

TEXTE

88/2025

Final report

How rapidly do per- and polyfluoroalkyl substances (PFAS) accumulate in different environmental compartments?

Monitoring of Samples from the German Environmental Specimen Bank

by:

Thorsten Reemtsma, Jana Rupp
Helmholtz Centre for Environmental Research - UFZ, Leipzig

Marc Guckert, Karsten Nödler, Gudrun Nürenberg
TZW: DVGW Water Technology Center, Karlsruhe

publisher:

German Environment Agency

TEXTE 88/2025

Ressortforschungsplan of the Federal Ministry for the
Environment, Nature Conservation and Nuclear Safety

Project No. (FKZ) 3718 64 423 0

FB001667

Final report

How rapidly do per- and polyfluoroalkyl substances (PFAS) accumulate in different environmental compartments?

Monitoring of Samples from the German Environmental
Specimen Bank

by

Thorsten Reemtsma, Jana Rupp
Helmholtz Centre for Environmental Research - UFZ, Leipzig

Marc Guckert, Karsten Nödler, Gudrun Nürenberg
TZW: DVGW Water Technology Center, Karlsruhe

On behalf of the German Environment Agency

Imprint

Publisher

Umweltbundesamt
Wörlitzer Platz 1
06844 Dessau-Roßlau
Tel: +49 340-2103-0
Fax: +49 340-2103-2285
buergerservice@uba.de
Internet: www.umweltbundesamt.de

Report performed by:

Helmholtz Centre for Environmental Research - UFZ
Permoserstraße 15
04318 Leipzig

Report completed in:

October 2024

Edited by:

Section IV 2.3 Chemicals
Wiebke Drost, Jona Schulze

Publication as pdf:

<http://www.umweltbundesamt.de/publikationen>

ISSN 1862-4804

Dessau-Roßlau, July 2025

The responsibility for the content of this publication lies with the author(s).

Acknowledgement

The authors gratefully acknowledge the financial support of this project by the Federal Ministry for the Environment, Nature Conservation, Nuclear Safety and Consumer Protection through the Federal Environment Agency (grant no 3718 64 423 0). The intensive collaboration with the colleagues at the German Environment Agency, namely with Wiebke Drost, Jan Koschorreck and Jona Schulze, Lena Vierke, Ina Fettig und Nina Vogel was an essential component for its success. This is gratefully acknowledged.

We are grateful to the personnel of Fraunhofer IME (Schmallenberg) for the support in receiving samples of the German Environmental Specimen Bank. We are indebted to colleagues of the following institutions for actively supporting this project by donating further samples for the PFAS monitoring: the German Federal Institute for Risk Assessment (BfR, Berlin), the German Wildlife Foundation (Hamburg), the Fraunhofer Institute for Molecular Biology and Applied Ecology (IME, Schmallenberg), the Institute for Terrestrial and Aquatic Wildlife Research at the University (ITAW) of Veterinary Medicine Hanover Foundation, the Leibniz Institute for Zoo and Wildlife Research (IZW, Berlin), the Bavarian Environment and Food Safety Agencies (LfU and LGL), Brumbachwild Outdoor Research and the District Office Rastatt.

We are grateful for the support we received from many individuals at UFZ: Heide Paschke, Steffi Schrader und Elias Flachowsky provided essential support in sample processing and analysis; Bettina Seiwert took care of the analyses by liquid-chromatography-high resolution-mass spectrometry; Theresa Döring and Kevin Jahn contributed to this project as master students; Laura Kahle curated the data for transfer to the ESB repository and supported the report finalization.

Our special thanks go to Urs Berger (now with Freiburg University Hospital) for initiating and conceptualizing this project and for this long-term scientific support.

Abstract: How rapidly do per- and polyfluoroalkyl substances (PFAS) accumulate in different environmental compartments?

A monitoring study was performed on the occurrence of per- and polyfluorinated alkyl substances (PFAS) in samples of the German Environmental Specimen Bank (ESB) covering the period 1990-2020 and in further biota samples, ensuring a wide geographic coverage of Germany. Terrestrial environment as well as riverine and coastal areas are covered by biomonitoring, each of it with animals of different trophic level, herbivores, omnivores and carnivores (28 different mammalian and avian species). Analytically, the study performed quantitative target analysis of > 60 PFAS, among them (ultra)short-chain perfluorinated carboxylic and sulfonic acids, long-chain PFAS, substitutes and precursors, by validated methods. This was complemented by the application of the total oxidizable precursor (TOP) assay including also (ultra)short-chain polyfluorinated carboxylic acids. The samples of the ESB were also analyzed by liquid-chromatography-high resolution-mass spectrometry to allow for retrospective screening.

While most of the data demonstrate the background contamination with large numbers of PFAS, also hot-spots were covered with contamination stemming from sludge application on agricultural land and industrial production of PFAS. This contamination was found to be well reflected in biota, namely the livers. Longer-chain PFAS clearly enrich along the terrestrial, aquatic and marine food chain, with highest concentrations found in organs of top-predators. Animals of lower trophic level better reflect the environmental contamination by (ultra)short-chain PFAS. The TOP assay provided valuable insight into the occurrence of unknown precursors namely in riverine biota, which would otherwise have remained undetected.

Time trends from 1990 to 2020 reflect the changes in PFAS market and the benefit of chemicals regulation with decreasing concentrations of the C8-PFAS since the early 2000s, first for PFOS and later also for PFOA. However, even today perfluorooctane sulfonic acid (PFOS) remains as the dominant PFAS in biota. Time trends for precursors and substitutes are less uniform and depend on the local contamination of the habitat under study and on the species studied. Contrary to C8-PFAS, the concentration of trifluoroacetic acid (TFA) is increasing clearly on a broad scale, as indicated by increasing concentrations in mussels as well as in terrestrial herbivores.

This comprehensive study proves the need for but also the effect of chemicals regulation of PFAS. In most compartments a clear but slow decrease of the environmental contamination by PFAS in Germany is visible. However, the data also outline the need for further regulatory action towards PFAS.

Kurzbeschreibung: Wie schnell akkumulieren Per- und Polyfluorierte Alkylsubstanzen (PFAS) in verschiedenen Umweltkompartimenten?

Diese Monitoring-Studie untersuchte die Gehalte per- und polyfluorierter Alkylsubstanzen (PFAS) in Proben der Umweltprobenbank (1990 -2020) und einer Vielzahl weiterer Biotaproben aus vielen Regionen Deutschlands. Die Proben stammten aus terrestrischen, aquatischen und marinen Kompartimenten von insgesamt 28 Säuger- und Vogelarten unterschiedlicher Trophiestufen (Herbiphore, Omniphore, Carniphore). Mehr als 60 PFAS-Verbindungen wurden quantifiziert, darunter (ultra)kurzkettige Carbon- und Sulfonsäuren, langkettige PFAS, Ersatzstoffe und Vorläuferverbindungen. Zudem wurde der "Total Oxidizable Precursor" (TOP) Assay angewendet. Die Proben der Umweltprobenbank wurden ferner mittels Flüssigchromatographie-hochauflösender Massenspektrometrie (LC-HRMS) untersucht, um ein retrospektives Screening zu ermöglichen.

Neben der weit verbreiteten sogenannten Hintergrundkontamination mit einer großen Breite an PFAS-Verbindungen wurden auch Proben aus hoch kontaminierten Bereichen untersucht, von mit Schlämmen beaufschlagten landwirtschaftlichen Flächen und aus dem Umfeld einer PFAS-Produktion. Diese hohen Kontaminationen spiegelten sich in den Biota-Proben wider, insbesondere in den Lebern, sowohl in der Höhe als auch in der Art der Belastung. In allen untersuchten Kompartimenten reicherten sich PFAS entlang der Nahrungsketten entlang der terrestrischen, aquatischen und marinen Nahrungsketten an. Die höchsten Belastungen fanden sich somit in hochstehenden räuberischen Arten. In herbiphore Arten fanden sich eher (ultra)kurzkettige PFAS. Die Anwendung des TOP-Assays auf Biotaprobe n erweiterte den Blick auf unbekannte Vorläuferverbindungen und Ersatzstoffe, die insbesondere in den Proben aus Flüssen sichtbar wurden.

Die zeitlichen Verläufe für den Zeitraum 1990 bis 2020 zeigen die seither erfolgten Veränderungen im PFAS-Markt und den Nutzen früherer PFAS-Regulationen, mit abnehmenden Konzentrationen der C8-PFAS seit 2000, zunächst für PFOS und später auch für PFOA. Allerdings ist auch heute PFOS zumeist noch die dominierende PFAS-Verbindung in Wildtierproben aus Deutschland. Die Konzentrationsverläufe für Vorläufersubstanzen und Ersatzverbindungen sind weniger einheitlich und abhängig von der Belastung des untersuchten Habitats und von der untersuchten Tierart. Im Gegensatz zu den C8-PFAS steigt die Konzentration von Trifluoressigsäure (TFA) seit den 1990er Jahren auf breiter Front an, sichtbar insbesondere in den Proben von Muscheln und terrestrischen Herbiphoren.

Diese sehr umfassende Monitoring-Studie zeigt klar den Nutzen früherer Regulationen von PFAS, aber auch den nur langsamen Rückgang der Kontamination mit PFAS in Deutschland. Die Befunde zeigen außerdem den anhaltenden Bedarf für regulatorische Aktivitäten hinsichtlich PFAS-Verbindungen.

Table of Content

Acknowledgement.....	5
List of Figures.....	12
List of Tables.....	15
List of Abbreviations.....	17
List of Abbreviations – PFAS.....	22
Summary	26
Zusammenfassung.....	31
1 Introduction.....	37
1.1 Per- and Polyfluoroalkyl Substances in the Environment.....	37
1.1.1 General.....	37
1.1.2 Regulation	37
1.1.3 PFAS Market.....	38
1.1.4 Analysis of PFAS	38
1.1.5 PFAS-Monitoring.....	39
1.2 Motivation.....	40
1.3 Study Objectives.....	40
1.4 Study Design.....	41
2 Materials and Methods	45
2.1 Chemicals Used	45
2.2 Samples.....	45
2.2.1 Samples from the German Environmental Specimen Bank.....	45
2.2.1.1 Work Package 2a: Initial Screening.....	45
2.2.1.2 Work Package 4: Trend Analyses.....	45
2.2.1.3 Sample Preparation	46
2.2.2 Samples from other Collections and Sampling Campaigns	46
2.2.2.1 Animal Tissues	47
2.2.2.2 Soil and Suspended Solids	48
2.2.2.3 Sample Preparation and Pooling	48
2.3 PFAS Screening for Targets and Oxidizable Precursors	50
2.4 Method Performance.....	51
2.5 Statistical Tools	52
2.6 PFAS Analysis by LC-Q-TOF-MS and FTICR-MS.....	53
2.6.1 Quality Assurance	53

2.6.2	Creation of a Suspect Screening Library	53
2.6.3	Quadrupole Time-of-Flight Mass Spectrometry	53
2.6.4	Fourier Transform Ion Cyclotron Resonance Mass Spectrometry (FTICR-MS)	54
3	Method Performance	56
3.1	Optimisation and Validation	56
3.1.1	Methods A and B.....	56
3.1.2	Method C.....	61
3.1.3	Quality Control.....	61
4	PFAS screening in samples of the Environmental Specimen Bank (work package 2a)	62
4.1	Diversity of PFAS included in this study	62
4.2	PFAS Concentrations and Patterns	63
4.3	TOP Assay.....	65
5	Time series analyses in marine and riverine organisms (work package 4)	68
5.1	Introduction	68
5.2	Spatiotemporal Trends in Freshwater Biota and Sample Selection.....	68
5.3	Sum Concentrations, Patterns and Trends	72
5.3.1	Are Sum Concentrations of Target PFAS decreasing?.....	72
5.3.2	What Information is gained by the TOP Assay?.....	73
5.4	Temporal Trends of Long-Chain PFAS and their Precursors	74
5.4.1	Is the C8 Phase-out mirrored in Monitoring Data?.....	74
5.4.2	How relevant are Precursors of C8 Chemistry?	74
5.4.3	Were all long-chain PFAS phased-out in parallel?	76
5.4.4	How relevant are precursors of >C8 PFAAs?	78
5.4.5	How relevant are Perfluoroalkyl Sulfonic Acids?	78
5.5	Temporal Trends of Short- and Ultrashort-Chain PFAS and their Precursors.....	78
5.5.1	Are Short-Chain PFAS replacing their Longer Homologues?	78
5.5.2	Which precursors contributed to the formation potential of short-chain PFCAs?.....	80
5.5.3	Is 6:2 FTSA-PrB an example of regrettable substitution?	80
5.5.4	Is trifluoroacetic acid a contaminant of emerging concern?	81
5.5.5	Has the risk of persistent and mobile PFAS been overlooked?	85
5.6	PFAS Trends in Comparison	85
5.6.1	PFAS trends in other aquatic biota	85
5.7	Conclusion	86
6	PFAS in German Wildlife and other environmental Samples (Work Package 2b).....	87

6.1	Abiotic Samples.....	87
6.1.1	PFAS Concentrations and Patterns	87
6.1.2	TOP Assay.....	88
6.2	Terrestrial Biota	90
6.3	PFAS patterns of herbivores, omnivores and carnivores.....	91
6.3.1	Introduction	91
6.3.2	Terrestrial species	91
6.3.3	Semi-aquatic herbivores and omnivores	95
6.3.4	Semi-aquatic freshwater and marine carnivores	96
6.3.4.1	Liver Tissue.....	96
6.3.4.2	Musculature Tissue.....	97
6.3.5	Interspecies comparison.....	97
6.3.6	TOP assay analysis.....	100
6.3.6.1	Interspecies comparison of the PFCA formation potential and pattern	100
6.3.6.2	Tissue specific PFCA formation potential and pattern	103
6.3.7	Conclusion.....	104
6.4	Wild Boar Liver as a Bioindicator for Environmental PFAS Contamination	104
6.4.1	Introduction	104
6.4.2	PFAS Profiles of Samples Associated with Different Contamination Sources	105
6.4.2.1	Background Contamination with PFAS	105
6.4.2.2	PFAS Contamination at the Hot-spot “Paper Sludges”	106
6.4.2.3	PFAS Contamination at Hot-spot “Industrial Emissions”	107
6.4.2.4	Variation in PFAS Patterns between the Areas	108
6.4.2.5	Formation Potential from Precursor PFAS.....	110
6.4.3	Comparison of PFAS Profiles in Wild Boar and the Local Environment.....	112
6.4.3.1	Soil Contamination at the Hot-spots	112
6.4.3.2	Contamination of Samples from a River Affected by Industrial Emissions	113
6.4.4	Dietary intakes and risks for human health.....	115
6.4.5	Conclusion.....	116
6.5	Human Risk Assessment	116
6.6	Conclusion.....	119
7	PFAS Suspect Screening.....	120
7.1	Archive of High-Resolution Mass Spectrometry Data (LC-TOF-MS)	120
7.2	Ultrahigh resolution MS (FTICR-MS) and Combination with LC-Q-TOF analysis	121

7.2.1	Work Flow	121
7.2.2	Application	122
8	Conclusion	128
9	List of References	130
A	Additional Information on Chemicals and Samples	147
A.1	PFAS reference standards and reagent purity	147
A.2	Sample overview	154
B	Overview of Analytical Methods Applied	170
B.1	Method A	170
B.2	Method B.....	172
B.3	Method C.....	173
B.4	Instrumental parameters for MS/MS detection of target compounds	174
B.5	Further Information on LC-HRMS screening.....	175
C	Screening Results.....	177
C.1	Time Series Analyses by LOESS Trend	177
D	Additional Information on Work Packages.....	187
D.1	Additional information on work package 4.....	187
D.2	Additional information on chapter 6.3	191
D.3	Additional information on chapter 6.4	197
D.4	Additional information on chapter 6	207
D.5	Samples of the study “Wild Boars Livers as Bioindicators for the Terrestrial Environment”	209
E	Attended Scientific Events as Part of the Project.....	210

List of Figures

Figure 1:	Analytical Concept of FLUORBANK.....	42
Figure 2:	Screening phases	43
Figure 3:	Sampling sites of the three times series.....	46
Figure 4:	Sample preparation of wild boar liver on dry ice	49
Figure 5:	Method overview	50
Figure 6:	Precision in quantitative LC-MS analysis	57
Figure 7:	Apparent recoveries in quantitative LC-MS analysis.....	58
Figure 8:	Limit of quantifications in target LC-MS analysis	59
Figure 9:	Precision in TOP assay analysis.....	59
Figure 10:	Apparent recovery in TOP assay analysis	60
Figure 11:	Limit of quantification in TOP assay analysis.....	60
Figure 12:	Organic fluorine in $\mu\text{g kg}^{-1}$ F (ww) in PFCAs found in bream liver.....	66
Figure 13:	Organic fluorine in $\mu\text{g kg}^{-1}$ F (wet weight) in PFCAs found in zebra mussel.....	66
Figure 14:	Mean PFCA patterns in % in bream liver and zebra mussel without and with oxidation via total oxidizable precursor assay	67
Figure 15:	Workflow to select samples for time series analyses	69
Figure 16:	Heatmap of temporal trends in (top) bream liver (pool size ≥ 20 fish) and (bottom) zebra mussel (pool size: 2000 – 5000 mussels)	70
Figure 17:	Spatiotemporal pattern of N-ethyl perfluorooctane sulfonamidoethanol (EtFOSE) in bream liver from German rivers.....	71
Figure 18:	Non-linear trends of PFOS and sum concentrations of PFAAs, target compounds (Σ_{42}) and results from target analysis and TOP assay (Σ_{23+TOP}).....	73
Figure 19:	Non-linear time trends of individual PFAS in herring gull egg from Mellum in the period 1980 to 2020 (North Sea; n=22; pool size ≥ 25 eggs).....	77
Figure 20:	Temporal trends of Deltas C4 and C7 (TOP assay) in (A) bream liver from Koblenz (Rhine; n=19; pool size ≥ 20 fish) and (B) herring gull egg from Mellum (North Sea; n=22; pool size ≥ 25 eggs).	79
Figure 21:	Temporal trend of TFA in herring gull egg (n=22; pool size ≥ 25 eggs) from Mellum (North Sea).....	82
Figure 22:	Temporal trends of (ultra)short-chain PFAS in zebra mussel (n=19; pool size: 2000–5000 mussels) from Blankenese (Elbe) depicting (A) the precursor 6:2 FTSA-PrB, (B) the formation potential of short-chain perfluorocarboxylic acids from precursors in the TOP assay and (C) trifluoroacetic acid (TFA)	83
Figure 23:	Temporal trends of C2 PFAS in bream liver from Koblenz (Rhine; n=19; pool size ≥ 20 fish).....	84
Figure 24:	Temporal trend (1990 – 2020) for C2, C3 - C7, C8 and C9 - C14 PFAS in aquatic biota.	86

Figure 25:	Experimental design of the monitoring study and of scientific publications generated from the data.....	87
Figure 26:	Formation potential from precursor PFAS in suspended matter and soil.....	89
Figure 27:	Increase of PFCAs in suspended matter after oxidation (TOP assay).....	89
Figure 28:	PFAS concentrations and results for the TOP assay in bird's eggs	90
Figure 29:	PFAS concentrations in livers from different wildlife species	92
Figure 30:	PFAS distribution patterns in livers from different wildlife species	93
Figure 31:	Principal component analysis of PFAS patterns in different wildlife species	99
Figure 32:	Pattern of the formation potential from precursor PFAS by the TOP-assay in different wildlife species	101
Figure 33:	PFAS sum concentrations in wild boar livers.....	108
Figure 34:	Principal component analysis of wild boar livers associated with different sources of contamination	109
Figure 35:	Formation potential from PFCA precursor compounds in wild boar livers.....	111
Figure 36:	Concentrations and patterns of perfluoroalkane carboxylic acids in wild boar livers and soil from area IE	113
Figure 37:	PFCA and PFAS concentrations in chub filet and suspended matter near an industrial park.....	114
Figure 38:	PFAS concentration in the liver of selected wild animals.....	117
Figure 39:	Scheme for the non-targeted search for PFAS	122
Figure 40:	Overview of tentatively identified candidates (with low and high confidence) and their associated PFAS subclasses detected in the four bream liver samples.....	124
Figure 41:	Overview of candidate annotations with low (LC) and high confidence (HC), detected in four bream liver samples from German rivers	127
Figure B 1:	Sample volume of beech leaves and soil in 10-mL headspace vials.....	174
Figure C 1:	Time Series Analyses by LOESS Trend.....	177
Figure D 1:	Temporal trends of (A) PFOA (target analysis) and (B) Delta C8 (TOP assay) in samples from the German Environmental Specimen Bank	187
Figure D 2:	Non-linear time trends of C10–C14 perfluoroalkyl carboxylic acids in (A) bream liver from Koblenz and (B) zebra mussel from Blankenese.....	188

Figure D 3:	Temporal trend of Delta C10 in herring gull egg (n=22; pool size≥25 eggs) from Mellum (North Sea).....	188
Figure D 4:	Temporal trends of Delta C9 and C10 in zebra mussels (n=19; pool size: 2000–5000 mussels) from Blankenese (Elbe).	188
Figure D 5:	Temporal trends of PFHxS in herring gull egg from Mellum (North Sea; n=22; pool size ≥25 eggs) and bream liver from Koblenz (Rhine; n=19; pool size ≥20 fish).....	189
Figure D 6:	Temporal trends of (top) (ultra)short-chain PFAS in zebra mussels (n=19; pool size: 50–100 mussels) from Blankenese (Elbe) in comparison to (bottom) related trends in zebra mussels and other biota.....	190
Figure D 7:	Total PFAS concentrations in liver (L) and musculature (F) tissue in grey seal (HG), harbour seal (PV), harbour porpoise (PP), cormorant (PC) and otter (LL).....	194
Figure D 8:	Differences in the PFAS composition between liver (L) and musculature (F) tissue in grey seal (HG), harbour seal (PV), harbour porpoise (PP), cormorant (PC) and otter (LL).	195
Figure D 9:	Scores along principle components (PC) 1 and 2 from the principle component analysis (PCA) of PFAS in wild boar liver from the paper sludge (PS, n=9), industrial emission (IE, n=1) and background contamination (BC, n=11) sites in Germany (collected in 2019 and 2020).....	198
Figure D 10:	Median PFCA pattern in soil (A, n=10) and wild boar liver (B, n=9) from area paper sludges (PS) in Germany.....	201
Figure D 11:	PFAS profiles of abiotic materials.....	207
Figure D 12:	PFAS profiles of aquatic samples – Filets	208

List of Tables

Table 1:	Reference materials used	52
Table 2:	Mean concentrations in $\mu\text{g kg}^{-1}$ of PFAS classes in different matrices screened in ESB samples from 2017–2019	64
Table 3:	Decreases in concentrations of PFOS and its precursors in biota from the German Environmental Specimen Bank for the years 2000–2010	76
Table 4:	p-values after testing for significant differences with student's T-test for the data of target analysis and TOP assay.	94
Table 5:	Validation results of TOP assay for bream liver (n=3).	96
Table 6:	Organic fluorine (OF) detected as ΣPFCA s in $\mu\text{g kg}^{-1}$ after TOP assay analysis.	100
Table 7:	Absolute and relative measures for the formation potential from precursor PFAS in wildlife samples	102
Table 8:	Comparison of PFOS and PFOA concentrations in wild boar livers from the present study (collected from three areas in Germany between 2019 and 2020) and literature for different study areas.	106
Table 9:	Risk assessment based on dietary human exposure by wild boar liver consumption from different sampling areas in Germany	115
Table 10:	Dietary risk assessment of different fish musculature	117
Table 11:	Overview on the four bream liver samples selected for the FTICR-MS and LC-HRMS screening exercise.....	123
Table 12:	List of assigned suspects with a high degree of confidence, identified in four bream liver samples.....	125
Table A 1:	List of target compounds and internal standards with acronym, corresponding PFAS family and group and information from the manufacturer	148
Table A 2:	Sample overview.....	154
Table A 3:	Samples from the German ESB for initial screening.....	157
Table A 4:	Samples from the German ESB for spatiotemporal trend analyses	160
Table A 5:	Details on samples and sampling procedures of the German ESB.....	161
Table A 6:	Samples from other collections and sampling campaigns	163
Table B 1:	Target compounds and selected instrumental parameters for LC-MS/MS detection.....	174
Table B 2:	Mix of standards used for quality control in LC-HRMS screening	175
Table D 1:	Mean sum concentrations in $\mu\text{g kg}^{-1}$ in liver samples from different species analysed within this study.....	191
Table D 2:	Mean sum concentrations in $\mu\text{g kg}^{-1}$ in pooled samples of musculature tissue from selected species analysed within this study.	195

Table D 3:	p-values after testing for significant differences between the wild boar livers from areas “background contamination” (BC, n=11) and “paper sludges” (PS, n=9).	197
Table D 4:	Organofluorine concentrations of PFCAs C2–C14 upon target analysis and TOP assay and the significance of their difference for wild boar liver from areas “background contamination” (BC, n=11) and “paper sludges” (PS, n=9), respectively.....	199
Table D 5:	Sample overview for the areas PS, IE and BC.	202
Table D 6:	Detailed information on individual sample materials and allocated source of contamination.	203
Table E 1:	Attended events as part of the project	210

List of Abbreviations

Abbreviation	Description
[M-H] ⁻ -ions	Molecular anion
ABF	Common bream filet (<i>Abramis brama</i>)
ABL	Common bream liver (<i>Abramis brama</i>)
AFFF	aqueous film forming foams
AOF	adsorbable organofluorine
area BC	sampling area with background contamination
area IE	sampling area (hot spot) with long-lasting industrial emissions
area PS	sampling area (hot spot) with deposition of paper sludges on arable land
AT	"after TOP-assay"
BBF	Common barbel filet (<i>Barbus barbus</i>)
BBL	Common barbel liver (<i>Barbus barbus</i>)
BC	background contamination
BfR	German Federal Institute for Risk Assessment (Bundesinstitut für Risikobewertung)
CASI	continuous accumulation of selected ions
CC	roe deer (<i>Capreolus capreolus</i>)
CCL	Roe deer liver (<i>Capreolus capreolus</i>)
CE	Red deer (<i>Cervus elaphus</i>)
CEL	Red deer liver (<i>Cervus elaphus</i>)
CF	Eurasian beaver (<i>Castor fiber</i>)
CF ₂	perfluorinated methylene group
CF ₃	perfluorinated methyl group
CFL	Eurasian beaver liver (<i>Castor fiber</i>)
CLP	chemical regulations for classification and labelling
CONTAM	EFSA Scientific Panel on Contaminants in the Food Chain
DI	direct injection
DPM	Zebra mussel soft body (<i>Dreissena polymorpha</i>)
DRM	Quagga mussel soft body (<i>Dreissena rostriformis</i>)
dTOP assay	modified form of TOP assay
dw	dry-weight
EOF	extractable organofluorine
ESB	German Environmental Specimen Bank

Abbreviation	Description
ESI	Electrospray ionisation
F	fluorine
F ₃ C-C	isolated carbon-bound trifluoromethyl group
FSL	Wildcat liver (<i>Felis silvestris</i>)
FSP	European beech (<i>Fagus sylvatica</i>)
FTICR-MS	Fourier transform ion cyclotron mass spectrometry
FVP	Bladder wrack (<i>Fucus vesiculosus</i>)
GC-MS	gas chromatography mass spectrometry
HC	high confidence
HGF	Grey seal filet (<i>Halichoerus grypus</i>)
HGL	Grey seal liver (<i>Halichoerus grypus</i>)
HRMS	high-resolution mass spectrometry
HS-SPME-GC-MS	headspace solid-phase-microextraction gas chromatography mass spectrometry
IC-QTOF-MS	ion chromatography quadrupole time of flight mass spectrometry
IE	industrial emission
IS	internal standard
JRC	European Union Joint Research Centre
K ⁺	Potassium ion
LAE	Herring gull egg (<i>Larus argentatus</i>)
LC	low confidence
LC PFCAs (C9-C21)	long-chain PFCAs
LC-HRMS	liquid chromatography high-resolution mass spectrometry
LC-MS	liquid chromatography mass spectrometry
LC-MS/MS	liquid chromatography tandem mass spectrometry
LC-QTOF-MS	liquid chromatography quadrupole-time-of-flight mass spectrometry
LE	Common/European hare (<i>Lepus europaeus</i>)
LEL	Common/European hare liver (<i>Lepus europaeus</i>)
Li ⁺	lithium ion
LLF	Common otter filet (<i>Lutra lutra</i>)
LLL	Common otter liver (<i>Lutra lutra</i>)
LOD	limit of detection
LOQ	limit of quantification

Abbreviation	Description
LTF	Earthworm filet (<i>Lumbricus terrestris</i> + <i>Aporrectodea longa</i>)
MCL	Coypu liver (<i>Myocastor coypus</i>)
MEM	Blue mussel soft body (<i>Mytilus edulis complex</i>)
Mg ²⁺	Magnesium ion
MRM	multiple-reaction monitoring
MS ^e	all-ion fragmentation mode
Na ⁺	Sodium ion
nano-ESI	nano-electrospray interface
nC	number of carbons
OECD	Organisation for Economic Co-operation and Development
OF	organic fluorine
PAP	Norway spruce plant (<i>Picea abies</i>)
PBT	persistent, bioaccumulative and toxic
PC	Great cormorant (<i>Phalacrocorax carbo</i>)
PC	principle component
PCA	principle component analysis
PCE	Great crested grebe egg (<i>Podiceps cristatus</i>)
PCI	positive chemical ionisation
PCL	Great cormorant liver (<i>Phalacrocorax carbo</i>)
PCU	Great cormorant lung (<i>Phalacrocorax carbo</i>)
PMT	persistent, mobile and toxic
PNP	Lombardy poplar plant (<i>Populus nigra 'Italica'</i>)
POPs	Persistent and Organic Pollutants
PP	harbour porpoise
PPF	harbour porpoise filet (<i>Phocoena phocoena</i>)
PPL	harbour porpoise liver (<i>Phocoena phocoena</i>)
PS	paper sludges
PSP	Scots pine plant (<i>Pinus sylvestris</i>)
PV	harbour seal (<i>Phoca vitulina</i>)
PVF	harbour seal filet (<i>Phoca vitulina</i>)
PVL	harbour seal liver (<i>Phoca vitulina</i>)
QA	quality assurance

Abbreviation	Description
RAC	ECHA's scientific committees for risk assessment
REACH	Regulation concerning the Registration, Evaluation, Authorisation and Restriction of Chemicals
RP-LC-MS/MS	reversed-phase liquid chromatography tandem mass spectrometry
RR	Chamois (<i>Rupicapra rupicapra</i>)
RRF	roach filet (<i>Rutilus rutilus</i>)
RRL	Chamois liver (<i>Rupicapra rupicapra</i>)
S/N ratio	signal to noise ratio
SCF	European chub filet (<i>Squalius cephalus</i>)
SEAC	ECHA's scientific committees for socio-economic analysis
SIM	single ion monitoring
SLF	Pike-perch filet (<i>Sander lucioperca</i>)
SML	Common eider duck liver (<i>Somateria mollissima</i>)
SO ₃ Cl	Chloro sulphate
SO ₃ F	Fluoro sulphate
SO ₃ H	Chlorosulfuric acid
SO ₄ H	Hydrogen sulphate
SPME-GC-MS	solid-phase-microextraction gas chromatography mass spectrometry
SPS	suspended matter sample
SS	wild boar (<i>Sus scrofa</i>)
SSL	Wild boar liver (<i>Sus scrofa</i>)
SVHC	substance of very high concern
TBF	emerald rockcod filet (<i>Trematomus bernachii</i>)
TOP assay	Total Oxidizable Precursor assay
TOP _{OF}	TOP assay organic fluorine
TSS	Top soil sample / soil A horizon
TTE	Black grouse egg (<i>Tetrao tetris</i>)
TWI	Tolerable Weekly Intake
UHR-MS	ultrahigh resolution mass spectrometry
vPvB	very persistent and very bioaccumulative
vPvM	very persistent and very mobile
WP	work package
ww	wet-weight

Abbreviation	Description
ZVF	Viviparous eelpout filet (<i>Zoarces viviparus</i>)
ZVL	Viviparous eelpout liver (<i>Zoarces viviparus</i>)
α	confidence level

List of Abbreviations – PFAS

Abbreviation	Description
10:2 diPAP	10:2 Fluorotelomer phosphate diester
10:2 diPAP- ² H ₄	Sodium bis(1 <i>H</i> ,1 <i>H</i> ,2 <i>H</i> ,2 <i>H</i> -[d4]-perfluorodecyl)phosphate
10:2 FTSA	10:2 Fluorotelomer sulfonic acid
10:2 monoPAP	10:2 Fluorotelomer phosphate monoester
4:2 diPAP	4:2 Fluorotelomer phosphate diester
4:2 FTSA	4:2 Fluorotelomer sulfonic acid
4:2 FTSA- ¹³ C ₂	Sodium 1 <i>H</i> ,1 <i>H</i> ,2 <i>H</i> ,2 <i>H</i> -perfluoro-1-[1,2- ¹³ C ₂]hexane sulfonate (4:2)
4:2 monoPAP	4:2 Fluorotelomer phosphate monoester
6:2 Cl-PFESA	9-chlorohexadecafluoro-3-oxanonane-1-sulfonate
6:2 diPAP	6:2 Fluorotelomer phosphate diester
6:2 diPAP- ¹³ C ₂	Sodium bis(1 <i>H</i> ,1 <i>H</i> ,2 <i>H</i> ,2 <i>H</i> -[1,2- ¹³ C ₂]perfluorooctyl)phosphate
6:2 FTMAC	6:2 fluorotelomer methacrylate
6:2 FTNO	6:2 fluorotelomer sulfonamide amine oxide (Capstone A)
6:2 FTSA	6:2 Fluorotelomer sulfonic acid
6:2 FTSA- ¹³ C ₂	Sodium 1 <i>H</i> ,1 <i>H</i> ,2 <i>H</i> ,2 <i>H</i> -perfluoro-1-[1,2- ¹³ C ₂]octane sulfonate (6:2)
6:2 FTSA-PrB	6:2 fluorotelomer sulfonamidopropyl betaine (Capstone B)
6:2 monoPAP	6:2 Fluorotelomer phosphate monoester
6:2 monoPAP- ¹³ C ₂	Sodium 1 <i>H</i> ,1 <i>H</i> ,2 <i>H</i> ,2 <i>H</i> -[1,2- ¹³ C ₂]perfluorooctylphosphate
6:2/10:2 diPAP	6:2/10:2 Fluorotelomer phosphate diester
6:2/12:2 diPAP	6:2/12:2 Fluorotelomer phosphate diester
6:2/8:2 diPAP	6:2/8:2 Fluorotelomer phosphate diester
6:6 PFPiA	6:6 perfluorinated phosphinic acids
6:8 PFPiA	6:8 perfluorinated phosphinic acids
8:2 Cl-PFESA	11-chloroeicosafluoro-3-oxaundecane-1-sulfonate
8:2 diPAP	8:2 Fluorotelomer phosphate diester
8:2 diPAP- ¹³ C ₂	Sodium bis(1 <i>H</i> ,1 <i>H</i> ,2 <i>H</i> ,2 <i>H</i> -[1,2- ¹³ C ₂]perfluorodecyl)phosphate
8:2 FTSA	8:2 Fluorotelomer sulfonic acid
8:2 FTSA- ¹³ C ₂	Sodium 1 <i>H</i> ,1 <i>H</i> ,2 <i>H</i> ,2 <i>H</i> -perfluoro-1-[1,2- ¹³ C ₂]decane sulfonate(8:2)
8:2 monoPAP	8:2 Fluorotelomer phosphate monoester
8:2 monoPAP- ¹³ C ₂	Sodium 1 <i>H</i> ,1 <i>H</i> ,2 <i>H</i> ,2 <i>H</i> -[1,2- ¹³ C ₂]perfluorodecylphosphate
8:2/10:2 diPAP	8:2/10:2 Fluorotelomer phosphate diester

Abbreviation	Description
8:2/12:2 diPAP	8:2/12:2 Fluorotelomer phosphate diester
Cl-PFBS	Chlorinated perfluorobutane sulfonic acid
Cl-PFDS	Chlorinated perfluorodecane sulfonic acid
Cl-PFESA	Chlorinated perfluoroalkyl ether sulfonic acid
Cl-PFHxS	chlorinated perfluorohexane sulfonic acid
Cl-PFNA	Chlorinated perfluorononanoic acid
Cl-PFNs	Chlorinated perfluorononanesulfonic acid
Cl-PFOS	Chlorinated perfluorooctane sulfonic acid
Cl-PFSA	Chloroperfluoroalkyl sulfonic acid
diPAPs	Fluorotelomer phosphate diesters
diSAmPAP	Perfluorooctane sulfonamido phosphate diester
DONA	4,8-dioxa-3 <i>H</i> -perfluorononanoic acid
EtFOSA	<i>N</i> -Ethyl perfluorooctane sulfonamide
EtFOSA- ² H ₅	<i>N</i> -Ethyl-d ₅ -perfluoro-1-octanesulfonamide
EtFOSAA	<i>N</i> -Ethylperfluorooctane sulfonamidoacetic acid
EtFOSAA- ² H ₅	<i>N</i> -Deuterioethylperfluoro-1-octanesulfonamidoacetic acid
EtFOSE	<i>N</i> -Ethyl perfluorooctane sulfonamidoethanol
EtFOSE- ² H ₉	2-(<i>N</i> -deuterioethylperfluoro-1-octanesulfonamido)- 1,1,2,2-tetradeuterioethanol
FASA	Perfluoroalkane sulfonamide (PFAS group)
FASAA	Perfluoroalkane sulfonamido acetic acid (PFAS group)
FASE	Non-alkylated perfluoroalkane sulfonamido ethanol (PFAS group)
FBSA	Perfluorobutane sulfonamide
FBSAA	Perfluorobutane sulfonamidoacetic acid
FBSE	Perfluorobutane sulfonamidoethanol
FHxSA	Perfluorohexane sulfonamide
FHxSAA	Perfluorohexane sulfonamidoacetic acid
FHxSE	Perfluorohexane sulfonamidoethanol
FOSA	Perfluorooctane sulfonamide
FOSA- ¹³ C ₈	Perfluoro-1-[¹³ C ₈]octanesulfonamide
FOSAA	Perfluorooctane sulfonamidoacetic acid
FOSE	Perfluorooctane sulfonamidoethanol
FPeSA	Perfluoro-1-pentanesulfonamide

Abbreviation	Description
FTAC	Fluorotelomer acrylate (PFAS group)
FTMAC	Fluorotelomer methacrylate (PFAS group)
FTNO	Fluorotelomer sulfonamide amine oxide (PFAS group)
FTOH	Fluorotelomer alcohol (PFAS group)
FTSA	Fluorotelomer sulfonic acid (PFAS group)
HFPO-DA, Gen X	Hexafluoropropylene oxide dimer acid or perfluoro-2-methyl-3-oxahexanoic acid
HFPO-DA- ¹³ C ₃	2,3,3,3-Tetrafluoro-2-(1,1,2,2,3,3,3-heptafluoropropoxy)- ¹³ C ₃ -propanoic acid
MeFOSA	N-Methyl perfluorooctane sulfonamide
MeFOSA- ² H ₃	N-Methyl-d ₃ -perfluoro-1-octanesulfonamide
MeFOSAA	N-Methylperfluorooctane sulfonamidoacetic acid
MeFOSAA- ² H ₃	N-Deuteriomethylperfluoro-1-octanesulfonamidoacetic acid
MeFOSE	N-Methyl perfluorooctane sulfonamidoethanol
MeFOSE- ² H ₇	2-(N-Deuteriomethylperfluoro-1-octanesulfonamido)- 1,1,2,2-tetradeuterioethanol
monoPAP	Fluorotelomer phosphate monoester (PFAS group)
monoSAmPAP	Perfluorooctane sulfonamido phosphate monoester (PFAS group)
PAP	Phosphate ester (PFAS group)
PFAA	Perfluoroalkyl acid (PFAS group)
PFAS	Per- and polyfluoroalkyl substances
PFBA	Perfluorobutanoic acid
PFBA- ¹³ C ₄	Perfluoro-n-[1,2,3,4- ¹³ C ₄]butanoic acid
PFBS	Perfluorobutane sulfonic acid
PFBS- ¹³ C ₃	Sodium perfluoro-1-[2,3,4- ¹³ C ₃]butane sulfonic acid
FHxSA	Perfluorohexane sulfonamide
PFCAs	Perfluoroalkyl carboxylic acids (PFAS group)
PFDA	Perfluorodecanoic acid
PFDA- ¹³ C ₂	Perfluoro-n-[1,2- ¹³ C ₂]decanoic acid
PFDoDA	Perfluorododecanoic acid
PFDoA- ¹³ C ₂	Perfluoro-n-[1,2- ¹³ C ₂]dodecanoic acid
PFDoDS	Perfluorododecanesulfonic acid
PFDPA	perfluorodecylphosphonic acid
PFDS	Perfluorodecanesulfonic acid
PFECA	Perfluoroalkyl mono- and di-ether carboxylic acid (PFAS group)

Abbreviation	Description
PFHpA	Perfluoroheptanoic acid
PFHpA- ¹³ C ₄	Perfluoro-n-[1,2,3,4- ¹³ C ₄]heptanoic acid
PFHpDA	Perfluoroheptadecanoic acid
PFHpS	Perfluoroheptane sulfonic acid
PFHxA	Perfluorohexanoic acid
PFHxA- ¹³ C ₂	Perfluoro-n-[1,2- ¹³ C ₂]hexanoic acid
PFHxS	perfluorohexanesulfonic acid
PFHxS- ¹⁸ O ₂	Perfluoro-1-hexane[¹⁸ O ₂]sulfonic acid
PFMOPrA	Perfluoromethoxypropionic acid
PFNA	Perfluorononanoic acid
PFNA- ¹³ C ₅	Perfluoro-n-[1,2,3,4,5- ¹³ C ₅]nonanoic acid
PFNS	Perfluorononanesulfonic acid
PFOA	Perfluorooctanoic acid
PFOA- ¹³ C ₄	Perfluoro-n-[1,2,3,4- ¹³ C ₄]octanoic acid
PFOS	Perfluorooctanesulfonic acid
PFOS- ¹³ C ₈	Perfluoro-1-[1,2,3,4- ¹³ C ₈]octane sulfonic acid
PFOSA	perfluorooctane sulfonamide
PFPeA	Perfluoropentanoic acid
PFPeA- ¹³ C ₅	Perfluoro-n-[1,2,3,4,5- ¹³ C ₅]pentanoic acid
PFPIA	Perfluorinated phosphinic acid (PFAS group)
PFPrA	Perfluoropropanoic acid
PFSA	Perfluoroalkyl sulfonic acid (PFAS group)
PFTeDA	Perfluorotetradecanoic acid
PFTeDA- ¹³ C ₂	Perfluoro-n-[1,2- ¹³ C ₂]tetradecanoic acid
PFTrDA	Perfluorotridecanoic acid
PFTrDS	Perfluorotridecane sulfonic acid
PFUnDA- ¹³ C ₂	Perfluoro-n-[1,2- ¹³ C ₂]undecanoic acid
PFUnDA	Perfluoroundecanoic acid
POSF	Perfluorooctansulfonylfluorid
TFA	Trifluoroacetic acid
triPAP	Polyfluoroalkyl phosphate tri-esters

Summary

Per- and polyfluorinated alkyl substances (PFAS) are one of the dominant groups of organic contaminants in the environment and in biota, today. Their persistence, in combination with their widespread use has led to a diffuse contamination of the environment as well as to large numbers of highly contaminated sites. The number of different PFAS used is very large and only partially known, and they are highly diverse in their molecular structure. The ongoing development in chemical industry, together with regulatory actions, leads to an ongoing change of the PFAS being produced and used, and eventually emitted to the environment. Some PFAS, i.e. the long-chain perfluoroalkyl acids (PFAA), accumulate along the food chain while others, i.e. the ultrashort-chain PFAA do travel along the water cycle. Some PFAS are highly persistent while others are transformed to such highly persistent PFAS in the environment or in biota.

For these reasons, the level of PFAS contamination in different environmental compartments and in biota as well as the respective PFAS patterns are only partially known, and subject to change.

The project FLUORBANK explored temporal trends as well as spatial differences in the PFAS burden of a large set of biota samples from different environmental compartments in Germany for a very broad set of PFAS. Besides the regularly studied long-chain PFCA and PFSA this includes:

- ▶ short-chain and ultra-short chain PFAS,
- ▶ new substitutes of long-chain PFAS,
- ▶ precursor PFAS, that can be oxidised to PFCAs (TOP-assay),
- ▶ unknown PFAS, i.e. the difference between the quantified PFAS and the outcome of the TOP-assay.
- ▶ previously overlooked, undetected PFAS (by suspect- and nontarget-screening).

With this approach FLUORBANK has extended the knowledge on the **distribution of PFAS in terrestrial, riverine and marine food webs** and on differences between **local hot spots and areas with diffuse pollution**. The project outlines **long-term temporal trends in the environmental contamination by PFAS** that may also reflect the effect of past regulatory actions. The results of this study are meant to provide a scientific basis to support the ongoing work of UBA on the European level with respect to the regulation of PFAS.

Overview

The project FLUORBANK aimed at a **comprehensive characterization of the level of contamination by PFAS in Germany with a focus on biota** with a set of validated, uniform analytical methods for the period 1980s to 2020.

For this purpose, a **combination of innovative analytical methods** was applied. These methods comprise four different approaches:

- ▶ Quantitative analysis of a broad range of PFAS with diverse physico-chemical properties employing validated methods that provide highest selectivity and sensitivity (LC-MS/MS).
- ▶ PFAS screening by liquid chromatography-high resolution-mass spectrometry (LC-HRMS) with the option to perform retrospective data search also after the completion of this project.

- ▶ Quantification of the totality of PFAS that form PFCA with the total oxidizable precursor (TOP) assay, including (unknown) precursor PFAS.
- ▶ Non-target screening for yet unknown PFAS by ultrahigh resolution-mass spectrometry (FTICR-MS).

These methods were applied to **samples of the Environmental Specimen Bank (ESB)** and to further samples provided by authorities from regional surveillance programs and from research institutes. FLUORBANK focussed on biota samples, covering plants (needles, leaves, algae) as well as animal samples (musculature, liver, egg, mussel tissue, lung tissue) from different trophic level including top predators (fish, birds and mammals) from terrestrial as well as riverine and coastal areas. Besides, also surface soil and riverine suspended matter were included.

Project results have been published in two **scientific publications**, thus far and were incorporated into two dissertations. Quantitative PFAS data for the samples received from the ESB were deposited in the **data repository of the ESB with open access**.

Besides, a **workshop “PFAS-Analytik für die Umweltüberwachung: Neue Anforderungen, Erfahrungen aus der Praxis, Erkenntnisse aus der Forschung”** was organized in November 2021 at UFZ Leipzig, with active contributions from academia and regulatory authorities. At this workshop, results of the project FLUORBANK were presented and the participants discussed about the recent challenges in PFAS analysis and risk assessment as well as about trends in PFAS regulation in Europe.

Results and Discussion

Monitoring of ESB samples

In FLUORBANK around 120 samples of the ESB, collected between 1980s and 2020, were quantitatively analyzed for 69 different PFAS. The target analysis was complemented by a modified TOP assay that included (ultra)short-chain PFCAs. This monitoring exercise generated the most comprehensive and uniform set on PFAS data in biota yet available for Germany.

Of the 69 PFAS analyzed 36 PFAS were determined at least once. A more detailed comparison of PFAS data was performed for 7 biota species (herring gull, viviparous eelpout filet, blue mussel, common bream liver, common bream filet, zebra mussel and roe deer liver) and riverine suspended matter and soils.

In biota, the level of \sum PFAS concentrations were highest in bream liver ($121 \mu\text{g kg}^{-1}$), followed by herring gull eggs ($30 \mu\text{g kg}^{-1}$) and bream musculature ($16 \mu\text{g kg}^{-1}$). For these three specimens the PFAS composition is dominated by PFOS (72 % for bream liver), followed by C8-C14 PFCA. Eelpout filet, blue mussel and zebra mussel exhibited much lower \sum PFAS levels of $1 - 4 \mu\text{g kg}^{-1}$ and a more diverse composition.

For most of the species the TOP assay, which screens for PFAS not accounted for by the quantitative analysis of the 69 individual PFAS, did not show a significant contribution of “unknown” precursors. This was, however, different for the samples of riverine biota, such as bream liver and mussel tissue in which the TOP assay led to mainly short-chain PFCAs.

The factors affecting PFAS levels in the diverse set of samples of the ESB collected over more than 20 years are discussed in more detail below. All data were imported into the ESB data repository for open access.

Subsequently, more detailed data analysis focused on animal samples, because of the higher PFAS concentrations found, compared to plants and soils and suspended matter.

Temporal trends

FLUORBANK studied temporal trends in the PFAS burden of ESB samples taken between the 1980s/1990s and 2020, for animal species of different habitats and with generally high detection frequencies for PFAS. On this basis herring gull egg from the North Sea (Mellum, 1988 – 2020), bream liver from River Rhine (Koblenz; 1996 – 2020), and zebra mussel from River Elbe (1995 – 2018) were selected.

On average 24, 23 and 13 PFAS were detected in herring gull egg, bream liver and zebra mussel, respectively, with maximum numbers of 30, 28 and 19 PFAS in samples from 2002, 1996 and 2007, respectively. The concentration for Σ PFAS ranged from 10 to 1000 $\mu\text{g F kg}^{-1}$ ww for zebra mussel, herring gull egg and bream liver.

Overall, 45 PFAS were detected at least once among all species and time points – with the substitutes 8:2 Cl-PFESA (bream) and DONA (herring gull and bream) determined only in single samples. PFCAs and PFSAs dominated among all analysed PFAS for all three sample types.

In herring gull egg and bream liver the Σ PFAS concentration decreased over time, reflecting a decreasing PFAS contamination both, in coastal and in the riverine benthic food chain. This is in accordance with the voluntary and regulatory-driven changes on the PFAS market.

Although the PFOS level in herring gull eggs and bream liver decreased by approximately 4 % per year on average during the study period, PFOS contamination remains on a high level and, still, accounts for more than 60 % of the PFAS load in 2020. The C10 – C14 PFCAs showed a less uniform pattern: in herring gull egg and bream liver they increased until around 2010 - 2015, and some but not all appear to decrease since then.

Temporal trends for the less contaminated zebra mussel are quite different from those in bream liver and herring gull eggs. Here, no decreasing trend but an increase is visible from 1990 onwards.

The TOP assay turned out to be a valuable tool in estimating the contribution of unknown precursors. In bream liver and zebra mussel, precursors significantly contributed to the overall PFAS load (on average 27 % and 39 %, respectively).

Contrary to many other PFAS, the level of the ultrashort-chain TFA exhibited an upwards trend in zebra mussel and herring gull eggs.

PFAS in food webs

In a comprehensive, quantitative analysis, the PFAS concentrations and patterns were investigated for 14 different mammalian and avian species, including herbivores, omnivores and carnivores from different ecological habitats (terrestrial, semi-aquatic, marine) and in different body tissues (liver and musculature).

Generally, PFAS concentrations in musculature are lower than those determined from liver of the same species. The Σ PFAS concentrations in liver tissue decreased in the order semi-aquatic carnivore ($1300 \mu\text{g kg}^{-1}$) > marine carnivore ($80 - 300 \mu\text{g kg}^{-1}$) > terrestrial omnivores ($120 \mu\text{g kg}^{-1}$) > terrestrial carnivores ($40 \mu\text{g kg}^{-1}$) > terrestrial herbivores ($20 - 40 \mu\text{g kg}^{-1}$) > semi-aquatic omnivores/herbivores ($20 \mu\text{g kg}^{-1}$). This reflects the increase in more proteinophilic/hydrophobic longer-chain PFAS along the food chain.

Also, the PFAS pattern in livers of the different species differed markedly. In carnivores PFOS (67–95 %) and, to a lesser extent, long-chain PFCAs (C \geq 8) dominated, whereas in predominantly herbivorous species TFA was the most dominant PFAS. Novel substitute compounds were detected only sporadically (wild boar, otter, cormorant) and at low concentrations.

The application of the TOP assay to the liver samples showed a generally low formation potential for PFCA. This may reflect *in vivo* transformation of precursors in the metabolically active liver.

Relationship between environmental contamination and contamination of biota

FLUORBANK explored if biomonitoring would be an option to localize sites of elevated PFAS contamination in terrestrial environment (hot-spots), many of which are not known, yet.

For this purpose, the PFAS load of livers of wild boars as terrestrial omnivorous species was compared for three sites with known differences in their contamination pattern: two hot-spots, one site of contaminated arable land (PS), one site affected by industrial emissions of PFAS (IE), and a rural background contamination (BC).

The livers of wild boars from the two contaminated sites both showed clearly elevated PFAS levels (480 and 960 $\mu\text{g kg}^{-1}$) compared to the background sites (120 $\mu\text{g kg}^{-1}$). For the PS and BC sites, PFOS was the major PFAS component, comprising 66 – 93 % of ΣPFAS . At the site IE, however, PFOA was dominating (69 % of ΣPFAS) in wild boar liver, while the concentration of PFOS was at the lower end of the BC values. Corresponding to the proximity to the industrial plant, also the substitutes HFPO-DA and DONA were found in wild-boar liver at the IE site, but not at the other sites. For the other hot-spot (area PS), short-chain PFCAs were formed by the TOP assay.

The environmental contamination by (ultra)short-chain PFAS is better monitored in aquatic organisms. In future environmental monitoring studies of PFAS, it is essential to include substitute PFAS and the TOP assay.

Human risk assessment

The maximum level set by the EU for PFOS and for PFAS₄ in fish meat were exceeded by most samples of bream analyzed in this study. In single cases also the maximum level of PFOA was exceeded. The human consumption of wild boar livers from Germany would significantly contribute to the dietary intake of PFAS and the tolerable weekly intake (TWI) could be exceeded easily. The investigated herbivorous game animals and fish from the remote Antarctica were also contaminated by PFAS, but at concentrations well below the maximum levels. In the terrestrial herbivores, other PFAS than those considered in dietary risk assessment prevail, such as TFA.

Suspect screening and HRMS data archive

Besides quantitatively analysing for a large set of PFAS available as reference compounds, FLUORBANK also improved methods for the suspect screening for unknown/undetected PFAS in biota samples. A novel approach was developed which combined direct injection-Fourier Transform Ion-Cyclotron-Resonance mass spectrometry (FTICR-MS) and LC-HRMS. This approach was exemplarily applied to four samples of bream liver of the ESB with a high proportion of unaccounted organofluorine compounds.

A larger number of previously undetected compounds were identified as PFAS in the bream livers samples, among them several precursors and substitutes and modified analogues of legacy compounds with branched side chains, H- and Cl-substitution, double bond/ring functionality insertion as well as variations of non-fluorinated polar head groups. Not all of these PFAS could be identified to the molecular level. Full confirmation or quantification would have required the availability of reference standards.

The complex matrix of biota samples and the comparatively low concentration of PFAS in such samples makes suspect screening and identification of unknown PFAS a challenging task. Methods for this purpose need further improvement.

A total of 249 samples of the FLUORBANK project, biota as well as soil and riverine suspended matter, were analysed by LC-HRMS with a time-of-flight mass spectrometer in the positive and in the negative mode using generic measurement conditions. The data are stored at UFZ and will be held available for retrospective search for 5 years.

Conclusions

FLUORBANK provided the most comprehensive set of PFAS data in terms of number of PFAS included (58 PFAS quantified), and the diversity of biota samples (five plant species, 28 animal species with 43 different sample types) of different trophic level and from terrestrial as well as riverine and coastal areas for Germany, covering a period from the 1980s to 2020. Samples of surface soil and riverine suspended matter were also included. This comprehensive data set is now publicly available through the ESB to inform authorities and the public.

From this data set it can be concluded:

- ▶ Beyond site-specific influences, the PFAS burden of wildlife animals is clearly dependent on their trophic level (herbivores, omnivores, carnivores) and their habitat (marine, semi-aquatic, terrestrial).
- ▶ The temporal development of the PFAS load of the biota samples clearly reflects the phase-out of PFOS in the early 2000s; there is a continuing decrease in the PFAS load of many of the studied animal species. However, PFOS remains environmentally relevant with high shares of the total PFAS burden in most organisms studied.
- ▶ Besides, also known and unknown C8 precursors can contribute markedly to the total PFAS load. Even if their levels are still low compared to PFOS, the overall increasing trends of >C8 PFCAs may be considered an early warning signal for ecosystem health and human food production.
- ▶ Biomonitoring with zebra mussel indicate an increasing trend for TFA and precursors of (ultra)short-chain PFAS, namely since 1995. This leads to an increase of the total PFAS concentration in zebra mussel.
- ▶ Of the animals collected in the ESB and studied more closely herring gull egg and bream liver turned out to be suitable for monitoring of such long-term trends for legacy PFAS, that enrich along the food chain and are considered problematic for human exposure. Animals of lower trophic level (e.g. deer and zebra mussels) appear to be better suited to monitor (ultra)short-chain PFAS in terrestrial and aquatic compartments.
- ▶ With respect to the characterization of PFAS contamination of soil, its level as well as site-specific contaminants, wild boars may be suitable organisms for biomonitoring; their PFAS burden can be analysed in their liver.
- ▶ Suspect screening for previously unrecognized PFAS in biota using high-resolution mass spectrometry remains challenging, due to the complexity of biota samples and their comparatively low level of unrecognized PFAS. However, if combined with suitable data processing pipelines, PFAS screening can provide a broader insight into the non-conventional PFAS burden of biota. Confirmation of suspects and their quantitative assessment depends on the availability of reference compounds.

Zusammenfassung

Per- und polyfluorierte Alkylsubstanzen (PFAS) sind eine der vorherrschenden Gruppen organischer Kontaminanten in der Umwelt und in Biota. Ihre Persistenz, zusammen mit ihrer weltweiten Nutzung hat sowohl zu einer diffusen Kontamination der Umwelt geführt, als auch zu einer sehr großen Zahl von örtlich hoch belasteten Flächen, sogenannten „Hot-Spots“. Die Anzahl der PFAS-Verbindungen, die genutzt wurden oder noch genutzt werden, ist sehr hoch; sie sind nur zum Teil bekannt und unterschieden sich stark in ihrer molekularen Struktur.

Eine anhaltende industrielle Fortentwicklung, zusammen mit regulatorischen Aktivitäten, führen zu einer stetigen Veränderung des PFAS-Portfolios, das produziert und eingesetzt wird und schließlich die Umwelt erreicht. Einige PFAS, z.B. die langkettigen Perfluoroalkyl-Säuren (PFAA), reichern sich in der Nahrungskette an, während andere, z.B. die ultrakurzkettigen PFAA, sich entlang des Wasserkreislaufs verbreiten. Einige PFAS sind hoch persistent, während andere erst in der Umwelt oder in Biota in diese hoch persistenten Verbindungen umgewandelt werden. Aus diesen Gründen ist der Konzentrationsbereich von PFAS in verschiedenen Umweltkompartimenten, ebenso wie die jeweiligen Belastungsmuster, nur teilweise bekannt und zudem stetiger Veränderung unterworfen.

Das Vorhaben FLUORBANK hat die PFAS-Belastung in einer großen Zahl an Wildtieren für eine sehr große Anzahl an PFAS erfasst und dabei sowohl zeitliche Trends als auch räumliche Unterschiede erfasst. Die untersuchten PFAS umfassten neben den häufig untersuchten langkettigen PFCA und PFSA:

- ▶ Kurzkettige und ultrakurzkettige PFAS,
- ▶ Ersatzstoffe für langkettige PFAS,
- ▶ Vorläufersubstanzen, die zu Perfluorcarbonsäuren oxidiert werden können (sog. „TOP-Assay“),
- ▶ Unbekannte PFAS, entsprechend der Konzentrationsdifferenz zwischen der Summe der quantifizierten PFAS und dem Ergebnis des TOP-Assays,
- ▶ Bisher übersehene PFAS, die durch Suspect- und Nontarget-Screening gefunden werden konnten.

Mit den durch das gewählte Vorgehen erzielten Ergebnissen hat FLUORBANK das Wissen über die **Verteilung von PFAS in Nahrungsnetzen terrestrischer, aquatischer und küstennaher mariner Habitate** erweitert. FLUORBANK hat auch Unterschiede zwischen der Belastung von Wildtieren in der Umgebung von **Hot-Spots und der diffusen Belastung** mit PFAS herausgearbeitet. FLUORBANK zeigt **langjährige Veränderungen in der Belastung mit PFAS** auf, in denen sich auch die Auswirkungen früherer regulatorischer Aktivitäten widerspiegeln. Die Ergebnisse dieser Studie bilden eine wissenschaftliche Basis für zukünftige regulatorische Aktivitäten hinsichtlich PFAS, auf nationaler ebenso wie auf europäischer Ebene.

Überblick

FLUORBANK hat das Ausmaß der **PFAS-Kontamination der Umwelt mit einem Fokus auf Wildtiere für den Zeitraum der 1980er Jahre bis in das Jahr 2020** umfassend erfasst. Zu diesem Zweck wurde eine **Kombination verschiedener analytischer Methoden** eingesetzt:

- ▶ Quantitative Analyse einer sehr großen Zahl an PFAS verschiedenster physiko-chemischer Eigenschaften mithilfe validierter Methoden mit höchster Sensitivität und Selektivität (LC-MS/MS).
- ▶ Screening für PFAS mittels Flüssigchromatographie und hochauflösender Massenspektrometrie (LC-HRMS) mit der Möglichkeit der späteren, retrospektiven Datenanalyse.
- ▶ Quantifizierung der Gesamtheit von PFAS, die sich durch Oxidation in PFCA überführen lassen (TOP Assay).
- ▶ Non-target Screening für bisher unbekannte PFAS mit LC-HRMS und mit ultrahoch auflösender Massenspektrometrie (FTICR-MS).

Mit diesen Methoden wurden **Proben der Umweltprobenbank des Bundes (UPB)** untersucht, aber auch weitere Proben anderer Wildtiere und aus anderen Habitaten, die von Behörden und Forschungsinstituten bereitgestellt wurden.

FLUORBANK hat sich auf Biota-Proben fokussiert und dabei Pflanzen (Nadeln, Blätter; Algen) und Tierproben (Muskelfleisch, Leber, Eier, Muscheln, Lungengewebe) verschiedener Trophiestufen untersucht. Diese Arbeiten schlossen Spitzenprädatoren (Fische, Vögel, Säugetiere) aus terrestrische, fluvialen und küstennahen Habitaten ein. Ergänzend wurden Oberböden und suspendiertes Material aus Flüssen untersucht.

Ein Teil der Projektergebnisse wurde in zwei **wissenschaftlichen Publikationen** veröffentlicht und fanden Eingang in zwei Dissertationsschriften. Die quantitativen Daten zur PFAS-Belastung der Proben der Umweltprobenbank wurden in der **zugehörigen Datenbank** eingepflegt und sind dauerhaft öffentlich zugänglich.

FLUORBANK hat ausserdem in November 2021 einen Workshop mit dem Titel **“PFAS-Analytik für die Umweltüberwachung: Neue Anforderungen, Erfahrungen aus der Praxis, Erkenntnisse aus der Forschung”** am Helmholtz-Zentrum für Umweltforschung in Leipzig organisiert, mit aktiver Beteiligung von Vertretern aus Forschungseinrichtungen und Behörden. Dabei wurden Ergebnisse des Vorhabens FLUORBANK präsentiert, gegenwärtige Herausforderungen in der Analytik von PFAS und in deren Risikobewertung diskutiert und aktuelle Trends in der europäischen Regulation zu PFAS vorgestellt.

Ergebnisse und Diskussion

Monitoring von Proben der Umweltprobenbank

Insgesamt wurden in FLUORBANK etwa 120 Proben der Umweltprobenbank des Bundes aus den Jahren 1980 – 2020 auf 69 verschiedene PFAS quantitativ untersucht. Diese quantitative Target-Analytik wurde ergänzt durch die Anwendung eines modifizierten TOP-Assays, der auch die (ultra)kurzkettigen PFCA als Reaktionsprodukte mit erfasst. Mit diesem Monitoring wurde der bisher umfassendste einheitliche Datensatz zur PFAS-Belastung von Wildtieren in Deutschland erzeugt.

Von den 69 analysierten PFAS wurden 36 zumindest einmal in den Proben detektiert. Ein detaillierter Vergleich der PFAS-Belastung wurde für sieben Wildtier-Spezies durchgeführt (Silbermöve, Aalmutter-Filet, Miesmuschel, Brassenleber und -filet, Dreikantmuschel und Reh-Leber) sowie für suspendiertes Material und Oberboden.

In den Wildtieren wurden die höchsten Gesamtgehalte (Σ PFAS) in Brassenleber gefunden ($121 \mu\text{g kg}^{-1}$), gefolgt von Silbermöven-Eiern ($30 \mu\text{g kg}^{-1}$) und Muskelfleisch von Brassen ($16 \mu\text{g kg}^{-1}$). In

diesen drei Probenarten wird die PFAS-Belastung von PFOS dominiert (72 % für Brassen-Leber), gefolgt von C8-C14 PFCA. Aalmutter-Filet, Miesmuschel und Dreikantmuschel zeigten deutlich geringere Gesamtbelastungen an PFAS von 1 – 4 $\mu\text{g kg}^{-1}$ sowie stärkere Unterschiede im Belastungsmuster.

Für diesen Probensatz ergab der TOP-Assay, der einen großen Teil der mit der Einzelstoff-Analytik nicht erfassten PFAS summarisch anzeigen kann, keine signifikanten Beiträge unbekannter Vorläuferverbindungen. Dies galt jedoch nicht für die Brassen; hier ergab sich ein deutlicher Zuwachs an kurzkettigen PFCA.

Die Faktoren, die den Grad und die Art der PFAS-Belastung in den verschiedenen, mehr als 20 Jahre abdeckenden Proben der Umweltprobenbank bestimmen, werden weiter unten diskutiert. Alle Einzeldaten sind in der zugehörigen Datenbank hinterlegt und öffentlich zugänglich. Die weitere detailliertere Betrachtung der PFAS-Belastungen konzentrierte sich auf die Proben der Wildtiere, weil diese grundsätzlich höher ausfiel als die von suspendiertem Material, Oberböden oder Pflanzen.

Zeitliche Veränderungen

Im Rahmen von FLUORBANK wurden zeitliche Trends der PFAS-Belastung von den 1980er Jahren bis 2020 erfasst und hier insbesondere Eier von Silbermöven an der Nordsee (Mellum, 1988 – 2020), Leber von Brassen aus dem Rhein (Koblenz; 1996 – 2020) und Dreikantmuschel aus der Elbe (Blankenese, 1995 – 2018) mit höherer Zeitauflösung untersucht.

Im Mittel wurden in Silbermöveneiern, Brassenleber und Dreikantmuscheln 24, 23 bzw. 13 PFAS detektiert, in einzelnen Proben sogar etwas höhere Anzahlen (30, 28 und 19 PFAS in Proben aus 2002, 1996 und 2007). Die Gesamtkonzentration der quantifizierten PFAS betrug 10 bis 1000 $\mu\text{g F kg}^{-1}$ FG für Dreikantmuschel, Silbermöveneiern, Brassenleber.

Insgesamt wurden in diesen drei Probenarten 45 PFAS zumindest einmal detektiert. Dabei wurden die Ersatzstoffe 8:2 Cl-PFESA (Brasse) und DONA (Silbermöveeier, Brasse) nur in einzelnen Proben gefunden. PFCA und PFSA dominierten die PFAS-Belastung in allen drei Probenarten.

Im zeitlichen Verlauf zeigte sich eine Abnahme der Gesamtbelastung mit PFAS sowohl in den Eiern der Silbermöve als auch in den Lebern der Brassen. Dieser Rückgang der PFAS-Belastung in den benthischen Nahrungsketten beider Habitats, Küstenraum und Flüsse, bezeugt mutmaßlich die positiven Auswirkungen der zunächst freiwilligen und dann regulatorisch erzwungenen Veränderungen in der PFAS-Verwendung.

Trotz dieses Rückgangs der PFAS-Belastung von etwa 4%/Jahr über den Untersuchungszeitraum blieb die PFOS-Belastung hoch und trug auch 2020 noch mehr als 60% zur Gesamtbelastung mit PFAS bei. Die C10 – C14 PFCA zeigten weniger einheitliche Trends: in den Eiern der Silbermöve und den Lebern der Brassen stiegen die Gehalte bis zum Zeitraum 2010 – 2015 an; Im Anschluss sanken sie für einige, aber nicht alle Vertreter dieser Gruppe.

Der zeitliche Verlauf für die weniger belasteten Dreikantmuscheln unterschied sich deutlich: hier war kein Rückgang der Gesamt-Belastung festzustellen, sondern vielmehr eine Zunahme seit etwa 1990.

Der TOP-Assay erwies sich als nützlich zur Erfassung der Belastung mit unbekanntem sog. Vorläufersubstanzen. In Brassenleber und Dreikantmuschel erwies sich, dass solche Vorläufersubstanzen signifikant zur PFAS-Belastung beitragen (im Mittel 27 % und 39 %).

Für die zu den ultrakurzkettigen PFAS zählende Trifluoressigsäure zeigte sich ein steigender Gehalt in Dreikantmuschel und herring gull eggs.

PFAS in Nahrungsnetzen

In einer weiteren umfassenden Untersuchung wurden die PFAS-Konzentrationen und Belastungsmuster für 14 Arten von Säugern und Vögeln aus verschiedensten Regionen Deutschlands ermittelt. Darunter waren Herbiphore, Omniphore und Carniphore unterschiedlicher Habitate (terrestrisch, semi-aquatisch, marin) und unterschiedliche Körpergewebe (Lebern, Muskelfleisch).

Dabei zeigte das Muskelfleisch durchgängig niedrigere Belastungen als die zugehörigen Lebern. Die PFAS-Gesamtbelastung der Lebern nahm in der folgenden Reihenfolge ab: semi-aquatische Carniphore ($1300 \mu\text{g kg}^{-1}$) > marine Carniphore ($80 - 300 \mu\text{g kg}^{-1}$) > terrestrische Omniphore ($120 \mu\text{g kg}^{-1}$) > terrestrische Carniphore ($40 \mu\text{g kg}^{-1}$) > terrestrische Herbiphore ($20 - 40 \mu\text{g kg}^{-1}$) > semi-aquatische Omniphore/Herbiphore ($20 \mu\text{g kg}^{-1}$). Diese Abnahme ergibt sich aus der Zunahme starker proteinophiler/hydrophober langkettiger PFAS in den jeweiligen Nahrungsketten.

Neben der Belastungshöhe variierte auch das Belastungsmuster der PFAS in den Lebern der unterschiedlichen Spezies. In Carniphoren dominierte PFOS (67–95 %), gefolgt von langkettigen PFCAs ($C \geq 8$); in Herbiphoren hingegen war TFA die dominierende PFAS-Verbindung. Neuere Ersatzstoffe wurden nur sporadisch und in Tieren höherer Trophiestufen gefunden (Wildschwein, Otter, Kormoran) und auch nur in vergleichsweise niedrigen Konzentrationen.

In diesem Teil der Untersuchungen zeigte der TOP-Assay generell ein sehr niedriges Bildungspotential von PFCA in den Leber-Proben. Dies kann daran liegen, dass in den Lebern mit ihrem hohen metabolischen Potential ein Großteil der Vorläufer bereits umgesetzt war.

Zusammenhang zwischen der PFAS-Belastung von Umwelt und Wildtieren

Im Vorhaben FLUORBANK wurde auch geprüft, ob das Biomonitoring mit Wildtieren dazu dienen könnte, sogenannte Hot-Spots der PFAS-Belastung von Böden zu lokalisieren. Von diesen Hot-Spots sind mutmaßlich sehr viele noch unentdeckt.

Für diesen Zweck wurde die PFAS-Belastung von Wildschweinen aus verschiedenen Untersuchungsgebieten mit unterschiedlicher Belastungsgeschichte verglichen: zwei Hot-Spots, eine kontaminierte landwirtschaftliche Fläche (PS) und ein Gebiet mit industrieller Emission von PFAS (IE), und zusätzlich eine Region mit ländlicher Hintergrundkontamination (BC).

Die Lebern der Wildschweine der beiden kontaminierten Standorte zeigten klar erhöhte PFAS-Gehalte (480 und $960 \mu\text{g kg}^{-1}$) im Vergleich zur Hintergrundbelastung von $120 \mu\text{g kg}^{-1}$. Nur an einem der kontaminierten Standorte (PS) war PFOS die dominierende Komponente wie bei der Hintergrundbelastung (BC) (66 – 93 % der Gesamtbelastung). Am Industriestandort IE hingegen dominierte PFOA (69 % der Gesamtbelastung) in der Wildschweinleber, während der Gehalt an PFOS am unteren Ende der für die Hintergrundbelastung (BC) gefundenen Werte lag. Der Einfluss des Industriestandorts (IE) wurde auch deutlich am Auftreten der Ersatzstoffe HFPO-DA und DONA, die in den Wildschweinlebern von den anderen Standorten nicht gefunden wurden. Am zweiten kontaminierten Standort (PS) wurden im TOP-Assay kurzkettige PFCAs gebildet.

Damit erscheint ein Biomonitoring zur Erfassung kontaminierter Standorte mittels der Lebern von Wildschweinen aussichtsreich. Die Umweltbelastung durch (ultra)kurzkettige PFAS wird besser aus der Belastung aquatischer Spezies oder herbiphorer terrestrischer Arten abzulesen ist.

Gesundheitliche Risikobewertung

Für die untersuchten Brassen wurden die zulässigen Höchstgehalte für PFOS und für die PFAS₄ in den meisten Proben überschritten, zudem in einigen Fällen auch der Höchstgehalt für PFOA. Der Verzehr von Wildschweinleber würde erheblich zur PFAS-Belastung über die Nahrung beitragen und es rechnerisch zu Überschreitungen der gesundheitlich zulässigen Aufnahmemenge (tolerable

weekly intake, TWI) kommen. Zwar hat FLUORBANK auch in herbiphoren Wildtieren und in Fisch aus der Antarktis PFAS nachgewiesen, jedoch in Konzentrationen deutlich unterhalb der zulässigen Höchstgehalte. In den terrestrischen herbiphoren Wildtieren dominieren (ultra)kurzkettige PFAS, vor allem Trifluoressigsäure, die bisher nicht in die gesundheitliche Risikobewertung einbezogen sind.

Suspect-Screening und massenspektrometrisches Datenarchiv

Neben den quantitativen Analysen für eine sehr große Anzahl an PFAS, die als Standards verfügbar waren, wurden in FLUORBANK auch Methoden für das Suspect-Screening auf PFAS in Biota fortentwickelt. Unter anderem wurde ein neues Vorgehen entwickelt, das Analysen mit Flüssigchromatographie und hochauflösender Massenspektrometrie (LC-HRMS) verknüpft mit Analysen mit einem Fourier Transform Ion-Cyclotron-Resonance Massenspektrometer (FTICR-MS) mit Direktinjektion.

Diese neue Vorgehensweise wurde anschließend exemplarisch auf vier Proben von Brassenleber angewendet, die einen hohen Anteil an unerklärter PFAS-Belastung aufwiesen. In diesen Analysen wurde eine größere Anzahl an zuvor nicht detektierten PFAS gefunden, darunter verschiedene Vorläufer-Verbindungen und Ersatzstoffe, sowie von den altbekannten PFAS abzuleitenden Verbindungen mit Seitenketten, H- bzw. Cl-Substitution oder mit Struktureinheiten wie Doppelbindungen oder alicyclischen Gruppen bzw. nicht-fluorierten Kopfgruppen. Nicht für alle diese PFAS konnten Strukturvorschläge erarbeitet werden. Eine vollständige Identifizierung hätte, ebenso wie eine Quantifizierung, die Verfügbarkeit entsprechender Referenzverbindungen erfordert.

Die komplexe Probenmatrix der Biotaprobe und die vergleichsweise niedrige Belastung mit unbekanntem PFAS der meisten untersuchten Proben erwies sich als eine Herausforderung für die Suche nach und die Identifizierung von zuvor nicht detektierten PFAS. Entsprechende Screening-Methoden bedürfen weiterer Verbesserung.

In diesem Arbeitspaket von FLUORBANK wurden schließlich 249 Proben, Biota, ebenso wie suspendiertes Material und Oberboden mit LC-HRMS im positiven und negativen Modus analysiert. Diese Daten werden am UFZ für retrospektive Analysen für einen Zeitraum von 5 Jahren zur Verfügung gehalten.

Schlussfolgerungen

Das Vorhaben FLUORBANK hat den bisher umfassendsten Datensatz zur PFAS-Belastung von Nahrungsnetzen in Deutschland erarbeitet, sowohl hinsichtlich der Anzahl an quantifizierten PFAS (58 PFAS) als auch der Diversität der Proben (fünf Pflanzen-Arten, 28 Tierarten mit zusammen 43 verschiedenen Probentypen) unterschiedlicher Trophiestufen aus terrestrischen, aquatischen und marinen Habitaten in Deutschland, und für einen Zeitraum von den 1980er Jahren bis 2020. Proben suspendierten Materials und von Oberböden waren ebenfalls eingeschlossen. Dieser Datensatz ist nun öffentlich zugänglich und für Forschungszwecke und regulatorische Aktivitäten nutzbar.

Dieser Datensatz zeigt auf:

- ▶ Neben standortspezifischen Einflüssen ist die PFAS-Belastung von Wildtieren vor allem von ihrer Trophiestufe (herbiphor, omniphor, carniphor) und ihrem Habitat (marin, aquatisch, terrestrisch) bestimmt.
- ▶ Die zeitlichen Veränderungen der PFAS-Belastung von Wildtieren im Zeitraum von den 1980er Jahren bis 2020 widerspiegeln den Ausstieg aus der PFOS-Nutzung in den frühen 2000er

Jahren; seither ist für viele der untersuchten Spezies und Habitate eine Abnahme der PFOS-Belastung sichtbar. Dennoch bleibt PFOS weiterhin die Umwelt stark belastende PFAS-Verbindung und dominiert in den meisten der untersuchten Spezies auch heute noch die Gesamtbelastung.

- ▶ Darüber hinaus tragen bekannte und unbekannte C8-Vorläuferverbindungen merklich zur PFAS-Belastung vieler der untersuchten Spezies bei. Auch wenn deren Konzentrationsniveau im Vergleich zu PFOS noch niedrig erscheint, ist ein ansteigender Trend erkennbar, der sowohl für die Umweltbelastung als auch für die Nahrungsmittelproduktion relevant werden kann.
- ▶ Das Biomonitoring mit Dreikantmuscheln zeigt deutlich ansteigende Konzentrationen für Trifluoressigsäure und Vorläufer anderer kruzettiger PFAS im aquatischen System seit 1995. Dieses bewirkt insgesamt steigende PFAS-Belastungen für Dreikantmuscheln.
- ▶ Von den Probenarten der Umweltprobenbank, die intensiv untersucht wurden, erwiesen sich die Eier der Silbermöven und die Lebern der Brassen als gut geeignet zum Erfassen langfristiger Veränderungen der Umweltbelastung aquatischer und mariner Systeme mit den PFAS-Verbindungen, die sich entlang der Nahrungsketten anreichern und die auch für die Humangesundheit relevant sind. Tierarten niedrigerer Trophiestufen (z.B. Reh, Dreikantmuschel) scheinen besser geeignet, spezifisch die Belastung terrestrischer und aquatischer Kompartimente mit (ultra)kurzkettigen PFAS zu erfassen. Erhöhte PFAS-Kontaminationen von Oberböden (Hot-Spots) könnten im Biomonitoring anhand der Lebern dort lebender Wildschweine lokalisierbar sein.
- ▶ Das Suspect-Screening zur Erfassung bisher nicht registrierter PFAS-Verbindungen in Biota mittels LC-HRMS zeigt das Vorhandensein einer noch größeren Vielfalt an PFAS, als sie durch die Target-Analysen erfasst wurden. Jedoch erschwert die hohe Komplexität der Probenmatrix die Detektion und Identifizierung zuvor nicht bekannter PFAS in Biota, wenn deren Gehalte eher niedrig sind. Zusammen mit geeigneten und stark automatisierten Auswerteprozeduren kann ein PFAS-Screening aber breiteren Einblick in die Belastung von Biota erlauben. Die finale Bestätigung von Befunden ebenso wie die Ermittlung ihrer quantitativen Bedeutung erfordert aber weiterhin die Verfügbarkeit der entsprechenden Referenzsubstanzen.

1 Introduction

1.1 Per- and Polyfluoroalkyl Substances in the Environment

1.1.1 General

Per- and polyfluoroalkyl substances (PFAS) are anthropogenic, highly fluorinated aliphatic compounds, differing in their carbon chain length and functional groups (Buck et al. 2011). Following the latest definition of the Organisation for Economic Co-operation and Development (OECD), PFAS contain at least one perfluorinated methyl group ($-CF_3$) or perfluorinated methylene group ($-CF_2-$) (OECD 2021). Based on this definition, the PFAS group covers more than six million individual substances (PubChem 2022); only a much smaller number of these, however, is commercially produced. Those PFAS bearing no carbon-hydrogen bond are called perfluorinated alkyl substances, while all others are called polyfluorinated alkyl substances.

Their chemical structure and the extremely strong and stable C–F bond render PFAS chemicals with unique properties (high thermal/chemical stability, dirt-/water-/fat-repellence), having led to a broad range of industrial applications since the 1950s (Buck et al. 2011). The strength of the C–F bond, however, also makes perfluorinated alkyl substances to resist to microbial mineralisation, photooxidation and hydrolysis (Sznajder-Katarzyńska et al. 2019).

Their persistence, in combination with the extensive use of PFAS in many different industrial applications and products, has led to a widespread, diffuse contamination of the environment. PFAS have been found in all environmental compartments worldwide and with some compounds being subject to (long-range) atmospheric transport, PFAS have been reported even in remote environments such as the Arctic and Antarctica (Houde et al. 2006, Lee and Mabury 2014, Kotthoff et al. 2020, Cousins et al. 2022, Guckert et al. 2022). Certain PFAS have toxic properties and can biomagnify in food webs, posing a toxicological risk to wildlife and humans (Giesy and Kannan 2001, Lau et al. 2004, Müller et al. 2011). Additionally, low molecular size PFAS such as trifluoroacetic acid (TFA) have received attention as contaminants in drinking water (Scheurer et al. 2017).

Hence, many PFAS are considered persistent, bioaccumulative and toxic (PBT) or very persistent and very bioaccumulative (vPvB) whereas the more polar, low molecular weight PFAS are considered persistent, mobile and toxic (PMT) or very persistent and very mobile (vPvM).

1.1.2 Regulation

The persistence and bioaccumulative properties of some PFAS led to regulatory actions, first on long chain perfluoroalkyl sulfonic acids (PFASs, with a number of carbons (nC) ≥ 6) and perfluoroalkyl carboxylic acids (PFCAs, $nC \geq 8$) and their corresponding anions (Buck et al. 2011, UNEP 2022). In addition, their precursor compounds were included, i.e. compounds that degrade in the environment to these persistent PFCAs and PFASs. These restricted PFAS are **often called legacy PFAS today**.

Meanwhile, two of the first substitutes of legacy PFAS, hexafluoropropylene oxide dimer acid (HFPO-DA, GenX) and perfluorobutane sulfonic acid (PFBS), were classified as substances of very high concern (SVHCs) under REACH in 2019 and 2020. Against this background and similar examples of regrettable substitution, the new PFAS are under scrutiny of being similarly concerning as the persistent legacy PFAS.

Perfluorooctanesulfonic acid (PFOS), perfluorooctanoic acid (PFOA), perfluorohexanesulfonic acid (PFHxS), their derivatives, salts and related compounds are listed in Annex I to the international

Stockholm Convention on Persistent and Organic Pollutants (POPs) to prohibit their production, commercialization and use (Stockholm Convention). Further PFAS such as the long-chain (LC) PFCAs (C9-C21) are being considered for inclusion therein. In the European Union PFOS/PFOA and their derivatives have already been restricted under the EU's POPs regulation (EC 2020).

Apart from that, chemical management of PFAS remains challenging. Not only is there debate on how to define the class of PFAS (OECD, EPA, EU...) within the different regulations – e. g. whether or not to include trifluoroacetic acid and its precursors – also the effect of regulatory and voluntary measures which were taken so far can retrospectively be considered regrettable.

This is one of the reasons for the submission of a proposal for restriction of all PFAS under REACH, which was submitted by five national authorities of the EU to the European Chemicals Agency (ECHA) in 2022. After its publication and the end of the consultation period in September 2023 ECHA's scientific committees for risk assessment (RAC) and for socio-economic analysis (SEAC) are presently evaluating the restriction proposal and the comments received.

Besides that, the ongoing emergence of reports on toxic effects of PFAS has led to a reevaluation of the health risks of PFAS (CONTAM et al. 2020), the consequence of a greatly reduced tolerable weekly intake (TWI) of 4.4 ng kg⁻¹ body weight for PFOA, PFNA, PFHxS and PFOS. As one of the consequences, the future limits for PFAS in drinking water was reduce to 0.1 µg L⁻¹ for the sum of 20 PFAS (EU 2020).

1.1.3 PFAS Market

Since the 1980s the PFAS market, first, shifted from C8 chemistry to homologues of the same chemical classes but shorter chain-length and, second, from perfluorinated alkyl chains to derivatives – e. g. with intermittent ether linkages, such as perfluoroalkyl ether acids (e. g. 4,8-dioxa-3H-perfluorononanoic acid (DONA) and HFPO-DA) or short chain PFAS (Ateia et al. 2019, Munoz et al. 2019, Zhang et al. 2019).

Generally, the PFAS market has become broader over the last decades and more dynamic, as it is constantly influenced by new chemical regulation, in Europe, the US or worldwide, by substitution of the regulated substances and subsequent evaluation of newly introduced substitutes (Glüge et al. 2020). However, information about fate, transport, exposure, toxicity and bioaccumulation of more recently introduced PFAS in the environment are still scarce (Wang et al. 2017, Ateia et al. 2019). Certain alternative PFAS were already detected in biotic and abiotic matrices and also their persistence, mobility and potential for long-range transport has been proven (Munoz et al. 2019). Furthermore, short chain perfluoroalkyl acids (PFAAs) have recently been shown to accumulate in plants and agricultural crops, leading to a novel route of exposure for humans and animals (Lesmeister et al. 2021).

1.1.4 Analysis of PFAS

The sheer number of PFAS in commerce – more than 4000 substances had been registered for commercial use already in 2018 (OECD 2018) - challenges the comprehensive quantitative analysis of PFAS on the level of single substances in environmental samples. Reference standards would have to be available; and quantitative analytical methods for all PFAS with very diverse physico-chemical properties for all relevant matrices would be needed. Both is not the case.

Quantitative analytical methods at trace level are well established for the so-called legacy PFAS and selected polyfluorinated precursor compounds. With PFAS regulation in place and owing to the changes in the PFAS market outlined above, however, legacy PFAS may become less relevant and precursors and substitutes may increase in concentration. Those compounds are, however, less frequently included in quantitative analytical methods.

In recent years, methods for the suspect screening and the non-target screening for PFAS have received increasing attention (Liu et al. 2019a, Bugsel et al. 2023). These approaches rely on comprehensive lists of suspects and on the high mass accuracy of high-resolution mass spectrometers.

Such methods aiming at detecting, identifying and, ultimately, quantifying large numbers of PFAS compounds at the molecular level can be complemented by methods determining the sum concentration of a certain group of PFAS compounds.

One such approach is the Total Oxidizable Precursor” (TOP) assay (Houtz and Sedlak 2012), which aims at detecting all PFAS that can be transformed into PFCA by oxidation. The TOP assay covers many known and unknown precursors; an increasing number of studies employed this approach (Janda et al. 2019, Simonnet-Laprade et al. 2019, Zhang et al. 2019, Göckener et al. 2021).

Other sum parameters determining the total concentration of organically bound fluorine, as extractable organofluorine (EOF) from solid materials or as adsorbable organofluorine (AOF) from aqueous samples (Wagner et al. 2013, Kärrman et al. 2021). Note that not all organically bound fluorine may stem from PFAS.

1.1.5 PFAS-Monitoring

As PFAS can persist in the environment for decades, the contamination found today is also a legacy of a production boom in PFAS from the early 70s to the early 2000s.

Today, an increasing number of PFAS is found worldwide, in soil (Lee and Mabury 2014, Washington et al. 2019), surface waters (Saito et al. 2003, Joeris et al. 2022) and seawater (Yamashita et al. 2005, Muir and Miaz 2021), in animal tissues and in environmental compartments worldwide (Giesy and Kannan 2001, Houde et al. 2006, Cousins et al. 2022, Guckert et al. 2022, Huang et al. 2022). This worldwide level of PFAS is also called **background concentration**.

Additionally, the production, usage and disposal of PFAS often results in **contamination hot spots** from point sources, e. g. near manufacturing facilities of fluoropolymer, textile or paper industry, on biosolid-amended fields or near military bases and airports where aqueous film forming foams (AFFFs) were used (Buck et al. 2011, Costello and Lee 2020, De Silva et al. 2021).

Food is the main **exposure pathway of PFAS** for mammalian and bird species (Giesy and Kannan 2001, Falk et al. 2012). Previous studies of PFAS in wildlife mainly investigated species that are in contact with each other (bioaccumulation along one food chain) and/or originate from the same ecosystem (e. g. terrestrial, marine, limnic), rather than comparing different environmental compartments (Kannan et al. 2005, Müller et al. 2011, Chen et al. 2021, Huang et al. 2022).

Furthermore, most studies on biota focused on legacy PFAS (PFASs and PFCAs) and selected polyfluorinated precursor compounds, covering only a fraction of those PFAS which can be captured by target analysis. Therefore, bioaccumulation of especially long-chain PFAAs along specific food chains has been reported, while information about **novel PFAS** (e. g. ultrashort-chain PFCAs, substitutes) and **information on PFAS levels in different ecosystems is lacking** (Kannan et al. 2005, Müller et al. 2011, Huang et al. 2022).

The existing knowledge on PFAS contamination in specific environmental compartments, individual animals, species, populations, and food webs is frequently generated with very different methodologies, for extraction, clean-up and analysis. As a consequence, the results of these **individual studies can only be compared to a limited degree**.

1.2 Motivation

The German Environmental Specimen Bank (ESB) provides samples that were collected and archived systematically, partially at sampling sites with the same methods for decades (<https://www.umweltprobenbank.de/en/documents>). This allows for retrospective analyses of all major environmental matrices, including soil and sediments, air, plants and biota. Moreover, the ESB covers different ecosystems, such as forest, agriculture, and rivers.

Therefore, contamination data of samples of the ESB should reflect the contamination level at the time of sampling, allowing to learn about long term temporal trends of environmental contamination. Thus, time-series of samples may also show the benefit of past regulatory action, by decreasing contamination levels for a regulated chemical. They may also outline the need for future regulatory activities on contaminants with increasing trends. Many samples of the ESB have been analysed for the legacy PFAS, previously (Kotthoff et al. 2020)).

However, data on short-chain and ultra-short chain PFAS were largely missing as well as information on precursor PFAS and substitutes for long-chain PFAS, such as various per- and polyfluorinated ethers. Furthermore, no balances have been possible to which extent the PFCA and PFSA yet analysed account for the organically bound fluorine in the different sample compartments.

A consistent set of such data, and the knowledge gathered from it on long term temporal trends of legacy PFAS as well as of substitutes, as well as on their level of transfer in different food webs would also inform chemicals regulation - about the benefit of past actions as well as of the need for future actions.

1.3 Study Objectives

The project FLUORBANK aimed at a more comprehensive characterization of the level of contamination by PFAS in Germany in environmental media and biota living therein.

For this purpose, a **combination of innovative analytical methods** was applied. These methods comprise four different approaches:

- ▶ Quantitative analysis of a broad range of PFAS with diverse physico-chemical properties employing validated methods that provide highest selectivity and sensitivity (liquid chromatography tandem mass spectrometry (LC-MS/MS)).
- ▶ PFAS screening by liquid chromatography-high resolution-mass spectrometry (LC-HRMS) with the option to perform retrospective data search also after the completion of this project.
- ▶ Quantification of the totality of PFAS that form PFCA with the total oxidizable precursor (TOP) assay, including (unknown) precursor PFAS.
- ▶ Non-target screening for yet unknown PFAS by ultrahigh resolution-mass spectrometry (Fourier transform ion cyclotron resonance mass spectrometry (FTICR-MS)).

These methods were applied to **samples of the Environmental Specimen Bank** and to further samples provided by authorities from regional surveillance programs. These activities focus on biota samples, covering five plant species (needles, leaves, algae) as well as 28 animal species of different trophic level including top predators, among them fish, birds and mammals from terrestrial as well as riverine and coastal areas. (with 36 sample types, Table A 2 for details). Besides, also terrestrial soil and riverine suspended matter was included.

By analysing a broad range of samples for a large number of chemically diverse PFAS the project FLUORBANK also explored the contribution of the following groups of PFAS to the exposure of environmental compartments and biota:

- ▶ short-chain and ultra-short chain PFAS
- ▶ new substitutes of long-chain PFAS, i.e. polyfluorinated compounds
- ▶ precursor PFAS, that can be oxidised to PFCAs (TOP-assay)
- ▶ unknown PFAS, i.e. the difference between the quantified PFAS and the outcome of the TOP-assay.

FLUORBANK explored temporal trends as well as spatial differences in the PFAS contamination in Germany and determines the PFAS burden of a large set of biota samples living in these environmental compartments.

The results of this study are meant to provide a scientific basis to support the work of UBA on the European level with respect to the regulation of PFAS, considering persistence of PFAS as well as enrichment in food webs and the long-range transport potential.

1.4 Study Design

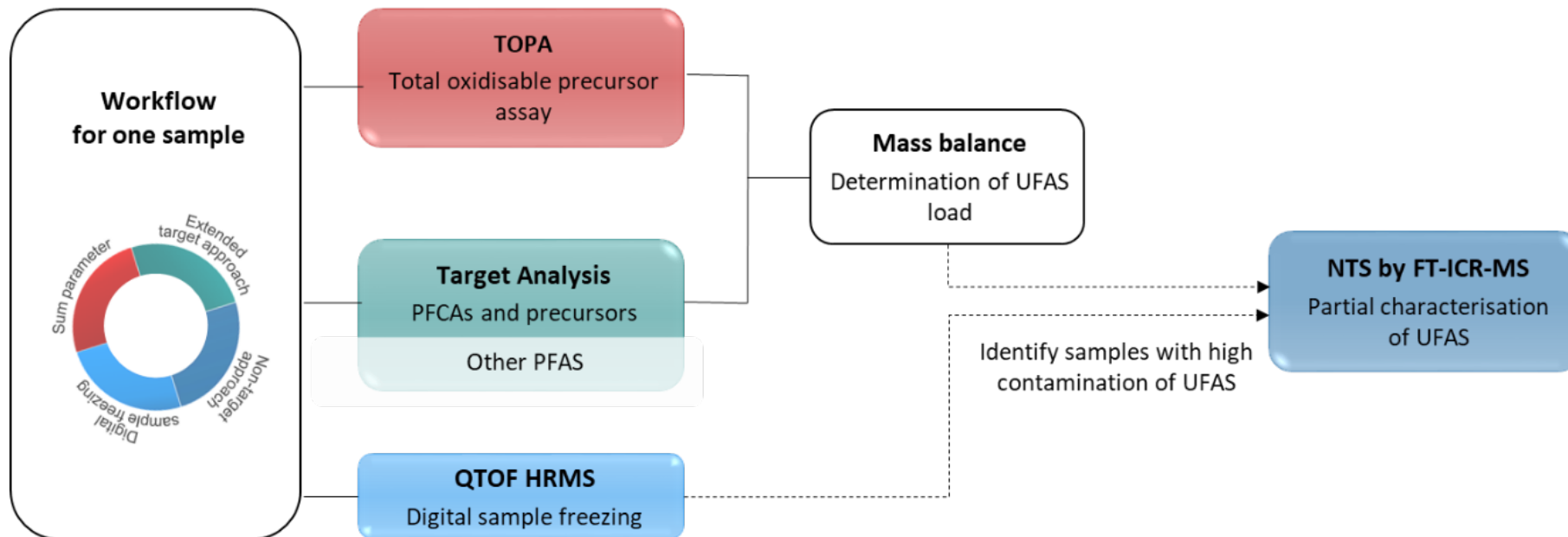
The project FLUORBANK was structured into six work packages

- ▶ Work package 1: Development of the analytical concept

Based on the expertise of UFZ and TZW and on literature knowledge, an analytical concept was developed in WP1 for FLUORBANK to fulfil the tasks in WP2, WP4 and WP5, with quantitative methods, screening methods and identification methods (Figure 1). This concept was developed in exchange with and upon agreement by UBA.

For the analysis of each sample, different analytical approaches were employed and combined in a mass balance of organically bound fluorine (Figure 1). In addition, LC-HRMS data was generated and archived in all-ion-fragmentation mode, which allows for retrospective data analyses. Based on the outcome of the mass balance, samples were selected for suspect screening.

Figure 1: Analytical Concept of FLUORBANK



PFCA: perfluorinated carboxylic acids; QTOF: quadrupole time of flight; HRMS: high resolution mass spectrometry; UFAS: unidentified PFAS; NTS: non target screening; FTICR MS: Fourier transform ion cyclotron resonance mass spectrometry.

Source: Own illustration, UFZ

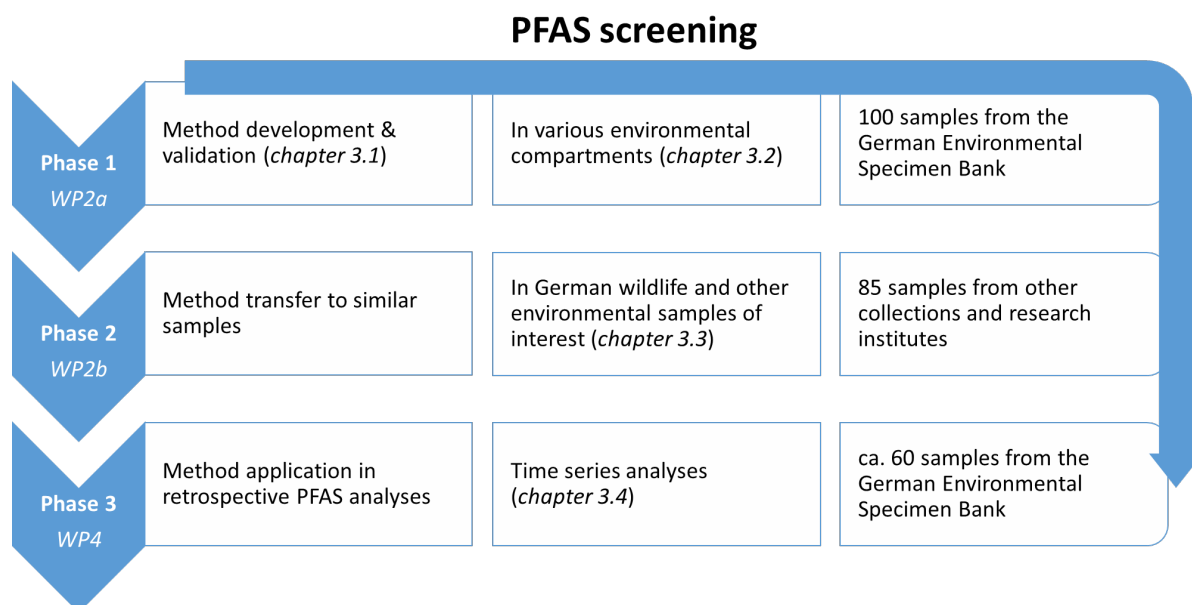
► Work package 2: Screening

This WP covered the major analytical activities foreseen for the application of the different analytical methods to samples of the ESB and of other sources.

The sample pool covered urbanised, less urbanised terrestrial ecosystems in forested, agrarian and riverine as well as coastal ecosystems. The biota included plants (needles, leaves, algae) as well as animals, of different trophic level including top predators (fish, birds, mammals). Therefore, terrestrial as well as aquatic food webs are considered. Only a small number of samples were obtained from recognised PFAS hotspots. Therefore, the majority of screening results are related to the local background contamination by PFAS.

The origin of the samples analysed in this and other work packages is illustrated in Figure 2.

Figure 2: Screening phases



Source: own illustration, UFZ.

► Work package 3: PFAS Workshop

The monitoring data were presented at a workshop and discussed with colleagues from authorities responsible for chemicals regulation and environmental and food control. Besides knowledge exchange, this workshop aimed at receiving recommendations for the ongoing work of FLUORBANK, taking into account recent development in science and regulation.

► Work package 4: Time series analyses for PFAS

Analyses of selected time-series of samples from the ESB were performed to discover temporal trends in PFAS contamination in relation to regulatory measures and market development.

► Work package 5: Additional PFAS analyses

Interpretation of the data gathered in the previous WPs led to new questions or novel hypotheses that required additional samples to be analysed. These activities increased the clarity of results and supported the final conclusions to be drawn (WP 6).

► Work package 6: Data analyses.

The data gathered in WP 2 – WP 5 were interpreted and the scientific results published. Data for the ESB samples were also made publicly available through the Umweltprobenbank des Bundes (UPB, <https://www.umweltprobenbank.de/en/documents>).

Data exploitation will specifically consider, but not be limited to, the following aspects:

- Behaviour in the environment and in aquatic food webs and possible sources of PFAS.
- Spatial differences and temporal trends in PFAS concentrations and in PFAS patterns.
- Importance of unknown PFAS in different environmental compartments and indications on their identity based on combining the findings of the different analytical approaches.
- Time series in the different environmental compartments are specifically exploited with respect to effects of previous PFAS regulation.
- Highly mobile PFAS of relevance as PMT substances with respect to REACH and the regulation in the water sector.

2 Materials and Methods

2.1 Chemicals Used

All reference standards and reagents were high purity grade as described in appendix A.1 and refer to the linear isomer. For quantification of 42 PFAS via LC-MS, reference standards were obtained for PFASs, PFCAs, precursors, substitutes and isotopically labelled standards (Table A 1). The precursors were fluorotelomer phosphate mono- and diesters (monoPAPs, diPAPs), fluorotelomer sulfonic acids (FTSAs) and perfluorooctane sulfonamides (PFOSAs) and their derivatives. The substitution compounds were chlorinated perfluoroalkyl ether sulfonic acids (Cl-PFESAs), a perfluoroalkyl mono- and di-ether carboxylic acid (PFECAs), a fluorotelomer sulfonamide amine oxide (FTNOs) and a fluorotelomer sulfonamidopropyl betaine (FTABs). In addition, 8 PFAS (class C) were analysed by gas chromatography mass spectrometry (GC-MS). These were fluorotelomer alcohols (FTOHs), fluorotelomer acrylates (FTACs) and fluorotelomer methacrylates (FTMACs). For additional 24 analytes, no reference standards were available. These PFAS were analysed qualitatively as part of method A and B and are listed in Table A 1.

2.2 Samples

Table A 2 gives an overview of the 43 sample types ranging from animal tissues over abiotic and plant materials. The table also explains the abbreviations of the different sample types used in the results section. An overview of all samples is available in the appendix (Table A 2).

2.2.1 Samples from the German Environmental Specimen Bank

2.2.1.1 Work Package 2a: Initial Screening

For initial screening, 100 environmental samples, including material for quality control duplicates, were obtained as annual composite samples from the German environmental specimen bank (ESB) for PFAS screening. In addition, pike perch reference material IRMM-427 (European Commission Joint Research Centre, Geel, Belgium), reference soil LUFA-2.4 (LUFA, Speyer, Germany), reference soil RefeSol 01-A-05 (Fraunhofer IME, Schmallenberg, Germany) and poplar leaves and pine tree needles, sampled in Leipzig and Dübener Heide in 1991 for the ESB, were used for calibration or quality control. Details of the samples are listed in Table A 3.

The majority of samples from the cryo-archive was sampled between 2017 and 2019 (95 samples) and chosen to investigate the current state of organofluorine contamination in as many environmental specimens as feasible. However, individual samples (16) date back until 1991 (poplar leaf). These older samples allow for comparison between different years or represent the most recent samples of the archive for specific matrices (2012 for bladder wrack and 2014 for soil collected in the Solling, a mountain range in Germany). The sampling sites of the selected ESB samples are spread across Germany and cover urban, forestry, agrarian and remote areas as well as coastal, terrestrial and limnic ecosystems.

2.2.1.2 Work Package 4: Trend Analyses

For (spatio-)temporal trend analyses, further samples were analysed. A pre-screening was performed for aquatic organisms (mostly zebra mussel and bream liver) from different sampling sites – sampled along River Elbe and Rhine in the years 2001 and 2018 (Table A 4). In few cases, an alternative year (2017) was used due to limited sample availability. Based on the results of the general initial screening and the spatiotemporal pre-screening, sampling sites and suitable sample types were selected. Altogether, three species from different origin within Germany were analysed:

(1) zebra mussel (*Dreissena polymorpha*) as a filter feeder in a benthic freshwater food web, in Blankenese (Elbe, 1995–2018), (2) common bream (*Abramis brama*) as a higher order consumer in a mainly benthic food web, in Koblenz (Rhine, 1996–2020) and (3) herring gull (*Larus argentatus*) as an opportunistic top predator in an intertidal food web at Island Mellum (North Sea, 1988–2020) (Figure 3).

Figure 3: Sampling sites of the three times series

Sampling sites of herring gull egg (*Larus argentatus*, LAE), common bream liver (*Abramis brama*, ABL) and zebra mussel soft body (*Dreissena polymorpha*, DPM).



Source: own illustration, UFZ.

2.2.1.3 Sample Preparation

Sampling and homogenisation of samples from the ESB followed standardised protocols of the ESB (<https://www.umweltprobenbank.de/de> and Table A 5). In general, the samples were frozen directly after sampling or shortly after, processed above liquid nitrogen in clean-air cabinets, cryo-milled, sub-divided into aliquots of 5–10 g and stored as wet-weight (ww) material at $-130\text{ }^{\circ}\text{C}$ in a cryo-archive. To keep manipulation of the sample matrix at minimum and analyte recovery high, freeze-drying was avoided. Therefore, all amounts and concentrations relate to ww in this study. An exception is suspended matter from rivers which was freeze-dried under controlled cool conditions. Details on the sampling sites can also be found on the web page of the ESB.

2.2.2 Samples from other Collections and Sampling Campaigns

In addition to the samples from the ESB, 85 environmental samples were obtained from various collections and institutes across Germany to broaden the sample spectrum with respect to

- ▶ the diversity of wildlife species
- ▶ the tissue type
- ▶ and the spatial distribution (including hot-spots).

Legacy PFAAs and many other PFAS bioaccumulate in liver at higher levels than in other types of tissue, which contain less protein. Therefore, this report focusses on liver samples for species comparison. Moreover, the tissue distribution between musculature and liver was studied for a subset of samples, that is three marine mammals and otter, and between lung and liver for cormorants. The specimens analysed in this study are both abiotic materials (suspended matter and soil), and animal tissues (liver, musculature, lung and bird's egg). When more than one tissue type was sampled, the same animals were dissected. A list of sample types and their corresponding Latin name can be found in the appendix (Table A 6).

The samples were taken between the Ammergau Alps in Bavaria and the German coast of the North and Baltic Sea with little to no overlap between the different sample types. Only in the area close to the industrial park in Gendorf, Bavaria, abiotic material (suspended matter and soil) was sampled in addition to biological material (wild boar and chub). Among all samples, two did not originate from Germany. The eider duck was from Denmark close to the German border and the emerald rockcod (Antarctica) was selected as a remote sampling site for fish comparison.

The samples were collected between 2015 and 2020 and stored at $-18\text{ }^{\circ}\text{C}$. The majority of specimens (73 %) was sampled after 2018. The samples from 2015 were considered only due to limitations in sample volume and pooled with more recent years for PFAS analysis.

Selected tissue samples were pooled to increase the representativeness for the given specimen type. The sample pools were defined by sex and age class and also by sampling area where appropriate (e.g. North or Baltic Sea or different federal state). Pooled liver and musculature samples consisted of three to five individuals and fish musculature samples of six to ten individuals.

2.2.2.1 Animal Tissues

Wild Boars

It should be noted that this study does neither aim to fully characterise the local concentrations nor to generalise them on a broader geographical scale. Livers from 50 wild boars were sampled by professional hunters in three German sampling areas in 2019 and 2020: (1) in Hügelsheim near Rastatt, Baden-Wuerttemberg, (2) in the direct surrounding of an industrial facility in southern Germany and (3) in a north-eastern region of Germany where research on the source of contamination revealed no prominent characteristics. The three sampling areas are located 300–600 km apart from each other. On request of the cooperating research units, areas 2 and 3 were anonymised. In the following, the latter source of contamination – as well as the sampling area – is referred to as background contamination (BC). Background contamination generally builds up in a diffuse way by a combination of several sources, pathways, events and distribution mechanisms such as formation from precursors, atmospheric deposition (Prevedouros et al. 2006, Björnsdotter et al. 2022), leaching from landfills (Knutsen et al. 2019), distribution via groundwater (Johnson et al. 2022) and plant uptake (Krippner et al. 2014). Areas 1 and 2 are, therefore, also affected by a background contamination. But more notably, they represent cases where the contamination can be attributed to a single major source.

Contamination in Hügelsheim (area 1), can be attributed to a particular historic case of contaminated paper sludges (hereafter called area PS) distributed on arable land (Brendel et al. 2018). Area PS is in the southwest of Germany and was presumably contaminated by PFAS-loaded paper sludges used repeatedly as compost on nearly 1000 ha fields for years. The PFAS in the paper sludges originate from their usage in fat and water-repellent paper and board food packaging as well as from printing inks (OECD 2020). In 2013, the contamination was discovered and the particular agricultural practices ceased. The paper sludge likely contained PFCAs and their

precursors, which were washed out and widely distributed in the local environment, including groundwater.

Sampling area 2 is contaminated by ongoing, long-lasting industrial emissions (hereafter called area IE). Exhaust air and wastewater from the local treatment facility as well as local entries from the ground of the fluoropolymer production facility contributed to contamination at the site and the surrounding environment. More specifically, PFOA and DONA were (are) emitted – the former being synthesised for over three decades until 2003 and the latter replacing it as a tentatively less problematic emulsifier in fluoropolymer production since 2008. While production rates increased, safety measures were developed to minimize the release of PFAS into the environment. The wild boar was shot 8 km downwind the industrial park.

Other Animals

Other terrestrial animal tissues include individual liver samples from three red deer (*Cervus elaphus*), three chamois (*Rupicapra rupicapra*) and nine European wildcats (*Felis silvestris*) and pool samples of liver from European hare (*Lepus europaeus*, n = 1), European beaver (*Castor fiber*, n = 4) and coypu (*Myocastor coypus*, n=4) as well as liver and musculature from Eurasian otter (*Lutra lutra*, both n = 2). Moreover, samples of four different bird species were obtained for PFAS screening: black grouse egg (*Tetrao tetris*, n = 1), great crested grebe egg (*Podiceps cristatus*, n = 2), common eider duck liver (*Somateria mollissima*, n = 1) and great cormorant (*Phalacrocorax carbo*) liver (n = 8) and lung (n = 2). One of the black grouse samples consisted of two eggs of an abandoned clutch of which one was rotten and contained underdeveloped offspring. The sample was sieved and treated like the other egg sample. Among the bird samples, three of the cormorant samples and the eider duck liver were pool samples.

Roach (*Rutilus rutilus*, n = 1) and European chub (*Squalius cephalus*, n = 3) were sampled in different Southern Germany rivers and Emerald rockcod (*Trematomus bernachii*, n = 1) at Terra Nova Bay, Antarctica. The sampling point of one of the European chubs was downstream the industrial park of area IE. Matching musculature and liver pool samples were obtained for seals and harbour porpoises (*Phocoena phocoena*, n = 2) from both North and Baltic Sea. The grey seals (*Halichoerus grypus*, n = 1) originated from the Baltic Sea whereas the harbour seals (*Phoca vitulina*, n = 1) samples originated from the North Sea. All biota samples from the aquatic environment refer to pool samples of at least five individuals.

2.2.2.2 Soil and Suspended Solids

Soil and suspended matter were sampled in area IE (both n=1), respectively. Another soil sample originated from arable land and a third one from an acre in a forest, both located close to a textile factory in Southern Germany. Suspended solids were also sampled in 2016 and 2019 in a Southern Germany river (n=5).

2.2.2.3 Sample Preparation and Pooling

The protocols of sample preparation were developed close to the model of the protocols from the German ESB for ease of method transfer. The samples were pooled and homogenised at the UFZ as described in Table A 6 of the appendix. Pool samples were obtained from equal weight proportions of the individual samples. Animal tissue was cut into small pieces (see Figure 4) and homogenised using a rotor stator disperser (ultra-turrax T25 from IKA Labortechnik, Staufen, equipped with an “S 25 N – 18 G – ST”). Eggs were defrosted, peeled if necessary and mixed manually by spatula. Sample material of suspended matter was freeze-dried and sieved to <2 mm. Also soil samples were sieved to <2 mm. Aliquots of approximately 10 g sample were filled into HDPE scintillation flasks or pressure lock bags for both analytical laboratories (UFZ and TZW).

Figure 4: Sample preparation of wild boar liver on dry ice

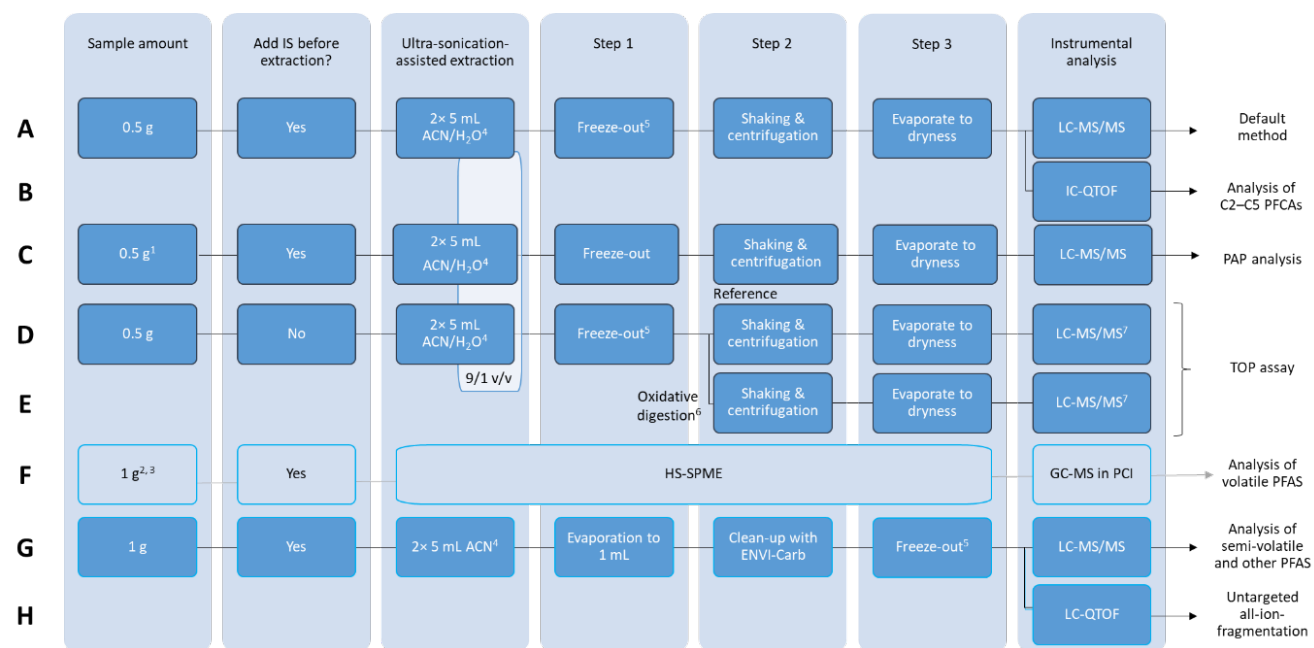
In preparation for homogenisation by the rotor stator disperser.



Source: own illustration, UFZ.

2.3 PFAS Screening for Targets and Oxidizable Precursors

Figure 5: Method overview



¹ In soil and SPM, PAP analysis was split into two methods. For analysis of diPAPs 0.5 g sample were extracted with MeOH and for analysis of monoPAPs 0.1 g with 7/3 MeOH/H₂O (v/v)

² Weigh-in adapted to density for constant filling volume

³ Animal tissue was not analysed since results of earthworm and literature suggest that volatile precursors are readily metabolised

⁴ Extraction in soil and SPM was carried out with 100 % MeOH. For the additional workflow of monoPAPs in soil and SPM, the extraction solvent was 7/3 MeOH/H₂O (v/v)

⁵ Freeze-out skipped for analysis in soil and SPM

⁶ Incubation for 20 h at 85 °C with K₂S₂O₈ and alkaline conditions

⁷ Extract divided and analysed separately by IC-QTOF for <C6 PFCAs.

Black frame: analyses at TZW; blue frame: analyses at UFZ. Dark blue background: LC-MS method; light blue background: GC-MS method. IS: internal standard; SPM: suspended matter; IC-QTOF: ion chromatography quadrupole time of flight mass spectrometry; PFCA: perfluorinated carboxylic acid; PAP: polyfluorinated alkyl phosphate; TOP assay: total oxidizable precursor assay; HS-SPME: headspace solid-phase-microextraction; GC-MS: gas chromatography mass spectrometry; PCI: positive chemical ionisation

Source: own illustration, UFZ.

Altogether, targeted methods were developed for 74 PFAS. For plants and abiotic solid sample materials, only the 66 PFAS of class A and B were analysed. For 19 target analytes, no reference standards were available at the beginning of the study. These PFAS were analysed qualitatively only. In addition, TFA was considered in the TOP assay. As three methods were applied for analysis the compounds are grouped accordingly in the list: 46 for method A, 16 for method B and eight for method C. The target analytes of method C (FTOHs, FTACs and FTMACs) are assumed to be readily eliminated in animals (Butt et al. 2010, Brandsma et al. 2011) and were thus not screened for in animal tissues except for earthworm.

The samples were analysed in two different laboratories by different LC-methods (summarised as methods A and B) and a GC-MS method (method C). For reasons of clarity, the principal method used in one lab for LC analysis is referred to as method A, while the analytical LC-method of the other lab is hereafter called method B. In short, basic PFAS target analysis was carried out by reversed-phase liquid chromatography tandem mass spectrometry (RP-LC-MS/MS) following the general extraction protocol of method A. For analysis of (ultra)short-chain PFAS (PFCAs C2–C5), the same extraction protocol was applied, but the analysis was carried out by ion chromatography quadrupole time-of-flight mass spectrometry (IC-QTOF-MS) for unequivocal determination of the PFAS. For analysis of fluorotelomer phosphate esters, the extraction and detection method were modified from the basic protocol of method A (e. g. different solvent and mobile phase). Method A also included the protocol and calculation of the TOP assay to quantify the formation potential of PFAS from their precursors. Method B – another RP-LC MS/MS method – was used for analysis of additional substitute compounds as well as for semi-volatile precursors (e. g. alkylated perfluorooctane sulfonamidoethanols (FOSEs)). For example, the extract was not evaporated to dryness to ensure good recovery rates. Table A 1 in the appendix shows how all target PFAS were distributed between the two laboratories. The protocols of solid-liquid extraction, clean-up and instrumental analysis are presented in appendices B.1. The cone voltages and collision energies were optimised for all analytes and are displayed in Table B 1 of the appendix together with the corresponding multiple-reaction monitoring (MRM) transitions. For qualitative analyses, the mass-to-charge ratios and compound-specific parameters were extrapolated from values of structurally similar reference standards (e. g. homologues of mono- and diPAPs).

2.4 Method Performance

For quantification, the isotope dilution approach was used. Where no corresponding mass-labelled reference standard was available, the internal standard approach was followed as indicated in Table A 1 (appendix). For LC-MS analyses, external calibration curves were analysed before and after the sample sequence to analyse instrumental drifts. For GC-MS analysis, matrix-matched calibrations were carried out in poplar tree leaves, pine needles and soil. All calibration curves consisted of at least six concentration levels.

The validation procedure for method A and B was based on extracts of seven different matrices (herring gull eggs, mussels, bream liver, top soil, suspended particular matter, beech leaves and bladder wrack). A reduced procedure, e. g. analysis of a reduced set of analytes or less replicates, was done for further six matrices (bream musculature, eelpout musculature, earthworm, roe deer liver, LUFA 2.4 (reference soil) and pine shoots). The extraction of spiked samples was done in triplicates for determining precision and apparent recovery, comparing the calculated concentrations corrected by internal standard (IS) to the theoretical spike levels. Precision was calculated as the relative standard deviation of the calculated concentrations. As no uncontaminated sample material was available, background concentrations were determined in sample material without spiking and considered in all calculations.

The daily method performance was investigated with method-specific reference materials (certified reference concentrations or known spiked concentrations, see Table 1).

Table 1: Reference materials used

Sample material	Corresponding reference material
Biological material	Pike perch IRMM-427 (PP); Poplar leaves from ESB (Leipzig 1991) spiked with 50 µL 20–100 ng mL ⁻¹ standard solution (Bp, method B, for plant material only)
Abiotic material	Soil LUFA 2.4 spiked with standard solution equal 5 µg kg ⁻¹ (KP, method A only); Soil RefeSol 01-A-05 spiked with 50 µL 20–100 ng mL ⁻¹ standard solution (method B only)

For method C (GC-MS) 7:1 FTOH was spiked to all samples to evaluate precision and the relative standard deviation of IS and 7:1 FTOH response (corrected by sample weight) was monitored within one matrix. Matrix-specific quality assurance (QA) samples were also analysed in duplicates by headspace solid-phase-microextraction gas chromatography mass spectrometry (HS-SPME-GC-MS).

Furthermore, instrumental and procedural background signals were determined routinely in blank samples. Procedural blanks were treated as the matrix samples over the whole procedure but without any sample matrix. Concentrations were blank-corrected and blank values were considered for determination of limits of quantification (LOQ ≥ 10fold standard deviation of procedural blanks).

LOQs were primarily determined for a signal-to-noise-ratio (S/N ratio) of ten. Due to the variation of matrix effects within one type of matrix, signals from all samples were considered as well as signals from spiked matrices from the validation, matrix-matched calibration (method C) and quality control. In the absence of a signal in any of these samples of the same sample type, the noise was integrated and quantified at the retention time of the analyte in question. In this case, the LOQ was obtained as ten times the concentration attributed to the noise.

The validated methods for biological and abiotic materials, described above, were transferred to samples of a similar sample type, these are roe deer liver for liver samples, herring gull egg for bird's eggs in general, bream musculature for musculatures and soil and suspended matter for the abiotic materials. In addition, the biota method was applied to the new sample type cormorant lung.

2.5 Statistical Tools

Concentrations refer to wet weight and are given as arithmetic means unless stated otherwise. Only suspended matter was freeze-dried and its PFAS concentrations refer to dry weight. Due to the large number of analytes with individual and highly variable LOQ, values <LOQ were treated as zero for sum concentrations and statistical tests. For temporal trend analyses, values <LOQ were replaced by the LOQ divided by 2.

Statistical analysis (test for normal distribution (Shapiro Wilk Test/significance (t-Test)) and the figures were done using the software R and Microsoft Excel. Significance was tested at confidence level $\alpha = 0.05$ for all tests. Before a principal component analysis (PCA) was carried out, the concentrations were transformed to molar concentrations and normalised to the sum of all concentrations.

Statistical analysis was conducted for wild boar livers from areas BC and PS only, as only one sample from area IE was available. Independent of gender and age, all wild boar samples were treated equally. Statistical analysis has to be interpreted with caution, as samples from area BC were pooled and samples from area PS were analysed at an individual level.

For analyses of temporal trends, the LOESS-Trend tool, version 1.1, Excel-based – provided by the German Environment Agency – and the USTAT trend tool (<https://ustat-trendtool.quodata.de>) – provided by Quodata GmbH in particular for analyses of combined effects from different factors (e. g. sample site and analyte) (Uhlig et al. 2014) - were used. Both tools are based on trend analyses described by Fryer and Nicholson (1999).

2.6 PFAS Analysis by LC-Q-TOF-MS and FTICR-MS

2.6.1 Quality Assurance

For validation purposes, extraction blanks were prepared for each batch of samples to monitor the possible occurrence of contamination during the extraction procedure. Instrumental blanks containing only mobile phase, were injected after an appropriate number of sample injections, in order to check for any background contamination.

2.6.2 Creation of a Suspect Screening Library

A suspect list of PFAS was compiled from the S46 NORMAN Suspect List (Liu et al. 2019b), which contains a list of PFAS reported in non-target HRMS studies compiled by Liu et. al. (2019) and the OECD PFAS global database edited by the U.S. EPA. The original database contains 747 unique substances with an assigned exact mass and sum formula. Among these, 604 substances included structural information in form of a Smiles code. The remaining PFAS listed without structural information were not considered within the scope of the present study. Moreover, the resulting database does not consider isomeric forms, thus the possibility of a multitude of molecular structures is still plausible. However, the original NORMAN bank does not offer further information.

In this study, the suspect PFAS were screened for their [M-H]⁻ molecular anions in negative ion mode. Therefore, all sum formulas correlating to a cationic structure had to be excluded, leaving 721 unique features. Negative ions were not considered in this workflow. The Norman database mentions all proposed structures in neutral salt form, thus all features including positive counter ions such as K⁺ and Na⁺ had to be formatted to a neutral formula without counter ions, as UNIFI requires a name and the sum formula in its ionic form for input data. Other counter ions included Mg²⁺, Li⁺ and various amine derivatives. The created library was formatted according to the UNIFI™ Scientific Information System (Waters, Milford, MA, USA), where both created library and datasets are uploaded and processed subsequently. For ease of processing, structural information converted to mol-files and integrated into the library would be beneficial for simplifying the identification process of suspects. For extending the library in the future, structural information of PFAS will be favourable. If absent, the formatted library entry will remain speculative. Nonetheless, knowledge about possible organic and inorganic counterions gathered in the present study may help to propose neutral formulas without counterions later on.

2.6.3 Quadrupole Time-of-Flight Mass Spectrometry

For the analysis by liquid chromatography-high resolution-mass spectrometry (LC-HRMS) a quadrupole-time-of-flight mass spectrometer (QTOF) (Xevo G2-S TOF, Waters, Manchester, UK) was used.

An injection volume of 10 μL of extract was separated on an Acquity UPLC BEH Shield RP18 column ($100 \times 2.1, 1.7 \mu\text{m}$, Waters) at a flow rate of 0.35 mL min^{-1} and a column temperature of $45 \text{ }^\circ\text{C}$. The gradient program started with 90 % solvent A (2 mM ammonium acetate in water/methanol, 95/5, v/v) and 10 % solvent B (2 mM ammonium acetate in water/methanol/acetonitrile, 5/75/20, v/v/v). After 1.5 min the proportion of solvent B was ramped to 65 %, after 4.5 min to 80 % and after 8.25 min to 99.9 %. This condition was held for 2.75 min before changing back to the initial conditions. The total run time was 15 min.

The measurements were conducted using electrospray ionization (ESI) in positive and negative mode, employing nitrogen as desolvation and cone gas (600 and 150 L hr^{-1} , respectively). The capillary voltage was set to 0.8 kV / -1.5 kV and an optimised desolvation and source temperature of 350 and $120 \text{ }^\circ\text{C}$ respectively, were employed. The MS^E -mode of the mass spectrometer was employed, alternating between low (recording of molecular ions) and high collision energy (recording of fragment ions). A collision energy ramp from 15 to 45 eV was applied as high collision energy and the mass window from 50 to 1200 Da was scanned in continuum mode. The scan time was 0.15 s .

The samples were analysed together with a procedural blank from extraction and a 2 ng mL^{-1} PFAS standard in a 2 mM ammonium acetate solution of methanol/water (1:1, v/v).

For data acquisition and processing in LC-HRMS, the software MassLynx v4.2 (Waters, Milford, USA) was used.

2.6.4 Fourier Transform Ion Cyclotron Resonance Mass Spectrometry (FTICR-MS)

The analyses by ultrahigh resolution mass spectrometry (UHR-MS) were performed on a Solaris XR 12 Tesla FTICR-MS (Bruker Daltonics, Billerica, USA).

This sample had been measured in continuous accumulation of selected ions (CASI) mode.

Before analysis, the sample extracts were diluted once again by a factor of 1:100 in a methanol/water mixture (1:1, v/v). The samples were introduced by direct injection (DI) and ionized with a nano-electrospray ionisation (nano-ESI) source operating in negative mode. A total volume of around $100 \mu\text{L}$ were injected via a gastight 1725 Hamilton syringe (Hamilton robotics, Bonaduz, Switzerland) at a flow rate of $240 \mu\text{L h}^{-1}$. Between each measurement, the capillary as well as the syringe were washed using a solution of methanol/water (1:1, v/v).

For the suspect screening, both CASI and full-scan spectra were acquired between a set mass range of m/z 147.41 to 1200.00 , whereas spectra acquired in full-scan mode were used for internal mass calibration, using the program "DataAnalysis" (Bruker Daltonics, Billerica, USA). All calibration points with mass errors above 0.2 ppm were subsequently excluded from calibration. According to the obtained signal intensities and respective methods, the selection for both the number of scans and accumulation times would vary.

Extraction and instrumental blanks were measured in FTICR-MS as well. However, no blank subtraction for quality control purposes was performed, since the probability of premature candidate exclusion was high, when many of the detected peaks displayed low intensities close to the S/N threshold. Nonetheless, various subsequent filtration steps followed the initial data processing, which should ensure that false positive annotations are kept to a minimum.

The Data Analysis software was used for data processing in FTICR-MS. After an internal calibration step, the obtained signals from the CASI measurements were exported to Excel for subsequent data clean-up, including a filtration step for the allowed mass windows. The filtered list of candidates was subsequently screened against an PFAS library, using an in-house created algorithm. The suspect library was compiled from the CompTox Chemicals Dashboard of the US Environmental

Protection Agency, containing an edited list of around 7000 unique PFAS entries previously reported in non-target HRMS studies by the OECD PFAS global database.

For a complete screening, DataAnalysis was utilised as a tool to generate in silico isotope patterns for suspected masses and their assigned formulae. A final isotope score was assigned and later used for suspect prioritization. After the screening step, the program compiled a comprehensive overview of all exact and measured masses, together with their mass errors, measured intensities, S/N ratio, isotope scores and assigned formulae, as well as corresponding Pubchem Database CIDs for ease of identification. Based on available data, the list further contained IUPAC names, assigned SMILES structures if available or InChIKey codes instead, all derived from the Pubchem Database. Later, the Pubchem database was also utilized for a cross-validation step for all assigned formulae, by searching for all plausible formulae that may correspond to a specific mass. Finally, the in-house algorithm was applied in the search for homologue masses. This approach is considered a non-targeted screening that complements the workflow, since all measured masses in the FTICR-MS data are screened for common mass differences, which hopefully produces new candidates of interest that can be integrated in the list for subsequent liquid chromatography quadrupole-time-of-flight mass spectrometry (LC-QTOF-MS) screening.

3 Method Performance

3.1 Optimisation and Validation

3.1.1 Methods A and B

Method validation was performed for seven representative matrices (see chapter 2.4) and for all 42 target analytes for quantitative analysis. The precision validation within one matrix group revealed a relative standard deviation <30 % for most analytes of the group A and B (Figure 6). The apparent recoveries were in an acceptable range (70–130 %) for most of the analytes (Figure 7). Poorer precision values were mostly limited to substances for which no authentic internal standard was available.

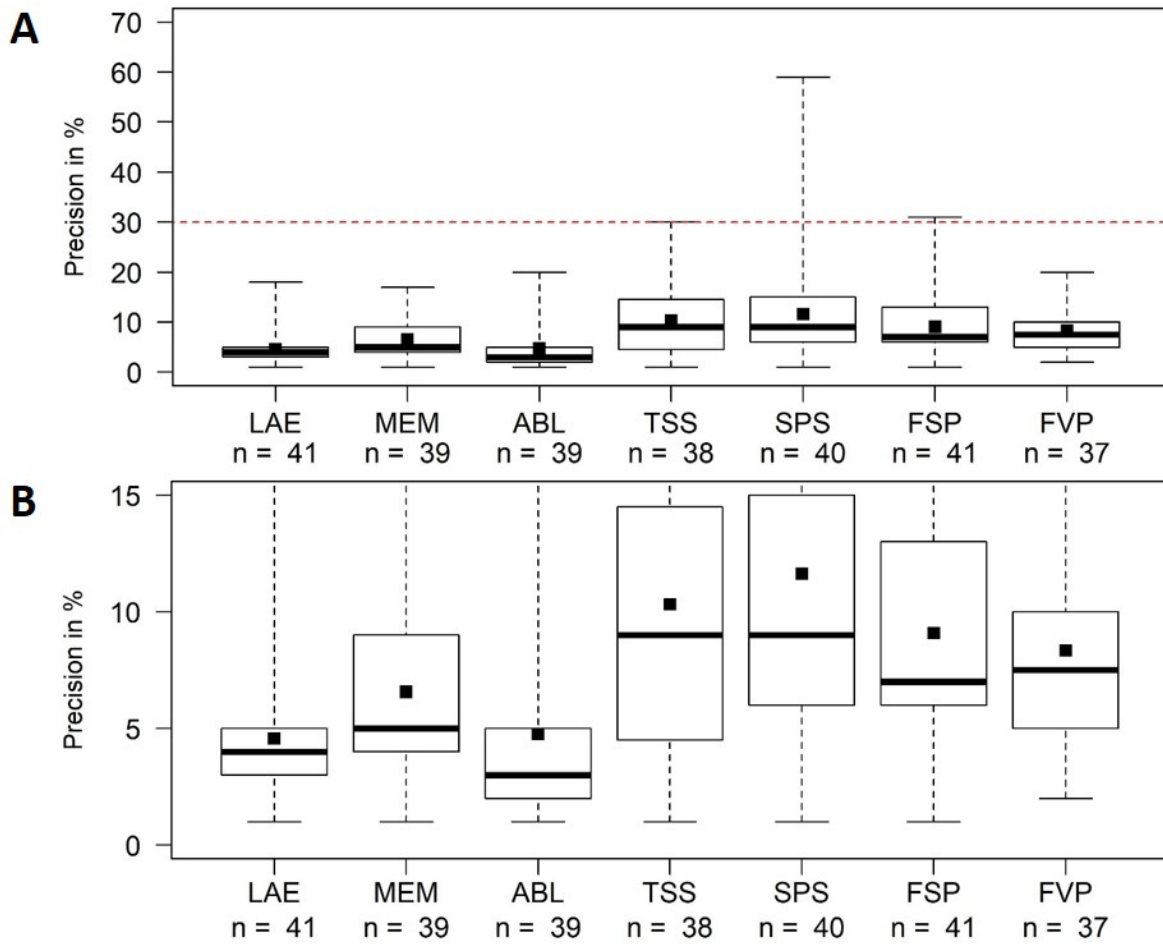
With respect to sensitivity, the median of all matrix-specific LOQs (PFAS group A and B) was less than 0.5 $\mu\text{g kg}^{-1}$ for most of the analytes. For aquatic biota (herring seagull egg (LAE), blue mussel soft body (MEM), common bream liver (ABL) and filet ABF and Viviparous eelpout filet (ZVF) also the mean was less than 0.5 $\mu\text{g kg}^{-1}$ (Figure 8). Earthworm (LTF) and plants (European beech (FSP), Scots pine (PSP) and Bladder wrack (FVP)), especially pine shoots (PSP), revealed higher LOQs. The evaluation of the LOQs for PFOS in the matrices LAE, ABL and Roe deer (liver (CCL)) was not feasible because of too high concentrations already present in the samples. Furthermore, the validation of top soil (TSS) was compared to a spiked reference soil (LUF 2.4) for the analytes of group A. The comparison within one matrix type showed that matrix effects varied for the same analytes and resulted in distinctive LOQs.

The validation of the TOP assay for PFCAs resulted in the values for precision shown in Figure 9 and for apparent recovery the ones shown in Figure 10. The comparison of TOP assay results from non-oxidised and oxidised extracts (pre- and post-oxidation) showed that oxidation influenced both performance criteria, but with no obvious trends. The median of the LOQs achieved for the analytes of the TOP assay methods (pre- and post-oxidation) ranged from 0.072 to 1.4 $\mu\text{g kg}^{-1}$ (Figure 11). Similar to the impact of the oxidation procedure on apparent recovery and precision, its impact on sensitivity of the methods is difficult to predict.

Analyte-matrix-combinations with insufficient validation results were excluded from further evaluation and are not included in the boxplots. One of these combinations was PFCAs determined by the IC-QTOF-MS method in plant matrices (FSP, PSP and FVP). These analytes could only be determined in the extract from the TOP assay method (pre- and post-oxidation). The determination of many analytes in the earthworm matrix (LTF) failed as recoveries were low. This was also true for the TOP assay method during the analysis of the earthworm samples, therefore TOP assay results were not considered for this matrix.

Figure 6: Precision in quantitative LC-MS analysis

(A) Relative standard deviation of three replicates for “n” PFAS for all matrices validated. (B) Extension of (A). Box: range from 25 to 75 percentile; whiskers: minimum and maximum. Bold line: median.

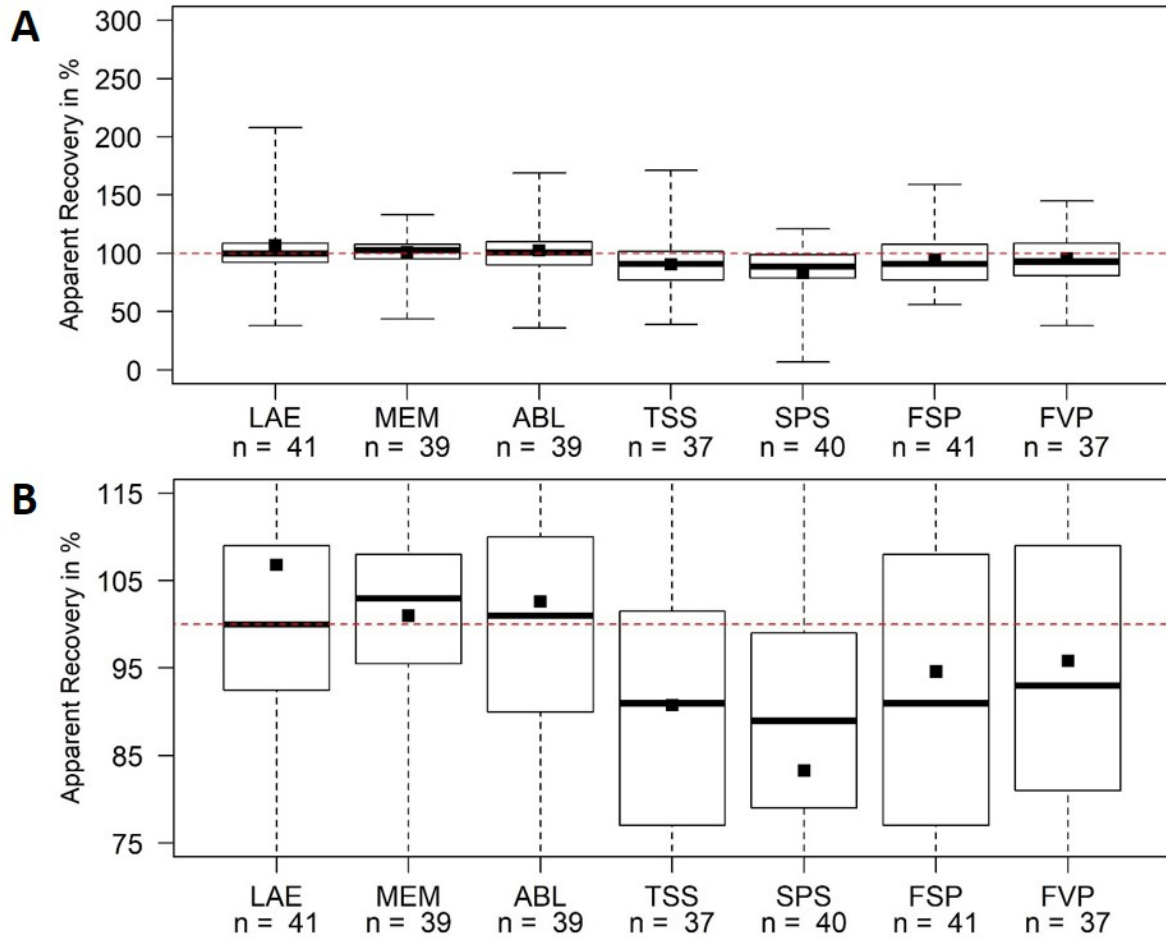


herring seagull egg (LAE), blue mussel (MEM), common bream liver (ABL), top soil sample (TSS), riverine suspended matter (SPS), European beech (FSP), bladder wrack (FVP).

Source: own illustration, TZW.

Figure 7: Apparent recoveries in quantitative LC-MS analysis

Apparent recovery (ratio between the measurement result and the spiked concentration) for all validated matrices, with “n” replicates. (B) extension of (A). Box: range from 25 to 75 percentile; whiskers: minimum and maximum. Bold line: median; dashed line (red): 100 %.

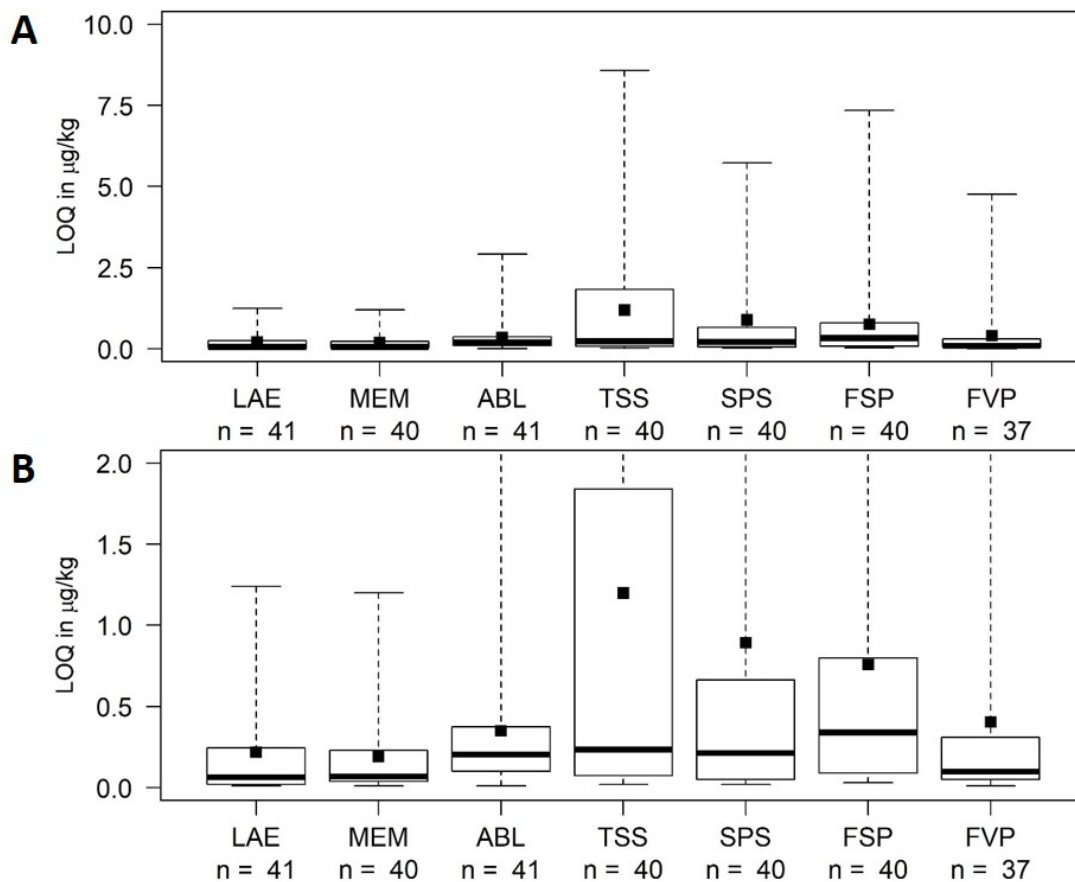


herring seagull egg (LAE), blue mussel (MEM), common bream liver (ABL), top soil sample (TSS), riverine suspended matter (SPS), European beech (FSP), bladder wrack (FVP).

Source: own illustration, TZW.

Figure 8: Limit of quantifications in target LC-MS analysis

(A) The limit of quantifications (LOQs) for “n” PFAS in one sample matrix. (B) extension of ‘(A). Box: range from 25 to 75 percentile; whiskers: minimum and maximum. Bold line: median.

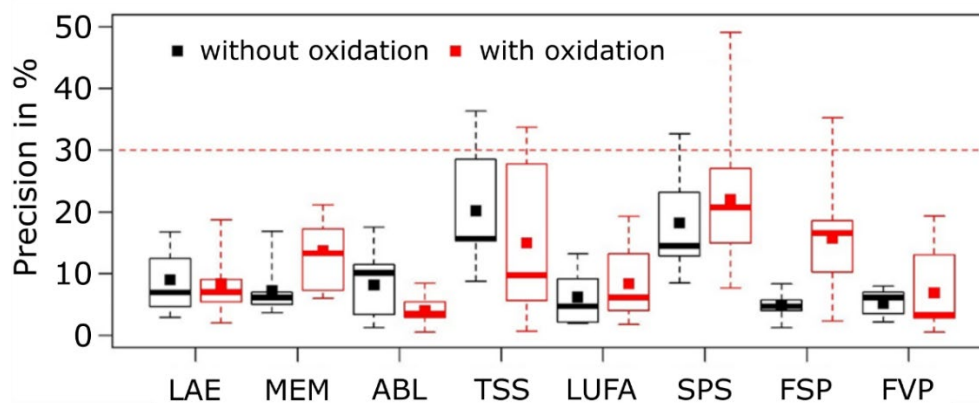


herring seagull egg (LAE), blue mussel (MEM), common bream liver (ABL), top soil sample (TSS), riverine suspended matter (SPS), European beech (FSP), bladder wrack (FVP).

Source: own illustration, TZW.

Figure 9: Precision in TOP assay analysis

Analytical precision expressed as relative determined of three replicates for PFCAs C2–C14 in each matrix and the spiked reference soil LUFA. Black: results of the non-oxidised extract, Red: results of the oxidised extract. Box: range from 25 to 75 percentile; whiskers: minimum and maximum; Bold line: median; dashed line (red): 30 %.

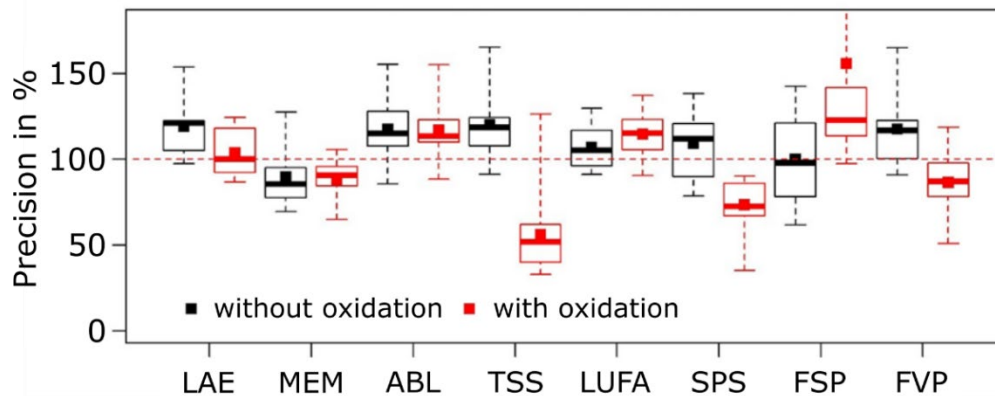


herring seagull egg (LAE), blue mussel (MEM), common bream liver (ABL), top soil sample (TSS), reference soil (LUFA), riverine suspended matter (SPS), European beech (FSP), bladder wrack (FVP).

Source: own illustration, TZW.

Figure 10: Apparent recovery in TOP assay analysis

Apparent recovery for the TOP assay (ratio between the measurement result and the spiked concentration) for the PFCAs C2–C14 in one matrix. Black: results of the non-oxidised extract, red: results of the oxidised extract. Box: range from 25 to 75 percentile; whiskers: minimum and maximum; bold line: median; dashed line (red): 100 %.

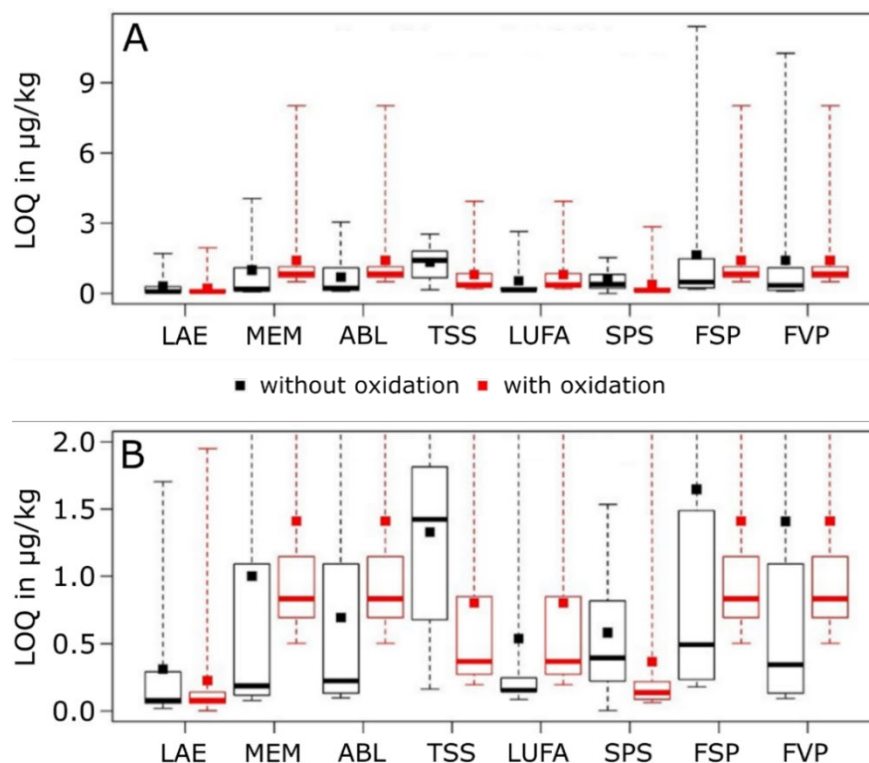


herring seagull egg (LAE), blue mussel (MEM), common bream liver (ABL), top soil sample (TSS), reference soil (LUFA), riverine suspended matter (SPS), European beech (FSP), bladder wrack (FVP).

Source: own illustration, TZW.

Figure 11: Limit of quantification in TOP assay analysis

- (A) Limit of quantification (LOQ) for the PFCAs C2–C14 in the TOP assay for each validation and the spiked reference soil LUFA, respectively. (B) extension of (A). In black: results of the non-oxidised extract, red: results of the oxidised extract. Box: range from 25 to 75 percentile; whiskers: minimum and maximum; bold line: median.



matrix (herring seagull egg (LAE), blue mussel (MEM), common bream liver (ABL), top soil sample (TSS), riverine suspended matter (SPS), European beech (FSP), bladder wrack (FVP).

source: own illustration, TZW.

3.1.2 Method C

In general, the precision of the SPME-GC-MS method (PFAS group C) was lower than for LC-MS analyses. The relative standard deviation of the IS response in tree leaves and bladder wrack was <40 % for fluorotelomers and <50 % for deuterated N-Methyl perfluorooctane sulfonamidoethanol (MeFOSE) and N-Ethyl perfluorooctane sulfonamidoethanol (EtFOSE). In tree needles and soil, deviations as high as 60% were determined for fluorotelomers and <65 % for deuterated Me- and EtFOSE. Spiked 7:1 FTOH had a precision <25 % in all matrices. Considering the high sensitivity of fluorotelomers (0.01–0.50 µg kg⁻¹) and their low abundance in all screened samples (99 % <LOQ, see Diversity of PFAS), the method was still deemed acceptable for screening purposes.

3.1.3 Quality Control

As quality control for selected PFAS, the certified JRC reference material IRMM 427, pikeperch (*Sander lucioperca*) musculature, was analysed with every batch of biota samples. For all reference values the difference to the measurement result was calculated and compared to the combined expanded uncertainty of measurement and reference value according to Dabrio Ramos et al. (2015) (Table A 1). The results of the reference material were found to be unbiased except for perfluorododecanoic acid (PFDoDA), which was systematically quantified too low (63 % of the reference value). In conclusion, the actual values of PFDoDA are presumably above the measurement results in all samples.

In the TOP assay analysis, complete oxidation of precursors was ensured by spiking separate samples of each matrix with N-ethylperfluorooctane sulfonamidoacetic acid (EtFOSAA) (i. e. 5 µg kg⁻¹ in wild boar liver, soil, suspended matter and bream musculature) prior oxidation. The absence of EtFOSAA after oxidation was considered a prerequisite of complete oxidation. Additionally, oxidation was controlled visually, as a clear and colourless extract was present after the oxidation process. Nonetheless, given the remaining uncertainty of complete oxidation, the findings for the TOP assay in this study have to be considered as a minimum formation potential.

4 PFAS screening in samples of the Environmental Specimen Bank (work package 2a)

4.1 Diversity of PFAS included in this study

In this part of the study, nine sample types were included, covering marine, riverine and terrestrial animals as well as suspended matter and surface soil. Of the 69 PFAS included in this study 36 were detected at least once (see UPB (<https://www.umweltprobenbank.de/de>)). Among these, 30 could be quantified with a reference and an internal standard whereas six were identified qualitatively. The analyte spectrum of this study exceeds routine analyses and may other broader screening exercises.

A preceding study on PFAS background contamination in Germany analysed for 41 substances, including substitutes and precursors (Kotthoff et al. 2020); of these, 31 PFAS were detected, in a sample set similar to this study (samples of the ESB, mainly from 2015–2017).

Substances identified in our study which are not part of present routine analyses, for instance, 8:2 FTOH, perfluorooctane sulfonamido phosphate diester (diSAmPAP), Capstone and DONA, i.e. substitutes introduced into the market before and after the start of the perfluorooctansulfonylfluorid (POSF) phase-out in 2000, FTSA, methylated and ethylated FOSEs, and perfluorobutane sulfonamide (FBSA) and perfluorohexane sulfonamide (FHxSA) as shorter chain homologues of POSF-based substances.

However, 33 of the 69 analytes were not detected in any of the samples. Among them are homologues of POSF-based substances perfluorobutane sulfonamidoacetic acid (FBSAA), perfluorohexane sulfonamidoacetic acid (FHxSAA), perfluorooctane sulfonamides (Me- and EtFOSA) and non-alkylated perfluoroalkane sulfonamido ethanols (FASEs), some short-chain PFCAs (perfluorobutanoic acid (PFBA), perfluoropentanoic acid (PFPeA) and perfluorohexanoic acid (PFHxA)), neutral fluorotelomers (FTOHs, FTACs and FTMACs), the substitutes HFPO-DA and perfluorooctane sulfonamido phosphate monoester (monoSAmPAP).

In addition, a broad range of PAPs (11) showed no signal in any of the extracts, although certain precursor diPAPs (sum < 0.20 $\mu\text{g kg}^{-1}$ and four identified) were detected in sea gull egg from 2001, fish liver and suspended matter. In addition, 6:2 and 8:2 Cl-PFESA were not detected. Both are constituents of the mist suppressant F-53B which is produced in China since the late 1970s and not expected to be used in Europe (Liu et al. 2018). Kotthoff et al. (2020) determined 6:2 Cl-PFESA in their retrospective screening in German bream as old as 1984 and sea gull eggs at levels $\leq 1.3 \mu\text{g kg}^{-1}$.

DONA was determined in single samples at concentrations $\leq 0.25 \mu\text{g kg}^{-1}$. These include bream liver from Blankenese and 27 % of all soil samples. DONA was already detected in soil from Scheyern in 2014 by Kotthoff et al. (2020) as well as in suspended matter from several German rivers. DONA was also found in suspended matter from River Saale, which was not screened for DONA before our study.

FTSAs were determined at substantial levels in most riverine specimens and all herring gull eggs. The 8:2 FTSA was determined with maximum concentrations of 0.93 and 0.97 $\mu\text{g kg}^{-1}$ in suspended matter from Cumlosen (Elbe) and Bimmen (Rhine). In agreement to Kotthoff et al. (2020) 4:2 FTSA was not detected.

Among the other fluorotelomers, which are feasible for GC analysis only and are therefore not screened for routinely, only 8:2 FTOH was detected. The compound was determined consistently in poplar and beech leaves at a background concentration of $0.074 \pm 0.068 \mu\text{g kg}^{-1}$ (maximum equals

0.20 $\mu\text{g kg}^{-1}$ dry-weight (dw)). The 8:2 FTOH is one of the compounds determined with high precision (<20 %) by SPME-GC-MS. Yoo et al. (2011) also reported FTOHs in plant material (tall fescue and Kentucky bluegrass) where 8:2 FTOH usually dominated among the homologues with concentrations $\leq 1.5 \mu\text{g kg}^{-1}$ (dw). The relatively high level of contamination in the study by Yoo et al. (2011) is presumably associated with biosolid field application at the sampling sites.

Besides plant and abiotic material, earthworm was analysed by GC-MS (method C). Again, none of the neutral PFAS were detected. This finding can be explained by a rapid biotransformation of fluorotelomer alcohols in animal tissue as shown by Zhao and Zhu (2017) in earthworm; the transformation ultimately leads to formation of the persistent end products perfluorononanoic acid (PFNA) and perfluorodecanoic acid (PFDA) which however showed no quantifiable signals in our study. Overall, only the long-chain PFCAs, perfluorotridecanoic acid (PFTrDA) and perfluorotetradecanoic acid (PFTeDA), were determined in earthworm at maximum concentrations of $0.60 \mu\text{g kg}^{-1}$ (sum concentration in recent sample from Saar Valley). However, the earthworm screening results are incomplete as the method was not applicable to this matrix for many PFAS.

4.2 PFAS Concentrations and Patterns

For comparisons between different sites and sample types, only the 62 most recent samples (2017–2019) were considered to avoid bias due to time trends. Mean concentrations of PFAS groups and the sum of all PFAS determined within one sample type are summarised in Table 2 for selected matrices. As discussed in chapter 2.4 the sensitivity for a specific compound strongly depends on the respective matrix: the spread of LOQs between different matrices ranges from 0.01 to $8 \mu\text{g kg}^{-1}$. This complicates direct comparisons between matrices if concentrations near the LOQ are determined. Group concentrations were calculated for mean concentrations of individual PFAS within a matrix group. If within a group of PFAS a single substance was quantified at least once, the mean for this matrix type is calculated considering levels below LOQ as half the LOQ. PFAS which were consistently not detected above LOQ for a given matrix were not considered at all for the group concentration.

Interestingly, roe deer and bream differ most in PFAS sum concentration (factor 200) although the data were obtained for the same organ (liver).

Overall, bream liver shows the highest PFAS contamination. The maximum total PFAS in bream was determined in Koblenz (Rhine, $209 \mu\text{g kg}^{-1}$). These high levels are mainly attributable to PFOS, which constitutes about 72 % of the sum concentration in bream liver. Similar proportions of PFOS are found for bream musculature and sea gull egg, which overall show second and third highest PFAS levels of all animal tissues.

The pattern of PFCAs in fish musculature from major German rivers is similar to fish from the North and the Baltic Sea (bream vs. eelpout, see Table 2). The PFAS patterns differ, however: in bream it is dominated by PFOS (factor 9 higher), whereas FOSA dominates in eelpout musculature. The difference in PFOS concentration is also reflected in the overall PFAS concentration (eelpout: $1.87 \pm 0.45 \mu\text{g kg}^{-1}$ and bream: $16.0 \pm 10.0 \mu\text{g kg}^{-1}$). This is, likely, due to the generally higher PFAS exposure in rivers than in marine systems, where river discharges are diluted by seawater.

PFDA is the compound determined frequently across all species (100 % in all fish, egg, suspended matter and roe deer liver; 75 % in zebra mussel; 9 % in soil); highest levels were, again, determined in bream liver ($7.5 \pm 3.2 \mu\text{g kg}^{-1}$) and sea gull egg ($2.5 \pm 0.15 \mu\text{g kg}^{-1}$). However, PFDA never dominates the PFAS pattern and was not found in blue mussel, earthworm and bladder wrack.

A comparison of samples from different sampling locations and times needs to consider that internal concentrations of PFAS are not only reflecting by the external (exposure) concentrations in

the habitat but are also influenced by the (species specific) exposure scenario, the food web structure and by matrix composition, with the latter factor also affecting method performance. This is even more critical for comparisons between different species (Chapter 6.3).

Table 2: Mean concentrations in $\mu\text{g kg}^{-1}$ of PFAS classes in different matrices screened in ESB samples from 2017–2019

Concentrations refer to wet weight (ww) except for suspended matter. For mean concentrations half the LOQ and for sum concentrations only mean concentrations >LOQ were considered.

	LAE n=2	ZVF n=2	MEM n=3	ABL n=10	ABF n=10	DPM n=8	CCL n=9	TSS n=11	SPS n=7
Sum of all PFAS	30.2 ± 4.2	1.87 ± 0.45	1.02 ± 1.14	121 ± 97	16.0 ± 10.0	3.99 ± 4.98	0.64 ± 0.12	1.49 ± 1.06	9.81 ± 3.70
PFCAs C3–C7	1.05 ± 0.03	< LOQs	< LOQs	< LOQs	0.11 ± 0.06	< LOQs	0.08 ± 0.04	0.03 ± 0.09	< LOQs
PFCAs C8–C10	4.74 ± 0.56	0.52 ± 0.34	< LOQs	8.95 ± 3.59	1.89 ± 0.67	0.04 ± 0.02	0.50 ± 0.10	0.20 ± 0.53	1.22 ± 0.54
PFCAs C11–14	3.20 ± 1.47	0.56 ± 0.27	0.01 ± 0.004	10.1 ± 5.1	2.19 ± 1.10	0.45 ± 0.37	0.06 ± 0.03	0.73 ± 0.22	1.28 ± 0.58
PFSA C4	< 0.014	< 0.039	< 0.21	< 0.15	< 0.075	< 0.079	< 0.29	0.06 ± 0.15	< 0.15
PFSA C6	2.55 ± 0.35	< 0.78	< 4.4	0.95 ± 0.60	< 0.41	< 1.4	< 0.86	0.42 ± 0.95	< 0.86
PFSA C8	18.5 ± 2.5	0.28 ± 0.11	< 1.1	97.7 ± 91.8	11.2 ± 8.6	0.24 ± 0.14	< 3.3	< 2.8	3.54 ± 2.49
PFSA C10	< 0.30	< 1.2	< 1.3	< 1.1	< 0.92	< 2.8	< 0.97	< 2.8	< 0.97
PAPs	< LOQs	< LOQs	< LOQs	0.01 ± 0.01	< LOQs	< LOQs	< LOQs	< LOQs	0.18 ± 0.13
diSAmpPAP	< 0.012	< 0.028	< 0.032	< 0.280	< 0.039	< 0.021	< 0.26	< 0.35	0.71 ± 0.78
FOSA	0.12 ± 0.01	0.49 ± 0.40	0.17 ± 0.15	1.75 ± 0.81	0.43 ± 0.21	0.40 ± 0.22	< 0.40	< 2.3	n. a.
POSF-based precursors	0.04 ± 0.005	0.02 ± 0.01	< LOQs	1.28 ± 0.89	0.17 ± 0.01	0.002 ± 0.003	< LOQs	0.03 ± 0.03	0.19 ± 0.12
Fluorotelomers	0.03 ± 0.01	< LOQs	< LOQs	0.12 ± 0.06	0.01 ± 0.002	0.01 ± 0.01	< LOQs	< LOQs	0.62 ± 0.45
Substitutes	< LOQs	< LOQs	0.84* ± 1.00	0.12** ± 0.05	< LOQs	2.56* ± 3.99	< LOQs	0.02+ ± 0.02	2.06+ ± 0.86

* 6:2 FTSA-PrB; + DONA. Herring gull (LAE), viviparous eelpout filet (ZVF), blue mussel (MEM), common bream liver (ABL), common bream filet (ABF), zebra mussel (DPM), roe deer liver (CCL), top soil (TSS), suspended matter (SPS).

4.3 TOP Assay

Assuming that all precursors were converted into measurable PFCAs, the organic fluorine (OF) was calculated from the PFCAs analysed (Houtz et al. 2013). The OF after TOP assay was calculated as the difference between the post TOP assay OF and the pre-TOP assay OF, summated to the native concentrations. Therefore, the calculated OF after oxidation describes the absolute increase and will be referred to as TOP assay OF (TOP_{OF}). The TOP assay showed no significant TOP_{OF} for the majority of the analysed samples, indicating generally low levels of precursors. This was true for all sampling sites. For the bulk of the matrices, a $TOP_{OF} < 10 \mu\text{g kg}^{-1} \text{F}$ was found, with only the barbel liver exceeding $10 \mu\text{g kg}^{-1} \text{F}$ ($14 \mu\text{g kg}^{-1} \text{F}$). This was verified by calculating the unknown OF and comparing it to the OF of the polyfluorinated substances (precursors) measured in the native analyses. The generated TOP_{OF} can be fully explained by the precursors quantified in this study.

However, two matrices (bream liver and zebra mussel) showed a more pronounced increase in TOP_{OF} , indicating a significant contamination with precursors.

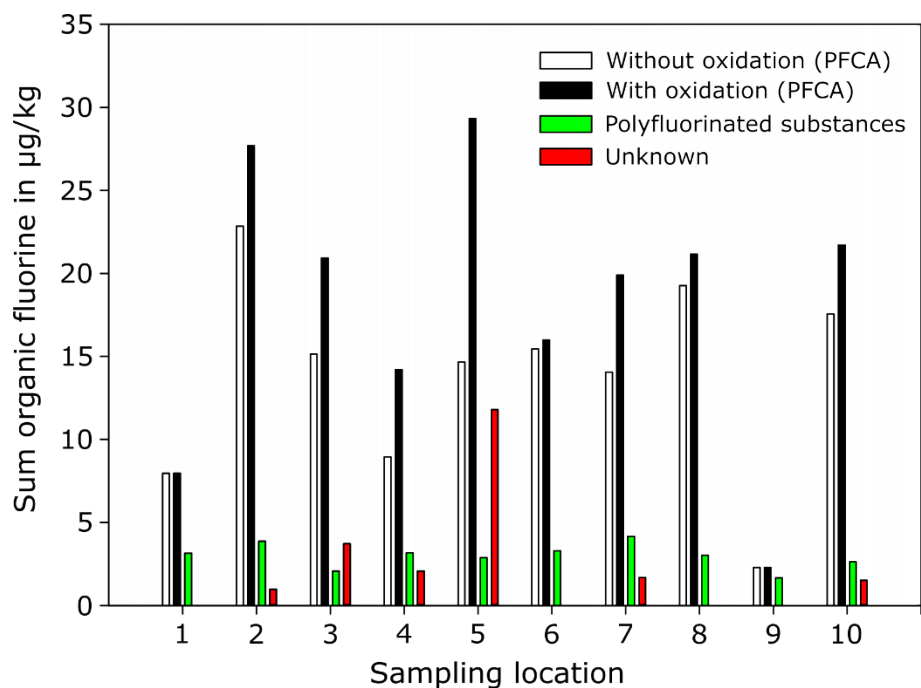
While *bream liver* exhibited generally elevated PFAS contamination, bream liver from one of the three sites also showed an elevated TOP_{OF} level (Figure 12): this was the sampling site Dessau (Mulde) with a 100 % increase in OF after the TOP assay; the sites Rehlingen (Saar) and Lake Belau showed no such increase. The Mulde River is significantly impacted by the industrial activity in the Bitterfeld region, which may be the origin of the unknown PFAS that become visible by the TOP assay.

For *zebra mussel* an even stronger increase in OF was observed after the TOP assay (Figure 13), most pronounced for the Wettin (Saale) and Jochenstein (Danube) sampling site, whilst mussels from Cumlosen (Elbe, after confluence with Saale river) showed no such increase. Similar to the Mulde River, the increase in OF after the TOP assay in Saale and Danube is probably linked to discharges from industry (Halle/Saale; Gendorf via the rivers Alz and Inn).

The different pattern for TOP_{OF} in bream liver and zebra mussel may either be due to species-specific bioaccumulation and biomagnification processes (bream versus zebra mussel) or be organ-specific (liver versus whole organism). The liver (of bream) exhibits high metabolic activity, which may transform so-called precursors into stable PFCA more effectively than the mussel tissue. For both kinds of specimen, however, the increase after TOP assay cannot be explained by the precursors measured in target analysis, indicating high levels of unknown precursors.

The fact that the polyfluorinated substances exceed the unknown OF in some samples can be explained by analyte loss during sample preparation. Given that the internal standard in TOP assay measurements is added after oxidation, to avoid oxidation of precursor internal standard, losses of precursors during the processes ahead of oxidation cannot be compensated. Thus, the actual contamination with precursors might be higher than the calculated unknown OF.

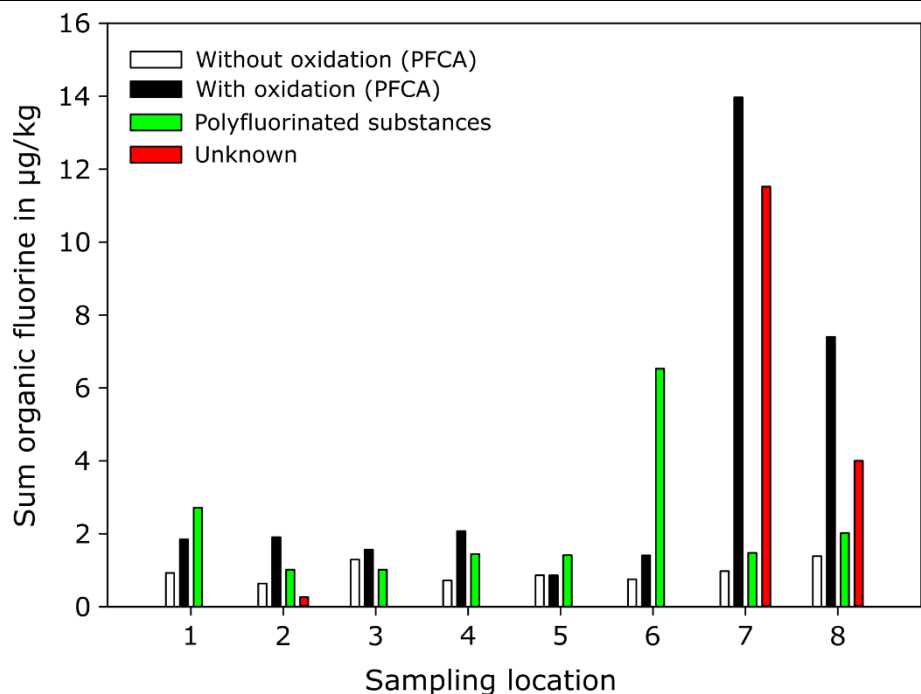
Figure 12: Organic fluorine in $\mu\text{g kg}^{-1}$ F (ww) in PFCAs found in bream liver.



Sampling sites: 1 Saar (Rehlingen), 2 Rhine (Bimmen), 3 Elbe (Cumlosen), 4 Elbe (Blankenese), 5 Mulde (Dessau), 6 Danube (Jochenstein), 7 Rhine (Koblenz), 8 Saale (Wettin), 9 Lake Belau, 10 Saale (Wettin, QA material).

Source: own illustration, TZW.

Figure 13: Organic fluorine in $\mu\text{g kg}^{-1}$ F (wet weight) in PFCAs found in zebra mussel



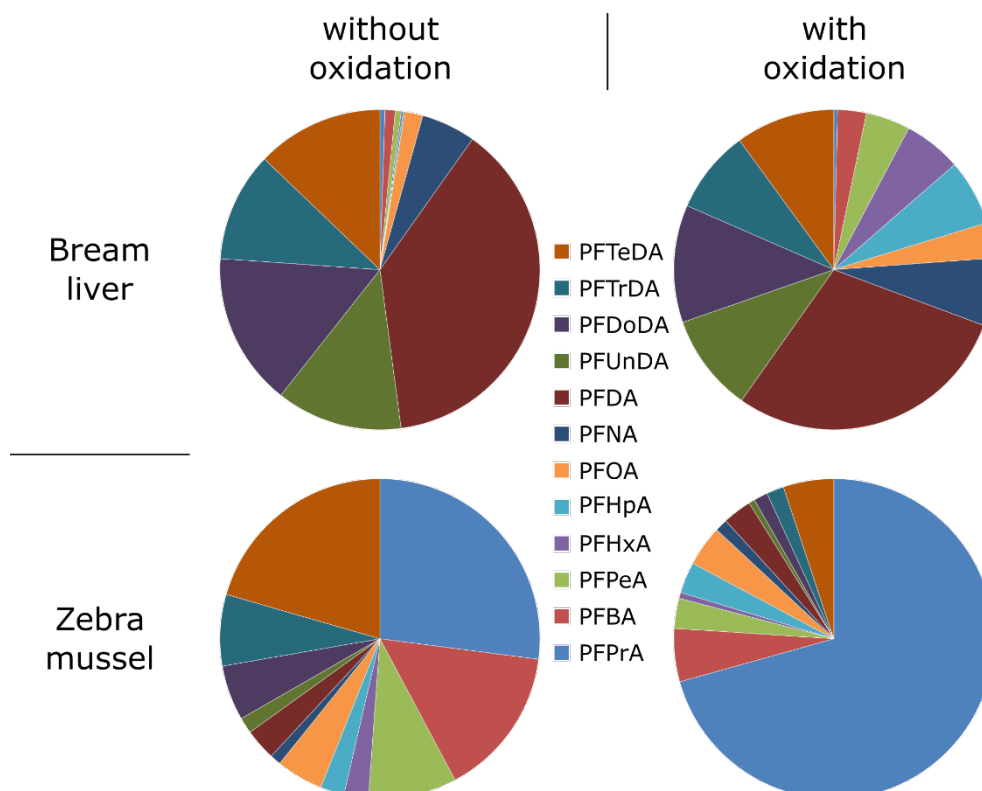
Sampling sites: 1 Saar (Rehlingen), 2 Lake Belau, 3 Rhine (Koblenz), 4 Prossen (Elbe), 5 Elbe (Cumlosen), 6 Elbe (Blankenese), 7 Saale (Wettin), 8 Danube (Jochenstein).

Source: own illustration, TZW.

Oxidation of precursors changed the relative PFCA pattern (Figure 14). For both matrices, a shift towards short-chained PFCAs by oxidation was observed, showing that most of the precursor

compounds carry structural moieties generating short-chained PFCAs. However, the precursors analysed in this study cannot account for this shift in PFCA pattern, indicating a high level of structurally different, unknown precursors. The zebra mussel for instance showed a significantly increasing perfluoropropanoic acid (PFPrA) concentration, accounting for up to 74 % of all PFCAs after oxidation. Possible precursors contributing to the observed shift are fluorotelomer sulfonamidoalkyl betaines and fluorotelomer carboxylic acids for example (Martin et al. 2019), both not analysed in the present study.

Figure 14: Mean PFCA patterns in % in bream liver and zebra mussel without and with oxidation via total oxidizable precursor assay



Source: own illustration, TZW.

5 Time series analyses in marine and riverine organisms (work package 4)

This chapter is based on the following manuscript:

Rupp J., Guckert M., Berger U., Nödler K., Nürnberg G., Koschorreck J., Schulze J., Reemtsma T. Temporal Trends of Legacy Per- and Polyfluoroalkyl Substances (PFAS), their Substitutes and Precursors in Archived Wildlife Samples from Germany (unpublished as of 19.09.24)

5.1 Introduction

Systematic archiving of samples in the German Environmental Specimen Bank (ESB) allows for retrospective long-term analysis of PFAS trends – also by methods which were not developed yet at the time of sampling. In this study, German wildlife samples were selected for temporal trend analyses based on results of an in-house pre-screening from the sample archive. To depict as many facets of the environmental PFAS load as possible by covering species from different ecological food webs and positions, herring gull from Island Mellum (North Sea, egg, 1988–2020), common bream from Koblenz (Rhine, liver, 1996–2020) and zebra mussel from Blankenese (Elbe, soft body and breathing water, 1995–2018) were selected.

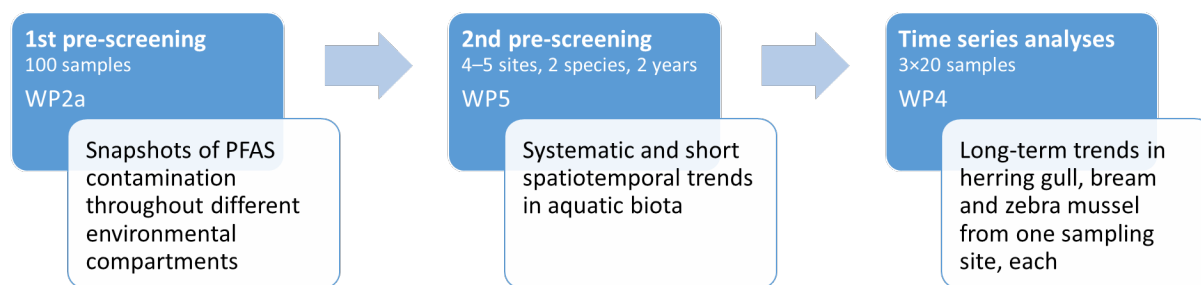
The objectives of the retrospective trend analyses were to test if internal PFAS contamination in German wildlife has changed as an effect of regulatory measures taken so far, how the patterns and levels of PFAS have developed in samples of different trophic levels and food chains and where the new trends are heading. For this purpose and to reduce the chemical gap of (ultra)short-chain and unknown PFAS, target analyses of 58 PFAS were combined with the TOP assay covering C2–C14 PFAAs.

The trend analyses extended routine analyses and included (ultra)short- and long-chain PFAS, legacy PFAS, their substitutes, precursors and degradation products, i.e. PFAAs. For the overall PFAS load, two proxies were calculated: (i) $\sum\text{PFAS}_{42}$ for target analyses of oxidisable and non-oxidisable compounds and (ii) $\sum\text{PFAS}_{23+\text{TOP}}$ for target analyses of non-oxidizable compounds and the TOP assay. In addition to the quantitative analyses, 16 PFAS were analysed qualitatively (without a reference standard).

5.2 Spatiotemporal Trends in Freshwater Biota and Sample Selection

Resources allowed only for analyses of one temporal trend (equalling one site) per biota. Therefore, for sample selection, two pre-screenings were carried out in >100 samples from the ESB (Figure 15). The first pre-screening was carried out with ca. 100 samples. The sample pool covered tissue of different animals, plants and abiotic materials. The results are discussed in chapter 4 and show a snapshot of PFAS contamination throughout different environmental compartments. For further analyses, animal samples were preferred due to the potential for bioaccumulation – which was mirrored in high PFAS concentrations as compared to concentrations in abiotic materials and plants.

Figure 15: Workflow to select samples for time series analyses



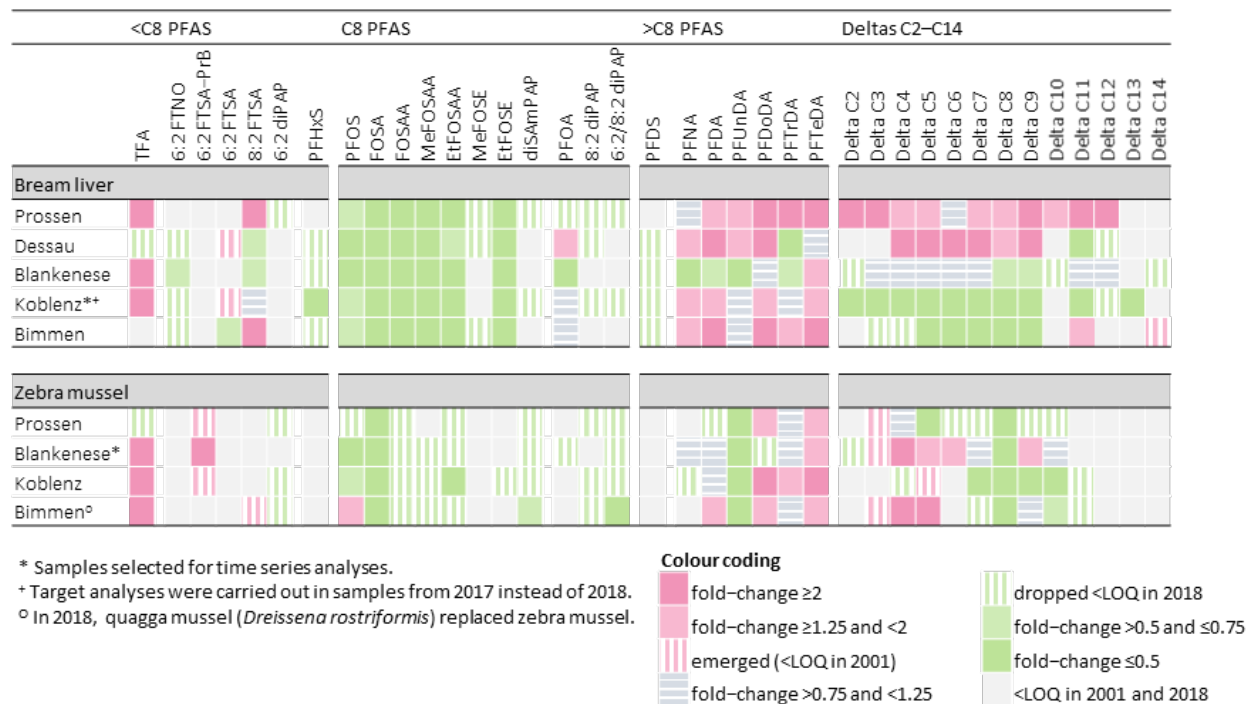
Source: own illustration, UFZ.

The objective of the time series analyses was to depict as many facets of the environmental PFAS load as possible by covering species from different ecological food chains and positions as well as PFAS from different classes. Samples were selected for the time series based on detection frequencies with focus on emerging substitutes and precursors which are not studied so well. By avoiding samples with low detection frequencies, chances of obtaining data gaps (<LOQ or <LOD (limit of detection)) were minimised. Herring gull egg from the North Sea, bream liver and zebra mussel (from different rivers and one lake) were identified as samples of interest for the time series analyses. Herring gull egg was selected for its variety of PFAS – in particular from the PAP family, zebra mussel as the only biota with positive detection of the substitute 6:2 fluorotelomer sulfonamidopropyl betaine (6:2 FTSA-PrB (Capstone B)) and bream liver for its high concentrations of the precursor EtFOSE.

To determine where and when contamination was highest in freshwater biota – either in the past (2001) or in more recent times (2017/2018) and at which sampling site – a second pre-screening was carried out before time series analyses. This screening allowed for a spatiotemporal comparison of four (zebra mussel) and five (bream liver) sample pairs from the same sampling site in two different years (overview of the trends in Figure 16). Blankenese was chosen for time series analyses as the sampling site with the highest concentration of 6:2 FTSA-PrB in zebra mussel. Similarly, bream from Koblenz was selected for its high concentrations of EtFOSE – especially in the past.

Figure 16: Heatmap of temporal trends in (top) bream liver (pool size ≥ 20 fish) and (bottom) zebra mussel (pool size: 2000 – 5000 mussels)

The colour indicates the fold-change between the years 2001 and 2018 (red for upwards trends and green for downwards trends). The shading indicates the magnitude of the change. Vertical stripes indicate that one of the results was $< LOQ$. Horizontal stripes indicate no clear change (within $\pm 0.25\%$). Samples originated from River Elbe (Prossen and Blankenese), its tributary Mulde (Dessau) and River Rhine (Koblenz and Bimmen).

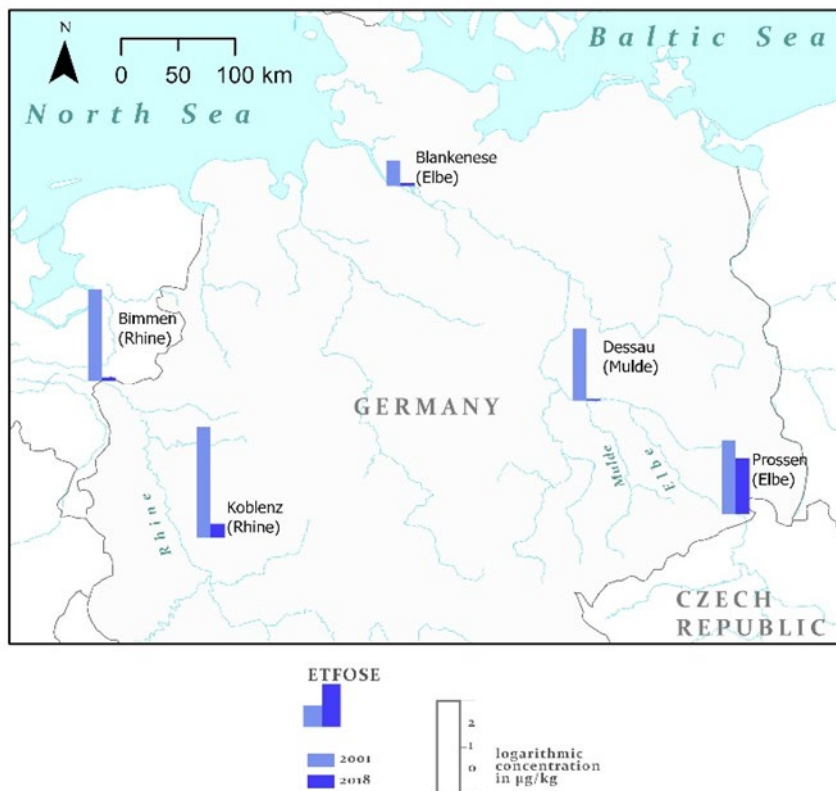


Source: own illustration, UFZ.

The second pre-screening did not only help in identifying suitable samples for time series analyses, but also in identifying common trends of zebra mussel and bream liver shared between sampling sites (or not). The C8 PFAS showed relatively uniform downwards trends in bream liver independent of the sampling site (Figure 16). Generally, trends of C8 PFAS mirrored those in zebra mussels from the same sampling sites. However, the sample set of zebra mussel includes more data gaps as results often fell $< LOQ$.

Figure 17: Spatiotemporal pattern of N-ethyl perfluorooctane sulfonamidoethanol (EtFOSE) in bream liver from German rivers

Pool samples of min. 20 individuals, sampled in 2001 or 2018, respectively, were obtained from the German Environmental Specimen Bank. Concentrations are given in $\mu\text{g kg}^{-1}$. The scale is logarithmic.



Source: own illustration, UFZ.

Besides Koblenz, EtFOSE was also determined at high concentrations in bream liver from the other four sites in 2001 (Figure 17). Until 2017/2018 the concentrations decreased: downstream River Rhine (Bimmen) and in River Mulde by $\geq 96\%$ and in River Elbe by 60–70%. In Prossen, near the Czech border, the concentration was still $17 \mu\text{g kg}^{-1}$ in 2018. In zebra mussels sampled at the same sampling sites, EtFOSE was only determined once $>\text{LOQ}$, in a sample from Koblenz from the year 2001 ($0.28 \mu\text{g kg}^{-1}$).

Concentrations of $>\text{C8}$ PFCA were mainly increasing at all sampling sites and in both aquatic biota (Figure 16). Exceptions include bream liver from Blankenese and perfluoroundecanoic acid (PFUnDA) in zebra mussel. In contrast, results of $<\text{C8}$ PFAS often fell $<\text{LOQ}$. The trends remaining for (ultra)short-chain PFAS – in particular the TFA trends – increased preponderantly as well (Figure 16).

In the pre-screening (data not shown), 6:2 FTSA-PrB was detected in 8 out of 8 samples of zebra mussel from 2018 in all major rivers of Germany (Rhine, Elbe and Danube) and the tributaries Saar and Saale. For example, it emerged in Koblenz (Rhine) and Prossen (Elbe) from $<0.22 \mu\text{g kg}^{-1}$ and increased by a fold-change of 1.4 in Rehlingen (River Saar) within two decades.

While increasing trends of 6:2 FTSA-PrB were indicated in zebra mussel from different sites, the compound did not accumulate in bream liver to measurable concentrations ($<0.44 \mu\text{g kg}^{-1}$ (LOQ), Figure D 11). The other way around, the short-chain precursor 6:2 FTNO was only detected in

bream liver from Rivers Elbe, Mulde and Rhine (with concentrations decreasing), but not in zebra mussel from the same sampling sites.

Except for PFOS, PFASs were mostly < LOQ in the spatiotemporal analyses (Figure 16). However, in 4 out of 5 analyses, PFHxS and perfluorodecanesulfonic acid (PFDS) were determined in bream liver from 2001. In most cases, their concentration dropped < LOQ until 2018.

Results of the TOP assay revealed opposing trends for bream liver from different sampling sites (Figure 16). Different to the common trends of C8 PFAS, the trends of Deltas C2–C14 were not necessarily shared between bream liver and zebra mussel. For example, in zebra mussel the concentration of Delta C8 decreased at all sites – also in Dessau and Prossen where monitoring of bream liver indicated upwards trends. Again, many results fell <LOQ. Primarily, this hindered trend analyses of Deltas C2 and >C11 (>50 % of results <LOQ).

In summary, the spatiotemporal comparison of PFAS concentrations in aquatic biota revealed local differences of PFAS trends (e.g. increasing trends in Blankenese vs. decreasing trends at the other sampling sites of bream liver). However, most trends were the same for bream and zebra mussel and/or sampling sites (e.g. the common downwards trend of FOSA). In particular, the changes in concentrations of C8 PFAS show a uniform contamination pattern. Thus, many qualitative patterns and trends of the time series analyses might have a generic rather than a species-specific and/or local character.

5.3 Sum Concentrations, Patterns and Trends

On average 24, 23 and 13 of the 58 analytes were detected in herring gull egg, bream liver and zebra mussel, respectively, with maximum numbers of 30, 28 and 19 PFAS in samples from 2002, 1996 and 2007, respectively. Overall, 45 PFAS were detected at least once among all species and time points – including the substitutes 8:2 Cl-PFESA (bream) and DONA (herring gull and bream). However, the species contamination by these ether compounds was negligible (mostly <LOQ) compared to the contamination by PFCAs and PFASs. These PFAAs dominated among all analysed PFAS in herring gull egg, bream liver and zebra mussel (Figure 18). The sum PFAS concentration for target $\sum\text{PFAS}_{42}$ ranged from 10 to 1000 $\mu\text{g F kg}^{-1}$ ww in the order zebra mussel < herring gull egg < bream liver (Figure 18).

The contributions of individual PFAS to the overall PFAS load are discussed after sum concentrations and separately for long- and (ultra)short-chain PFAS. The division of PFAS by chain length is usually limited to PFAAs and excludes precursors. In this study, the chain length of the terminal degradation product – as reported in literature e.g. for the TOP assay – is used to determine the class of the precursor. However, it should be noted that many precursors may degrade to PFAAs of different chain length (depending on environmental or experimental conditions) or to degradation products which are not identified for a given precursor yet. Therefore, the division by chain length can be ambiguous for precursors and may change with new knowledge on chemical fate.

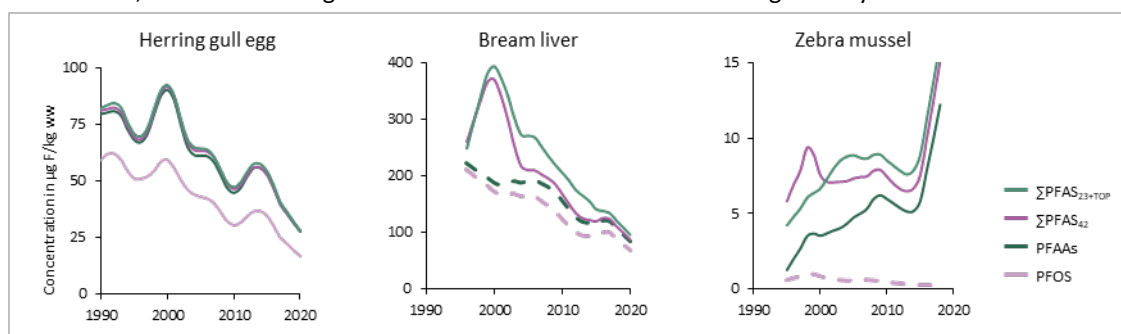
5.3.1 Are Sum Concentrations of Target PFAS decreasing?

In herring gull egg (1988–2020) and bream liver (1996–2020), the fluorine sum concentration decreased linearly over time whereas in zebra mussel (1995–2018), it increased in a non-linear manner (Figure 18), or in a linear manner if not normalized to fluorine. The decreasing trends of total PFAS concentrations in herring gull egg and bream liver suggests that PFAS contamination decreased both in the coastal and in the riverine benthic food chain in accordance with the voluntary and regulatory-driven changes on the PFAS market. Previous studies also showed

decreasing concentrations in various environmental compartments and human blood, but rather inconsistent trends in wildlife (e.g. Land et al. (2018)).

Figure 18: Non-linear trends of PFOS and sum concentrations of PFAAs, target compounds (Σ_{42}) and results from target analysis and TOP assay (Σ_{23+TOP})

All concentrations are expressed as mass concentrations of PFAS fluorine. Herring gull eggs (n=22; pool size ≥ 25 eggs) originated from Mellum (North Sea), bream livers (n=19; pool size ≥ 20 fish) from Koblenz (Rhine) and zebra mussel (n=19; pool size: 2000–5000 mussel) from Blankenese (Elbe). Values <LOQ were treated as zero. Solid line: significant trends; dashed line: insignificant trends. Note the different scaling of the y-axes.



Source: own illustration, UFZ.

Compared to results of previous time series analyses of the same species and/or sampling sites, the findings of the present study generally agreed well. Moreover, the present study prolonged existing time series (as for herring gull egg), complemented them with a new sampling site (Koblenz for bream liver) or with advanced analytical methodology (extended target analyses, TOP assay for PFAS $\geq C2$). Monitoring studies of PFAS in mussel are particularly scarce with signals of PFAS usually falling below LOQ (e.g. 48: 39/40 or 40/40 PFAS). However, advancing analytical techniques promoted sensitivity (median LOQ in zebra mussel: $0.5048 \pm 0.07 \mu\text{g kg}^{-1}$) so that the present study could reveal trends of low PFAS concentration in freshwater mussel.

5.3.2 What Information is gained by the TOP Assay?

Similar to ΣPFAS_{42} sum concentrations (target analyses), downwards trends were also obtained for the concentrations of $\Sigma\text{PFAS}_{23+TOP}$ (target analyses and TOP assay combined, Figure 18) In zebra mussel, the upwards trend of the overall PFAS load, normalized to the fluorine content, became significant only when results of the TOP assay were considered besides target analyses (linear trend for $\Sigma\text{PFAS}_{23+TOP}$ in contrast to non-linear trend for ΣPFAS_{42}).

The contribution of precursors (both known and unknown) was nearly negligible in herring gull egg (approximately 4 %, Figure 18: $\Sigma\text{PFAS}_{42} \approx \Sigma\text{PFAS}_{23+TOP} \approx \text{PFAAs}$). Literature already indicated that concentrations of precursors are generally low in herring gull eggs from the North Sea (ECHA 2023). The capacity of herring gulls to metabolise FOSA to PFOS was already suggested in 2009 based on a predator/prey comparison of PFOS:FOSA for the Great Lakes (Gebbinck et al. 2009). While the transfer to the egg has been described as an efficient way of PFAS depuration for female breeding birds (Gebbinck and Letcher 2012), *in-ovo* paths of biotransformation are still widely unknown.

In contrast to herring gull egg, in bream liver and zebra mussel, precursors significantly contributed to the overall PFAS load $\Sigma\text{PFAS}_{23+TOP}$ (on average 27 % and 39 %, respectively). For both species, the TOP assay was a valuable tool in estimating the contribution of unknown precursors. The unknowns emerged after the year 1997 in bream liver and after 2000 in zebra mussel (Figure 18: $\Sigma\text{PFAS}_{42} < \Sigma\text{PFAS}_{23+TOP}$). Generally, $\Sigma\text{PFAS}_{23+TOP}$ was expected to exceed ΣPFAS_{42}

as any combination of target analyses is limited in its scope whereas the scope of the TOP assay is unspecific (all oxidizable precursors – if present) and thus larger.

However, the TOP assay may also reach its limits which become visible when comparing the proxies of the overall PFAS load, $\sum\text{PFAS}_{42}$ and $\sum\text{PFAS}_{23+\text{TOP}}$, before the year 1997 in bream liver and 2000 in zebra mussel. First, in bream liver, the known precursors from the extended target analyses already accounted for the formation potential of the TOP assay ($\sum\text{PFAS}_{42} \approx \sum\text{PFAS}_{23+\text{TOP}}$) making the TOP assay redundant. Second, in zebra mussel, the TOP assay underestimated the formation potential from precursors ($\sum\text{PFAS}_{42} > \sum\text{PFAS}_{23+\text{TOP}}$) possibly due to a (matrix-specific) impairment of the oxidation process and/or a reduced recovery of the dominating precursor FOSA.

To date, the TOP assay has only been applied to few biota samples. This study is the first report on results of the TOP assay in herring gull egg and zebra mussel. In bream liver, precursors were studied before, by a modified form of the TOP assay called dTOP, in Bimmen located 275 km downstream Koblenz (Göckener et al. 2021). While the temporal profile determined by dTOP was similar to the results of TOP assay in the present study (peak concentration at about 2005/2007, trends not shown), the authors of the earlier study determined a higher ratio between precursor and PFCA concentration (ratio 5 vs. ratio 2).

5.4 Temporal Trends of Long-Chain PFAS and their Precursors

Long-chain PFAS – which include PFHxS, PFOA and PFAS of a longer alkyl chain – generally also belong to the class of legacy PFAS because nowadays they are – with a few exceptions – regulated under European law, e.g. EU (2010) and EU (2020).

5.4.1 Is the C8 Phase-out mirrored in Monitoring Data?

In herring gull egg, bream liver and zebra mussel, the concentration of PFOS decreased by approximately 4 % annually on average (Figure 18). However, in recent samples of herring gull egg and bream liver, PFOS still accounted for more than 60 % of the total PFAS load with PFOA concentrations being 100–1000 times lower. Similar to PFOS, the concentrations of PFOA also decreased significantly (by ≥ 40 %) over the course of the time series (Figure 19A). However, in zebra mussel, the signal of PFOA was often $< \text{LOQ}$ (reported as $\text{LOQ}/2 = 0.30 \mu\text{g kg}^{-1}$), so no trend could be deduced.

The PFOS decline in herring gull egg, bream liver and zebra mussel illustrate the effect of 3M's POSF-based phase-out between 2000 and 2002 (Weppner 2000) which was already described in aquatic, terrestrial and human samples (Yeung et al. 2013, Falk et al. 2019, Göckener et al. 2021). However, first steps in a global phase-out apparently started before 3M's announcement – as can be seen by the early decline of PFOS concentrations in bream liver from Koblenz and herring gull egg from Mellum (Figure 18). Similarly, PFOA started to decrease in concentration (Figure 19A) before it was identified as Substance of Very High Concern (SVHC) in 2013 under the European Chemicals Regulation REACH (ECHA 2013) and also before the US EPA's "PFOA Stewardship program 2010/2015" (US EPA and Johnson 2006, US EPA 2017).

5.4.2 How relevant are Precursors of C8 Chemistry?

The EU POP regulation which regulates the use of PFOS and PFOA since 2010 (EU 2010) and 2020 (EU 2020) also covers the use of precursors. As readily degradable precursors, these PFAS are considered as problematic as their persistent terminal degradation products in the environment.

In target analysis, herring gull egg showed a high diversity of C8 precursors (up to 12 PFAS in one sample (2002)). However, the concentrations were relatively low compared to PFOS and PFOA

(lower vs. upper $\mu\text{g kg}^{-1}$ range) and the temporal profiles varied from those of the terminal degradation products.

While certain PFOS precursors, N-methylperfluorooctane sulfonamidoacetic acid (MeFOSAA), EtFOSAA and diSAmPAP, decreased in herring gull egg after a maximum concentration in 1995/1996 or constantly over the course of the time series (starting in 1990, perfluorooctane sulfonamidoacetic acid (FOSAA)), the PFOA precursors 8:2 diPAP and 6:2/8:2 diPAP increased until 2004 and decreased afterwards (Figure 19A). In turn, PFOS – as the terminal degradation product⁶¹ – already decreased in concentration while its precursors still increased (approx. until 1996, Figure 18 vs. Figure 19A). Therefore, degradation from precursors seems to be a minor source of PFOS contamination as compared to direct exposure.

Different to PFOA, its precursors – fluorotelomer phosphate diesters (diPAPs) (Zabaleta et al. 2017) – dropped markedly in concentration only after 2010 in herring gull egg. Before that time, they even increased. Therefore, in herring gull egg, the temporal contamination profiles (Figure 19A) directly followed the timeline of regulatory measures and substitution on the chemical market: First, diSAmPAP and other precursors of PFOS were used – e.g. in the food packaging industry. Next, POSF-based chemistry was replaced by diPAPs (Zabaleta et al. 2017) which were in turn replaced themselves by short-chain PFAS (discussed below) and later on by polymer-based and fluorine-free alternatives (not covered in this study) (OECD 2020). In the food packaging industry, market shares of PFAS-free alternatives are still $\leq 1\%$ (OECD 2020) whereas knowledge on the environmental fate of the new fluorinated substitutes – the polymers – and their degradation products is still lacking. (Minet et al. 2022, Lohmann and Letcher 2023).

The low concentrations of precursors in herring gull egg should be interpreted with caution. Nonetheless, their temporal profile may indicate a changing source of PFAS in the environment with possibly higher concentrations closer to the source (before undergoing distribution processes, biotransformation and elimination). For herring gull eggs in Germany, the major source of contamination is presumably associated with the terrestrial and less with the marine environment because the female bird prefers terrestrial feeding grounds before egg laying (Enners et al. 2018).

In bream liver and zebra mussel, the trends of PFOS precursors generally agreed well with those in herring gull egg (Table 3). However, this comparison of target results is limited to the years 2000–2010 when concentrations were consistently decreasing (before they increasing in some instances and later falling $< \text{LOQ}$ in many cases). In bream liver, a decreasing temporal trend was found for six precursors – including EtFOSE and those precursors, which also decreased in herring gull egg. Moreover, the concentrations of FOSA, FOSAA and EtFOSAA decreased in herring gull egg, bream liver and zebra mussel. The precursor EtFOSE and its intermediate degradation products EtFOSAA, FOSAA and FOSA show similar temporal profiles in bream liver.

Table 3: Decreases in concentrations of PFOS and its precursors in biota from the German Environmental Specimen Bank for the years 2000–2010

Samples of bream liver (n=11; pool size ≥ 20 fish) originate from Koblenz (Rhine), herring gull egg (n=11; pool size ≥ 25 eggs) from Mellum (North Sea) and zebra mussel (n=9; pool size: 2000–5000 mussel) from Blankenese (Elbe). “NA”: not applicable as the trend is not significant or the majority of values is $< LOQ$.

	Linear fit for 2000–2010 Annual decrease in $\mu\text{g kg}^{-1}$			Non-linear fit based on whole time series Percentage decrease for 2000–2010		
	Bream liver	Herring gull egg	Zebra mussel	Bream liver	Herring gull egg	Zebra mussel
PFOS	-5.55	-4.66	-0.03	-28%	-48%	-47%
FOSA	-1.86	-0.04	-0.27	-74%	-67%	-80%
FOSAA	-0.41	-0.02	-0.01	-85%	-78%	-80%
EtFOSAA	-0.99	-0.02	-0.02	-90%	-93%	-95%
MeFOSAA	-0.36	-0.01	NA	-82%	-84%	-68%
diSAmPAP	-0.01	-0.02	NA	-77%	-98%	NA
EtFOSE	-37.5	NA	NA	-97%	NA	NA

The TOP assay confirmed the decreasing trends of known and unknown C8 precursors in bream liver and zebra mussel (Figure D 1). For herring gull egg however, results from the TOP (called Delta C8) assay were below the LOQ of C8.

In wildlife, concentrations of C8 PFAS reported in literature are inconsistent because of regional differences (Land et al. 2018). Monitoring data and temporal trends on precursor PFAS are still scarce. Eriksson et al. (2016) determined PAPs in eggs of osprey from Sweden with the maximum concentration in a sample from 2008/2009. Similarly, Göckener et al. (2022) described their concentration dropping in suspended matter from three major German rivers between 2005 and 2013.

In summary, three decades after PFOS has been phased out, legacy PFAS persist in the riverine and the coastal environment. In particular, PFOS remains environmentally relevant with high shares of the total PFAS contamination in herring gull and bream – species which are prone to bioaccumulation. Nevertheless, also known and unknown C8 precursors can contribute markedly to the total PFAS load as demonstrated by target analyses (e.g. EtFOSE in bream liver) and the TOP assay (Delta C8 in bream liver and zebra mussel).

5.4.3 Were all long-chain PFAS phased-out in parallel?

In parallel with PFOS and PFOA, other long-chain PFAS became subject to regulatory scrutiny – first, within the scope of the US EPA’s “PFOA Stewardship program 2010/2015” (US EPA and Johnson 2006, US EPA 2017) and later, in 2023, under EU REACH regulation (C9–C14 PFCAs) (EU 2021). Unlike PFOA, the other long-chain PFCAs were only present as impurities in mixtures and products of the EU (Wirth et al. 2019).

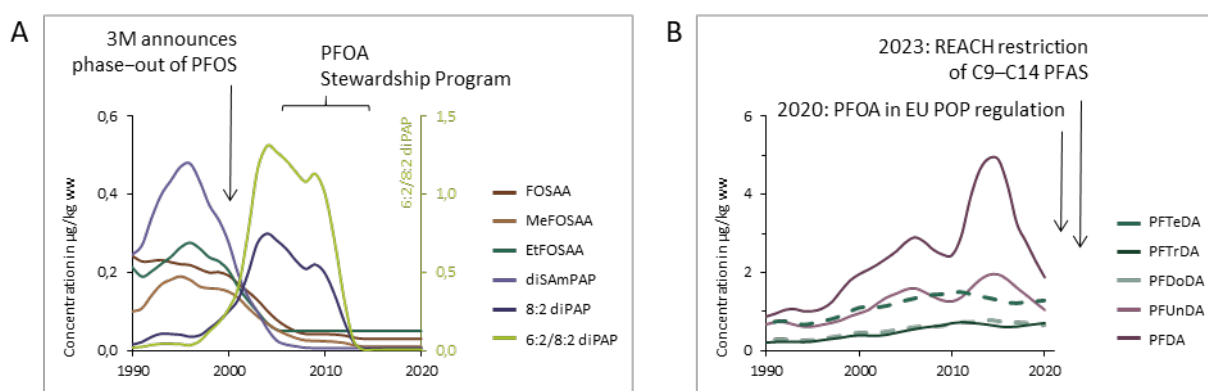
Monitoring results of the present study show that the C10 – C14 PFCAs followed a different trend compared to PFOA. In herring gull egg, their concentrations increased until 2010 or more recent years. For PFTeDA (C14 PFCA), the long-term trend was still increasing in 2020 without having reached a maximum (Figure 19B). In bream liver (Figure D 2A) and zebra mussel (Figure D 2B) in

turn, the concentration dropped for all >C10 PFCAs, including PFTeDA, after reaching a maximum. From visual observation, the maximum was reached approximately at the same time for C10–C13 PFCAs (in 2011 or before).

Among all >C8 PFCAs, largest shares were reached by PFTeDA in zebra mussel (median: 31 %) and PFDA (C10) in bream liver (33 %) and herring gull egg (28 %). In all three species, stable concentrations of PFNA (C9) were observed at a relatively low level over the course of the time series (no trend, 4 %, 7 % and 22 %, respectively).

Figure 19: Non-linear time trends of individual PFAS in herring gull egg from Mellum in the period 1980 to 2020 (North Sea; n=22; pool size ≥25 eggs)

Trends are shown for (A) precursors of C8 PFAS and (B) C10–C14 perfluoroalkyl carboxylic acids. Solid line: trend is significant; dashed line: not significant. Note the different scaling of the y-axes and the separate y-scale of the precursor 6:2/8:2 diPAP.



Source: own illustration, UFZ.

The phase-out of PFCAs >C8 was expected to follow that of PFOA – at the latest in 2020 when the EU POP regulation became effective (EU 2020). However, data presented in the present study illustrate that > C8 PFCAs are still present in the environment and some might still increase in concentration as implied by the trend of PFTeDA in herring gull egg from Mellum. Moreover, PFOA already started to decrease in concentration early, in parallel with PFOS (see chapter above) and apparently without an (immediate) effect on environmental loads of >C8 PFCAs.

Even if their levels are still low compared to PFOS, the overall increasing trends of >C8 PFCAs may be considered an early warning signal for ecosystem health and human food production. In particular C12–C14 PFCAs – have a high bioaccumulation potential in the food chain as compared to their homologues of shorter chain length (Gobas et al. 2020). To assess the effectiveness of the EU's new restriction on overlooked long-chain PFCAs, future studies should continue to monitor time trends of long-chain PFAS. As the EU regulation became effective in 2023 (EU 2021), its effects were outside the scope of the present study.

Increasing trends of long-chain PFCAs were reported before in birds' eggs (UK Northern gannets (*Morus bassanus*, 1988–2013 for C10, C11 and C13) (Holmström et al. 2010) and Swedish peregrine falcons (*Falco peregrinus*, 1974–2007 for C9–C15)) (Bustnes et al. 2022) but also in mammals (Scandinavian otters (*Lutra lutra*, 1972–2011 for C9–C14) (Roos et al. 2013) and grey seals (*Halichoerus grypus*, 1974–2008 for C12–C14)) (Kratzer et al. 2011) and fish (eelpout from the Baltic Sea (*Zoarces viviparus*, 2003–2017 for C9–C11)) (Flidner et al. 2020).

5.4.4 How relevant are precursors of >C8 PFAAs?

Besides PFCAs, few long-chain PFAS were detected. Similar to C8 chemistry, among precursors of longer chain-length, PAPs (e.g. 10:2 mono- or diPAP) were also determined occasionally in samples of all three biota – but not in recent samples. In herring gull egg, a change from detects to non-detects of 4:2/10:2 diPAP co-occurred with the peak concentrations of the 8:2 homologues in 2010 (see chapter above). Thus, the results of >C8 further illustrate the market shift from diSAMPAP to long-chain diPAPs and later on to other alternatives e.g. in the food packaging industry. (Zabaleta et al. 2017, OECD 2020).

In total, the results of long-chain precursors – determined either by target analyses or by TOP assay – corresponded to a low potential for formation of PFCAs as compared to direct contamination by perfluorinated compounds. Due to the wider scope, the TOP assay also revealed more trends than the analyses of targeted precursors. For example, in herring gull egg, it revealed that the concentration of Delta C10 reached a maximum approximately in 2015 (Figure D 3) and in zebra mussel it revealed that the concentrations of Deltas C9 and C10 followed an increasing trend until 2010 before reaching a plateau at approx. $0.3 \mu\text{g kg}^{-1}$, respectively (Figure D 4).

The cumulative formation potential of long-chain PFCAs from precursors determined in this study is lower than expected for bream liver from River Rhine. When Gökener et al. (2021) analysed comparable samples from Koblenz by dTOP assay (method explained above), the concentrations were multiple times higher than those determined in the present study for Koblenz where sample extracts were oxidised. Nonetheless, the temporal patterns of individual PFCAs were similar, following non-linear trends with peak concentrations roughly in between 2007 and 2015 (trends not shown).

5.4.5 How relevant are Perfluoroalkyl Sulfonic Acids?

The perfluoroalkyl sulfonic acids PFHxS and PFDS are homologues of PFOS which occurred less frequently (only in bream liver and in herring gull egg, not detected in zebra mussel) and at lower concentrations than PFOS (approx. 10 – 100-fold lower concentrated). In bream liver, the concentration of PFDS decreased, by 92 % after a peak concentration in 2002 (trend not shown). Afterwards, the trend levelled off at about $0.4 \mu\text{g kg}^{-1}$. The concentration of PFHxS decreased both in herring gull egg and in bream liver (Figure D 5). The decreasing trends of PFHxS and PFDS might be the effect of an advancing phase-out of all long-chain PFAS and not only of the C8 chemistry (and long-chain PFCAs as discussed above).

However, previous studies in wildlife samples reported a rather inconsistent temporal development of PFDS concentration over time (1969–2012) – in particular for birds whereas mammals tended towards increasing concentrations and fish towards decreasing concentrations (Land et al. 2018). Moreover, the decreasing concentrations of PFHxS are opposed to results reviewed by Land et al. (2018) on biota of different species and geographical origin. In the majority of studies, the authors found increasing trends or insignificant trends, but individual time series were also decreasing (e.g. fish (Sweden) and marine mammals (Germany)). Since 2023, PFHxS is listed under EU POP regulation. (EU 2023)

5.5 Temporal Trends of Short- and Ultrashort-Chain PFAS and their Precursors

5.5.1 Are Short-Chain PFAS replacing their Longer Homologues?

With regulatory pressure growing to phase-out long-chain PFAS, industry generally switched to alternatives of shorter chain length – in particular to C6-based PFAS which were assumed to be environmentally safe (Wang et al. 2013). This early development in chemical management was

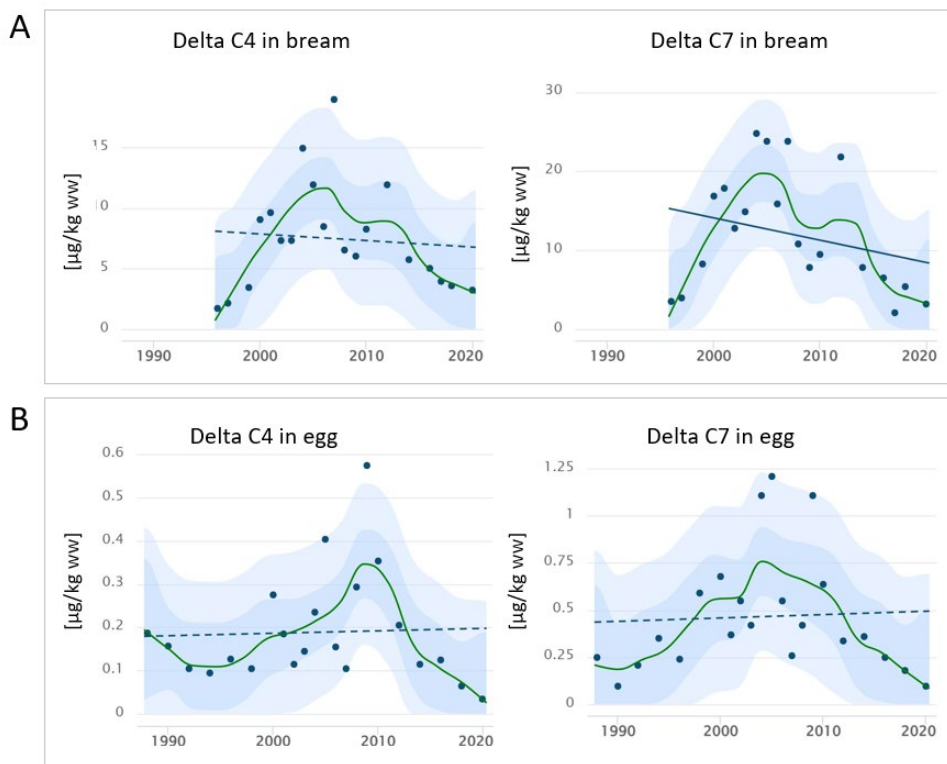
mirrored by results of the TOP assay in zebra mussel (Figure 19B). The trends of Deltas C4–C7 were commonly increasing and peaked approx. in 2005. The same level of concentration was reached again (or exceeded) at the end of the time series (in 2018), respectively. The retrospective long-term trends (1995–2018) correspond to precursor concentrations of short-chain PFAAs being on the rise already for decades in zebra mussel.

In contrast, concentrations of short-chain PFAAs were too low (<LOQ) to see an effect of the market shift if present. The different findings of precursors and PFAAs in zebra mussel could be explained by increased sorption affinity to sediments combined with lower water solubility of the perfluorinated compounds as compared to their precursors of similar chain length. Similarly, Langberg et al. (2020) hypothesised that sediment acts as a sink of PFAS after degradation of precursors. Consequently, the sample of zebra mussel and breathing water presumably represents the dissolved rather than the particle-bound fraction of PFAS in the aquatic system.

In TOP assay data from bream liver (Figure 20A the examples of Deltas C4 and C7), the temporal profiles also reached a maximum between 2003 and 2007. However, afterwards, when the concentrations dropped, they dropped for a longer time than in zebra mussel. Therefore, in 2020, the concentrations approximated the initial concentrations from 1995 again. In herring gull egg, full profiles (detection frequency $\geq 80\%$) were obtained only for Deltas C4 and C7 (Figure 20B). For Delta C7, the profile matched those in aquatic biota. For Delta C4, the peak concentration was reached later, in 2010.

Figure 20: Temporal trends of Deltas C4 and C7 (TOP assay) in (A) bream liver from Koblenz (Rhine; n=19; pool size ≥ 20 fish) and (B) herring gull egg from Mellum (North Sea; n=22; pool size ≥ 25 eggs).

Solid line: significant linear or non-linear fit; dashed line: not significant; blue line: linear fit; green line: non-linear fit; shadowed areas: 95% confidence (dark blue) and 95% prediction interval (light blue). Note the different scaling of the y-axis.



Source: own illustration, UFZ.

Among short-chain PFCAs (C4–C7), full temporal profiles (detection frequency $\geq 80\%$) were obtained only for PFBA (C4) and/or perfluoroheptanoic acid (PFHpA) (C7) in herring gull egg and bream liver. In herring gull egg for example, both short-chain PFCAs were determined at a relatively stable concentration of $0.2 \mu\text{g kg}^{-1}$ (no linear trend, profiles not shown).

5.5.2 Which precursors contributed to the formation potential of short-chain PFCAs?

While the TOP assay determined the quantity of precursors and differentiated approximately between short- and long-chain PFAS, individual PFAS could only be identified by target analyses. The precursors of short-chain PFCAs which were identified included FBSA in herring gull egg (detection frequency: 77%), FBSA and FHxSA in bream liver (detection frequencies: 18/19) and 6:2 diPAPs (occurring occasionally), FHxSA (consistently since 1995), FBSA (emerging in 2010) and 6:2 FTSA-PrB (Figure D 6C, trend discussed in next chapter) in zebra mussel. Moreover, in the egg, 4:2 FTSA followed a non-linear trend with concentrations ranging between <0.01 and $0.73 \mu\text{g kg}^{-1}$. In bream liver, perfluorohexane sulfonamidoethanol (FHxSE) and its intermediate degradation product FHxSAA emerged and disappeared in the past (in line with trends of EtFOSE and other C8 precursors).

Generally, monitoring data on the occurrence of short-chain PFAS in biota is scarce, although the compounds are suggested as contaminants of emerging concern (Brendel et al. 2018, Ateia et al. 2019). Mostly, literature reports on a high abundance (e.g. of PFBS and PFBA) in surface waters (Zhao et al. 2015, Pan et al. 2018, Muir and Miaz 2021). If short-chain PFAS are monitored in biota, they often range in concentrations between $< \text{LOQ}$ and $1 \mu\text{g kg}^{-1}$ (Chu et al. 2016, Kärman et al. 2019, Huang et al. 2022, Guckert et al. 2023). Chu et al. (2016) reported a widespread contamination of FBSA as a new contaminant in Canadian fish. In the present study, the precursor of PFBS was detected in herring gull eggs, bream liver and zebra mussel, also occasionally in samples from before the market shift.

5.5.3 Is 6:2 FTSA-PrB an example of regrettable substitution?

Many substitutes were on the market even before the phase-out of long-chain legacy PFAS and promoted then as safer alternatives – e.g. 6:2 FTSA-PrB – formerly known as 6:2 fluorotelomer sulfonamidopropyl betaine (FTAB) (Nguyen et al. 2020) and now marketed as Capstone B (EU 2022). In zebra mussel, 6:2 FTSA-PrB increased in concentration (Figure 19A) at a similar rate and to a similar concentration as the one FOSA had reached in 1997 and fallen from afterwards (until 2018: $+4$ vs. $-2 \mu\text{g kg}^{-1} \text{a}^{-1}$, max. approximately $10 \mu\text{g kg}^{-1}$). This illustrates exemplarily the relation between phase-out of legacy PFAS and emergence of fluorinated alternatives which were or are used in aqueous film-forming foams (Favreau et al. 2017).

Often, the compound 6:2 FTSA-PrB is associated with contamination at incident sites after firefighting activities (D'Agostino and Mabury 2017). However, the compound is rarely monitored elsewhere. With concentrations in zebra mussel from Blankenese increasing constantly over time, the cause for the contamination of 6:2 FTSA-PrB is presumably a continuous emission source upstream River Elbe. Hence, the increasing trend should be an early warning for the local industry.

Contamination by the precursor 6:2 FTSA-PrB alone only partially accounts for the formation potential of C4–C7 PFCAs whereas the contributions of other precursors of short-chain PFAS remain largely unknown. This follows Ruyle et al. (2021) who determined that 6:2 FTSA-PrB is oxidised to 8% PFPeA, 33% PFBA and 21% PFPrA in TOP assay. To fill this gap, more quantitative methods for precursors of short chain length are needed.

5.5.4 Is trifluoroacetic acid a contaminant of emerging concern?

Ultrashort-chain PFAS have unique exposure pathways, which diverge from those of short-chain and long-chain PFAS. Further, the concentration of TFA in atmospheric deposition and surface water is typically most abundant among PFAS (Björnsdotter et al. 2022). Much of it originates from the decay of anthropogenic fluorinated gases (used as refrigerants and blowing agents) (Wallington et al. 1994, Kotamarthi et al. 1998) in the atmosphere. Temporal trends have not been reported for samples of animal origin before.

In zebra mussel (Figure 22 C) and in herring gull egg (Figure 21), TFA also showed an increasing concentration trend – similar to short-chain PFAS. However, the annual increase was lower in herring gull egg (0.23 vs. 0.33 $\mu\text{g kg}^{-1}$ in zebra mussel). While first concentrations exceeded those in zebra mussel, this changed approximately in 2006. Despite sharing the same trend direction, TFA contributed less to the total PFAS concentration in herring gull egg (30 % vs. 80 % in 2018).

In zebra mussel, a high concentration at the end of the series (2018) might be considered an outlier. However, the concentration (34 $\mu\text{g kg}^{-1}$) is within the 95 % prediction interval of the non-linear trend. Even if the last measurement value was to be excluded, the trend would still be increasing.

In bream liver, only a non-linear trend was determined for TFA (Figure 23 A) with starting and end concentration (1995 vs. 2020) not being significantly different to each other ($p \gg 0.05$). A similarity between starting and end concentrations was also observed in the time series of DeltaC2 (Figure 23 B). Overall, the profile of DeltaC2 dominated the time series of the ΣC2 concentration (sum of TFA and DeltaC2; Figure 23 C). For zebra mussel and herring gull egg, the formation potential of TFA from precursors was often zero so that no trend analyses were carried out.

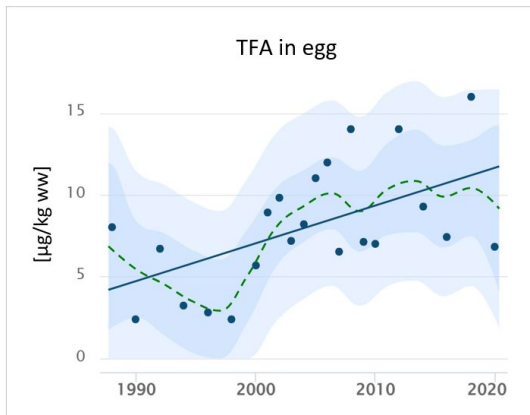
Besides C2 PFAS, the ultrashort-chain PFCA PFPrA was analysed. In herring gull egg, the concentration was relatively stable at 2 $\mu\text{g kg}^{-1}$ without showing a trend. In bream liver and zebra mussel, PFPrA was < LOQ.

Temporal profiles of TFA (in all three biota), PFPrA (in herring gull egg) and their precursors (DeltaC2 and DeltaC3 in bream liver) indicated a long-lasting contamination of these ultrashort-chain PFAS in different food chains. The upwards trends of TFA in zebra mussel and herring gull egg are in line with trends reported previously for wet precipitation (Wang et al. 2014), surface water (Cahill 2022) and plants (Freeling et al. 2022).

In non-marine environments, TFA is generally attributed to anthropogenic sources whereas natural sources are considered controversial (Frank et al. 2002). Sources of TFA are multiple including atmospheric degradation of anthropogenic fluorinated gases (used as refrigerants and blowing agents) (Wallington et al. 1994, Kotamarthi et al. 1998), thermolysis of fluoropolymers (Ellis et al. 2001) and biotransformation of precursors such as CF_3 -containing pesticides (Bhat et al. 2022), pharmaceuticals (Scheurer et al. 2017) and industrial chemicals (Sun et al. 2020).

Figure 21: Temporal trend of TFA in herring gull egg (n=22; pool size ≥ 25 eggs) from Mellum (North Sea).

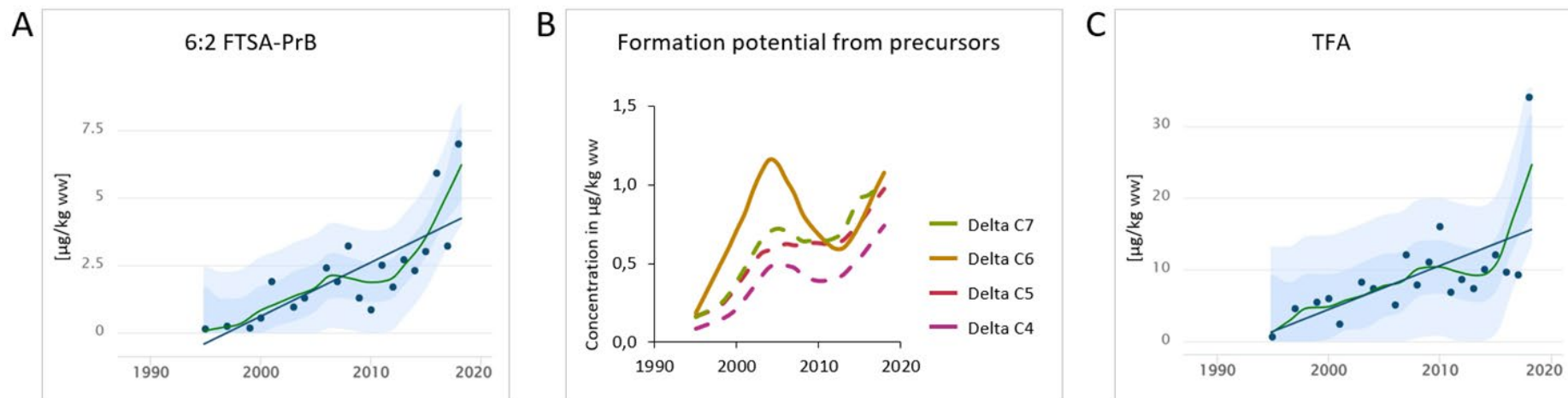
Solid blue line: significant linear fit; dashed green line: not significant, non-linear fit; shadowed areas: 95% confidence (dark blue) and 95% prediction interval (light blue).



Source: own illustration, UFZ.

Figure 22: Temporal trends of (ultra)short-chain PFAS in zebra mussel (n=19; pool size: 2000–5000 mussels) from Blankenese (Elbe) depicting (A) the precursor 6:2 FTSA-PrB, (B) the formation potential of short-chain perfluorocarboxylic acids from precursors in the TOP assay and (C) trifluoroacetic acid (TFA)

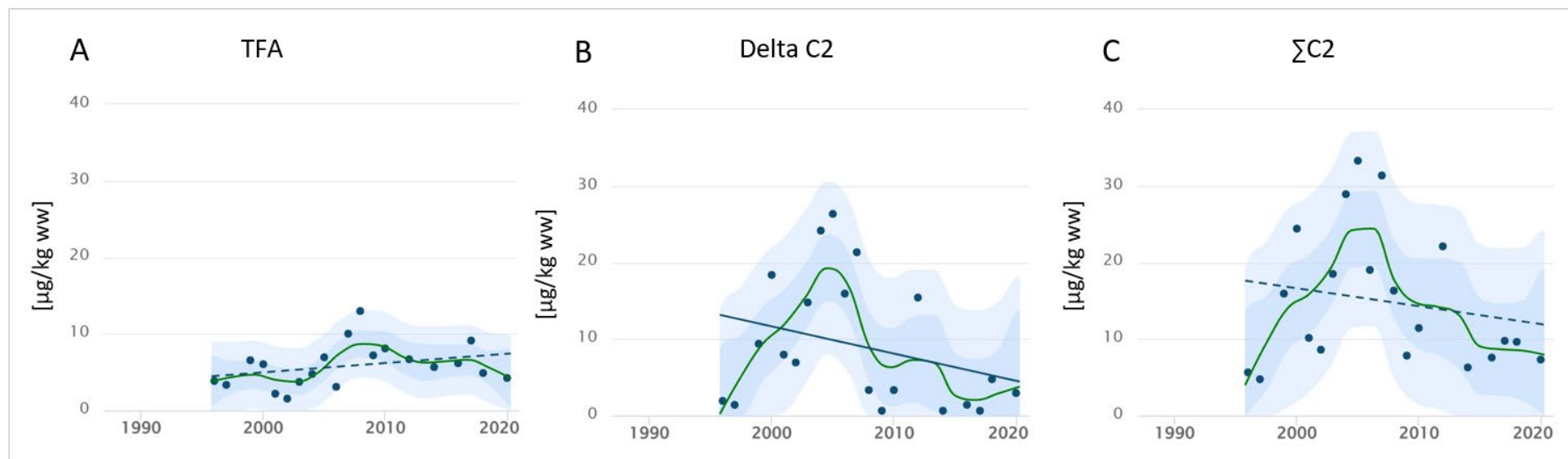
Blue lines: linear curve fit; other colours: non-linear fit; solid line: significant fit; dashed line: not significant; shadowed areas: 95% confidence (dark blue) and 95 % prediction interval (light blue). Note the different scaling of the y-axes.



Source: own illustration, UFZ.

Figure 23: Temporal trends of C2 PFAS in bream liver from Koblenz (Rhine; n=19; pool size≥20 fish).

Solid line: significant linear or non-linear fit; dashed line: not significant; blue line: linear fit; green line: non-linear fit; shadowed areas: 95 % confidence (dark blue) and 95 % prediction interval (light blue). The sum of TFA (target analysis) and Delta C2 (TOP assay) is $\Sigma C2$.



Source: own illustration, UFZ.

5.5.5 Has the risk of persistent and mobile PFAS been overlooked?

The increasing use of (ultra)short-chain PFAS is of high concern for reasons that deviate from the “classical” assessment criteria of POPs (Ateia et al. 2019). While being similarly persistent as long-chain PFAS, the same level of performance is only achievable in applications if higher concentrations of the short-chain PFAS are used (Scheringer et al. 2014). Once released to the environment, the mobile substitutes are hardly removable from water bodies where they can travel long distances (Ateia et al. 2019). Ultimately, they will contaminate the groundwater. Long-term effects are still poorly understood but first studies report on adverse health effects (Wolf et al. 2008, Zhou et al. 2020).

With increasing trends of (ultra)short-chain PFAS dominating in the biota from the bottom of the food chain (zebra mussel) as compared to those from higher levels (herring gull egg and bream liver), the findings of the present study illustrate a variety of effects caused by the persistent nature of PFAS. The upwards trends in zebra mussel in parallel with the downwards trends of many long-chain PFAS in bream liver and herring gull egg indicate that (ultra)short-chain PFAS building in the aquatic system might eventually become a higher concern than legacy PFAS biomagnifying in the food web.

The emerging risk of mobile chemicals has been underestimated in the past due to a lack of data – linked to the analytical gap for highly polar compounds (Reemtsma et al. 2016) – and due to the rigid hazard criteria of POPs in risk assessment. Against this background, in 2020, the EU started a process of refining chemical regulations for classification and labelling (CLP) and REACH (EC 2020) by adding new hazard classes (i.e. persistent, mobile and toxic (PMT) and very persistent and very mobile (vPvM)) (Arp and Hale 2023).

Further, after restriction of the long-chain PFAS, regulatory pressure is growing to phase-out short-chain PFAS as well (Scheringer et al. 2014). First, the short-chain PFAS HFPO-DA, PFBS and PFHpA were identified as SVHCs in 2019, 2020 and 2023 under EU REACH regulation (ECHA 2023). Further, restrictions might follow soon in the EU e.g. for PFHxA (ECHA 2023) or the entire class of PFAS – as proposed by five member states (ECHA 2023).

Moreover, the effects of the new regulatory developments still need to be assessed in future monitoring studies. The precursor 6:2 FTSA-PrB was already recommended for inclusion in PFAS analyses of food by the European Commission (EU 2022).

5.6 PFAS Trends in Comparison

5.6.1 PFAS trends in other aquatic biota

Since the production peak of legacy PFAS in 2000 and the first regulatory measures, the commercial use of PFAS chemicals has changed markedly. These changes were well reflected in the contamination patterns of zebra mussel which appears to react fast to changes in the environmental contamination.

In 1998, zebra mussels from Blankenese were contaminated by PFAS in the order: FOSA > TFA > DeltaC8 > PFOS >> other PFAS (e.g. DeltaC6) > 6:2 FTSA-PrB ≈ DeltaC5 and DeltaC7, each. Afterwards, the market shift resulted in opposing trends of C8 PFAS and (ultra)short-chain PFAS which changed the order markedly at the riverine sampling spot. In 2018, it was: TFA >> 6:2 FTSA-PrB > DeltaC3–DeltaC8, each ≥ FOSA > PFOS.

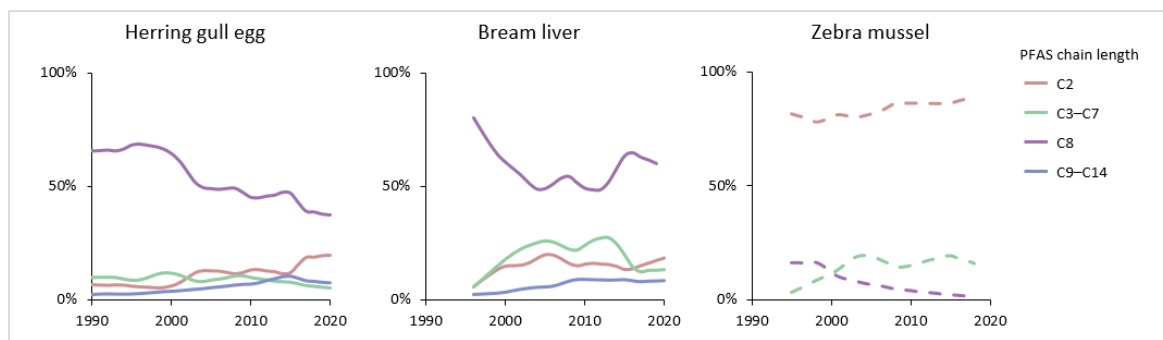
The temporal changes were less pronounced in the contamination patterns of bream liver and herring gull egg – i.e. organisms which are prone to bioaccumulation (Kannan et al. 2005, Morganti et al. 2021, Colomer-Vidal et al. 2022, Parolini et al. 2022). However, PFAS screening in samples of

those organisms revealed that contamination by long-chain PFAS is still a major concern for the safety of the food web – in particular contamination by PFOS. On the one hand, two decades after the market shift from C8 chemistry to fluorinated alternatives, the absolute concentrations are still high. On the other hand, the relative concentration of C8 PFAS remains largely unchanged if considered on a molar basis in bream liver and herring gull egg (approximately 50 % of the total molar PFAS concentration, Figure 24). In contrast, C2 PFAS clearly dominate in zebra mussel at a relatively constant rate (approximately 90 %, Figure 24).

For this comparison, molar concentrations were used for equal weighting of every molecule. Mind that mass concentrations can show a different contamination pattern (e.g. C8 > C2 in zebra mussel from 1998) as the molecular weight increases with chain length.

Figure 24: Temporal trend (1990 – 2020) for C2, C3 - C7, C8 and C9 - C14 PFAS in aquatic biota.

Relative proportion of C2, C3-C7, C8 and C9-C14 PFAS in herring gull eggs (Mellum, North Sea), bream liver (Koblenz, River Rhine) and zebra mussel (Blankenese, River Elbe).



Source: own illustration, UFZ.

5.7 Conclusion

In conclusion, legacy PFAS continue to accumulate in different food chains and (ultra)short-chain PFAS seem to be an emerging risk to the quality of water resources due to their persistent and mobile nature. Therefore, future monitoring programs should consider both risks of contamination by selection of suitable sentinel species. Inter-species differences in PFAS patterns and levels found in the present study suggest that samples of zebra mussel are suitable sentinel species for monitoring the environmental contamination by (ultra)short-chain PFAS (TFA and precursors of short-chain PFAS) whereas herring gull egg and bream liver are suitable for monitoring of legacy PFAS.

Further, a combination of different methods is recommended for future monitoring studies of PFAS when resources allow. This study found extended target analyses and the TOP assay to be useful, complementary tools in retrospective PFAS screening –shedding light on hidden trends of (ultra)short-chain PFAS and the overall load of PFAS in German wildlife.

In chemical management, it is imperative that both compound classes – the bioaccumulative and the mobile PFAS – are addressed consequently by policy makers. For this purpose, i.e. in support of the EU restriction of the entire PFAS class, the present study provides additional examples of “regrettable substitution” in chemical management (e.g. 6:2 FTSA-PrB) and illustrates that persistence alone is cause of high concern with unforeseeable, poorly manageable consequences for the environmental health.

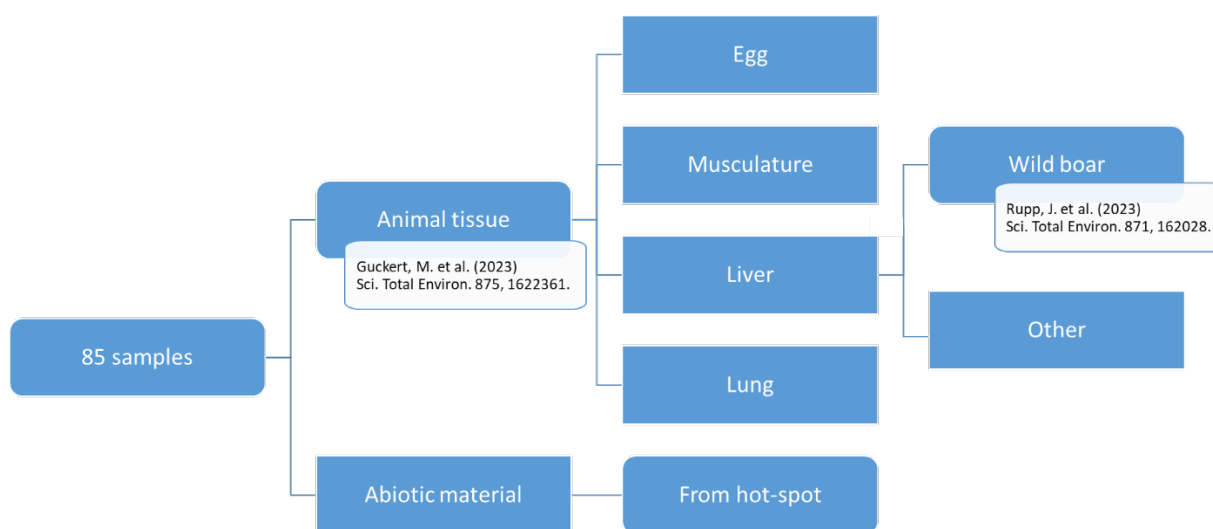
6 PFAS in German Wildlife and other environmental Samples (Work Package 2b)

In this chapter, the monitoring data for the following sample types are presented and discussed:

- ▶ abiotic samples, namely suspended matter and soils
- ▶ terrestrial animals
- ▶ aquatic animals.

Because the LOQs differed strongly for the different matrices, data < LOQ were treated as zero.

Figure 25: Experimental design of the monitoring study and of scientific publications generated from the data



Source: own illustration, UFZ.

6.1 Abiotic Samples

Soils and sediments are an important sink for PFAS in terrestrial and freshwater systems and, at the same time, a source for the contamination of terrestrial and aquatic food webs. For that reason, surface soil from one site and suspended matter from two German rivers were included in this part of the study. These samples were analysed for 66 PFAS of class A and B were analysed.

6.1.1 PFAS Concentrations and Patterns

Comparing the median PFAS contamination in suspended matter from River Saale, PFCA with chain length C8–C14 exhibit the highest concentrations (Figure D 11). However, their concentrations decreased significantly ($p < 0.05$) from 2016 to 2019, likely due to decreasing production of PFOA and its longer chained homologues (Cousins et al. 2020). Furthermore, the concentration of POSF-based precursors and fluorotelomers also slightly decreased. Presumably, as a consequence of the restrictions, the concentrations of substitutes slightly increased. Aside from the substitutes, one sample from River Saale in 2019 contained high concentrations of phosphate esters (PAP) and interestingly diSAMPAP, which was phased out in the early 2000s.

In contrast to PFCAs, PFOS concentration did not decrease in the time period. Having been phased-out in 2002, contamination levels already decreased before the monitoring period of FLUORBANK. However, the steady concentration of PFOS demonstrates its widespread use in the past, persistence, strong sorption and bioaccumulation in the environment. Samples of suspended matter from a river in proximity to site IE Alz showed a higher contamination with PFCAs (especially short chained PFCA C2–C7) and substitutes than River Saale, presumably due to emissions from the IE site, which might also explain the substitute concentrations measured (HFPO-DA, DONA) (Scheurer et al. 2017).

The level of contamination in soil is lower than in suspended matter. Other than the already for suspended matter reported PFCA and PFOS, the soil samples also exhibit a low contamination with diSAMPAP whereas the concentration of substitutes is negligible.

The soil samples were also analyzed by GC-MS analysis. However, no PFAS signal were obtained >LOQ. The suspended matter samples were freeze-dried so that volatiles and semi-volatiles are expected to be evaporated in the process.

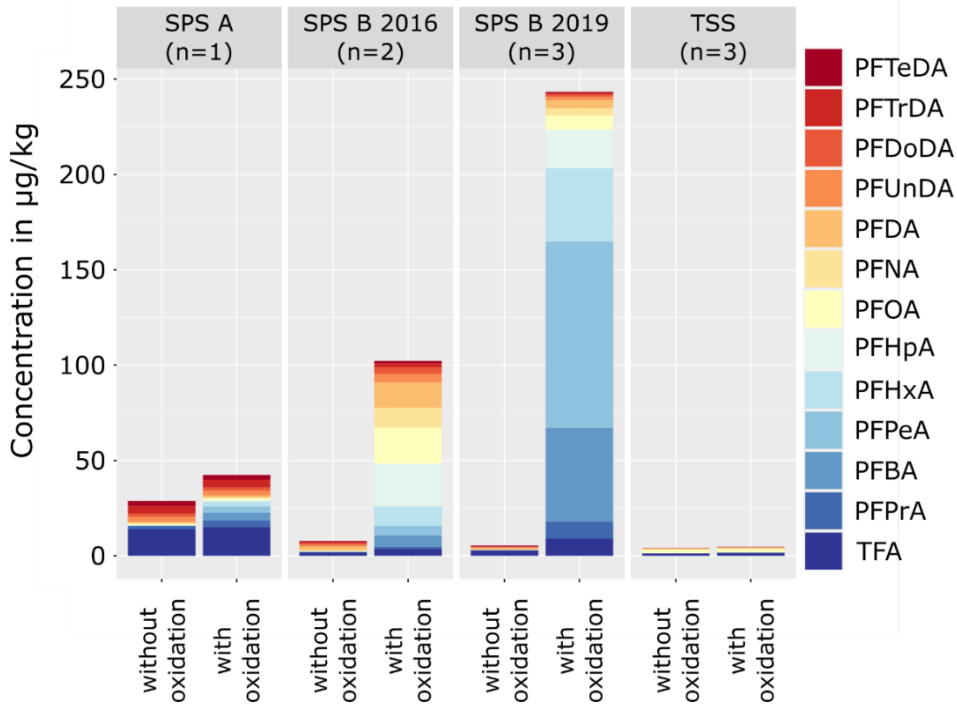
6.1.2 TOP Assay

The highest absolute growth in sum PFCA after TOP-Assay was observed in samples of suspended matter from southern German river (Site SPS B) with 238 $\mu\text{g kg}^{-1}$ (45-fold, 2019) and 94 $\mu\text{g kg}^{-1}$ (13-fold, 2016, Figure 26). In 2016 the growth derived from PFCAs with chain length C6–C10, whereas in 2019 C4–C6 were dominant (Figure 27). The shift in PFCAs toward shorter chain length might result from the restriction of PFOA, it's longer chained homologues and precursors (Cousins et al. 2020). The strong increase in PFCA cannot be explained by the precursors analysed in this study as their concentrations were low. The sample of suspended matter from River Alz showed a lower increase by the top assay (14 $\mu\text{g kg}^{-1}$). Similar to River Saale 2019, the increase derived from short chained PFCAs (C2 – C6) and cannot be explained by the precursors determined in this study, as the substitutes (HFPO-DA and DONA) detected are not transformed into PFCA by the TOP assay (Zhang et al. 2019).

It is noteworthy that the European chub sampled in a southern German river also showed a high increase by the TOP assay (70 $\mu\text{g kg}^{-1}$), the highest gain of all biota measured in this study. Unlike the sample of suspended matter from that river, the gain derived from all PFCA measured in this study (C2–C14) but its origin is also unclear. Presumably, it is due the industrial park in its proximity. It is noteworthy, that in the European chub from River Saale, the increase in PFCA derives predominantly from C4, indicating a different precursor spectrum, whereas no difference was observed in the PFCA growth of the suspended matter samples.

Figure 26: Formation potential from precursor PFAS in suspended matter and soil

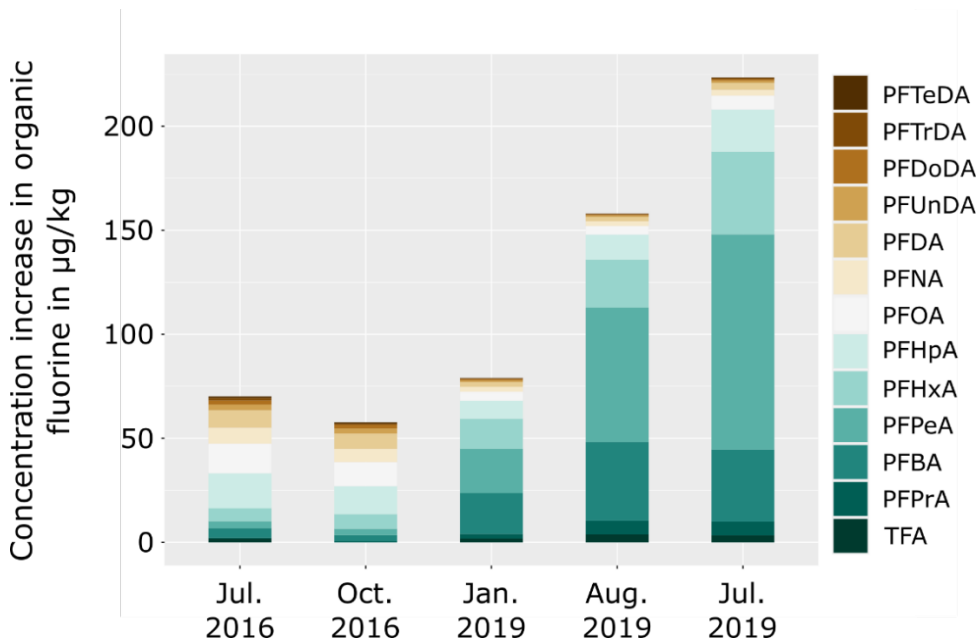
Examples for PFCA concentrations without and with oxidation (TOP assay) in abiotic samples from anonymized sampling sites. For samples with n >1, the arithmetic mean was calculated. SPS: riverine suspended matter, TSS: top soil.



Source: own illustration, TZW.

Figure 27: Increase of PFCAs in suspended matter after oxidation (TOP assay)

The samples originated from one sampling point in a Southern German river.



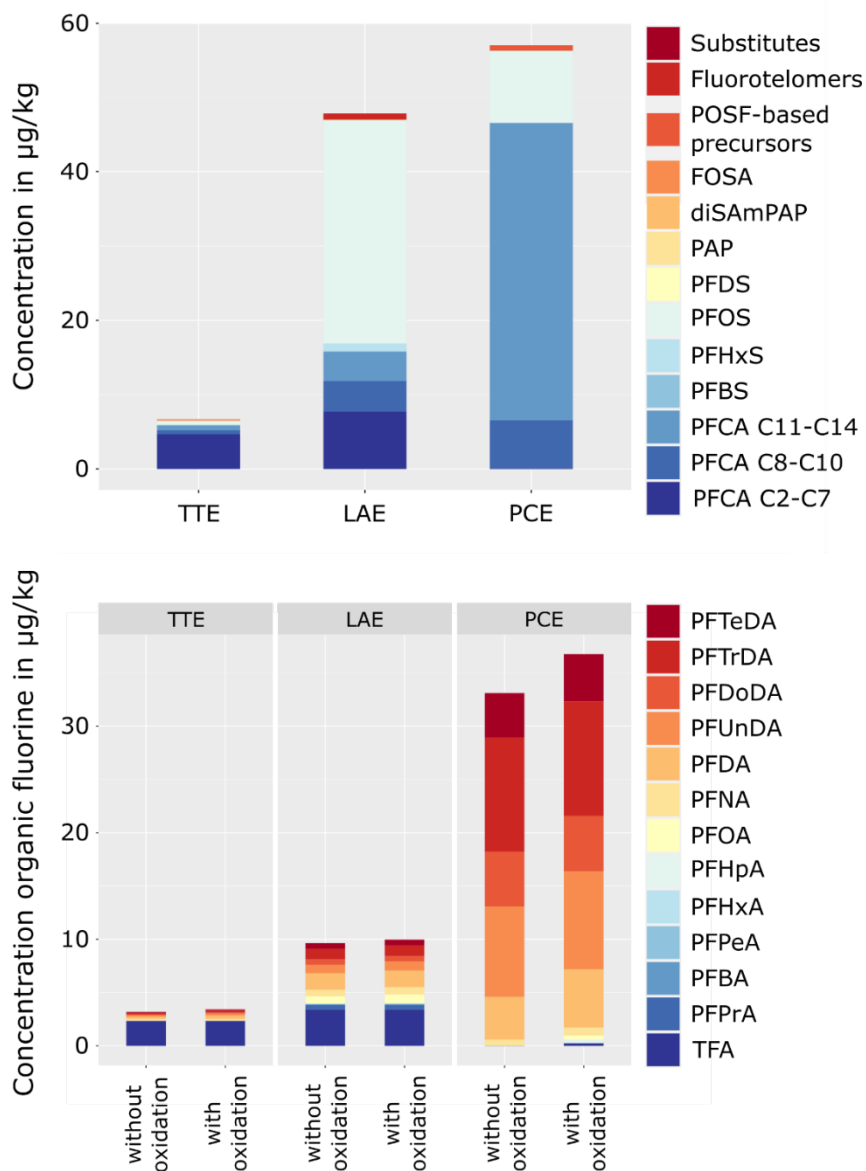
Source: own illustration, TZW.

6.2 Terrestrial Biota

In egg from great crested grebe (PCE), PFOS was the dominant PFAS, followed by C11–C14 PFCAs, while PFCAs C2–C7 were dominant in egg from black grouse (TTE). This difference may reflect the different diet of these two species, since great crested grebe mainly feed from fish whereas black grouse feeds on insects and invertebrates (Wegge and Kastdalen 2008, Ulenaers 2020). For comparison between all bird's eggs analysed in the study, PFAS concentrations for black grouse and great crested grebe are shown together with herring gull egg from the Environmental Specimen Bank (ESB) (first mentioned in chapter 4 in Figure 28).

Figure 28: PFAS concentrations and results for the TOP assay in bird's eggs

PFAS concentrations without oxidation (top) and comparison of PFCA concentrations with and without oxidation (bottom) for Black grouse (*Tetrao tetris*) (TTE), Herring gull egg (*Larus argentatus*) (LAE) and Great crested grebe (*Podiceps cristatus*) (PCE).



Source: own illustration, TZW.

6.3 PFAS patterns of herbivores, omnivores and carnivores

This chapter is based on the following publication:

Guckert M., Rupp J., Nürenberg G., Nödler K., Koschorreck J., Berger U., Drost W., Siebert U., Wibbelt G., Reemtsma T. (2023) Differences in the internal PFAS patterns of herbivores, omnivores and carnivores - lessons learned from target screening and the total oxidizable precursor assay. *Sci. Tot. Environ.* 875, 162361. <https://doi.org/10.1016/j.scitotenv.2023.162361>

6.3.1 Introduction

It was one of the aims of FLUORBANK to provide information on the PFAS concentrations in mammalian and bird species of different trophic level (herbivores, omnivores and carnivores) and from different habitat (marine, semi-aquatic, terrestrial). While such data may be available for legacy PFAS, they were lacking for novel PFAS (e. g. ultrashort-chain PFCAs, substitute compounds) as well as for precursor compounds.

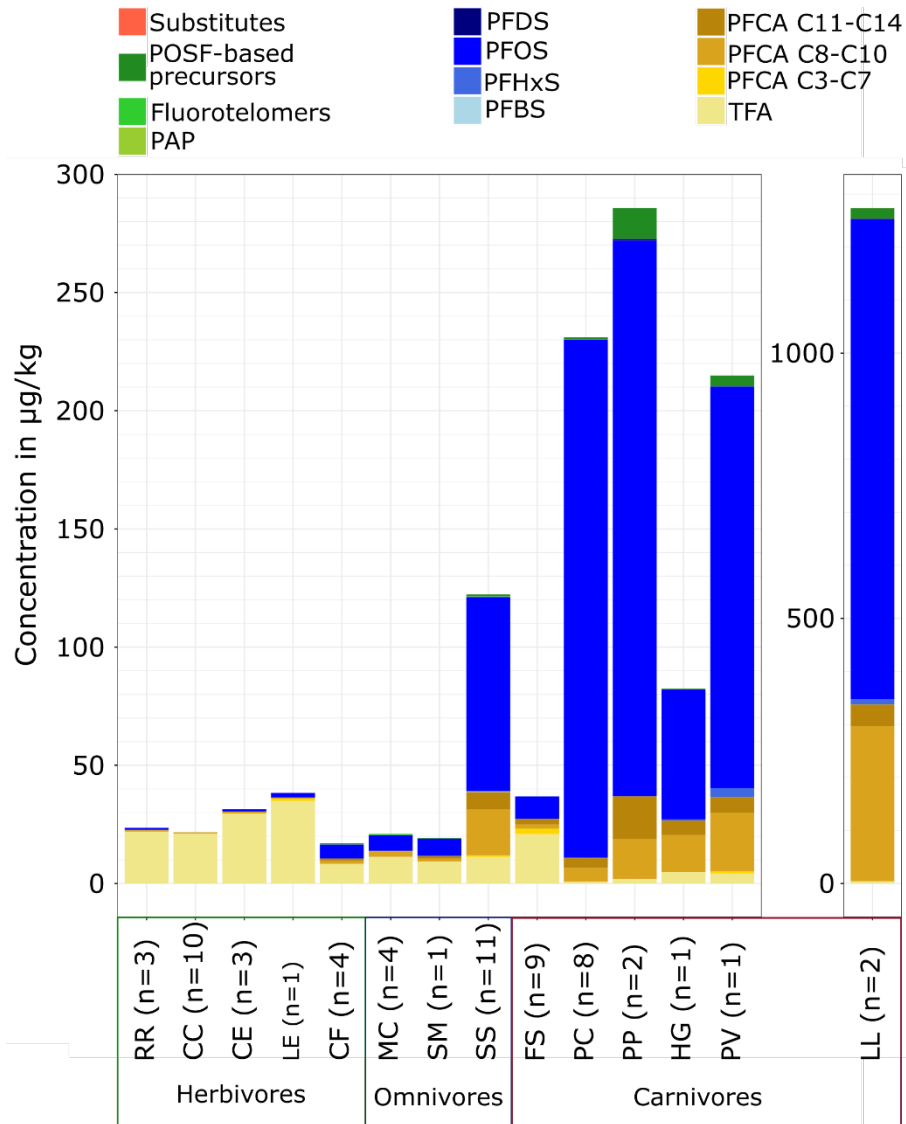
For this purpose, liver samples of 14 different mammalian and bird wildlife species collected from 2015 – 2020 in Germany and Denmark were analysed for a very broad range of 66 PFAS. In addition, the Total Oxidizable Precursors (TOP) assay was applied. To complement the interspecies comparison, musculature tissue from selected species was analysed in parallel to allow for a comparison with the PFAS found in the respective livers.

6.3.2 Terrestrial species

The mean \sum PFAS concentration in the terrestrial liver species analysed followed the order wild boar > wildcat > hare > red deer > chamois > roe deer (Figure 29, Table D 1). In herbivores, PFCAs dominated the PFAS pattern, especially the ultrashort-chain PFCA, TFA which accounted for more than >90 % of the total PFAS load (Figure 30). In addition to TFA, PFCAs with chain-length C8–C14 were detected, with individual PFCA concentrations <0.4 $\mu\text{g kg}^{-1}$. Among PFSAs, only PFOS was detected in terrestrial herbivores (max. 1.9 $\mu\text{g kg}^{-1}$ in hare). In roe deer, PFOS was not detected. However, this was the only species without PFOS findings in this study.

Figure 29: PFAS concentrations in livers from different wildlife species

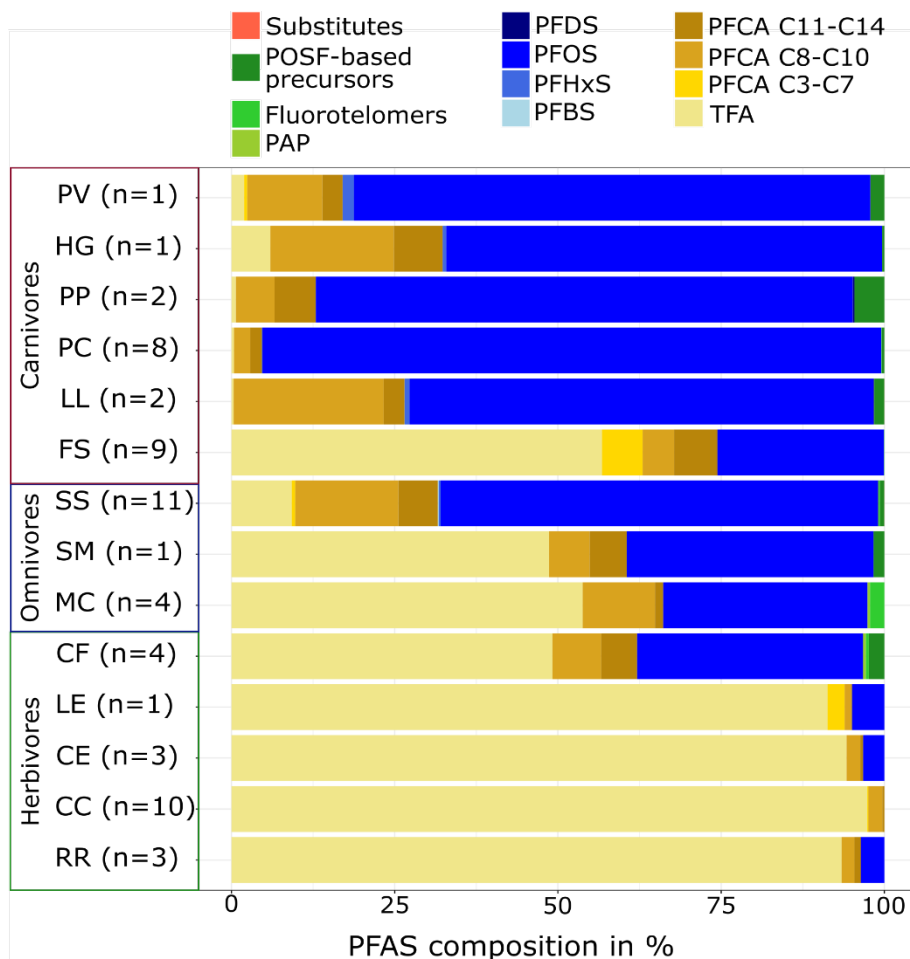
PFAS concentrations (mg/g) by target analysis. Species with n=1 are pooled samples, consisting of 5 individuals. Samples were pooled, except for RR, CE, MC and FS. Used abbreviations: red deer (CE), roe deer (CC), chamois (RR), hare (LE), beaver (CF), coypu (MC), common eider duck (SM), wild boar (SS, from (Rupp et al. 2023)), wildcat (FS), otter (LL), cormorant (PC), harbour porpoise (PP), grey seal (HG), harbour seal (PV).



Source: own illustration, TZW.

Figure 30: PFAS distribution patterns in livers from different wildlife species

PFAS composition (%) in livers from different species determined by target analysis. Species with n=1 are pooled samples, consisting of 5 individuals. Samples were pooled, except for RR, CE, MC and FS. Used abbreviations: red deer (CE), roe deer (CC), chamois (RR), hare (LE), beaver (CF), coypu (MC), common eider duck (SM), wild boar (SS, from (Rupp et al. 2023)), wildcat (FS), otter (LL), cormorant (PC), harbour porpoise (PP), grey seal (HG), harbour seal (PV).



Source: own illustration, TZW.

Similar to the PFAS pattern in herbivores, PFCAs, in particular the ultrashort-chain PFCAs were also the dominant group of PFAS in wildcat, the only terrestrial carnivore in this study (TFA 21 $\mu\text{g kg}^{-1}$, PFPrA 2.2 $\mu\text{g kg}^{-1}$). However, wildcats had comparatively higher concentrations of C7–C14 PFCAs (max. 1 $\mu\text{g kg}^{-1}$ PFDA and PFTrDA) and PFOS (9.4 $\mu\text{g kg}^{-1}$). In both, herbivores and wildcat only few polyfluorinated compounds were detected in concentrations $\leq 0.04 \mu\text{g kg}^{-1}$ – i. e. diSAmPAP and EtFOSAA in herbivores and 6:2 diPAP, 8:2 FTSA as well as qualitatively FBSA in wildcat.

Contrary to the terrestrial herbivores and wildcat, in wild boar PFOS was the dominant PFAS (82 $\mu\text{g kg}^{-1}$), followed by the PFCAs TFA and PFNA (both 11 $\mu\text{g kg}^{-1}$, Figure 29). Furthermore, the PFSAs PFBS, PFHxS, PFDS, and the PFCAs with chain-lengths C4 and C7–C14 were detected. In addition to the PFAAs, several polyfluorinated compounds (10:2 diPAP, diSAmPAP, 6:2 and 8:2 FTSA, Me- and EtFOSAA, EtFOSE and FBSA) were detected in wild boar with a maximum concentration of 5.9 $\mu\text{g kg}^{-1}$ for EtFOSE. Wild boar was the only terrestrial species in which PFAS substitutes (6:2 Cl-PFESA, 6:2 FTNO) were identified (first reported in Rupp et al. (2023)).

The high TFA concentrations in herbivorous species are consistent with recent TFA results in terrestrial German ecosystems (Freeling et al. 2020, Freeling et al. 2022). In general, TFA is not expected to accumulate in animal tissue because it is hydrophilic and rapidly eliminated (Holaday 1977, Frank et al. 2002). Therefore, the TFA is assumed to mainly reflect the level of TFA content of the current diet and local habitat at the time of sampling. Nevertheless, it can be expected that due to its persistence, TFA will remain in the environment which leads to a continuous and long-lasting exposure. Recently, significant correlations were reported between TFA in locusts and in plants on which they feed, collected from the same farmland in China (Lan et al. 2020). Atmospheric transformation and deposition of halogenated refrigerants are discussed as sources of TFA, as well as pesticides that form TFA during biotic and abiotic transformation (Behringer et al. 2021, Seiber and Cahill 2022).

PFOS and long-chain PFCAs were present at significantly higher concentrations in wildcat compared to terrestrial herbivores ($p < 0.05$, Table 4), likely due to the exclusively carnivorous diet of wildcat (Lozano et al. 2006) and the accumulation of longer chained PFAAs in food webs (Lozano et al. 2006, Kelly et al. 2009). Nevertheless, overall PFCA levels in wildcat were low, with a high TFA contribution to Σ PFAS (57 %). This could be explained by consuming small herbivorous rodents or insects as the main diet in a short food chain with low bioaccumulation potential (Lozano et al. 2006, Shukla et al. 2021).

The omnivorous species wild boar exhibited the highest PFAS contamination of the terrestrial species analysed. Its opportunistic feeding behaviour, including e. g. plants, insects, and small rodents provides a wide range of different PFAS sources (Cuevas et al. 2010). Due to its digging and rooting behaviour (Kowalczyk et al. 2018), wild boar is in close contact with soil and therefore particularly exposed to atmospheric deposition of PFAS, as soils are a major repository for PFAS (Rankin et al. 2016, Kowalczyk et al. 2018, Söregård et al. 2022).

The Σ PFAS findings in the present study for the herbivorous species exceed previous reports for livers of terrestrial herbivores (roe deer and chamois; mean 1.6–10.1 $\mu\text{g kg}^{-1}$) (Falk et al. 2012, Riebe et al. 2016, Falk et al. 2019, Kotthoff et al. 2020). This is primarily due to the inclusion of TFA in the present study, as it was not considered in the cited studies. After subtracting TFA concentrations from Σ PFAS (mean 0.6–3.3 $\mu\text{g kg}^{-1}$), the results of the present study are slightly lower than in the previous studies. The concentrations of Σ PFAS and PFOS determined in the omnivorous wild boar are consistent with previously reported data (Brambilla et al. 2016, Kowalczyk et al. 2018).

Table 4: p-values after testing for significant differences with student's T-test for the data of target analysis and TOP assay.

P-values < 0.05 indicate significant differences and are indicated in bold.

Parameter	p-value
Target analysis	
PFOS (wildcat vs. terrestrial herbivores)	1.26E-09
Long-chain PFCAs (wildcat vs. terrestrial herbivores)	4.47E-06
% Short-chain PFCAs (liver vs. musculature)	1.54E-02
% Long-chain PFCAs (liver vs. musculature)	1.54E-01
% PFOS (liver vs. musculature)	1.08E-01

Parameter	p-value
Σ PFAS (liver vs. musculature)	3.82E-02
TOP assay	
% Σ PFCAs increase (terrestrial vs. semi-aquatic habitat)	1.66E-01
% Σ PFCAs increase (terrestrial vs. marine)	3.15E-01
% Σ PFCAs increase (marine vs. semi-aquatic habitat)	9.09E-01
% Σ PFCAs increase (herbivores vs. carnivores)	3.07E-01
% Σ PFCAs increase (herbivores vs. omnivores)	5.97E-02
% Σ PFCAs increase (omnivores vs. carnivores)	4.73E-01
% Σ PFCAs increase (liver vs. musculature)	8.23E-02
% Short-chain Σ PFCAs increase (liver vs. musculature)	2.10E-01
% Long-chain Σ PFCAs increase (liver vs. musculature)	2.10E-01
% Explainable increase of Σ PFCAs via precursors measured in target analysis (liver vs. musculature)	3.13E-02
Σ PFCAs increase (liver vs. musculature)	5.23E-01
Σ PFCAs (target analysis vs. after TOP assay in roe deer)	1.00E+00
Σ PFCAs (target analysis vs. after TOP assay in wildcat)	1.00E+00
Σ PFCAs (target analysis vs. after TOP assay in cormorant)	9.86E-01
Σ PFCAs (target analysis vs. after TOP assay in wild boar)	5.39E-01

6.3.3 Semi-aquatic herbivores and omnivores

Despite beaver and coypu inhabiting inland and common eider duck inhabiting coastal areas, the profiles and patterns in livers of these three species were similar, with mean Σ PFAS concentrations of 17 to 21 $\mu\text{g kg}^{-1}$ (Figure 28). Major contributions to the Σ PFAS concentrations were determined for TFA (8.4–11.3 $\mu\text{g kg}^{-1}$) and PFOS (5.9–7.3 $\mu\text{g kg}^{-1}$). In addition, long-chain PFCAs C8–C14 were determined.

While beaver and coypu are predominantly herbivorous, the common eider duck is mainly carnivorous (Laurson and Møller 2022). Smaller differences might be accounted for by the different diet. Larger differences are not expected as the common eider duck mainly feeds on biota of low trophic classes e. g. bivalves (Laurson and Møller 2022). Beaver and coypu exhibited multiple findings of polyfluorinated compounds (e. g. 10:2 diPAP, diSAmPAP, FTSA, FBSA) whereas in common eider duck only FBSA, FHxSA and FOSA were detected. As the beaver and coypu were both sampled in urban catchments, the higher detection frequency of polyfluorinated substances of the Σ PFAS (Figure 29) might derive from urban contamination (Chen et al. 2019, Lan et al. 2020). The levels of PFOS in beaver and common eider duck are consistent with data reported in the literature (6.6 $\mu\text{g kg}^{-1}$, respectively 7.7 $\mu\text{g kg}^{-1}$) (Falandysz et al. 2007, Kelly et al. 2009).

6.3.4 Semi-aquatic freshwater and marine carnivores

6.3.4.1 Liver Tissue

Mean Σ PFAS concentrations in the livers of semi-aquatic (otter, cormorant) and marine fish-feeding top predators followed the order otter > harbour porpoise > cormorant > harbour seal > grey seal (Figure 28, Table D 1). For all those species the predominant PFAS was PFOS (67–95 %, Figure 29), followed by PFNA and PFDA. In otter, the PFASs PFBS, PFHxS and PFDS were also detected, while no PFASs other than PFHxS were found in the other species (except for harbour porpoise). The long-chain PFCAs C8–C14 were detected in species from both ecosystems. In the species from marine ecosystem, diSAmPAP, 8:2 FTSA and FOSA were the only polyfluorinated compounds determined. The pattern of polyfluorinated compounds in otter and cormorant was more diverse (e. g. 10:2 diPAP, diSAmPAP, FTSA, perfluoroalkane sulfonamides (FASAs), perfluoroalkane sulfonamido acetic acid (FASAAs)). Besides, multiple substitute compounds (6:2 Cl-PFESA, 8:2 Cl-PFESA, 6:2 FTNO) were also detected at low concentrations in the semi-aquatic freshwater species.

The otter results are consistent with previously reported concentrations of Σ PFAS and PFOS concentrations for otter in Northern Europe (Roos et al. 2013, Androulakakis et al. 2022). The high level of Σ PFAS is associated with more frequent detections of polyfluorinated compounds and substitutes and could be explained by higher concentrations of PFAS emissions in freshwater systems compared to coastal and marine systems (Androulakakis et al. 2022).

The cormorant accounted for the highest percentage of PFOS in the total PFAS load (mean 95 %) compared to the other piscivorous species. However, a strong spread in the Σ PFAS and PFOS concentration could be observed for the eight cormorant samples (29–640 $\mu\text{g kg}^{-1}$, Table 5), which is likely attributable to the sampling site, as there seemed to be no correlation with sex or age. Nevertheless, the results for PFOS in cormorant liver are in agreement with piscivorous birds reported in the early 2000s (Kannan et al. 2002, Houde et al. 2006) – despite the fact that PFOS and PFOA concentrations in Western Europe tend to decrease since then (Falk et al. 2019, Kotthoff et al. 2020).

Table 5: Validation results of TOP assay for bream liver (n=3).

Liver of bream (*Abramis brama*) was used as proxy for the biota samples analysed in this study.

Analyte	Relative standard deviation in %	Apparent Recovery in %
TFA	7	109
PFPrA	4	117
PFBA	7	144
PFPeA	3	116
PFHxA	3	108
PFHpA	8	123
PFOA	4	118
PFNA	11	112
PFDA	18	155

Analyte	Relative standard deviation in %	Apparent Recovery in %
PFUnDA	11	136
PFDoDA	13	112
PFTTrDA	5	128
PFTeDA	10	155

The marine species share a similar PFAS profile, with the harbour porpoise and harbour seal having higher Σ PFAS concentrations compared to the grey seal. The reason for this discrepancy cannot be fully explained within the scope of this study as all three marine species share the same ecological niche and feeding behaviour. However, because the harbour porpoise enters adjacent estuaries in search for food, it may be more exposed to anthropogenic influences than the seal species, which could result in higher levels of contamination (Taupp 2022). In general – and despite targeting more analytes in the present study – the Σ PFAS results for the marine species are lower or at the lower limit compared to data in the literature from previous years (Kannan et al. 2002, van de Vijver et al. 2003, van de Vijver et al. 2007, Ahrens et al. 2009, Galatius et al. 2013, Androulakakis et al. 2022), which reflects the decreasing environmental concentrations of legacy PFAS.

6.3.4.2 Musculature Tissue

PFAS are known to preferentially bioaccumulate in liver tissue (Müller et al. 2011, Greaves et al. 2012). To complement the interspecies comparison in liver, PFAS profiles were also determined in musculature tissue for the piscivorous species.

Indeed, concentrations of Σ PFAS in liver were significantly higher than in musculature tissue (5-fold (grey seal) to 28-fold (otter), Figure D 7), but in both tissue types PFOS was the dominant PFAS (Figure D 8). The relative amount of PFOS and long-chain PFCAs ($nC \geq 8$) did not differ significantly, while the relative concentration of short-chain PFCAs ($nC < 8$) was significantly higher in musculature than in liver tissue. In general, the relative concentration of precursors in musculature was also higher than in liver tissue.

In contrast to liver tissue, in the musculature tissue, the differences in the total PFAS concentrations between the species were minor. The results for the PFAS trends in liver and musculature tissue are consistent with data reported in harbour seal, polar bears and fish (Ahrens et al. 2009, Greaves et al. 2012, Kowalczyk et al. 2020, Chen et al. 2021). However, data on the accumulation of short-chain PFAS in different animal body tissues is scarce, as previous studies mainly focus on long-chain PFAS, lacking information on the differences in tissue distribution of short-chain PFAS.

6.3.5 Interspecies comparison

PFAS concentrations in the investigated species decreased in the order semi-aquatic carnivore > marine carnivore > terrestrial omnivore > terrestrial carnivore > terrestrial herbivore > semi-aquatic omnivore/herbivore.

A principal component analysis (PCA) was performed to obtain unbiased insight into the differences in the PFAS patterns of the liver samples of the different species (Figure 31). The principal components (PC) 1 and 2 explain 61 % of the total variance in the data. PC2 clearly separates the terrestrial herbivores from aquatic carnivores. A unique distribution pattern can be seen between the carnivorous wildcat and terrestrial herbivores rather than a clear separation of

the wild cat. In general, terrestrial herbivores cluster identically and are strongly affected by high TFA and low PFOS concentrations resulting in high scores of PC2. Similar clustering can be seen for the omnivorous common eider duck and coypu and herbivorous beaver. The clustering is also influenced by TFA, but to a smaller extent than in the terrestrial herbivores.

Most of all, clustering of beaver and coypu is affected by polyfluorinated compounds. Clustering of wild boar is driven by PC2, being influenced by PFOS and TFA. Due to the high PFOS content, wild boar clearly separates from the other clusters of terrestrial species. The piscivorous species are mainly affected by PFOS and the long-chain PFCAs and therefore group differently from the herbivorous species but overlap with wild boar due to PFOS. However, separation of wild boar and piscivorous species is achieved when PC3 is considered. PC3 explains 6.4 % of the total variance, so that 67.4 % of the total variance is explained by the first three PC. While wild boar clustering is mainly affected by PFBS, PFBA, PFOA and the polyfluorinated EtFOSE via PC3, piscivores are influenced by the long-chain PFUnDA, PFDS, PFOS and especially FOSA.

The large differences in the PFAS pattern and concentrations between the carnivorous terrestrial (wildcat) and all aquatic species might be explained by the differences in trophic classes and the ecological habitat. In general, food chains are longer in aquatic environments than in terrestrial ecosystems, resulting in aquatic prey having higher PFAS levels (Chase 2000, Eriksson et al. 2016). Furthermore, species-specific physiological processes (e. g. absorption, excretion, distribution, conversion rate) and prey pattern also affect the PFAS burden. For example, research on the faeces of domestic cats showed high excretion rates for long-chain PFCAs ($nC \geq 8$) (Ma et al. 2020).

6.3.6 TOP assay analysis

Clear trends in the concentrations and patterns of the PFAS analysed in dependence of the trophic class and/or habitat of the different species were found in this study. These relationships were further studied by TOP assay to determine the formation potential for PFCAs from partially unknown precursor compounds. Due to the aggressive conditions in the process, the TOP assay only forms PFCAs and does not simulate the biotransformation processes in the environment, in which also PFSAs and intermediate products may be formed (Houtz and Sedlak 2012, Casson and Chiang 2018). However, the TOP assay gives a good estimate for both PFSA and PFCA precursors in the environment. The PFCA formation potential is expressed as organic fluorine, for which the organic fluorine content of each analyte was calculated with the respective PFAS concentrations.

6.3.6.1 Interspecies comparison of the PFCA formation potential and pattern

The formation potential in liver tissue ranged from $<0.01 \mu\text{g kg}^{-1}$ (common eider duck, roe deer, hare) to $13.2 \mu\text{g kg}^{-1}$ organic fluorine (grey seal, Table 6). Except for the grey seal, however, the release of PFCAs by the TOP assay was negligible compared to the PFCAs determined by target analysis.

Table 6: Organic fluorine (OF) detected as Σ PFCAs in $\mu\text{g kg}^{-1}$ after TOP assay analysis.

Species with $n=1$ are always pooled samples, consisting of 5 individuals. Used abbreviations: red deer (CE), roe deer (CC), chamois (RR), hare (LE), beaver (CF), coypu (MC), common eider duck (SM), wild boar (SS, from (Rupp et al. 2023)), wildcat (FS), otter (LL), cormorant (PC), harbour porpoise (PP), grey seal (HG), harbour seal (PV).

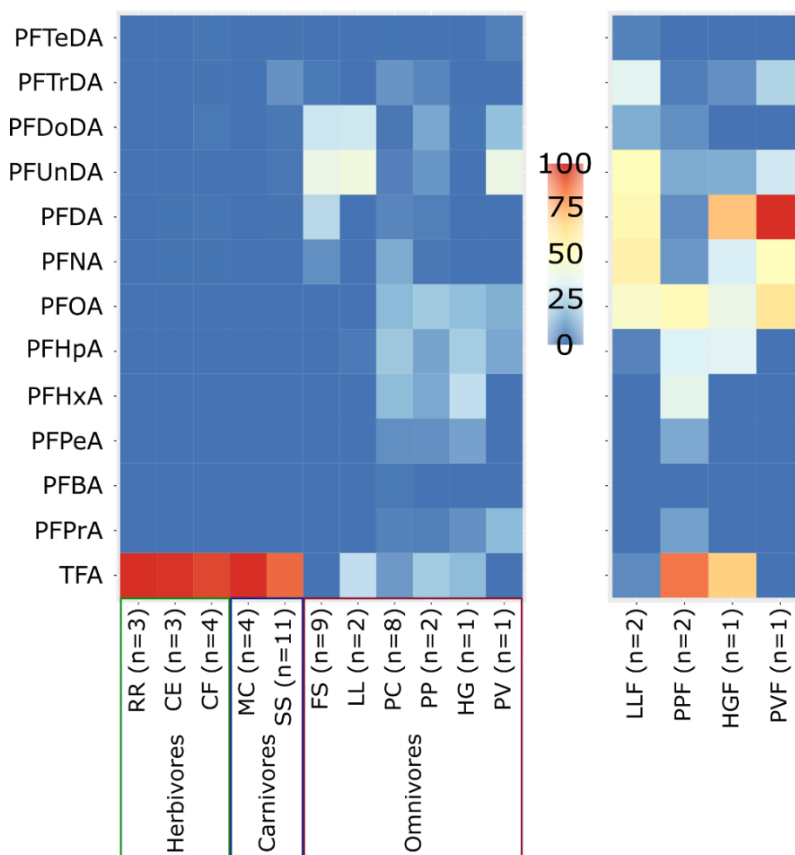
Species	Tissue type	Increase in Σ PFCAs in $\mu\text{g kg}^{-1}$ OF	Increase in Σ PFCAs relative to the Σ PFCA concentration from target analysis in %
RR (n=3 ^l)	Liver	3.00	125
CE (n=3 ^l)	Liver	3.80	124
CC (n=10)	Liver	<0.01	-
LE (n=1)	Liver	<0.01	-
CF (n=4)	Liver	0.7*	119
MC (n=4 ^l)	Liver	0.60	111
SM (n=1)	Liver	<0.01	-
SS (n=11)	Liver	7.1*	130
FS (n=9 ^l)	Liver	0.20	101
LL (n=2)	Liver	6.00	102
PC (n=8)	Liver	3.7*	147
PP (n=2)	Liver	5.80	122
HG (n=1)	Liver	13.20	174
PV (n=1)	Liver	1.10	104
LLF (n=2)	Musculature (F)	3.10	147
PPF (n=2)	Musculature (F)	8.10	350
HGF (n=1)	Musculature (F)	1.20	138

Species	Tissue type	Increase in Σ PFCA in $\mu\text{g kg}^{-1}$ OF	Increase in Σ PFCA relative to the Σ PFCA concentration from target analysis in %
PVF (n=1)	Musculature (F)	1.30	122

While the TOP assay analysis showed no significant differences in the PFCA formation potential for either the trophic class or the ecological habitat of the analysed species, it exhibited different patterns of PFCAs for herbivores, omnivores and carnivores. In terrestrial herbivores and coypu TFA accounted for >99 % of the total PFCAs formed (Figure 32). In contrast, in beaver and the omnivorous wild boar TFA accounted for 74 %, and 90 %, respectively. The percentage of TFA in the total formation potential was much lower for carnivores, with a maximum of 27 % determined in otters. In carnivorous species, the pattern of PFCAs formed is broad, covering all the analysed PFCAs. Their patterns differed between species, with PFUnDA and PFDoDA dominating in wildcat and otter, and PFHxA, PFHpA and PFOA dominating in grey seal. While the PFCA pattern of wildcat from target analysis resembled that of the herbivores, the pattern of PFCAs formed by the TOP assay resembled that of a carnivore.

Figure 32: Pattern of the formation potential from precursor PFAS by the TOP-assay in different wildlife species

Heatmap showing the pattern of PFCAs formed upon TOP assay analysis (i. e. with oxidation). Species with $<0.01 \mu\text{g kg}^{-1}$ PFCA formation potential are excluded. Species with n=1 are pooled samples, consisting of 5 individuals. Samples are pooled, except for RR, CE, MC and FS. Left: difference between livers (L) from different species; right: PFCA formation potential in organs other than liver (musculature (F)) for certain species. Species with n=1 are always pooled samples, consisting of 5 individuals. Used abbreviations: red deer (CE), roe deer (CC), chamois (RR), hare (LE), beaver (CF), coypu (MC), common eider duck (SM), wild boar (SS), wildcat (FS), otter (LL), cormorant (PC), harbour porpoise (PP), grey seal (HG), harbour seal (PV)



Source: own illustration, TZW.

The low PFCA formation potential of all liver samples agrees with the low concentration of known precursors determined in target analysis (Table D 1). Both findings may reflect in vivo transformation of precursors in the metabolically active liver (Rand and Mabury 2014, Chen et al. 2015, Liu et al. 2020). The data of body tissues points into the same direction.

The TFA formation potential in herbivores and omnivores possibly derives from fluorinated compounds containing only isolated CF₃-groups, which are released upon oxidation, such as agrochemicals (Kaczyński et al. 2021, Seiber and Cahill 2022). The low findings of polyfluorinated PFAS by target analysis support this thesis (Table D 1). Additionally, for the semi-aquatic beaver and coypu, which have been sampled in close proximity to urban catchment, fluorinated compounds in wastewater might also account for the TFA formation potential (Scheurer et al. 2017).

For the carnivorous species, due to variability of PFCAs formed (C2–C14), the organic fluorine is likely to result from precursor compounds with fluorinated alkyl chains, which were not included in target analysis, such as perfluorinated phosphinic acids (PFPIAs). PFPIAs were found in different prey fish and could, among other unknown precursors compounds, account for the organic fluorine formation in cormorant and grey seal (Chen et al. 2021).

For certain carnivorous species (otter, harbour porpoise and harbour seal) the concentration of precursor compounds determined by target analysis exceeded the formation potential determined by the TOP assay (Table D 1). This could either be due to: i) non-detectable/unknown/not extractable PFAS/oxidation products (e. g. perfluoromethoxypropionic acid (PFMOPrA)) (Zhang et al. 2019, Göckener et al. 2022), ii) poor correction by internal standard (IS) which is only added after the oxidation step, iii) loss of precursor compounds by the TOP assay, e. g. volatilisation (i.e. FOSA/FOSE) (Del Vento et al. 2012) or iv) depending on the precursor compound, loss of organic fluorine due to oxidative mineralization of precursor compounds (Janda et al. 2019).

Altogether, the broad spectrum of PFCAs released by the TOP assay in carnivores indicates the presence of different precursor compounds and outlines the bioaccumulation potential of precursor compounds in the food web. According to the different patterns of the formed PFCAs, this bioaccumulation potential differs between herbivores, carnivore and omnivores.

Table 7: Absolute and relative measures for the formation potential from precursor PFAS in wildlife samples

Organic fluorine (OF) detected as Σ PFCAs in $\mu\text{g}/\text{kg}$ after TOP assay analysis. Species with n=1 are always pooled samples, consisting of 5 individuals. Used abbreviations: red deer (CE), roe deer (CC), chamois (RR), hare (LE), beaver (CF), coypu (MC), common eider duck (SM), wild boar (SS, from (Rupp et al. 2023)), wildcat (FS), otter (LL), cormorant (PC), harbour porpoise (PP), grey seal (HG), harbour seal (PV)]

Species	Tissue type	Increase in Σ PFCAs in $\mu\text{g kg}^{-1}$ OF	Increase in Σ PFCAs relative to the Σ PFCA concentration from target analysis in %
RR (n=3 ^l)	Liver	3.00	125
CE (n=3 ^l)	Liver	3.80	124
CC (n=10)	Liver	<0.01	-
LE (n=1)	Liver	<0.01	-
CF (n=4)	Liver	0.7*	119

Species	Tissue type	Increase in Σ PFCAs in $\mu\text{g kg}^{-1}$ OF	Increase in Σ PFCAs relative to the Σ PFCAs concentration from target analysis in %
MC (n=4 [!])	Liver	0.60	111
SM (n=1)	Liver	<0.01	-
SS (n=11)	Liver	7.1*	130
FS (n=9 [!])	Liver	0.20	101
LL (n=2)	Liver	6.00	102
PC (n=8)	Liver	3.7*	147
PP (n=2)	Liver	5.80	122
HG (n=1)	Liver	13.20	174
PV (n=1)	Liver	1.10	104
LLF (n=2)	Musculature (F)	3.10	147
PPF (n=2)	Musculature (F)	8.10	350
HGF (n=1)	Musculature (F)	1.20	138
PVF (n=1)	Musculature (F)	1.30	122

*Outliers identified via Shapiro-Wilco-Test excluded; !: Individual samples.

6.3.6.2 Tissue specific PFCAs formation potential and pattern

In liver and musculature tissue of piscivorous predators, the formation potential in musculature and liver is similar (Table 7). Both, the absolute and the relative increase in organic fluorine between musculature and liver were insignificant. However, due to the lower PFCAs concentrations determined in musculature by target analysis, the relative increases appear higher. Especially striking was the high formation potential in musculature of harbour porpoise (350 %), which fits the high percentage (19 %) of perfluorinated compounds seen in the PFAS pattern (Figure D 8). The largest discrepancies between the PFCAs formation potential in liver and musculature were observed for the grey seal (tenfold higher in liver tissue). The formation potential is likely to derive from unknown precursor compounds.

Regarding the pattern of formed PFCAs, only minor differences between liver and musculature tissue were observed (Figure 32). In musculature tissue, the long-chain PFCAs had the highest formation potential (77 %, respectively 68 %). For liver tissue, the ratio between short-chain PFCAs and long-chain (nC \geq 8) PFCAs was equal (50 % each). However, between musculature and liver tissue, differences in the formation potential of short-/long-chain PFCAs were not significant.

Significant differences, though, were observed for the amount of explainable organic fluorine by the target analysis between liver and musculature tissue. Musculature tissue shows significantly higher ratios of unidentified precursor compounds (Table D 2), which might be due to a lower metabolic activity in musculature tissue.

6.3.7 Conclusion

In a comprehensive, quantitative analysis, the PFAS concentrations and patterns of 66 PFAS were investigated in 14 different mammalian and avian species including herbivores, omnivores and carnivores from different ecological habitats (terrestrial, semi-aquatic, marine) and in different body tissues (liver and musculature). This study confirms a ubiquitous presence of PFAS in wildlife.

In general, PFAS concentrations in liver tissue decreased in the order semi-aquatic carnivore > marine carnivore > terrestrial omnivore > terrestrial carnivore > terrestrial herbivore > semi-aquatic omnivore/herbivore, due to PFAS enrichment in longer food chains. PFAS patterns differed significantly, with TFA dominating in (predominantly) herbivorous species, whereas in carnivores PFOS, and to a lesser extent long-chain PFCAs ($n_c \geq 8$) dominated. Novel substitute compounds were detected only sporadically (wild boar, otter, cormorant) and at low concentrations. The major contribution of TFA to the total PFAS contamination in herbivores highlights the importance of including TFA in future biota screening studies.

TFA was also the dominant PFCA formed in the liver of herbivores in the TOP assay, whereas in carnivores, the PFCAs C2–C14 were formed. It appears important to extend the target analysis and TOP assay analyte spectrum with respect to additional precursor compounds (e. g. PFPiAs and phosphonic acids) and transformation compounds (e. g. PFMOPrA) in future studies.

For the first time, the PFCA formation potential and patterns in different body tissues was investigated, which neither differed significantly for the absolute formation potential, nor the pattern of formed PFCAs, between liver and musculature. However, as the samples sizes for musculature tissues were comparatively small, further research in regards to the formation potential in different body tissues is necessary.

6.4 Wild Boar Liver as a Bioindicator for Environmental PFAS Contamination

This chapter is based on the following publication:

Rupp J., Guckert M., Berger U., Drost W., Mader A., Nödler K., Nürnberg G., Schulze J., Söhlmann R., Reemtsma, T. (2023) Comprehensive target analysis and TOP assay of per- and polyfluoroalkyl substances (PFAS) in wild boar livers indicate contamination hot-spots in the environment. *Sci. Tot. Environ.* 871, 162028. <https://doi.org/10.1016/j.scitotenv.2023.162028>

6.4.1 Introduction

Biomonitoring is an approach in which biota samples are analysed for certain contaminants to learn about the contamination of the habitat from which they stem from. In selected cases even environmental quality standards are defined by a certain contaminant level in biota: this is the case for mercury in river systems, which is defined by a mercury level in fish (EC 2008).

The PFAS contamination of terrestrial environment is characterised by a widely distributed so-called “background contamination” plus a large number of hot-spots. These are sites with high PFAS concentration originating from specific local point sources, e. g. near manufacturing facilities producing or using fluoropolymer, textile or paper industry, on biosolid-amended fields or near military bases and airports where aqueous film forming foams (AFFFs) were used (Buck et al. 2011, Costello and Lee 2020, De Silva et al. 2021).

Spatially resolved monitoring data of the terrestrial environment are particularly scarce – even for legacy PFAS such as PFCAs and PFSA (Falk et al. 2019, Death et al. 2021). Biomonitoring can help to provide such spatially distinct information on the level of PFAS contamination, namely to localise PFAS hot-spots. Kowalczyk et al. (2018) proposed wild boars (*Sus scrofa*) as a sensitive bioindicator for environmental pollution by PFOA and PFOS.

The general suitability of wild boar livers as a generic bioindicator is attributable to their omnivorous diet and the widespread lack of effective predators (Garza et al. 2018), practically placing them at the top of the food chain in the majority of occupied regions. Their global geographical distribution is one of the largest among all species stretching across all continents except Antarctica (Garza et al. 2018). Wild boars are considered a destructive species to be controlled by hunting since the population has been increasing both in native and more substantially non-native ranges (Massei et al. 2015, Lewis et al. 2019). Therefore, sample material can often be provided by local hunters.

The typical foraging behaviour of wild boars brings them in direct contact with multiple environmental media including soil, water and feed from lower levels in the trophic chain (e. g. plants, worms, small rodents). Moreover, carrion scavenging (Tobajas et al. 2021) and access to dumpsites (CONTAM et al. 2018) can expose boars to particularly high PFAS concentrations. Their home range can vary between 0.62 and 48.3 km² depending on various biotic and abiotic factors such as climate and vegetation (Garza et al. 2018). In Germany, they are resident all year in a rather limited home range, for example, 7.7 km² for female adult animals in northeast Germany (Keuling et al. 2008).

Elimination half-lives of PFAS are usually in the range of days to weeks for domestic and wild terrestrial livestock (Death et al. 2021). However, in the porcine species *Sus scrofa* they are comparatively long, for example, 1.7 years for PFOS in domestic pigs (Numata et al. 2014). Elimination half-lives are even higher for humans (5.4 to 8.7 years for PFOS). Correspondingly, wild boars are expected to exhibit remarkably high PFAS concentrations due to the extensive exposure, slow elimination half-lives and trophic magnification. The highest concentrations are expected to be found in protein rich tissues. Therefore, the liver is the preferred organ for analysis of PFAS in wild boars (Numata et al. 2014, Kowalczyk et al. 2018).

This study explores the suitability of wild boar liver as a bioindicator for environmental contamination by different PFAS encompassing one short-chain PFSA, six (ultra)short-chain PFCAs, three long chain PFSA, seven long chain PFCAs, 32 precursors and six substitute compounds. Furthermore, the TOP assay is performed to assess the formation potential of PFAS from (untargeted) precursors.

Livers of 50 wild boars from three areas in Germany, associated with (1) contaminated paper sludges distributed on arable land (PS), (2) industrial emissions from a fluoropolymer production facility (IE) and (3) background contamination (BC) were investigated.

6.4.2 PFAS Profiles of Samples Associated with Different Contamination Sources

PFAS in wild boar livers from one background area (area BC) and two hot-spots (areas PS and IE) in Germany were analysed. One hot-spot contaminated by paper sludges distributed on arable land (PS) and the other one with industrial emissions of PFAS from a fluoropolymer production facility (IE). In total, 31 different PFAS were detected in the wild boar livers and 30 of these could be quantified. These cover legacy PFAAs, (ultra)short-chain PFAAs, precursor compounds and the substitutes HFPO-DA, DONA, 6:2 Cl-PFESA and 6:2 FTNO. PFAS concentrations and patterns in wild boar livers are distinctively different between the three areas of this study (Figure 32).

6.4.2.1 Background Contamination with PFAS

For wild boar livers from area BC, the Σ PFAS concentration is 124 $\mu\text{g kg}^{-1}$. The PFAS contamination in area BC was primarily composed of PFOS (82 $\mu\text{g kg}^{-1}$). Σ PFCA contributes 40 $\mu\text{g kg}^{-1}$, with TFA and PFNA being the dominant PFCAs (each with 11 $\mu\text{g kg}^{-1}$). The most frequently detected PFAA precursors were 6:2 and 8:2 FTSA (in 100% of the samples, max. 0.2 $\mu\text{g kg}^{-1}$) followed by EtFOSE

(max. 5.9 $\mu\text{g kg}^{-1}$) and EtFOSAA. The only substitute compound detected multiple times – i. e. in 6 of 11 samples with background contamination – was 6:2 Cl-PFESA (median 0.022 $\mu\text{g kg}^{-1}$).

The PFOS and PFOA concentrations determined in the present study for area BC as well as their ratio (22:1) were in line with recently reported data in wild boar livers from other parts of Germany (Stahl et al. 2012, Kowalczyk et al. 2018) and Italy (Brambilla et al. 2016) (Table 8). Due to its hydrophilic nature and short elimination half-life, bioaccumulation of TFA is unlikely (Holaday 1977, Seiber and Cahill 2022). For this reason, the TFA in the wild boar livers is suspected to mainly reflect the recent wild boar diet at the time of sampling.

Table 8: Comparison of PFOS and PFOA concentrations in wild boar livers from the present study (collected from three areas in Germany between 2019 and 2020) and literature for different study areas.

Concentrations are given in $\mu\text{g kg}^{-1}$ and refer to wet weight. Values < LOQ were treated as zero for mean calculations. The number of samples is abbreviated as n.

Study area (source of contamination)	Study	n	PFOS mean (min–max)	PFOA mean (min–max)	PFOS:PFOA mean
Area PS (paper sludges)	Present study	9	426 (150–800)	5* (3.0–35)	85:1
Area BC (background contamination)	Present study	11	82* (46–450)	4 (0.60–9.30)	22:1
Area IE (Industrial emissions)	Present study	1	64	650	1:10
Sauerland in north-western region of Germany (industrial sludges in fertilizers distributed on arable land)	Arenholz <i>et al.</i> (2011)	50	432 (4–1200)	max 38	NA
North, south and west of Germany (background contamination)	Kowalczyk <i>et al.</i> (2018)	91	179 (<LOQ–1084)	8.8 (<LOQ–114)	21:1
Hesse in west-central Germany (background contamination)	Stahl <i>et al.</i> (2012)	529	117 (<LOQ–1780)	4.0 (<LOQ–45)	29:1
North, south and central Italy (background contamination)	Brambilla, Testa and Fedrizzi (2016)	62	95 (9.1–397)	6.7 (6.0–11)	14:1

*Excluding outliers identified via Shapiro-Wilk-Test.

6.4.2.2 PFAS Contamination at the Hot-spot “Paper Sludges”

The mean Σ PFAS concentration in livers of wild boar sampled in area PS (458 $\mu\text{g kg}^{-1}$) was significantly higher ($p < 0.05$, Table D 3) than for those in area BC (Figure 33). Similar to the PFAS pattern in livers from area BC, PFSAs (433 $\mu\text{g kg}^{-1}$) – and in particular PFOS (426 $\mu\text{g kg}^{-1}$) – dominated. Nevertheless, PFBS, PFHxS, and PFDS also contributed to the contamination, with concentrations and detection frequencies being higher than in area BC. Cumulatively, the PFSAs accounted for 85 % of the targeted PFAS, which was significantly higher than in area BC (69 %). The Σ PFCA concentration (51 $\mu\text{g kg}^{-1}$) was only slightly higher. The pattern, however, differed strongly with long-chain perfluorocarboxylic acids (C8–C14) being significantly higher and the ultrashort chain PFCA TFA being significantly lower than in area BC (Figure 33).

The significantly higher PFOS concentrations in area PS may be due to degradation of polyfluorinated compounds as described in the literature, e. g. for the PFOS precursor diSAmPAP in soil (Bugsel and Zwiener 2020). Similarly, the higher concentrations of long-chain PFCAs in area PS are possibly the result of degradation of PFCA precursors as reported, e. g. for selected diPAPs in rats (D'eon and Mabury 2011) and soil (Liu and Liu 2016). In fact, diPAPs of different chain-lengths as well as diSAmPAP (both being fluorinated phosphate esters) were recently identified in soil collected at the investigated area PS and were also found in impregnated paper that may be related to the paper sludges deposited in area PS (Janda et al. 2019, Bugsel and Zwiener 2020, Kotthoff et al. 2020, Bugsel et al. 2022). In the wild boar liver, however, the concentrations of fluorinated phosphate esters were low (6:2 monoPAP: <LOQ–0.24 µg kg⁻¹), below LOQ or below limit of detection (LOD, all other analytes). This observation might be explained either by transformation of the esters into PFOS/PFCAs in vivo (D'eon and Mabury 2011) or by environmental degradation prior to intake – e. g. in soil (Lee et al. 2014). Overall, the PFAS profile in wild boar liver in area PS distinguishes itself from the background contamination (area BC). But it is not directly indicative of the contamination source that was presumably paper sludges loaded with phosphate esters. Furthermore, the findings of comparatively low TFA concentrations suggest that this compound is not associated with the paper sludge contamination in the area.

The PFOS:PFOA ratio in area PS was much higher than in area BC (85:1 vs. 22:1), indicating a high PFOS contamination. These findings are comparable to previous findings of PFOS and PFOA in wild boar liver from the region Sauerland (Germany, Table 8) (Arenholz et al. 2011), which was one of the first reported cases with PFAS contamination in Germany. Also, in that area, PFAS-loaded material was distributed on arable lands (Wilhelm et al. 2008).

6.4.2.3 PFAS Contamination at Hot-spot “Industrial Emissions”

In contrast, the Σ PFAS concentration in the wild boar liver from area IE (944 µg kg⁻¹, one individual) was dominated by PFCAs (864 µg kg⁻¹, Figure 33) and PFOA in particular (650 µg kg⁻¹, Table 8). The concentration of PFOS (64 µg kg⁻¹) was even lower than in wild boars from area BC. Furthermore, the wild boar from area IE exhibited considerable amounts of HFPO-DA (0.30 µg kg⁻¹) and an even higher concentration of DONA (15 µg kg⁻¹), clearly distinguishing the liver collected in area IE from those in areas BC and PS.

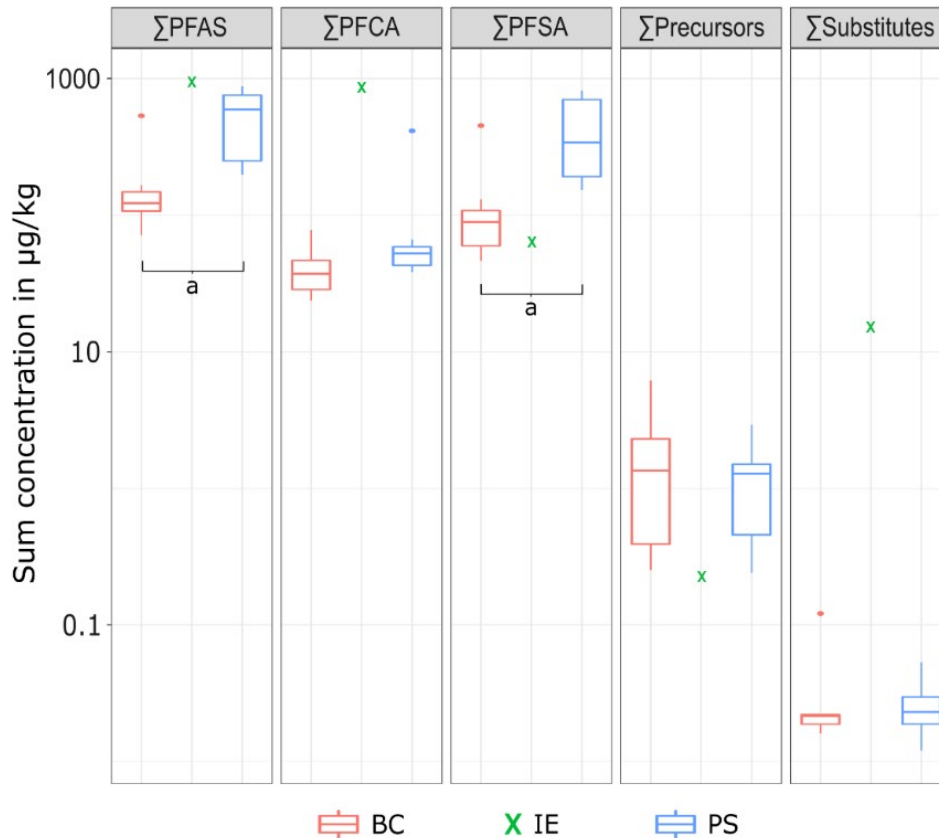
The high PFOA concentration in the wild boar liver from area IE led to an inverse PFOS:PFOA ratio (1:10) as compared to those observed in the other areas. Together with the high concentration of DONA, this points at (former) local industrial emissions of PFOA and ongoing use of its substitute DONA. However, while the PFAS pattern of the wild boar liver from the area IE is very specific, it is obtained from one animal, only, and needs further confirmation.

On a global level, DONA has only been reported in very few other studies on wildlife, e. g. in one egg of an Arctic seabird (0.11 µg kg⁻¹) (Jouanneau et al. 2021) or one locust in Tianjin, China (0.21 µg kg⁻¹) (Lan et al. 2020). To date, DONA is not subject to regulation, though it is within the scope of the planned broad PFAS restriction in the EU (ECHA 2022b). It possesses a structure closely related to the substances of very high concern (SVHC) HFPO-DA. HFPO-DA has been identified as a SVHC under the REACH regulation primarily based on its high persistence and mobility in water and soil, but also due to high potential for long-range transport, difficulty in remediation, moderate bioavailability and multiple adverse effects (ECHA 2023). Both HFPO-DA and DONA are ether carboxylic acids with a maximum of five perfluorinated carbon atoms. Hence, the physicochemical properties – that is high specific sorption affinity to structural proteins, storage lipids, membrane lipids and serum albumin (Allendorf et al. 2021) as well as low sorption potential to soil (Nguyen et al. 2020) – are probably of similar concern for DONA as for HFPO-DA.

HFPO-DA is commonly detected in the environment downwind or downstream fluoropolymer production sites, e. g. in soil (Galloway et al. 2020), grass and leaves (Brandsma et al. 2019). The determination of both ether compounds at substantial levels in wild boar liver suggests a high bioaccumulation potential of these compounds in wild boars hitherto unknown in its dimensions.

Figure 33: PFAS sum concentrations in wild boar livers

The boxplots (logarithmic scale) illustrate the results of samples from the years 2019/2020 – associated with different PFAS contamination sources in Germany. The wild boar liver from the “industrial emission” (IE) area is an individual sample marked with “x” (green). The brackets marked with “a” describe significant ($p < 0.05$) differences between the samples from the “background contamination” (BC) area ($n = 11$, red) and “paper sludges” (PS) area ($n = 9$, blue).



Source: own illustration, TZW.

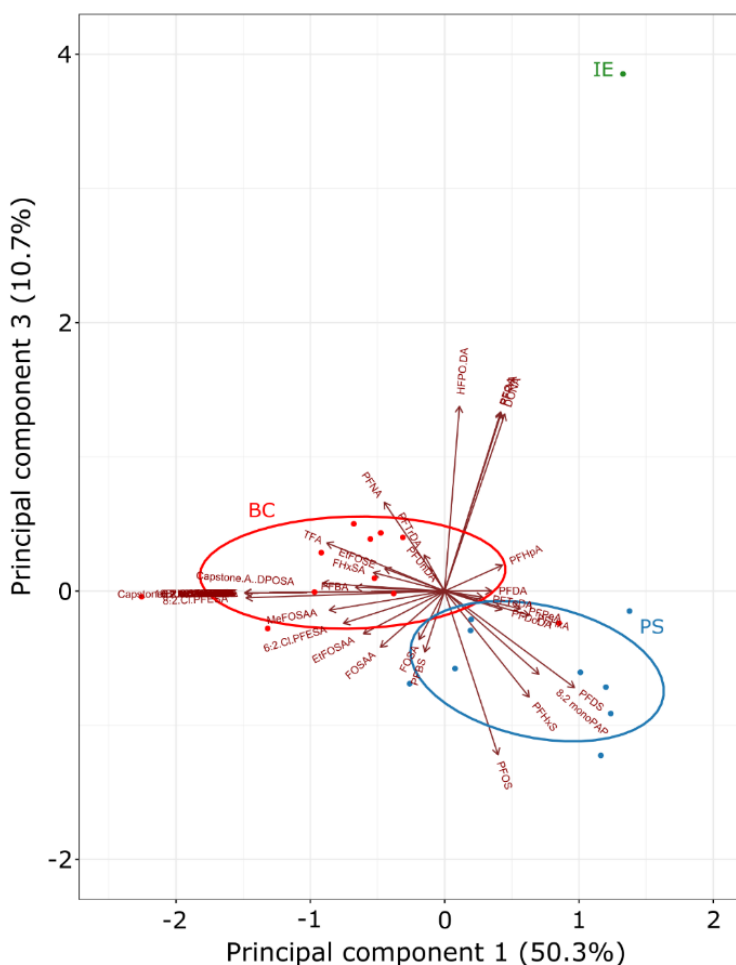
6.4.2.4 Variation in PFAS Patterns between the Areas

The extensive target analyte spectrum covered in this study enabled a precise characterisation of the PFAS patterns in wild boar livers from the different areas. However, the detections and concentrations of precursors did not differ substantially between the areas, potentially indicating that the precursors that were ingested were readily transformed in the wild boars. For substitutes (HFPO-DA and DONA), differences were found, which clearly distinguish the wild boar liver collected in area IE from those collected in areas PS and BC. Besides DONA and HFPO-DA, the patterns in the livers mainly differed due to high concentrations of either PFOS (PS) or PFOA (IE). Nonetheless, it is important to emphasize that the PFAS exposure history of any wildlife species – including wild boars – cannot be fully traced back. However, the strong correlations between the known PFAS contamination and PFAS patterns observed in the livers for each site suggest a source-specific accumulation of PFAS in the wild boar livers.

A principal component analysis (PCA) was conducted to illustrate the variation inherent in the different sample sets of the wild boar liver. Separation between livers from area BC and the two hotspot areas (PS and IE) was achieved via the principal components 1 and 2 (PC 1 and PC 2, explaining 66 % of the total variance inherent in the data, Figure D 9). PC 3 distinguishes between livers from the two contaminated areas PS and IE. Together with PC 1 it explains 61 % of the total variance inherent in the data (Figure 34). On one hand, high concentrations of HFPO-DA, DONA and PFOA have a large effect on PC 3 loadings and describe the main characteristics of livers from area-IE. On the other hand, PFHxS, PFOS and PFDS correlate negatively with PC 3, characterising area PS. The clustering of the BC samples is determined by their higher shares of TFA, PFNA and EtFOSE, separating them from those collected in area PS via PC 1. The PCA supports the hypothesis that PFAS profiles in wild boar livers vary between sampling areas which is a consequence of different exposure patterns in the environment and likely also of the three different contamination sources.

Figure 34: Principal component analysis of wild boar livers associated with different sources of contamination

Loadings of the principal components (PC) 1 and 3 based on normalized molar concentrations from target analysis of PFAS in wild boar liver from the “paper sludges” (PS, n=9), “industrial emission” (IE, n=1) and “background contamination” (BC, n=11) areas. The wild boar livers were collected in Germany between 2019 and 2020. The arrows show the loadings of individual analytes, dots indicate the scores of individual samples. Ellipses show 68 % confidence intervals for the respective sample groups. PC 1 and 3 combined explain 61 % of the total variance inherent in the data.



Source: own illustration, TZW.

6.4.2.5 Formation Potential from Precursor PFAS

TOP assay analyses were performed to estimate the exposure to precursor compounds that were not included in the target analysis. The data were also used to investigate whether differences in the contamination source are also reflected in the PFCA formation potential or the pattern of formed PFCAs from oxidation of precursor compounds. Compared to the PFCA concentrations from target analysis, the PFCA formation potential in the wild boar livers was relatively low for all areas (Figure 35). Low concentrations of precursor compounds were also determined via target analysis (see Figure 32). Certain PFAS undergo biotransformation primarily in liver – as reported in vivo for example for perfluoroalkyl phosphinic acids (Joudan et al. 2017), PAPs, FTOHs (both Rand and Mabury (2014)) and 6:2 Cl-PFESA (Yi et al. 2022) in rats. Therefore, in liver, precursor concentrations might generally be lower than in other mammalian tissues.

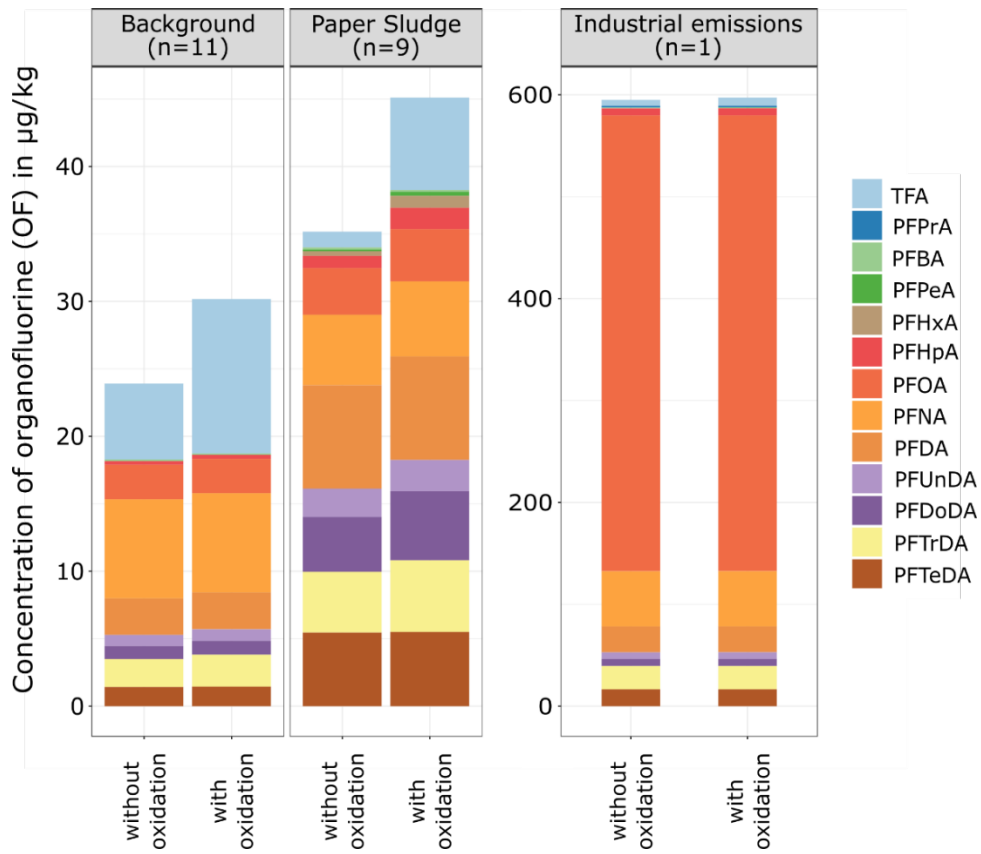
The patterns of PFCAs formed in the TOP assay varied between the different areas: In livers from areas BC and IE, >90 % of the formed PFCAs were attributable to TFA. Concentrations of formed PFCAs C3–C14 were either low or below LOQ. TFA was also the dominant reaction product formed in the liver extracts from area PS, but accounts for only 57 % of formed PFCAs. However, TFA is one of the few formation products which shows a significantly higher concentration after the TOP assay as compared to the concentration from target analysis ($p < 0.05$, Table D 4). The other PFCAs are the C5–C7 homologues which contribute 2 %, 5 % and 7 %, respectively. In general, in livers from area PS, all PFCAs except for PFPrA, PFBA and PFDA were formed.

The target compounds 6:2 and 8:2 FTSA only partially explain the formation potential of short-chain PFCAs C5–C7 in the TOP assay ($\sum(\text{target analysis}): 0.51 \mu\text{g kg}^{-1} \text{F}$ vs. $\sum(\text{TOP assay}): 9.6 \mu\text{g kg}^{-1} \text{F}$, concentrations normalised to the molecular fluorine content). However, formation of the PFCAs is most likely also attributable to unknown precursor compounds not included in the target analysis spectrum – e. g. organophosphorus compounds like perfluoroalkyl phosphinic acids and polyfluoroalkyl phosphate tri-esters (triPAPs). These compounds have recently been reported to be present in the soils from area PS (Bugsel and Zwiener 2020). However, as PAPs were reported to be transformed in vivo, (Rand and Mabury 2014), the impact of triPAPs on the PFCA formation potential likely remains low.

The dominance of TFA among the PFCAs formed in the TOP assay may be due to bioaccumulation of multiple compounds with an isolated carbon-bound trifluoromethyl group ($\text{F}_3\text{C-C}$) by wild boars. These may include fluorinated pesticides and/or their metabolites. For instance, the occurrence of the $\text{F}_3\text{C-C}$ -containing herbicide trifluralin has been reported in Polish wild boar meat (Kaczyński et al. 2021). This demonstrates its relevance and persistence in the soil environment even 12 years after its ban in the EU (EC 2007). Previously, trifluralin was used e. g. in rapeseed and sunflower cultivation (Lewis et al. 2016) – both representing relevant feeding grounds for wild boars (Massei et al. 2015). In the present study, liver samples were not screened for fluorinated compounds with an isolated trifluoromethyl group. This may be recommended for further studies of combined TOP assay and target analysis in animal tissues.

Figure 35: Formation potential from PFCA precursor compounds in wild boar livers

Organofluorine (OF) concentrations (arithmetic mean) in wild boar livers determined without and with oxidation. The differences represent the amount of PFCAs formed by precursor oxidation. Wild boar liver samples (collected in 2019 and 2020) from different regions in Germany were compared. The regions are associated with different sources of contamination. Mean values and standard deviation of individual PFAS are given in Table A 1.



Source: own illustration, TZW.

6.4.3 Comparison of PFAS Profiles in Wild Boar and the Local Environment

The findings of the wild boar livers showed site-specific PFAS patterns which are in line with the local PFAS exposure history. To better understand their origin as well as advantages and disadvantages of wild boar liver as a bioindicator, further samples – from different environmental compartments – were analysed.

6.4.3.1 Soil Contamination at the Hot-spots

Compared to reference soil samples from Germany without a specific contamination history, soil in proximity to the industrial plant (IE) was found to be contaminated by a broad range of PFAS, namely the C2–C14 PFCAs (Figure 36 A), PFOS and DONA (1.7 and 0.43 $\mu\text{g kg}^{-1}$, respectively). PFOA dominated the PFCA pattern (Figure 36 C), although its production ceased eleven years before the soil sample was collected.

The PFAS pattern in the boar liver from area IE largely reflected the soil contamination, in particular for the PFCAs (Figure 36 C–D). However, the total PFAS concentration in liver was about two orders of magnitude higher than that in the soil (Figure 36 A–B). For DONA and PFOS, the difference was less pronounced (35- and 38-fold higher in liver as compared to soil, respectively).

For area PS, the PFAS concentrations of wild boars were compared to those of soil samples from literature (Kotthoff et al. 2020). The respective top soil samples (n=10) originated from different sites in area PS. The median Σ PFCA concentration was 8-fold higher than that of the soil sample from area IE (192 vs. $\mu\text{g kg}^{-1}$, for comparability expressed in dw). The PFCA patterns (C3–C14) of wild boar and soil resembled each other not only in area IE, but largely also in area PS (Figure D 10). However, perfluorodecanoic acid (C10) dominated in area PS whereas it is PFOA for both samples in area IE.

Soil acts as a long-term storage compartment for many PFAS (Liu et al. 2015). Global mean background concentrations of individual legacy PFCAs and PFOS are in the range 0.01–0.06 $\mu\text{g kg}^{-1}$ (Washington et al. 2019). Therefore, given the results in the present study and in the study of Kotthoff et al. (2020), the soil samples from area IE and PS are confirmed as being contaminated. The presence of PFOS, DONA and/or other PFAS in the boar liver may indicate long-term exposure to contaminated soil as well as the dietary uptake of organisms living in the soil and of plants grown on it. Moreover, the monitoring examples of the soil and wild boar samples underline the persistence and dispersion of PFAS in the environment. It is likely that PFAS exposure of the wild boars to soil contaminants occurs both directly – due to intense digging and rooting behaviour of the wild boar – and indirectly via the food chain. In comparison to other uptake routes of PFOS, soil intake has been modelled to account for >80 % in domestic outdoor pigs (Brambilla et al. 2015). The contribution of soil uptake strongly depends on contamination levels in all exposure media and feed as well as on the feeding habits. The modelled value should be seen as an estimate.

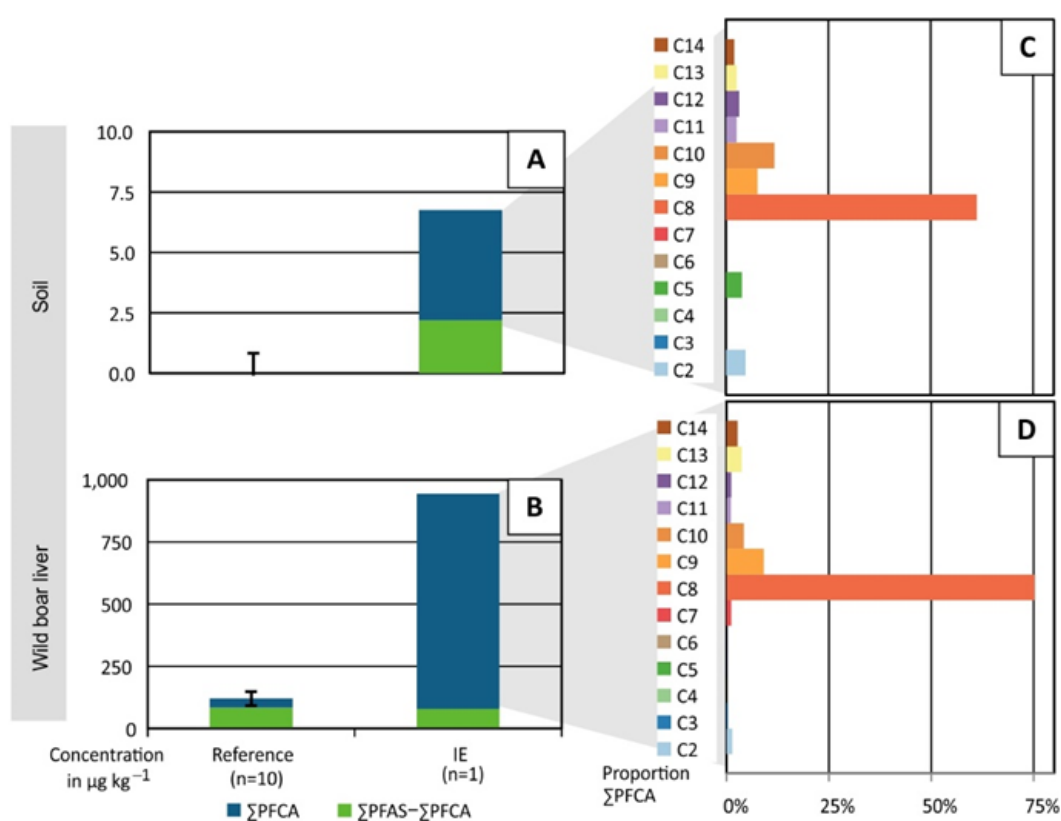
Studies on contamination levels in wild boars in relation to their local environment have not been published, yet. Also, for other terrestrial organisms such data are scarce. For example, in the Arctic food chain the PFCA concentration increases from lichen (primary producer) to caribou (prey) and wolf (predator) (Müller et al. 2011). Meanwhile, the pattern remains the same at all trophic levels. Other monitoring studies come to different results, e. g. in a Norwegian skiing area, where the PFCA pattern of soil is reflected in that of local earthworm (*Eisenia fetida*) only for high loads of PFOA, and where for bank voles (liver, *Myodes glareolus*), PFCA screening shows an entirely different pattern (Grønnestad et al. 2019).

The agreement in the PFAS patterns between soil and wild boar liver clearly supports the potential of wild boar livers as bioindicators of terrestrial contamination. Moreover, factors of bioconcentration seem to be high like the one for the sample pair from area IE. However, these

conclusions can be drawn tentatively only as they are based on two sample pairs of soil and boar liver from a different sampling area, respectively. Altogether, such a good agreement of the PFAS patterns is not necessarily expected, as the processes involved in bioaccumulation of PFAS are very complex. For example, PFCAs of higher chain-length tend to accumulate in biota to a higher degree than those of shorter chain lengths and PFASs have a higher bioaccumulation potential than PFCAs – as demonstrated by Zhao et al. (2013) for earthworm.

Figure 36: Concentrations and patterns of perfluoroalkane carboxylic acids in wild boar livers and soil from area IE

(A–B) PFCA and PFAS sum concentrations and (C–D) PFCA patterns in 905 soil (top) and wild boar liver (bottom) near an industrial park (area IE). The first columns on the left show median sum concentrations of reference samples (n=10 and 11) with error bars indicating the standard deviation. Detailed information on reference samples is available in Table D 6. For wild boars, the liver samples from area BC are depicted as reference samples. The samples were collected in Germany between 2018 and 2020.



Source: own illustration, TZW.

6.4.3.2 Contamination of Samples from a River Affected by Industrial Emissions

For comparison to the terrestrial samples, samples from a riverine environment (pooled European chub musculature and suspended matter) located downstream the wastewater treatment plant of the industrial site in area IE were analysed. In the fish musculature, PFOA was determined at a relatively low concentration (Figure 37). Instead, other PFCAs with longer chain length (C10–C14) dominated the PFCA pattern in the riverine fish.

For suspended matter and chub musculature, the PFCA (Figure 37 C-D) and PFAS patterns differ in parts. Generally, the formation potential from precursors was higher for (ultra)short-chain PFAS ($\Sigma\text{C2-C7}$: $8.1 \mu\text{g kg}^{-1}$ F dw in suspended matter and $23 \mu\text{g kg}^{-1}$ F ww in chub musculature) than for long-chain PFAS ($\Sigma\text{C8-C14}$: $0.5 \mu\text{g kg}^{-1}$ F dw and $20 \mu\text{g kg}^{-1}$ F ww, respectively). In suspended

matter, TFA ($14 \mu\text{g kg}^{-1}$) was more pronounced than in chub musculature and dominated the PFCA pattern (Figure 37 D). Moreover, in suspended matter, the ratio HFPO-DA:DONA was reversed as compared to the fish (1:3 vs. 3:1) whereas in wild boar liver DONA predominated (ratio: 1:52). The high concentration of the hydrophilic compound TFA in suspended matter may partially originate from its pore water.

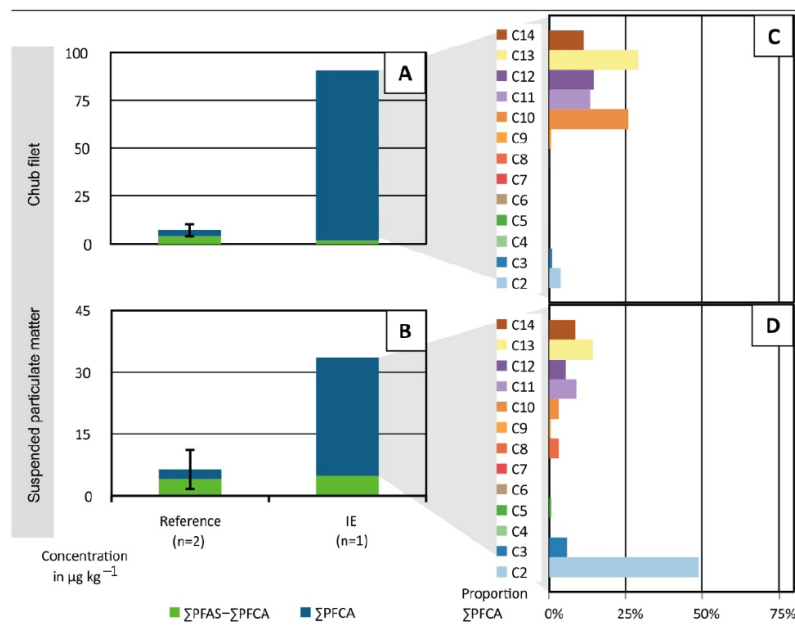
In the riverine ecosystem, industrial contamination by PFOA and other PFCAs is retained only by suspended matter and in sediments – with sorption affinity increasing with chain length (Chen et al. 2018). Opposed to that, in soil environments, PFAS are likely to accumulate over long time periods (Söregård et al. 2022). Consequently, in aquatic organisms, the PFAS pattern should integrate over shorter periods of time than in terrestrial organisms like wild boars.

However, by biomonitoring terrestrial organisms, contamination by very polar PFAS may be overlooked as their terminal degradation products – the (ultra)short-chain PFCAs and PFSAs – are eliminated comparatively fast in biota; i.e. largely within days as compared to long-chain PFCAs and PFSAs with half-lives of ≥ 1 year (Holaday 1977, Numata et al. 2014). Moreover, polar compounds quickly migrate into deeper soil layers and into groundwater.

Therefore, the very polar PFAS are most relevant for the aquatic system. In the present study they were shown to accumulate in fish and suspended matter from area IE rather than in the liver of wild boars. In conclusion, short chain PFAS may be better monitored in aquatic specimens – like suspended matter or fish – or directly in water.

Figure 37: PFCA and PFAS concentrations in chub filet and suspended matter near an industrial park

PFCA and PFAS sum concentrations (A) in chub filet and (B) suspended matter near an industrial park (area IE), with median sum concentrations of reference samples (n=2 and 6) for comparison. PFCA patterns in (C) in chub filet and (D) suspended matter of the same site. Detailed information on reference samples is available in Table D 6. The samples were collected in Germany between 2016 and 2019.



Source: Own illustration, TZW.

6.4.4 Dietary intakes and risks for human health

Wild boar monitoring data can be used to indicate PFAS contamination of terrestrial environment - as shown above - but also in risk assessment of human health. The EFSA Scientific Panel on Contaminants in the Food Chain (CONTAM) considers dietary exposure as the main uptake route for PFAS to humans (CONTAM et al. 2020). Dietary intake of game meat is rather low (in Germany: 200–400 g year⁻¹, Bundesamt für Risikobewertung (BfR) (2011)) and boar liver is consumed to an even minor extent, as most consumers prefer musculatures or meat products (e. g. ham or sausage) of wild boar. On the other hand, hunters and their families consume liver of wild boars on a more regular basis (median in Italy: 13 g week⁻¹ (Danieli et al. 2012)). In Germany, many federal food administrations already recommend to abstain from consuming boar liver from specific hunting grounds (e. g. Laufer et al. (2019) and BJV and Gangl (2020)). In 2020, the European Food Safety Authority (EFSA) introduced a general group safety threshold for four PFAS for human dietary exposure. The Tolerable Weekly Intake (TWI) was set to 4.4 ng kg⁻¹ body weight for the sum of PFHxS, PFOS, PFOA and PFNA (Bundesamt für Risikobewertung (BfR) 2011).

The weekly intake of PFAS for the hunter population – assuming consumption of the studied wild boar livers – was calculated (Table 9 a). The calculations show that even livers from the least contaminated area (BC) are not suitable for consumption by this group of people. Also, for the general population, the consumption of one portion of 0.20 kg of this wild boar liver per year – with a mean sum concentration of 101 µg kg⁻¹ for the four EFSA-PFAS – would exceed the TWI (Table 9 b). This exceedance is primarily driven by high PFOS concentrations.

Table 9: Risk assessment based on dietary human exposure by wild boar liver consumption from different sampling areas in Germany

Sum concentrations of PFHxS, PFOS, PFOA and PFNA (Σ PFAS-4) and their corresponding weekly intake for (a) the hunter population and (b) one portion (200 g) a year are given for comparison to the tolerable (weekly) intake (TWI = 4.4 ng kg⁻¹ body weight) set by EFSA (CONTAM et al. 2020). Individual PFAS concentrations below LOQ are set to zero for the calculations.

	Area “Paper sludges” (PS, n=9), median (1st–3rd quartile)	Area “Industrial emissions” (IE, n = 1)	Area “Background contamination” (BC, n = 11), median (1st–3rd quartile)
Σ PFAS-4 in ng kg ⁻¹	432 (201–706)	792.00	101 (75–121)
(a) Weekly intake via consumption of wild boar liver by hunter population in ng kg ⁻¹ body weight*, +	80 (37–131) \cong 18 \times TWI	147 \cong 33 \times TWI	19 (14–23) \cong 4 \times TWI
(b) Annual consumption of 200 g wild boar liver expressed as weekly intake in ng kg ⁻¹ body weight*	24 (11–39) \cong 5 \times TWI	44 \cong 10 \times TWI	5.6 (4.1–6.7) > TWI

* normalized to a human body weight of 70 kg (EFSA Scientific Committee, 2012); + calculated with the median amount of wild boar liver consumed by the Italian hunter population according to Danieli et al. (2012).

6.4.5 Conclusion

This study on wild boar livers from sampling sites with different contamination history shows the co-occurrence of a wide range of PFAS (up to 31 compounds) in the liver as well as considerable amounts of Σ PFAS – between 100 (BC) and 1000 $\mu\text{g kg}^{-1}$ – and spatial differences in the PFAS patterns. The site-specificity is associated with different contamination sources ranging from background contamination (BC) to industrial emissions (IE) and the distribution of PFAS-loaded sludges on arable land (PS). For the wild boar liver from the industrial hot-spot (IE), a subset of the monitoring data was characteristic, i. e. a reversed ratio of PFOS:PFOA and the presence of individual emerging substitutes (HFPO-DA and DONA). For the other hot-spot (area PS), the formation potential of short-chain PFCAs from precursors was site-specific. Shown exemplarily for these areas (IE and PS), PFAS profiling in wild boar liver seems to represent the environmental contamination in soil.

In conclusion, these results support the notion that wild boar liver is a suitable bioindicator for PFAS in the terrestrial environment – due to the omnivorous diet and the high trophic level of this species. The bioindicator reflects long-term PFAS trends in the environment and is particularly sensitive for PFAS that are considered problematic for human health. However, the environmental contamination by (ultra)short chain PFAS is better assessed in aquatic organisms, suspended matter or water – as shown exemplarily for riverine samples from area IE. In future environmental monitoring studies of PFAS, it is essential to include substitute PFAS and the TOP assay.

Since PFAS monitoring has not yet been carried out comprehensively on a geographical scale, many hot-spots are yet to be detected. The screening of wild boar livers appears promising for monitoring the terrestrial environment at a relatively wide geographical scale. It can determine both historic contamination by legacy PFAS – like PFOS and PFOA – and the emergence of substitutes – such as DONA and HFPO-DA – that all will shape the environmental PFAS contamination of the future.

6.5 Human Risk Assessment

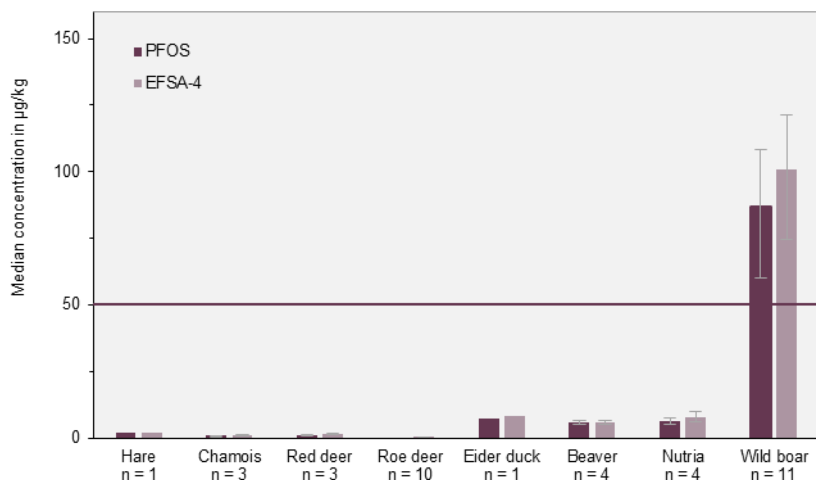
High PFAS concentrations in wild animals may affect the health of the respective animals (Ankley et al. 2021). In game animals and fish, they may also affect the health of humans when consuming the meat of the animals (CONTAM et al. 2018). In 2023, new maximum levels were introduced for PFAS in offal of game animals, fish meat and other foodstuffs (EU 2023). Products exceeding these levels by high levels of PFOS, PFHxS, PFOA and PFNA or the sum of these PFAS may not be placed on the market or processed for other food products.

In offal of game animals, the maximum levels were set at 50 $\mu\text{g kg}^{-1}$ for PFOS and the sum of the four PFAS. This threshold was exceeded in eleven out of eleven liver samples originating from wild boars (area BC), among them nine exceeded the threshold because of PFOS (Figure 38). The median concentration of all four PFAS was 101 $\mu\text{g kg}^{-1}$ (lower bound). This concentration corresponds to a weekly exposure of 5.6 ng kg^{-1} body weight if one portion wild boar liver is consumed by an average adult with a body weight of 70 kg per year. The calculated weekly intake fully exploits the TWI of 4.4. ng kg^{-1} body weight (CONTAM et al. 2020). In absence of representative consumption data, the calculation intake was based on a 200 g-portion consumed once a year.

In the investigated livers of hare, chamois, red deer, roe deer, eider duck, beaver and nutria, sum concentrations of PFOS, PFHxS, PFOA and PFNA were less than 10 % of the concentrations determined in wild boar livers and collectively below the maximum levels for offal of game animals (Figure 38). The consumption of one liver portion of these animals would be equivalent to a 10 %-exploitation of the TWI or less. It should be noted that concentrations in musculature, which is consumed more frequently, are generally lower than in livers (Felder et al. 2023).

Figure 38: PFAS concentration in the liver of selected wild animals

Median concentrations of PFOS and the sum of PFOS, PFHxS, PFOA and PFNA (EFSA-4, lower bound) in livers of selected animals. The horizontal line indicates the maximum level for PFOS and the EFSA-4 in offal of game animals which is effective since 2023 (EU 2023). Error bars indicate the range between the first and the third quartile.



Source: own illustration, UFZ.

For PFAS in fish musculature, lower maximum levels apply than for offal of game animals and these levels vary between fish species. The maximum level of $45 \mu\text{g kg}^{-1}$ ww for the sum concentration in roach, common bream and common barbel was exceeded in one of the respective fish (Table 10). The only fish with concentrations above this fish-specific maximum level was sampled in 2001 (common bream with $47 \mu\text{g kg}^{-1}$). For the other investigated fish a lower maximum level of $2 \mu\text{g kg}^{-1}$ ww applies. This was exceeded in one of three chubs.

Moreover, in one eelpout sample from the Baltic Sea, a PFNA concentration was determined which fully exploits the maximum level for the individual PFAS ($0.5 \mu\text{g kg}^{-1}$ ww). It should be noted that PFAS intake also occurs via other foodstuffs. In 2021, the German Federal Institute for Risk Assessment (Bundesinstitut für Risikobewertung (BfR) 2021) estimated that, the PFAS exposure of the German population is higher than deemed tolerable for the intake of all foodstuffs.

For aquatic biota, an Environmental Quality Standard (EQS) of $9.1 \mu\text{g kg}^{-1}$ applies for PFOS in addition to maximum levels for human consumption. The environmental threshold was exceeded in approximately half of the freshwater fish (see Table 10 for comparison). The EQS also covers human intake as a risk factor and rates it as the most sensitive protection goal for deriving the threshold. The quality standard is currently under revision and will probably be lowered soon (EU 2023).

Table 10: Dietary risk assessment of different fish musculature

Median concentrations of PFOS, PFOA and PFNA and the sum of PFOS, PFHxS, PFOA and PFNA (EFSA-4, lower bound) in fish musculature ($\mu\text{g/kg}$ wet weight) (PFHxSA always below LOD). The asterisk indicates samples from 2001. The other fish were sampled between 2015 and 2018. Bold indicates values which exceed EU maximum levels (EU 2023).

Sample Origin	Sample type	Sample code	PFOS	PFOA	PFNA	ΣEFSA-4
Maximum levels in fish meat			2.0	0.20	0.50	2.0
Antarctica	Emerald rockcod (<i>Trematomus bernachii</i>)	B015	< 0.068	< 0.034	< 0.016	0
South Germany	Roach (<i>Rutilus rutilus</i>)	B016	15	< 0.034	< 0.016	15
South Germany	European chub (<i>Squalius cephalus</i>)	B017	1.2	0.048	0.72	2.0
South Germany	European chub (<i>Squalius cephalus</i>)	B018	5.7	< 0.034	0.036	5.7
South Germany	European chub (<i>Squalius cephalus</i>)	B019	1.9	< 0.034	0.072	2.0
ESB	Viviparous eelpout (<i>Zoarces viviparus</i>)	A005*	< 0.33	< 0.025	0.064	0.064
ESB	Viviparous eelpout (<i>Zoarces viviparus</i>)	A006	< 0.33	0.027	0.22	0.25
ESB	Viviparous eelpout (<i>Zoarces viviparus</i>)	A007	< 0.33	0.17	0.50	0.67
ESB	Viviparous eelpout (<i>Zoarces viviparus</i>)	A008	0.39	0.042	< 0.03	0.43
ESB	Common bream (<i>Abramis brama</i>)	A020	0.24	0.12	0.14	0.50
ESB	Common bream (<i>Abramis brama</i>)	A021	14	0.17	0.20	14
ESB	Common bream (<i>Abramis brama</i>)	A022	2.9	0.13	0.21	3.2
ESB	Common bream (<i>Abramis brama</i>)	A023	9.9	0.046	0.27	10
ESB	Common bream (<i>Abramis brama</i>)	A024	5.0	< 0.025	0.12	5.1
ESB	Common bream (<i>Abramis brama</i>)	A025	7.8	0.10	0.23	8.1
ESB	Common bream (<i>Abramis brama</i>)	A026	7.8	0.15	0.20	8.2
ESB	Common bream (<i>Abramis brama</i>)	A027	15	0.19	0.40	16
ESB	Common bream (<i>Abramis brama</i>)	A028	29	0.25	0.34	30

Sample Origin	Sample type	Sample code	PFOS	PFOA	PFNA	ΣEFSA-4
ESB	Common bream (<i>Abramis brama</i>)	A029*	47	0.21	0.28	47
ESB	Common bream (<i>Abramis brama</i>)	A030	20	0.20	0.41	21
ESB	Common barbel (<i>Barbus barbus</i>)	A031	4.2	0.35	0.33	4.9

Beyond PFOS, PFHxS, PFOA and PFNA, many other PFAS, known or presumed to be harmful to human health, were determined in this project, including PFDA, PFUnDA, PFDoDA, PFTrDA and perfluorotetradecanoic acid (PFTeDA), each with a higher liver toxicity than PFOA (Bil et al. 2021). Currently, toxicological data are insufficient to deduce a health-based guidance value for any but the four PFAS considered in the TWI.

Consumption of wild boars, which are consumed more frequently (12 t per year in Germany; DJV (2024)) and exhibit higher PFAS concentrations than other game animals, was identified as a major source of dietary PFAS exposure. Similarly, consumption of fish may significantly contribute to the dietary PFAS intake.

6.6 Conclusion

- ▶ PFAS were determined in all environmental samples across Germany with a wide spread in concentration levels from sub-ppb to ppm.
- ▶ Obvious differences in concentration and PFAS pattern were detected for contaminated sites.
- ▶ An accumulation of PFAS over the food web was observed in concentration levels and PFAS pattern, as the pattern allowed drawing conclusions on the nutrition of the species, with herbivores clustering separately from omnivores and carnivores in PCA.
- ▶ Highest levels were consistently obtained in liver samples, as PFAS accumulate stronger in blood- and lipid rich tissues.
- ▶ The increase in PFCAs after application of TOP-Assay could not be explained by the precursors measured in this study (exception: harbour porpoise), indicating high concentrations of still unidentified precursors (“dark matter”).
- ▶ Suspended solids contained the highest proportions of unidentified precursors whereas concentrations of undefined precursors in biota samples were lower, indicating that precursors are subject to metabolic processes.
- ▶ No explicit difference in unknown PFAS between terrestrial and aquatic biota was observed. All wild boar livers analysed in this study, regardless of their origin, are not suited for human consumption, based on the new grouped EFSA TWI for PFAS.
- ▶ In this study, also fish filet was considered a potential health risk if consumed too frequently.

7 PFAS Suspect Screening

7.1 Archive of High-Resolution Mass Spectrometry Data (LC-TOF-MS)

It has been shown that stored mass spectrometric data generated by liquid chromatography-high resolution-mass spectrometry (LC-HRMS) allow for a later, retrospective search for molecular ions of analytes, one was not interested in while the LC-HRMS analysis was performed. Sometimes the term “digital sample freezing” is used for the generation of such LC-HRMS data from samples.

However, “digital sample freezing” is an erroneous terminology, as LC-HRMS screening cannot detect and, thus, “conserve” the totality of components in a sample. Rather, as any analytical technique LC-HRMS is selective. It detects analytes only:

- ▶ that were extracted and not lost in any sample processing step (e.g. volatiles lost in solvent evaporation),
- ▶ then passed the chromatographic column (of a given polarity range), providing a pronounced chromatographic peak,
- ▶ were effectively ionised in the electrospray process in presence of a large amount of co-eluting matrix constituents,
- ▶ were stable enough to not fragment in the electrospray ionisation process and,
- ▶ generate molecular ions within the m/z - range suitable for the mass spectrometer used,
- ▶ at an ion intensity high enough to generate a signal that can be clearly distinguished from the background noise.

Correspondingly, one may find a molecular ion that fits to an analyte of interest by a retrospective search in an LC-HRMS data set only if all aspects mentioned above were fulfilled during the previous sample processing and LC-HRMS analysis.

A search in such an LC-HRMS data set may provide a hit for a suspected PFAS, that may indicate the presence of the compound of interest in the original sample processed years ago (positive finding). Such a hit would then need to be confirmed and to exclude a false positive finding. The absence of such a hit does imply, that the compound of interest was not present in that sample. It may well be a false negative finding.

Experiences

Such non-targeted screening approaches bring about some specific challenges. For a broad coverage of PFAS in a non-target screening and for generating a comprehensive data set for archiving a generic extraction with no clean-up is needed. This should avoid losses of analytes of interest (PFAS). Without a clean-up, however, extracts contain much co-extracted sample matrix (lipids etc.) and the LC-HRMS data are then dominated by native sample constituents. This makes the later selection of signals that may represent a previously unknown PFAS extremely challenging.

In screening approaches generic measurement conditions have to be selected for both, the liquid chromatographic separation as well as for the mass spectrometric analysis to cover a wide range of the structurally very diverse PFAS. The conditions, therefore, cannot be optimized for certain PFAS classes. Consequently, some classes of PFAS may not be seen because of unfavourable LC-HRMS conditions. For example, it may not be possible to avoid fragmentation of labile molecules during electrospray ionization; this could specifically affect the detection of certain carboxylates or ethers.

The extent of in-source fragmentation also depends upon the temperature applied to the ESI-source. For the LC-TOF-MS analyses this source temperature was lowered from 600 °C to 300 °C.

Data dependent acquisition of product ion spectra is not suitable for a fully non-targeted analysis with reasonable effort. Therefore, the all-ion fragmentation mode (MS^E) was applied in this study, where all coeluting molecular ions are fragmented together in the collision cell. For analytes lacking highly diagnostic fragment ions, the MS^E -mode may not provide useful structural information to support tentative identification. For example, sulfonated PFAS tend to form a $[SO_3]^-$ fragment ion (Table 12). However, this fragment ion is formed from many other, non-fluorinated sulfonates. Therefore, if a PFAS signal of low intensity is accompanied by a coeluting sulfonate of high intensity, these fragments cannot be well distinguished and assigned to one of the molecular ions in the MS^E -mode. This, then, hampers the confirmation of PFAS suspects.

Results

A total of 249 samples of the FLUORBANK project were analysed by RPLC-HRMS with a TOF-mass spectrometer in the positive and in the negative mode using generic measurement conditions. In addition, standard mixes (containing different classes of PFAS and additionally isotope-labelled internal standards (Table B 2) and blanks were analysed repeatedly in each of the sequences for quality assurance and control.

The data are stored at UFZ and are available for retrospective search for 5 years. If a suspect list used to search in the LC-HRMS-data contains not only molecular formulas but MOL files, the data can be searched automatically for software predicted fragment ions. The data set recorded at low collision energies can also be exported to mzML format to allow for data mining using non-proprietary software such MZmine.

7.2 Ultrahigh resolution MS (FTICR-MS) and Combination with LC-Q-TOF analysis

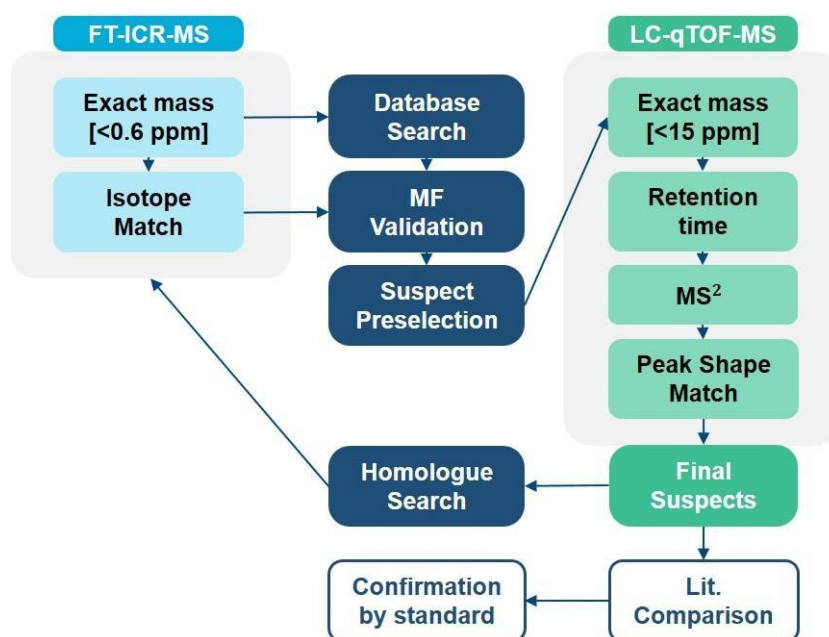
An even higher mass resolving power is achieved by so-called ultra-high resolution-mass spectrometry utilizing a FTICR-mass spectrometer. Selected samples were analysed by FTICR-MS in the infusion mode, meaning that no chromatographic separation was applied. The lack of chromatographic separation is partially compensated for by the ultrahigh mass resolution and high mass accuracy and precision of FTICR-MS. This makes molecular formula selection much more straightforward than in LC-HRMS analysis. However, structure assignment is hardly possible because information on chromatographic retention time as well as on fragment ions is missing.

On this basis it was decided to combine both approaches, LC-QTOF-MS and FTICR-MS for a non-targeted search for previously undetected PFAS in samples of the environmental specimen bank.

7.2.1 Work Flow

This approach (Figure 39) combines analytical evidence from exact mass and isotope pattern (FTICR-MS) to diagnostic fragments (LC-QTOF-MS) and mass defects (FTICR-MS) that are characteristic for PFAS. All of these criteria are commonly utilised in suspect screening efforts but were combined here in a new workflow.

Figure 39: Scheme for the non-targeted search for PFAS



Source: T. Döring, UFZ.

In its first stage the workflow uses an in-house database of PFAS to search for the exact masses of their molecular ions (with a mass error $\leq 0.6 \text{ ppm}$) in the DI-FTICR-MS data, making use also of the isotopic pattern visible from the FTICR-MS data. As the PFAS database was not curated with respect to mass spectrometry, the list of preselected suspects required further filtering. This included deletion of salts and of pure fluorohydrocarbons and similar compounds that are unlikely to ionise in the negative mode of electrospray ionisation

In the second stage, the LC-TOF-MS data are searched for the molecular ions of the suspects preselected from the FTICR-MS data (with a mass error $\leq 15 \text{ ppm}$). The MS^E-data recorded by the LC-TOF-MS are used to search for expected fragment ions to verify the identity suggested from the FTICR-MS data and, on this basis, to generate a list of final suspects.

A third step, then, is to search for homologues of the final suspects in the DI-FTICR-MS data. As for all suspect screenings it is mandatory to confirm suspects as far as possible by using literature data and analysis of standard compounds, where applicable.

7.2.2 Application

For this exercise four bream liver samples were selected that exhibited a) high concentrations of known PFAS and b) a comparatively high proportion of non-explained EOF (Table 11). It has to be noted, though, that concentrations of PFAS in these samples were still low, compared to samples previously used for non-targeted search for PFAS. In literature reports on non-target screening for unknown PFAS the samples often originated from contamination hot-spots, e.g. from AFFF applications (Barzen-Hanson et al. 2017) or from sludge deposition (Zweigle et al. 2024).

Table 11: Overview on the four bream liver samples selected for the FTICR-MS and LC-HRMS screening exercise

	BL8	BLDE	BLPr	BL20
Sampling Site	Bimmen (Rhine)	Dessau (Mulde)	Prossen (Elbe)	Koblenz (Rhine)
Sampling Year	2001	2018	2018	2020
Precursor Potential ¹⁾	74 %	51 %	75 %	48 %
Σ PFAS target \geq C2 [$\mu\text{g kg}^{-1}$]	87.83	147.14	128.07	656.63

1) Precursor potential denotes the difference between the sum concentration of quantified PFAS and the concentration of total extractable organic fluorine (EOF) determined in the respective sample

The work-flow outlined above (Figure 39) was applied to the set of four samples of bream liver (Table 11). Of the initial >7000 features in the FTICR-MS data this process was able to select 154 suspects with variable degree of confidence (Figure 40). A number of 21 of those agreed to PFAS previously determined by the quantitative target analysis, while 133 were not detected in these samples before.

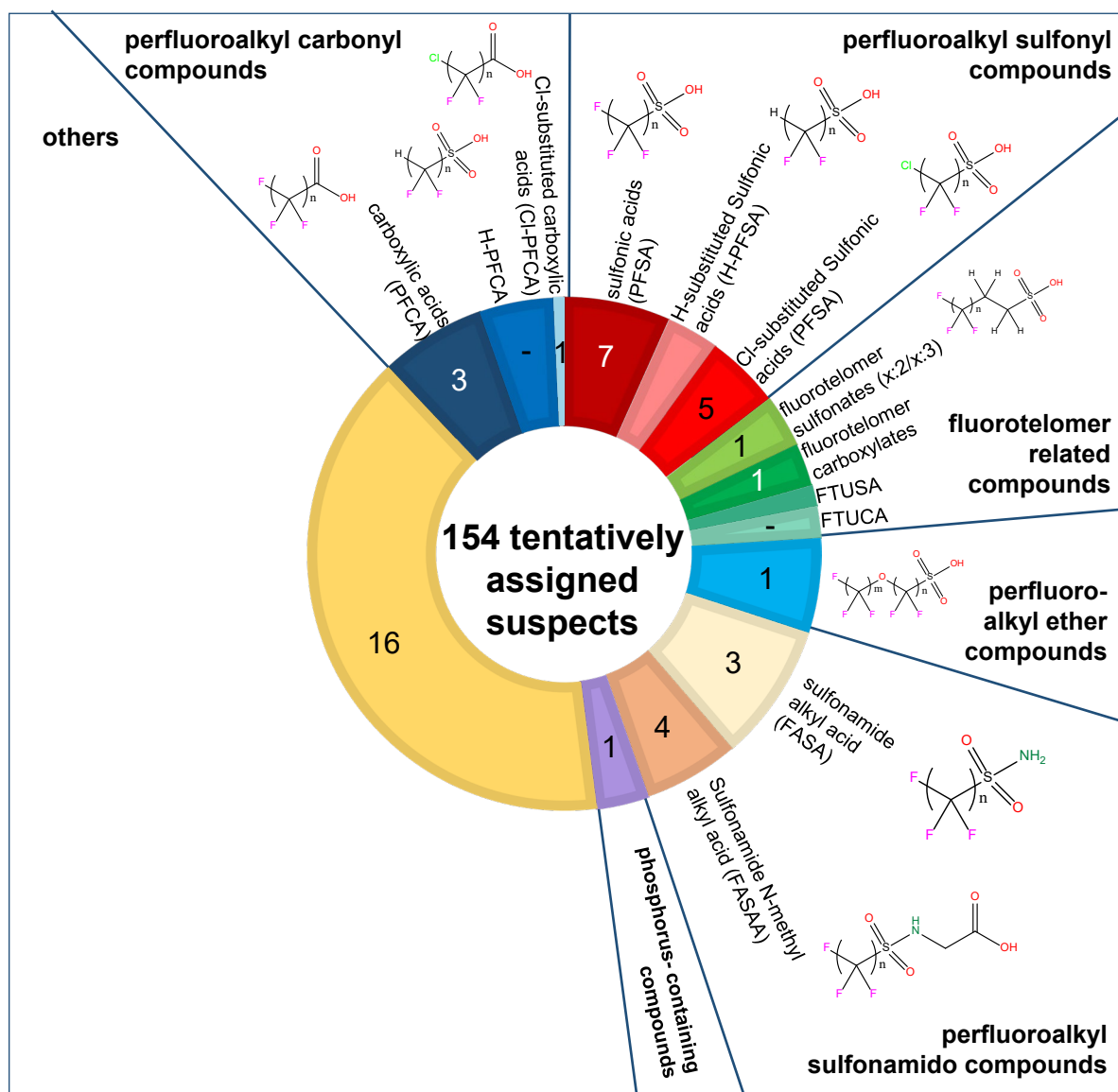
To several suspects fragment ions could be ascribed from the MS^e data recorded by the LC-TOF-MS that supported the proposed structures. These 43 compounds were classified as being identified with “high confidence” (HC), while the remaining 90 of the newly detected PFAS remained at the level of “low confidence” (LC).

Overall, 14 PFAS classes were annotated in the analysed samples using the established workflow (Figure 40). Most of the classes that were identified have been reported in PFAS-contaminated environmental samples in the past. PFCA, PFSA, FTS and FASA combined, comprise around 82 % of the detected PFAS classes in recent suspect screening studies (Liu et al. 2019a). In the four liver samples studied here, these four PFAS classes made up around half of all annotations, only.

Of the PFAS candidates ascribed with high confidence (HC) four exhibit carboxylic acid-derived structures, 12 sulfonic acid-derived structures, two are fluorotelomer-based, seven sulfonamide-based, one is carboxylic ether-based and one exhibits a phosphinic acid-derived structure. Another 16 additional HC candidates are not belonging to any of these classes.

The homologue series of PFSA and PFCA were the longest, ranging from C3 and C4 up to C15. Besides that, a series of chloroperfluoroalkyl sulfonic acid (Cl-PFSA) with seven consecutive members was putatively identified with the support of homologue search and isotope matches, although it was of low abundance (Table 12).

Figure 40: Overview of tentatively identified candidates (with low and high confidence) and their associated PFAS subclasses detected in the four breast liver samples.



Source: T. Döring, UFZ; Master Thesis, Univ. of Leipzig.

Table 12 shows the PFAS identified with high confidence, that have not been included in the previous quantitative analysis. Many of the HC candidates are sulfonic acids, which is due to the fact that they exhibit characteristic fragment ions that support identification: besides $[SO_3]^-$ several related fragment ions exist for PFAS containing additional elements, including SO_3H , SO_4H , SO_3F or SO_3Cl , which further support the identification of members of these PFAS classes. For many of the other classes of PFAS, only less characteristic fragment ions could be recorded, so that they remained in the LC class.

Table 12: List of assigned suspects with a high degree of confidence, identified in four bream liver samples.

No	Acronym	Formula	Mass Error (ppm)	m/z of fragment anions (corresponding elemental composition)
1	PFHpS	C7HF15O3S	-0.891	79.957 (SO3); 99.062 (FSO3); 119.049 (C2F5)
2	PFNS	C9HF19O3S	0.0364	79.957 (SO3); 80.964 (SO3H)
3	PFDoS	C12HF25O3S	-0.5723	79.957 (SO3)
4	PFTTrDS	C13F27O3HS	-7.6110	93.969 (C2F2S, CH2SO3)
5	FPeSA	C5H2F11NO2S	0.0364	79.960 (SO3); 80.961 (C2F3); 81.954 (C2F4); 94.980 (CH3O3S); 106.979 (C2H3O3S)
6	8-F5S-PFOS	C8HF21O3S2	2.6364	79.957 (SO3); 80.964 (SO3H); 118.992 (C2F5)
7	Cl-PFBS	C4HF8ClO3S	3.1755	96.961 (SO4H)
8	Cl-PFHxS	C6HF12ClO3S	-7.2305	96.961 (SO4H); 98.955 (FSO3); 279.962 (C4F8O3S)
9	Cl-PFOS	C8HF16ClO3S	1.9421	79.956 (SO3); 80.964 (SO3H); 94.980 (CH3O3S); 95.952 (SO4); 96.960 (SO4H); 97.961 (SO4H2); 98.957 (SO3F); 106.977 (C2H3O3S); 107.986 (C2H4O3S); 134.989 (C2F5O); 136.996 (C2F5OH); 136.996 (C2H5OF3Cl); 138.988 (C3H4O3FS); 168.989 (C3F7)
10	Cl-PFNS	C9HF18ClO3S	0.5311	118.992 (C2F5)
11	Cl-PFDS	C10HF20ClO3S	8.1315	(79.957 (SO3); 80.918 (SO3H); 96.962 (SO4H); 99.009 (FSO3); 119.049 (C2F5))
12	Cl-PFNA	C9F16O2ClH	-2.2968	78.957 (CO2Cl); 106.981 (C2O4F)
13	10:2 FTS	C12F21O3H5S	-8.9321	73.979 (C2H2OS); 79.956 (SO3); 80.967 (C2F3); 96.973 (SO4H); 99.007 (SO3F); 119.060 (C2F5); 168.957 (C3F7); 606.948 (C12F20SO3H3 M-H-HF)
14	6:2 FTMAC	C12H9F13O2	4.6400	(169.088 (C3F7))
15	FTA-OH derivative	C6F6O3H6	-9.6229	80.964 (C2F3); 81.950 (C2F3H)
16	FTA derivative	C10F6O2H14	10.7495	68.982 (CF3)
17	-	C11F4O3H11N	-2.4995	115.947 (C2F4O)
18	FTA derivative	C11H10F12O2	2.2442	331.000 (C7H3F12O)
19	PFOES	C8F17O4HS	8.5449	79.958 (SO3); 80.965 (C2F3); 95.950 (SO4); 96.961 (SO4H); 97.948 (SO4H2); 98.956 (SO3F); 109.970 (CH2O4S); 110.972 (CH3O4S)
20	EtFOSAA derivative	C10F13O6H11PNS	0.1819	122.985 (C2H4O4P); 123.990 (C2H5O4P); 126.997 (C2H5O3FP); 140.998 (C2H6O5P)

No	Acronym	Formula	Mass Error (ppm)	m/z of fragment anions (corresponding elemental composition)
21	PFDPA	C10F21O3H2P	-9.6839	331.985 (C8H5O3F8P); 379.933 (C5H3O4F10PS)
22	6:8 PFPiA	C14HF30O2	1.6231	69.038 (CF3); 83.020 (C2H2F3); 166.991 (C4H5O4FP); 400.940 (C6O2F14P); 500.935 (C8O2F18P)

This screening exercise led to the detection of a variety of PFAS, including legacy compounds as well as several precursors and substitutes in the liver of bream. Furthermore, several modified analogues of legacy compounds with branched side chains, H- and Cl-substitution, double-bond/ring functionality insertion as well as variations of non-fluorinated polar head groups could be detected.

Ketone-PFOS, known to be a PFOS metabolite, was also detected in fish sera of the Great Lakes region (U.S.) at low concentrations. (Baygi et al. 2021).

Another emerging class of potential PFAS metabolites include the homologue series of Cl-substituted PFSA. These less known substitutes have already been identified in industrial wastewater and river water in China (Wang et al. 2013).

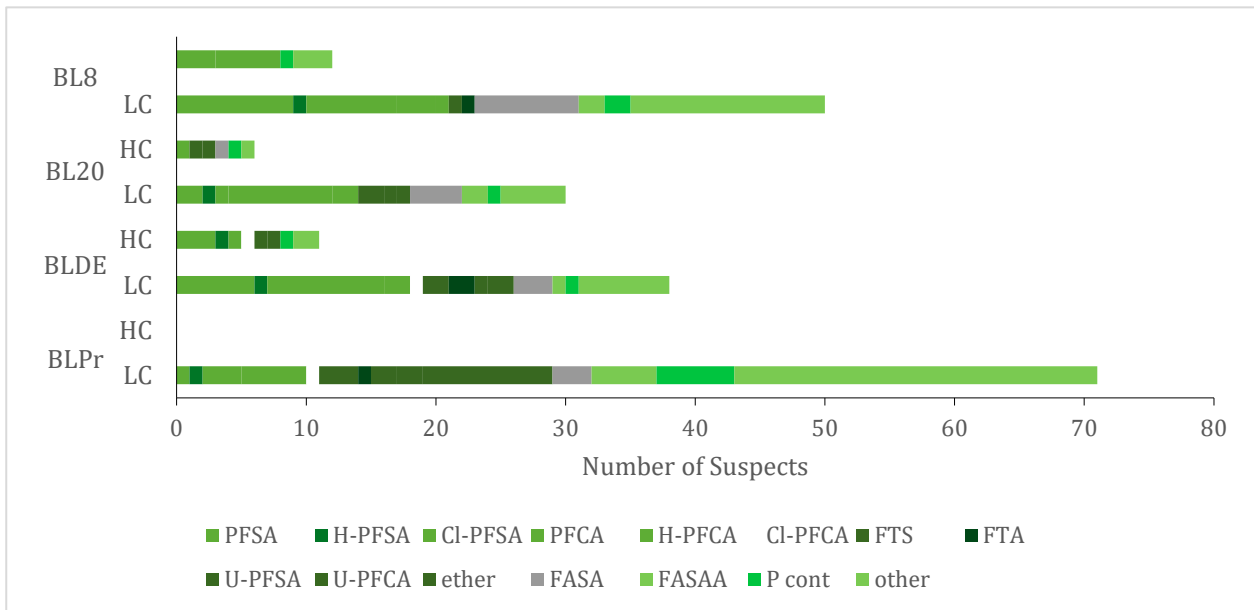
Unlike the structurally related perfluoroalkyl phosphonic acids, little is known about the biological fate of the phosphinic acids (PFPiA) and their persistent metabolites. To date, there have only been a few studies, reporting screening results for PFPiA in humans and the environment (Joudan et al. 2017). In organisms, PFPiA may be metabolized to more reactive transformation products such as 1H-perfluoroalkanes, or result in more persistent compounds such as phosphonic acids. PFPiA is eliminated approximately twice as fast as PFOA, even though they have more perfluorinated carbon groups.

In an earlier screening study, PFPiA has been reported to occur in human sera. The most commonly detected species were 6:6 PFPiA and 6:8 PFPiA, which were found in >50 % of samples at concentrations ranging between 4 – 38 pg mL⁻¹ (Lee and Mabury 2011).

Figure 41 shows which of the low and high confidence PFAS occurred in the individual samples of bream liver. For all samples, the number of PFAS detected with high confidence is much lower than that with low confidence. The highest diversity of suspect PFAS was detected in the sample BLPr, which was the one with the largest proportion of unidentified PFAS determined by the TOP assay (Table 11). However, none of the suspected PFAS in this sample could be confirmed. Rather, all remained in the LC group.

The complex matrix of biota samples and the comparatively low concentration of PFAS in such samples makes identification of unknown PFAS a challenging task, still. Methods for this purpose need further improvement. Because of its high sensitivity and extremely high mass resolving power, FTICR-MS remains as an attractive option in this field.

Figure 41: Overview of candidate annotations with low (LC) and high confidence (HC), detected in four bream liver samples from German rivers



Source: T. Döring, UFZ.

8 Conclusion

Based on the results elaborated in the project FLUORBANK the following conclusions can be drawn:

- ▶ For PFAS monitoring, in the environment and in biota, a combination of different analytical methods is recommended for future monitoring studies of PFAS when resources allow. Target analyses of a larger number of PFAS (long-chain-PFAS, (ultra)short-chain PFA, substitutes and precursors) in combination with the TOP assay also extended towards (ultra)short-chain PFAS, proved to be complementary tools, needed to adequately cover the increasingly diverse PFAS burden of the environment.
- ▶ Suspect- as well as nontarget-screening analysis for PFAS by LC-HRMS can provide a broader insight into the PFAS burden of biota that is not typically covered by target analysis. The benefit of screening analyses, however, strongly relies on PFAS specific data processing strategies. Moreover, confirmation of suspects and their quantitative assessment depends on the availability of reference compounds.
- ▶ FLUORBANK outlined that PFAS are omnipresent in wildlife in all regions of Germany with a wide spread in concentration levels from sub-ppb to ppm and PFAS patterns.
- ▶ PFAS levels in wildlife are determined by the level of contamination of the respective habitat and the trophic level of the species studied. PFAS contamination increased from herbivorous to carnivorous species. Also, the PFAS pattern differed with (ultra)short-chain PFAS and precursors being more relevant for the herbivores, both in riverine (mussel) and in terrestrial environment (deer).
- ▶ Long-chain legacy PFAS and precursors continue to accumulate in food chains and PFOS remains as the dominant PFAS compound in most instances. This contamination can be monitored by analysing the liver of wild boar (terrestrial environment) and bream (riverine systems) and herring gull eggs (marine).
- ▶ Monitoring for the PFAS contamination of the terrestrial environment in Germany has not been carried out comprehensively. Analysis of PFAS from the liver of wild boars appears suitable to detect contamination hot-spots. It is expected to indicate not only the level of contamination but also the respective PFAS pattern, thus providing indications of the potential origin of a contamination.
- ▶ The major contribution of TFA to the total PFAS contamination in herbivores highlights the importance of including TFA in future (bio-) monitoring studies. Herbivorous terrestrial animals (e.g. deer) and zebra mussel are suitable sentinel species for biomonitoring.
- ▶ The application of the TOP assay showed that riverine suspended matter contained the highest proportion of unidentified PFAS precursor compounds.
- ▶ The temporal development of the PFAS load of the biota samples clearly reflects the phase-out of PFOS in the early 2000s; it decreased continuously since then in many of the studied animal species. However, PFOS remains environmentally relevant with high shares of the total PFAS burden in most organisms studied.
- ▶ Contrary to this general trend, the level of known and unknown C8 precursors and the trend for > C 8 PFAS is increasing in some of the species monitored.

- ▶ Also, the burden of TFA and precursors of (ultra)short-chain PFAS increases, namely since 1995; this was clearly reflected in zebra mussels. TFA and its precursors appears as an emerging risk for biota – and for the quality of water resources due to the persistent and mobile nature.
- ▶ The monitoring data of FLUORBANK have outlined that both, the bioaccumulative and the mobile PFAS classes, occur throughout the environment and in wildlife. Thus, both these classes should be considered in monitoring and be addressed by policy makers.
- ▶ All wild boar livers analysed in FLUORBANK, regardless of their origin, are not suited for human consumption, based on the newly derived TWI for the PFAS group. Also, fish filet was considered a potential health risk if consumed too frequently.

9 List of References

- Ahrens, L.; Plassmann, M.; Xie, Z. and Ebinghaus, R. (2009). "Determination of polyfluoroalkyl compounds in water and suspended particulate matter in the river Elbe and North Sea, Germany." Frontiers of Environmental Science & Engineering **3**(2): 152–170. DOI: <https://doi.org/10.1007/s11783-009-0021-8>.
- Ahrens, L.; Siebert, U. and Ebinghaus, R. (2009). "Total body burden and tissue distribution of polyfluorinated compounds in harbor seals (*Phoca vitulina*) from the German Bight." Marine Pollution Bulletin **58**(4): 520-525. DOI: <https://doi.org/10.1016/j.marpolbul.2008.11.030>.
- Allendorf, F.; Goss, K.-U. and Ulrich, N. (2021). "Estimating the Equilibrium Distribution of Perfluoroalkyl Acids and 4 of Their Alternatives in Mammals." Environmental Toxicology and Chemistry **40**(3): 910-920. DOI: <https://doi.org/10.1002/etc.4954>.
- Androulakis, A.; Alygizakis, N.; Gkotsis, G.; Nika, M. C.; Nikolopoulou, V.; Bizani, E.; Chadwick, E.; Cincinelli, A.; Claßen, D.; Danielsson, S.; Dekker, R. W. R. J.; Duke, G.; Glowacka, N.; Jansman, H. A. H.; Krone, O.; Martellini, T.; Movalli, P.; Persson, S.; Roos, A.; O'Rourke, E.; Siebert, U.; Treu, G.; van den Brink, N. W.; Walker, L. A.; Deaville, R.; Slobodnik, J. and Thomaidis, N. S. (2022). "Determination of 56 per- and polyfluoroalkyl substances in top predators and their prey from Northern Europe by LC-MS/MS." Chemosphere **287**(May 2021). DOI: <https://doi.org/10.1016/j.chemosphere.2021.131775>.
- Ankley, G. T.; Cureton, P.; Hoke, R. A.; Houde, M.; Kumar, A.; Kurias, J.; Lanno, R.; McCarthy, C.; Newsted, J.; Salice, C. J.; Sample, B. E.; Sepúlveda, M. S.; Steevens, J. and Valsecchi, S. (2021). "Assessing the Ecological Risks of Per- and Polyfluoroalkyl Substances: Current State-of-the Science and a Proposed Path Forward." Environmental Toxicology and Chemistry **40**(3): 564-605. DOI: <https://doi.org/10.1002/etc.4869>.
- Arenholz, U.; Bergmann, S.; Bosshammer, K.; Busch, D.; Dreher, K.; Eichler, W.; Geueke, K.-J.; Grubert, G.; Hähnle, J.; Harff, K.; Kraft, M.; Leisner-Saab, J.; Oberdörfer, M.; Rauchfuss, K.; Respondek, R.; Reupert, R.; Rose-Luther, J.; Schroers, S.; Tiedt, M.; Just, P.; Poschner, A. and Susset, B. (2011). "Verbreitung von PFT in der Umwelt : Ursachen, Untersuchungsstrategie, Ergebnisse, Maßnahmen." LANUV-Fachbericht 34. Recklinghausen, Landesamt für Natur, Umwelt und Verbraucherschutz: 118. <https://www.lanuv.nrw.de/landesamt/veroeffentlichungen/publikationen/fachberichte>.
- Arp, H. P. H. and Hale, S. (2023). "REACH: Guidance and Methods for the Identification and Assessment of PMT/vPvM Substances." Umweltbundesamt. **19**: 66. ISBN/ISSN: 1862-4804. DOI: <https://doi.org/10.13140/RG.2.2.24980.48001>.
- Ateia, M.; Maroli, A.; Tharayil, N. and Karanfil, T. (2019). "The overlooked short- and ultrashort-chain poly- and perfluorinated substances: A review." Chemosphere **220**: 866–882. DOI: <https://doi.org/10.1016/j.chemosphere.2018.12.186>.
- Bach, C.; Boiteux, V.; Hemard, J.; Colin, A.; Rosin, C.; Munoz, J. F. and Dauchy, X. (2016). "Simultaneous determination of perfluoroalkyl iodides, perfluoroalkane sulfonamides, fluorotelomer alcohols, fluorotelomer iodides and fluorotelomer acrylates and methacrylates in water and sediments using solid-phase microextraction-gas chromatography/mas." Journal of Chromatography A **1448**: 98-106. DOI: <https://doi.org/10.1016/j.chroma.2016.04.025>.
- Barzen-Hanson, K. A.; Roberts, S. C.; Choyke, S.; Oetjen, K.; McAlees, A.; Riddell, N.; McCrindle, R.; Ferguson, P. L.; Higgins, C. P. and Field, J. A. (2017). "Discovery of 40 Classes of Per- and Polyfluoroalkyl Substances in Historical Aqueous Film-Forming Foams (AFFFs) and AFFF-Impacted Groundwater." Environmental Science & Technology **51**(4): 2047-2057. DOI: <https://doi.org/10.1021/acs.est.6b05843>.
- Baygi, S. F.; Fernando, S.; Hopke, P. K.; Holsen, T. M. and Crimmins, B. S. (2021). "Nontargeted Discovery of Novel Contaminants in the Great Lakes Region: A Comparison of Fish Fillets and Fish Consumers." Environmental Science & Technology **55**(6): 3765–3774. DOI: <https://doi.org/10.1021/acs.est.0c08507>.

Behringer, D.; Heydel, F.; Gschrey, B.; Osterheld, S.; Schwarz, W.; Warncke, K.; Freeling, F.; Nödler, K.; Henne, S.; Reimann, S.; Blepp, M.; Jörß, W.; Liu, R.; Ludig, S.; Rüdener, I. and Gartiser, S. (2021). "Persistent degradation products of halogenated refrigerants and blowing agents in the environment: type, and fate with particular regard to new halogenated substitutes with low global warming potential." Dessau-Roßlau, Umweltbundesamt. **73**: 259. ISBN/ISSN: 1862-4 804. <http://www.umweltbundesamt.de/publikationen>.

Bhat, A. P.; Pomerantz, W. C. K. and Arnold, W. A. (2022). "Finding Fluorine: Photoproduct Formation during the Photolysis of Fluorinated Pesticides." *Environmental Science & Technology* **56**(17): 12336-12346. DOI: <https://doi.org/10.1021/acs.est.2c04242>.

Bil, W.; Zeilmaker, M.; Fragki, S.; Lijzen, J.; Verbruggen, E. and Bokkers, B. (2021). "Risk Assessment of Per- and Polyfluoroalkyl Substance Mixtures: A Relative Potency Factor Approach." *Environmental Toxicology and Chemistry* **40**(3): 859-870. DOI: <https://doi.org/10.1002/etc.4835>.

Björnsdotter, M. K.; Yeung, L. W. Y.; Kärrman, A. and Jogsten, I. E. (2022). "Mass Balance of Perfluoroalkyl Acids, Including Trifluoroacetic Acid, in a Freshwater Lake." *Environmental Science & Technology* **56**(1): 251–259. DOI: <https://doi.org/10.1021/acs.est.1c04472>.

BJV and Gangl, C. (2020, 09.02.2020). "NEU: PFC – Belastung beim Schwarzwild (PFC=per- oder polyfluorierte Chemikalien)." from <https://www.bjv-ffb.de/chemie>.

Brambilla, G.; D'Hollander, W.; Oliyai, F.; Stahl, T. and Weber, R. (2015). "Pathways and factors for food safety and food security at PFOS contaminated sites within a problem based learning approach." *Chemosphere* **129**(2015): 192–202. DOI: <https://doi.org/10.1016/j.chemosphere.2014.09.050>.

Brambilla, G.; Testa, C. and Fedrizzi, G. (2016). "Occurrence of selected perfluoroacids in muscle and liver from wild boar: Relevance for food safety/food security issues." *Conference: 36th International Symposium On Halogenated Persistent Organic Pollutants*. Florence. *Organohalogen Compounds* **78** (2016): 338–340.

Brandsma, S. H.; Koekkoek, J. C.; van Velzen, M. J. M. and Boer, J. d. (2019). "The PFOA substitute GenX detected in the environment near a fluoropolymer manufacturing plant in the Netherlands." *Chemosphere* **220**: 493–500. DOI: <https://doi.org/10.1016/j.chemosphere.2018.12.135>.

Brandsma, S. H.; Smithwick, M.; Solomon, K.; Small, J.; Boer, J. d. and Muir, D. C. G. (2011). "Dietary exposure of rainbow trout to 8:2 and 10:2 fluorotelomer alcohols and perfluorooctanesulfonamide: Uptake, transformation and elimination." *Chemosphere* **82**(2): 253–258. DOI: <https://doi.org/10.1016/j.chemosphere.2010.09.050>.

Brendel, S.; Fetter, É.; Staude, C.; Vierke, L. and Biegel-Engler, A. (2018). "Short-chain perfluoroalkyl acids: environmental concerns and a regulatory strategy under REACH." *Environmental Sciences Europe* **30**(1): 9. DOI: <https://doi.org/10.1186/s12302-018-0134-4>.

Buck, R. C.; Franklin, J.; Berger, U.; Conder, J. M.; Cousins, I. T.; de Voogt, P.; Jensen, A. A.; Kannan, K.; Mabury, S. A. and van Leeuwen, S. P. J. (2011). "Perfluoroalkyl and polyfluoroalkyl substances in the environment: Terminology, classification, and origins." *Integrated Environmental Assessment and Management* **7**(4): 513-541. DOI: <https://doi.org/10.1002/ieam.258>.

Bugsel, B.; Bauer, R.; Herrmann, F.; Maier, M. E. and Zwiener, C. (2022). "LC-HRMS screening of per- and polyfluorinated alkyl substances (PFAS) in impregnated paper samples and contaminated soils." *Analytical and Bioanalytical Chemistry* **414**(3): 1217–1225. DOI: <https://doi.org/10.1007/s00216-021-03463-9>.

Bugsel, B.; Zweigle, J. and Zwiener, C. (2023). "Nontarget screening strategies for PFAS prioritization and identification by high resolution mass spectrometry: A review." *Trends in Environmental Analytical Chemistry* **40**: e00216. DOI: <https://doi.org/10.1016/j.teac.2023.e00216>.

Bugsel, B. and Zwiener, C. (2020). "LC-MS screening of poly- and perfluoroalkyl substances in contaminated soil by Kendrick mass analysis." *Analytical and Bioanalytical Chemistry* **412**(20): 4797–4805. DOI: <https://doi.org/10.1007/s00216-019-02358-0>.

- Bundesamt für Risikobewertung (BfR). (2011). "Dioxin- und PCB-Gehalte in Wild stellen keine Gesundheitsgefahr dar." *BfR-Stellungnahmen*, 048/2011, from <https://www.bfr.bund.de/cm/343/dioxin-und-pcb-gehalte-in-wild-stellen-keinegesundheitsgefahr-dar.pdf>.
- Bundesamt für Risikobewertung (BfR) (2021). "PFAS in food: BfR confirms critical exposure to industrial chemicals : BfR Opinion No 020/2021 of 28 June 2021." *BfR-Stellungnahmen*. **020**: 71. DOI: <https://doi.org/10.17590/20210914-121236>. <https://www.bfr.bund.de/cm/349/pfas-in-food-bfr-confirms-critical-exposure-to-industrial-chemicals.pdf>.
- Bustnes, J. O.; Bårdsen, B. J.; Herzke, D.; Bangjord, G.; Bourgeon, S.; Fritsch, C. and Eulaers, I. (2022). "Temporal Trends of Organochlorine and Perfluorinated Contaminants in a Terrestrial Raptor in Northern Europe Over 34 years (1986–2019)." *Environmental Toxicology and Chemistry* **41**(6): 1508-1519. DOI: <https://doi.org/10.1002/etc.5331>.
- Butt, C. M.; Muir, D. C. G. and Mabury, S. A. (2010). "Biotransformation of the 8:2 fluorotelomer acrylate in rainbow trout. 1. In vivo dietary exposure." *Environmental Toxicology and Chemistry* **29**(12): 2726–2735. DOI: <https://doi.org/10.1002/etc.349>.
- Cahill, T. M. (2022). "Increases in Trifluoroacetate Concentrations in Surface Waters over Two Decades." *Environmental Science & Technology* **56**(13): 9428-9434. DOI: <https://doi.org/10.1021/acs.est.2c01826>.
- Casson, R. and Chiang, S. Y. D. (2018). "Integrating total oxidizable precursor assay data to evaluate fate and transport of PFASs." *Remediation* **28**(2): 71–87. DOI: <https://doi.org/10.1002/rem.21551>.
- Chase, J. M. (2000). "Are there real differences among aquatic and terrestrial food webs?" *Trends in Ecology and Evolution* **15**(10): 408-412. DOI: [https://doi.org/10.1016/S0169-5347\(00\)01942-X](https://doi.org/10.1016/S0169-5347(00)01942-X).
- Chen, H.; Reinhard, M.; Yin, T.; Nguyen, T. V.; Tran, N. H. and Yew-Hoong Gin, K. (2019). "Multi-compartment distribution of perfluoroalkyl and polyfluoroalkyl substances (PFASs) in an urban catchment system." *Water research* **154**: 227–237. DOI: <https://doi.org/10.1016/j.watres.2019.02.009>.
- Chen, H.; Yao, Y.; Zhao, Z.; Wang, Y.; Wang, Q.; Ren, C.; Wang, B.; Sun, H.; Alder, A. C. and Kannan, K. (2018). "Multimedia Distribution and Transfer of Per- and Polyfluoroalkyl Substances (PFASs) Surrounding Two Fluorochemical Manufacturing Facilities in Fuxin, China." *Environmental Science & Technology* **52**(15): 8263-8271. DOI: <https://doi.org/10.1021/acs.est.8b00544>.
- Chen, M.; Qiang, L.; Pan, X.; Fang, S.; Han, Y. and Zhu, L. (2015). "In Vivo and in Vitro Isomer-Specific Biotransformation of Perfluorooctane Sulfonamide in Common Carp (*Cyprinus carpio*)." *Environmental Science & Technology* **49**(23): 13817–13824. DOI: <https://doi.org/10.1021/acs.est.5b00488>.
- Chen, M.; Zhu, L.; Wang, Q. and Shan, G. (2021). "Tissue distribution and bioaccumulation of legacy and emerging per-and polyfluoroalkyl substances (PFASs) in edible fishes from Taihu Lake, China." *Environmental Pollution* **268**: 115887-115887. DOI: <https://doi.org/10.1016/j.envpol.2020.115887>.
- Chu, S.; Letcher, R. J.; McGoldrick, D. J. and Backus, S. M. (2016). "A New Fluorinated Surfactant Contaminant in Biota: Perfluorobutane Sulfonamide in Several Fish Species." *Environmental Science & Technology* **50**(2): 669-675. DOI: <https://doi.org/10.1021/acs.est.5b05058>.
- Colomer-Vidal, P.; Bertolero, A.; Alcaraz, C.; Garreta-Lara, E.; Santos, F. J. and Lacorte, S. (2022). "Distribution and ten-year temporal trends (2009–2018) of perfluoroalkyl substances in gull eggs from Spanish breeding colonies." *Environmental Pollution* **293**: 118555. DOI: <https://doi.org/10.1016/j.envpol.2021.118555>.
- CONTAM; Knutsen, H. K.; Alexander, J.; Barregård, L.; Bignami, M.; Brüschweiler, B.; Ceccatelli, S.; Cottrill, B.; Dinovi, M.; Edler, L.; Grasl-Kraupp, B.; Hogstrand, C.; Hoogenboom, L.; Nebbia, C. S.; Oswald, I. P.; Petersen, A.; Rose, M.; Roudot, A.-C.; Vleminckx, C.; Vollmer, G.; Wallace, H.; Bodin, L.; Cravedi, J.-P.; Halldorsson, T. I.; Haug, L. S.; Johansson, N.; van Loveren, H.; Gergelova, P.; Mackay, K.; Levorato, S.; van Manen, M. and Schwerdtle, T.

(2018). "Risk to human health related to the presence of perfluorooctane sulfonic acid and perfluorooctanoic acid in food." *EFSA Journal* **16**(12): e05194. DOI: <https://doi.org/10.2903/j.efsa.2018.5194>.

CONTAM; Schrenk, D.; Bignami, M.; Bodin, L.; Chipman, J. K.; del Mazo, J.; Grasl-Kraupp, B.; Hogstrand, C.; Hoogenboom, L.; Leblanc, J.-C.; Nebbia, C. S.; Nielsen, E.; Ntzani, E.; Petersen, A.; Sand, S.; Vleminckx, C.; Wallace, H.; Barregård, L.; Ceccatelli, S.; Cravedi, J.-P.; Halldorsson, T. I.; Haug, L. S.; Johansson, N.; Knutsen, H. K.; Rose, M.; Roudot, A.-C.; Van Loveren, H.; Vollmer, G.; Mackay, K.; Riolo, F. and Schwerdtle, T. (2020). "Risk to human health related to the presence of perfluoroalkyl substances in food." *EFSA Journal* **18**(9): e05194. DOI: <https://doi.org/10.2903/j.efsa.2020.6223>.

Costello, M. C. S. and Lee, L. S. (2020). "Sources, Fate, and Plant Uptake in Agricultural Systems of Per- and Polyfluoroalkyl Substances." *Current Pollution Reports* **10**(4): 799-819. DOI: <https://doi.org/10.1007/s40726-020-00168-y>.

Cousins, I. T.; DeWitt, J. C.; Glüge, J.; Goldenman, G.; Herzke, D.; Lohmann, R.; Miller, M.; Ng, C. A.; Scheringer, M.; Vierke, L. and Wang, Z. (2020). "Strategies for grouping per- and polyfluoroalkyl substances (PFAS) to protect human and environmental health." *Environmental Science: Processes & Impacts* **22**(7): 1444–1460. DOI: <https://doi.org/10.1039/d0em00147c>.

Cousins, I. T.; Johansson, J. H.; Salter, M. E.; Sha, B. and Scheringer, M. (2022). "Outside the Safe Operating Space of a New Planetary Boundary for Per- and Polyfluoroalkyl Substances (PFAS)." *Environmental Science & Technology* **56**(16): 11172–11179. DOI: <https://doi.org/10.1021/acs.est.2c02765>.

Cuevas, M. F.; Novillo, A.; Campos, C.; Dacar, M. A. and Ojeda, R. A. (2010). "Food habits and impact of rooting behaviour of the invasive wild boar, *Sus scrofa*, in a protected area of the Monte Desert, Argentina." *Journal of Arid Environments* **74**(11): 1582-1585. DOI: <https://doi.org/10.1016/j.jaridenv.2010.05.002>.

D'Agostino, L. A. and Mabury, S. A. (2017). "Certain Perfluoroalkyl and Polyfluoroalkyl Substances Associated with Aqueous Film Forming Foam Are Widespread in Canadian Surface Waters." *Environmental Science and Technology* **51**(23): 13603-13613. DOI: <https://doi.org/10.1021/acs.est.7b03994>.

D'eon, J. C. and Mabury, S. A. (2011). "Exploring Indirect Sources of Human Exposure to Perfluoroalkyl Carboxylates (PFCAs): Evaluating Uptake, Elimination, and Biotransformation of Polyfluoroalkyl Phosphate Esters (PAPs) in the Rat." *Environmental Health Perspectives* **119**(3): 344–350. DOI: <https://doi.org/10.1289/ehp.1002409>.

Dabrio Ramos, M.; van der Veen, I.; Emteborg, H.; Weiss, J. and Schimmel, H. (2015). "Certification of the mass fraction of perfluoroalkyl substances (PFASs) in fish tissue (*pike-perch*): IRMM-427." *Reference Materials Report by the European Commission's Joint Research Centre*. DOI: <https://doi.org/10.2787/486905>.

Danieli, P. P.; Serrani, F.; Primi, R.; Ponzetta, M. P.; Ronchi, B. and Amici, A. (2012). "Cadmium, Lead, and Chromium in Large Game: A Local-Scale Exposure Assessment for Hunters Consuming Meat and Liver of Wild Boar." *Archives of Environmental Contamination and Toxicology* **63**(4): 612-627. DOI: <https://doi.org/10.1007/s00244-012-9791-2>.

De Silva, A. O.; Armitage, J. M.; Bruton, T. A.; Dassuncao, C.; Heiger-Bernays, W.; Hu, X. C.; Kärrman, A.; Kelly, B.; Ng, C.; Robuck, A.; Sun, M.; Webster, T. F. and Sunderland, E. M. (2021). "PFAS Exposure Pathways for Humans and Wildlife: A Synthesis of Current Knowledge and Key Gaps in Understanding." *Environmental Toxicology and Chemistry* **40**(3): 631-657. DOI: <https://doi.org/10.1002/etc.4935>.

Death, C.; Bell, C.; Champness, D.; Milne, C.; Reichman, S. and Hagen, T. (2021). "Per- and polyfluoroalkyl substances (PFAS) in livestock and game species: A review." *Science of The Total Environment* **774**: 144795. DOI: <https://doi.org/10.1016/j.scitotenv.2020.144795>.

Del Vento, S.; Halsall, C.; Gioia, R.; Jones, K. and Dachs, J. (2012). "Volatile per- and polyfluoroalkyl compounds in the remote atmosphere of the western Antarctic Peninsula: an indirect source of perfluoroalkyl acids to Antarctic waters?" *Atmospheric Pollution Research* **3**(4): 450–455. DOI: <https://doi.org/10.5094/apr.2012.051>.

DJV. (2024). "Mehr als 25.500 Tonnen Wild haben die Deutschen verzehrt." Retrieved 19.09.2024, from <https://www.jagdverband.de/mehr-als-25500-tonnen-wild-haben-die-deutschen-verzehrt>.

2007/629/EC: Commission Decision of 20 September 2007 concerning the non-inclusion of trifluralin in Annex I to Council Directive 91/414/EEC and the withdrawal of authorisations for plant protection products containing that substance (notified under document number C(2007) 4282). **L255**: 42–43. <http://data.europa.eu/eli/dec/2007/629/oj>.

Directive 2008/105/EC of the European Parliament and of the Council of 16 December 2008 on environmental quality standards in the field of water policy, amending and subsequently repealing Council Directives 82/176/EEC, 83/513/EEC, 84/156/EEC, 84/491/EEC, 86/280/EEC and amending Directive 2000/60/EC of the European Parliament and of the Council. **L348**: 84-97. <http://data.europa.eu/eli/dir/2008/105/oj>.

Commission Staff Working Document: Poly- and perfluoroalkyl substances (PFAS) Accompanying the document Communication from the Commission to the European Parliament, the Council, the European Economic and Social Committee and the Committee of the Regions: Chemicals Strategy for Sustainability Towards a Toxic-Free Environment, EC. <https://op.europa.eu/en/publication-detail/-/publication/2614f1f2-0f02-11eb-bc07-01aa75ed71a1/language-en>.

ED/69/2013: Inclusion of Substances of Very High Concern in the Candidate List. , European Chemicals Agency. <https://echa.europa.eu/documents/10162/092663e6-b14a-4a06-aadf-fc0e56bc0a23>.

ECHA. (2022b). "Registry of restriction intentions until outcome." Retrieved 20.06.2022, from <https://echa.europa.eu/de/registry-of-restriction-intentions/-/dislist/details/0b0236e18663449b>.

ECHA. (2023). "Candidate List of substances of very high concern for Authorization (published in accordance with Article 59(10) of the REACH Regulation)." Retrieved 28.02.2023, from <https://echa.europa.eu/en/candidate-list-table>.

Ellis, D. A.; Mabury, S. A.; Martin, J. W. and Muir, D. C. G. (2001). "Thermolysis of fluoropolymers as a potential source of halogenated organic acids in the environment." *Nature* **412**(6844): 321-324. DOI: <https://doi.org/10.1038/35085548>.

Enners, L.; Schwemmer, P.; Corman, A.-M.; Voigt, C. C. and Garthe, S. (2018). "Intercolony variations in movement patterns and foraging behaviors among herring gulls (*Larus argentatus*) breeding in the eastern Wadden Sea." *Ecology and Evolution* **8**(15): 7529-7542. DOI: <https://doi.org/10.1002/ece3.4167>.

Eriksson, U.; Roos, A.; Lind, Y.; Hope, K.; Ekblad, A. and Kärrman, A. (2016). "Comparison of PFASs contamination in the freshwater and terrestrial environments by analysis of eggs from osprey (*Pandion haliaetus*), tawny owl (*Strix aluco*), and common kestrel (*Falco tinnunculus*)." *Environmental Research* **149**: 40–47. DOI: <https://doi.org/10.1016/j.envres.2016.04.038>.

Commission Regulation (EU) No 757/2010 of 24 August 2010 amending Regulation (EC) No 850/2004 of the European Parliament and of the Council on persistent organic pollutants as regards Annexes I and III Text with EEA relevance. **L223**: 29-36. <http://data.europa.eu/eli/reg/2010/757/oj>.

Commission Delegated Regulation (EU) 2020/784 of 8 April 2020 amending Annex I to Regulation (EU) 2019/1021 of the European Parliament and of the Council as regards the listing of perfluorooctanoic acid (PFOA), its salts and PFOA-related compounds. **L188I**: 1-3. http://data.europa.eu/eli/reg_del/2020/784/oj.

Directive (EU) 2020/2184 of the European Parliament and of the Council of 16 December 2020 on the quality of water intended for human consumption (recast). **L435**: 1-62. <http://data.europa.eu/eli/dir/2020/2184/oj>.

Commission Regulation (EU) 2021/1297 of 4 August 2021 amending Annex XVII to Regulation (EC) No 1907/2006 of the European Parliament and of the Council as regards perfluorocarboxylic acids containing 9 to 14 carbon atoms in the chain (C9-C14 PFCAs), their salts and C9-C14 PFCA-related substances (Text with EEA relevance). **L282**: 29-32. <http://data.europa.eu/eli/reg/2021/1297/oj>.

Commission Recommendation (EU) 2022/1431 of 24 August 2022 on the monitoring of perfluoroalkyl substances in food. **L221**: 105-109. <http://data.europa.eu/eli/reco/2022/1431/oj>.

Commission Delegated Regulation (EU) 2023/1608 of 30 May 2023 amending Annex I to Regulation (EU) 2019/1021 of the European Parliament and of the Council as regards the listing of perfluorohexane sulfonic acid (PFHxS), its salts and PFHxS-related compounds (Text with EEA relevance). **L198**: 24–26. http://data.europa.eu/eli/reg_del/2023/1608/oj.

Commission Regulation (EU) 2023/915 of 25 April 2023 on maximum levels for certain contaminants in food and repealing Regulation (EC) No 1881/2006. **L119**: 103-157. <http://data.europa.eu/eli/reg/2023/915/oj>.

Falandysz, J.; Taniyasu, S.; Yamashita, N.; Rostkowski, P.; Zalewski, K. and Kannan, K. (2007). "Perfluorinated compounds in some terrestrial and aquatic wildlife species from Poland." *Journal of Environmental Science and Health, Part A* **42**(6): 715-719. DOI: <https://doi.org/10.1080/10934520701304369>.

Falk, S.; Brunn, H.; Schröter-Kermani, C.; Failing, K.; Georgii, S.; Tarricone, K. and Stahl, T. (2012). "Temporal and spatial trends of perfluoroalkyl substances in liver of roe deer (*Capreolus capreolus*)." *Environmental Pollution* **171**: 1–8. DOI: <https://doi.org/10.1016/j.envpol.2012.07.022>.

Falk, S.; Stahl, T.; Fliedner, A.; Rüdell, H.; Tarricone, K.; Brunn, H. and Koschorreck, J. (2019). "Levels, accumulation patterns and retrospective trends of perfluoroalkyl acids (PFAAs) in terrestrial ecosystems over the last three decades." *Environmental Pollution* **246**: 921-931. DOI: <https://doi.org/10.1016/j.envpol.2018.12.095>.

Favreau, P.; Poncioni-Rothlisberger, C.; Place, B. J.; Bouchex-Bellomie, H.; Weber, A.; Tremp, J.; Field, J. A. and Kohler, M. (2017). "Multianalyte profiling of per- and polyfluoroalkyl substances (PFASs) in liquid commercial products." *Chemosphere* **171**: 491-501. DOI: <https://doi.org/10.1016/j.chemosphere.2016.11.127>.

Felder, C.; Trompeter, L.; Skutlarek, D.; Färber, H.; Mutters, N. T. and Heinemann, C. (2023). "Exposure of a single wild boar population in North Rhine-Westphalia (Germany) to perfluoroalkyl acids." *Environmental Science and Pollution Research* **30**(6): 15575-15584. DOI: <https://doi.org/10.1007/s11356-022-23086-6>.

Fliedner, A.; Rüdell, H.; Dreyer, A.; Pirntke, U. and Koschorreck, J. (2020). "Chemicals of emerging concern in marine specimens of the German Environmental Specimen Bank." *Environmental Sciences Europe* **32**(1). DOI: <https://doi.org/10.1186/s12302-020-00312-x>.

Frank, H.; Christoph, E. H.; Holm-Hansen, O. and Bullister, J. L. (2002). "Trifluoroacetate in ocean waters." *Environmental Science & Technology* **36**(1): 12-15. DOI: <https://doi.org/10.1021/es0101532>.

Freeling, F.; Behringer, D.; Heydel, F.; Scheurer, M.; Ternes, T. A. and Nödler, K. (2020). "Trifluoroacetate in precipitation: deriving a benchmark data set." *Environmental Science & Technology* **54**(18): 11210-11219. DOI: <https://doi.org/10.1021/acs.est.0c02910>.

Freeling, F.; Scheurer, M.; Koschorreck, J.; Hoffmann, G.; Ternes, T. A. and Nödler, K. (2022). "Levels and Temporal Trends of Trifluoroacetate (TFA) in Archived Plants: Evidence for Increasing Emissions of Gaseous TFA Precursors over the Last Decades." *Environmental Science & Technology* **9**(5): 400–405. DOI: <https://doi.org/10.1021/acs.estlett.2c00164>.

Fryer, R. J. and Nicholson, M. D. (1999). "Using smoothers for comprehensive assessments of contaminant time series in marine biota." *ICES Journal of Marine Science* **56**(5): 779-790. DOI: <https://doi.org/10.1006/jmsc.1999.0499>.

- Galatius, A.; Bossi, R.; Sonne, C.; Rigét, F. F.; Kinze, C. C.; Lockyer, C.; Teilmann, J. and Dietz, R. (2013). "PFAS profiles in three North Sea top predators: metabolic differences among species?" Environmental Science and Pollution Research **20**(11): 8013–8020. DOI: <https://doi.org/10.1007/s11356-013-1633-x>.
- Galloway, J. E.; Moreno, A. V. P.; Lindstrom, A. B.; Strynar, M. J.; Newton, S.; May, A. A. and Weavers, L. K. (2020). "Evidence of Air Dispersion: HFPO–DA and PFOA in Ohio and West Virginia Surface Water and Soil near a Fluoropolymer Production Facility." Environmental Science & Technology **54**(12): 7175–7184. DOI: <https://doi.org/10.1021/acs.est.9b07384>.
- Garza, S. J.; Tabak, M. A.; Miller, R. S.; Farnsworth, M. L. and Burdett, C. L. (2018). "Abiotic and biotic influences on home-range size of wild pigs (*Sus scrofa*)." Journal of Mammalogy **99**(1): 97-107. DOI: <https://doi.org/10.1093/jmammal/gyx154>.
- Gebbink, W. A.; Hebert, C. E. and Letcher, R. J. (2009). "Perfluorinated carboxylates and sulfonates and precursor compounds in herring gull eggs from colonies spanning the Laurentian Great Lakes of North America." Environmental Science & Technology **43**(19): 7443-7449. DOI: <https://doi.org/10.1021/es901755g>.
- Gebbink, W. A. and Letcher, R. J. (2012). "Comparative tissue and body compartment accumulation and maternal transfer to eggs of perfluoroalkyl sulfonates and carboxylates in Great Lakes herring gulls." Environmental Pollution **162**: 40-47. DOI: <https://doi.org/10.1016/j.envpol.2011.10.011>.
- Giesy, J. P. and Kannan, K. (2001). "Global distribution of perfluorooctane sulfonate in wildlife." Environmental Science & Technology **35**(7): 1339–1342. DOI: <https://doi.org/10.1021/es001834k>.
- Glüge, J.; Scheringer, M.; Cousins, I. T.; DeWitt, J. C.; Goldenman, G.; Herzke, D.; Lohmann, R.; Ng, C. A.; Trier, X. and Wang, Z. (2020). "An overview of the uses of per- and polyfluoroalkyl substances (PFAS)." Environmental Science: Processes and Impacts **22**(12): 2345-2373. DOI: <https://doi.org/10.1039/D0EM00291G>.
- Gobas, F. A. P. C.; Kelly, B. C. and Kim, J. J. (2020). "Final Report-SERDP Project ER18-1502: A Framework for Assessing Bioaccumulation and Exposure Risks of Per- and Polyfluoroalkyl Substances in Threatened and Endangered Species on Aqueous Film Forming Foam (AFFF)-Impacted Sites." Burnaby, US, SERDP. ISBN/ISSN: 978-1-922345-88-2. <https://serdp-estcp.org/projects/details/09c93894-bc73-404a-8282-51196c4be163>.
- Göckener, B.; Fliedner, A.; Rüdél, H.; Badry, A. and Koschorreck, J. (2022). "Long-Term Trends of Per- and Polyfluoroalkyl Substances (PFAS) in Suspended Particular Matter from German Rivers Using the Direct Total Oxidizable Precursor (dTOP) Assay." Environmental Science & Technology **56**(1): 208-217. DOI: <https://doi.org/10.1021/acs.est.1c04165>.
- Göckener, B.; Fliedner, A.; Rüdél, H.; Fettig, I. and Koschorreck, J. (2021). "Exploring unknown per- and polyfluoroalkyl substances in the German environment – The total oxidizable precursor assay as helpful tool in research and regulation." Science of The Total Environment **782**: 146825-146825. DOI: <https://doi.org/10.1016/j.scitotenv.2021.146825>.
- Göckener, B.; Lange, F. T.; Lesmeister, L.; Gökçe, E.; Dahme, H. U.; Bandow, N. and Biegel-Engler, A. (2022). "Digging deep—implementation, standardisation and interpretation of a total oxidisable precursor (TOP) assay within the regulatory context of per- and polyfluoroalkyl substances (PFASs) in soil." Environmental Sciences Europe **34**(1): 1-9. DOI: <https://doi.org/10.1186/s12302-022-00631-1>.
- Greaves, A. K.; Letcher, R. J.; Sonne, C.; Dietz, R. and Born, E. W. (2012). "Tissue-specific concentrations and patterns of perfluoroalkyl carboxylates and sulfonates in East Greenland polar bears." Environmental Science & Technology **46**(21): 11575-11583. DOI: <https://doi.org/10.1021/es303400f>.
- Grønnestad, R.; Vázquez, B. P.; Arukwe, A.; Jaspers, V. L. B.; Jenssen, B. M.; Karimi, M.; Lyche, J. L. and Krøkje, Å. (2019). "Levels, Patterns, and Biomagnification Potential of Perfluoroalkyl Substances in a Terrestrial Food Chain in a Nordic Skiing Area." Environmental Science & Technology **53**(22): 13390–13397. DOI: <https://doi.org/10.1021/acs.est.9b02533>.

Guckert, M.; Rupp, J.; Nürenberg, G.; Nödler, K.; Koschorreck, J.; Berger, U.; Drost, W.; Siebert, U.; Wibbelt, G. and Reemtsma, T. (2023). "Differences in the internal PFAS patterns of herbivores, omnivores and carnivores - lessons learned from target screening and the total oxidizable precursor assay." *Science of The Total Environment* **875**: 162361. DOI: <https://doi.org/10.1016/j.scitotenv.2023.162361>.

Guckert, M.; Scheurer, M.; Schaffer, M.; Reemtsma, T. and Nödler, K. (2022). "Combining target analysis with sum parameters-a comprehensive approach to determine sediment contamination with PFAS and further fluorinated substances." *Environmental Science and Pollution Research International* **29**(57): 85802–85814. DOI: <https://doi.org/10.1007/s11356-022-21588-x>.

Holaday, D. A. (1977). "Absorption, biotransformation, and storage of halothane." *Environmental Health Perspectives* **Vol. 21**: 165–169. DOI: <https://doi.org/10.1289/ehp.7721165>.

Holmström, K. E.; Johansson, A.-K.; Bignert, A.; Lindberg, P. and Berger, U. (2010). "Temporal Trends of Perfluorinated Surfactants in Swedish Peregrine Falcon Eggs (*Falco peregrinus*), 1974–2007." *Environmental Science & Technology* **44**(11): 4083-4088. DOI: <https://doi.org/10.1021/es100028f>.

Houde, M.; Martin, J. W.; Letcher, R. J.; Solomon, K. R. and Muir, D. C. G. (2006). "Biological Monitoring of Polyfluoroalkyl Substances: A Review." *Environmental Science & Technology* **40**(11): 3463-3473. DOI: <https://doi.org/10.1021/es052580b>.

Houtz, E. F.; Higgins, C. P.; Field, J. A. and Sedlak, D. L. (2013). "Persistence of perfluoroalkyl acid precursors in AFFF-impacted groundwater and soil." *Environmental Science & Technology* **47**(15): 8187–8195. DOI: <https://doi.org/10.1021/es4018877>.

Houtz, E. F. and Sedlak, D. L. (2012). "Oxidative conversion as a means of detecting precursors to perfluoroalkyl acids in urban runoff." *Environmental Science & Technology* **46**(17): 9342–9349. DOI: <https://doi.org/10.1021/es302274g>.

Huang, K.; Li, Y.; Bu, D.; Fu, J.; Wang, M.; Zhou, W.; Gu, L.; Fu, Y.; Cong, Z.; Hu, B.; Fu, J.; Zhang, A. and Jiang, G. (2022). "Trophic Magnification of Short-Chain Per- and Polyfluoroalkyl Substances in a Terrestrial Food Chain from the Tibetan Plateau." *Environmental Science & Technology* **9**(2): 147–152. DOI: <https://doi.org/10.1021/acs.estlett.1c01009>.

Jahnke, A.; Berger, U.; Ebinghaus, R. and Temme, C. (2007). "Latitudinal Gradient of Airborne Polyfluorinated Alkyl Substances in the Marine Atmosphere between Germany and South Africa (53° N–33° S)." *Environmental Science & Technology* **41**(9): 3055-3061. DOI: <https://doi.org/10.1021/es062389h>.

Janda, J.; Nödler, K.; Scheurer, M.; Happel, O.; Nürenberg, G.; Zwiener, C. and Lange, F. T. (2019). "Closing the gap – inclusion of ultrashort-chain perfluoroalkyl carboxylic acids in the total oxidizable precursor (TOP) assay protocol." *Environmental Science: Processes & Impacts* **21**(11): 1926-1935. DOI: <https://doi.org/10.1039/C9EM00169G>.

Joerss, H.; Menger, F.; Tang, J.; Ebinghaus, R. and Ahrens, L. (2022). "Beyond the Tip of the Iceberg: Suspect Screening Reveals Point Source-Specific Patterns of Emerging and Novel Per- and Polyfluoroalkyl Substances in German and Chinese Rivers." *Environmental Science & Technology* **56**(9): 5456–5465. DOI: <https://doi.org/10.1021/acs.est.1c07987>.

Johnson, G. R.; Brusseau, M. L.; Carroll, K. C.; Tick, G. R. and Duncan, C. M. (2022). "Global distributions, source-type dependencies, and concentration ranges of per- and polyfluoroalkyl substances in groundwater." *Science of the Total Environment* **841**: 156602. DOI: <https://doi.org/10.1016/j.scitotenv.2022.156602>.

Jouanneau, W.; Léandri-Breton, D.-J.; Corbeau, A.; Herzke, D.; Moe, B.; Nikiforov, V. A.; Gabrielsen, G. W. and Chastel, O. (2021). "A Bad Start in Life? Maternal Transfer of Legacy and Emerging Poly- and Perfluoroalkyl Substances to Eggs in an Arctic Seabird." *Environmental Science & Technology* **56**(10): 6091-6102. DOI: <https://doi.org/10.1021/acs.est.1c03773>.

- Joudan, S.; Yeung, L. W. Y. and Mabury, S. A. (2017). "Biological cleavage of the C-P bond in perfluoroalkyl phosphinic acids in male Sprague-Dawley rats and the formation of persistent and reactive metabolites." Environmental Health Perspectives **125**(11): 117001–117009. DOI: <https://doi.org/10.1289/ehp1841>.
- Kaczyński, P.; Łozowicka, B.; Perkowski, M.; Zoń, W.; Hrynkó, I.; Rutkowska, E. and Skibko, Z. (2021). "Impact of broad-spectrum pesticides used in the agricultural and forestry sector on the pesticide profile in wild boar, roe deer and deer and risk assessment for venison consumers." Science of The Total Environment **784**: 147215. DOI: <https://doi.org/10.1016/j.scitotenv.2021.147215>.
- Kannan, K.; Corsolini, S.; Falandysz, J.; Oehme, G.; Focardi, S. and Giesy, J. P. (2002). "Perfluorooctanesulfonate and related fluorinated hydrocarbons in marine mammals, fishes, and birds from coasts of the Baltic and the Mediterranean Seas." Environmental Science & Technology **36**(15): 3210-3216. DOI: <https://doi.org/10.1021/es020519q>.
- Kannan, K.; Tao, L.; Sinclair, E.; Pastva, S. D.; Jude, D. J. and Giesy, J. P. (2005). "Perfluorinated compounds in aquatic organisms at various trophic levels in a Great Lakes food chain." Archives of Environmental Contamination and Toxicology **48**(4): 559–566. DOI: <https://doi.org/10.1007/s00244-004-0133-x>.
- Kärrman, A.; Wang, T.; Kallenborn, R.; Langseter, A. M.; Ræder, E. M.; Lyche, J. L.; Yeung, L.; Chen, F.; Eriksson, U.; Aro, R. and Fredriksson, F. (2019). "PFASs in the Nordic environment." Copenhagen, Nordic Council of Ministers. ISBN/ISSN: 9789289360623/ISSN. DOI: <https://doi.org/10.6027/TN2019-515>.
- Kärrman, A.; Yeung, L. W. Y.; Spaan, K. M.; Lange, F. T.; Nguyen, M. A.; Plassmann, M.; de Wit, C. A.; Scheurer, M.; Awad, R. and Benskin, J. P. (2021). "Can determination of extractable organofluorine (EOF) be standardized? First interlaboratory comparisons of EOF and fluorine mass balance in sludge and water matrices." Environmental Science: Processes & Impacts **23**(10): 1458-1465. DOI: <https://doi.org/10.1039/D1EM00224D>.
- Kelly, B. C.; Ikonomou, M. G.; Blair, J. D.; Surridge, B.; Hoover, D.; Grace, R. and Gobas, F. A. P. C. (2009). "Perfluoroalkyl contaminants in an arctic marine food web: Trophic magnification and wildlife exposure." Environmental Science & Technology **43**(11): 4037–4043. DOI: <https://doi.org/10.1021/es9003894>.
- Keuling, O.; Stier, N. and Roth, M. (2008). "Annual and seasonal space use of different age classes of female wild boar *Sus scrofa* L." European Journal of Wildlife Research **54**(3): 403-412. DOI: <https://doi.org/10.1007/s10344-007-0157-4>.
- Klein, R.; Paulus, M.; Tarricone, K. and Teubner, D. (2018a). "Guideline for Sampling and Sample Processing Bream (*Abramis brama*)." Standard Operating Procedure (SOP) Retrieved 25.06.2024, from <https://www.umweltprobenbank.de/en/documents/publications/26845>.
- Klein, R.; Paulus, M.; Tarricone, K. and Teubner, D. (2018b). "Guideline for Sampling and Sample Processing Eelpout (*Zoarces viviparus*)." Standard Operating Procedure (SOP) Retrieved 25.06.2024, from <https://www.umweltprobenbank.de/en/documents/publications/26543>.
- Klein, R.; Tarricone, K.; Teubner, D. and Paulus, M. (2018c). "Guideline for Sampling and Sample Processing Norway Spruce (*Picea abies*) / Scots Pine (*Pinus sylvestris*)." Standard Operating Procedure (SOP) Retrieved 25.06.2024, from <https://www.umweltprobenbank.de/en/documents/publications/26583>.
- Knutsen, H.; Mæhlum, T.; Haarstad, K.; Slinde, G. A. and Arp, H. P. H. (2019). "Leachate emissions of short- and long-chain per- and polyfluoroalkyl substances (PFASs) from various Norwegian landfills." Environmental Science: Processes & Impacts **21**(11): 1970–1979. DOI: <https://doi.org/10.1039/c9em00170k>.
- Kotamarthi, V.; Rodriguez, J.; Ko, M.; Tromp, T.; Sze, N. and Prather, M. (1998). "Trifluoroacetic Acid from Degradation of HCFCs and HFCs: A Three-Dimensional Modeling Study." Journal of Geophysical Research **103**: 5747-5758. DOI: <https://doi.org/10.1029/97JD02988>.

Kotthoff, M.; Fliedner, A.; Rüdell, H.; Göckener, B.; Bücking, M.; Biegel-Engler, A. and Koschorreck, J. (2020). "Per- and polyfluoroalkyl substances in the German environment - Levels and patterns in different matrices." Science of the Total Environment **740**: 140116. DOI: <https://doi.org/10.1016/j.scitotenv.2020.140116>.

Kowalczyk, J.; Flor, M.; Karl, H. and Lahrssen-Wiederholt, M. (2020). "Perfluoroalkyl substances (PFAS) in beaked redfish (*Sebastes mentella*) and cod (*Gadus morhua*) from arctic fishing grounds of Svalbard." Food Additives and Contaminants: Part B - Surveillance **13**(1): 34-44. DOI: <https://doi.org/10.1080/19393210.2019.1690052>.

Kowalczyk, J.; Numata, J.; Zimmermann, B.; Klinger, R.; Habedank, F.; Just, P.; Schafft, H. and Lahrssen-Wiederholt, M. (2018). "Suitability of Wild Boar (*Sus scrofa*) as a Bioindicator for Environmental Pollution with Perfluorooctanoic Acid (PFOA) and Perfluorooctanesulfonic Acid (PFOS)." Archives of Environmental Contamination and Toxicology **75**(4): 594–606. DOI: <https://doi.org/10.1007/s00244-018-0552-8>.

Kratzer, J.; Ahrens, L.; Roos, A.; Bäcklin, B.-M. and Ebinghaus, R. (2011). "Reprint of: Temporal trends of polyfluoroalkyl compounds (PFCs) in liver tissue of grey seals (*Halichoerus grypus*) from the Baltic Sea, 1974–2008." Chemosphere **85**(2): 253-261. DOI: <https://doi.org/10.1016/j.chemosphere.2011.09.001>.

Krippner, J.; Brunn, H.; Falk, S.; Georgii, S.; Schubert, S. and Stahl, T. (2014). "Effects of chain length and pH on the uptake and distribution of perfluoroalkyl substances in maize (*Zea mays*)." Chemosphere **94**: 85–90. DOI: <https://doi.org/10.1016/j.chemosphere.2013.09.018>.

Lan, Z.; Yao, Y.; Xu, J.; Chen, H.; Ren, C.; Fang, X.; Zhang, K.; Jin, L.; Hua, X.; Alder, A. C.; Wu, F. and Sun, H. (2020). "Novel and legacy per- and polyfluoroalkyl substances (PFASs) in a farmland environment: Soil distribution and biomonitoring with plant leaves and locusts." Environmental Pollution **263**(Pt A): 114487. DOI: <https://doi.org/10.1016/j.envpol.2020.114487>.

Land, M.; De Wit, C. A.; Bignert, A.; Cousins, I. T.; Herzke, D.; Johansson, J. H. and Martin, J. W. (2018). "What is the effect of phasing out long-chain per- and polyfluoroalkyl substances on the concentrations of perfluoroalkyl acids and their precursors in the environment? A systematic review." Environmental Evidence **7**(1): 1-32. DOI: <https://doi.org/10.1186/s13750-017-0114-y>.

Langberg, H. A.; Breedveld, G. D.; Slinde, G. A.; Grønning, H. M.; Høisæter, Å.; Jartun, M.; Rundberget, T.; Jensen, B. M. and Hale, S. E. (2020). "Fluorinated Precursor Compounds in Sediments as a Source of Perfluorinated Alkyl Acids (PFAA) to Biota." Environmental Science & Technology **54**(20): 13077-13089. DOI: <https://doi.org/10.1021/acs.est.0c04587>.

Lau, C.; Butenhoff, J. L. and Rogers, J. M. (2004). "The developmental toxicity of perfluoroalkyl acids and their derivatives." Toxicology and Applied Pharmacology **198**(2): 231–241. DOI: <https://doi.org/10.1016/j.taap.2003.11.031>.

Laufer, S.; Zwickel, T.; Riemenschneider, C. and Lippold, R. (2019, 22.10.2019). "Befunde und Beurteilung perfluorierter Alkylsubstanzen (PFAS) in Leber und Fleisch von Wildschweinen." from https://www.ua-bw.de/pub/beitrag.asp?subid=3&Thema_ID=5&ID=3061&lang=DE&Pdf=No.

Laursen, K. and Møller, A. P. (2022). "Diet of eiders and body condition change from the late 1980s to the mid 2010s." Journal of Sea Research **187**: 102244. DOI: <https://doi.org/10.1016/j.seares.2022.102244>.

Lee, H. and Mabury, S. A. (2011). "A pilot survey of legacy and current commercial fluorinated chemicals in human sera from United States donors in 2009." Environmental Science & Technology **45**(19): 8067–8074. DOI: <https://doi.org/10.1021/es200167q>.

Lee, H. and Mabury, S. A. (2014). "Global Distribution of Polyfluoroalkyl and Perfluoroalkyl Substances and their Transformation Products in Environmental Solids." Transformation Products of Emerging Contaminants in the Environment. D. A. Lambropoulou and L. M. L. Nollet, Wiley: 797–826. ISBN/ISSN: 9781118339596. DOI: <https://doi.org/10.1002/9781118339558.ch27>.

- Lee, H.; Tevlin, A. G. and Mabury, S. A. (2014). "Fate of polyfluoroalkyl phosphate diesters and their metabolites in biosolids-applied soil: Biodegradation and plant uptake in greenhouse and field experiments." *Environmental Science & Technology* **48**(1): 340–349. DOI: <https://doi.org/10.1021/es403949z>.
- Lesmeister, L.; Lange, F. T.; Breuer, J.; Biegel-Engler, A.; Giese, E. and Scheurer, M. (2021). "Extending the knowledge about PFAS bioaccumulation factors for agricultural plants - A review." *Science of the Total Environment* **766**: 142640. DOI: <https://doi.org/10.1016/j.scitotenv.2020.142640>.
- Lewis, J. S.; Corn, J. L.; Mayer, J. J.; Jordan, T. R.; Farnsworth, M. L.; Burdett, C. L.; VerCauteren, K. C.; Sweeney, S. J. and Miller, R. S. (2019). "Historical, current, and potential population size estimates of invasive wild pigs (*Sus scrofa*) in the United States." *Biological Invasions* **21**(7): 2373-2384. DOI: <https://doi.org/10.1007/s10530-019-01983-1>.
- Lewis, K. A.; Tzilivakis, J.; Warner, D. J. and Green, A. (2016). "An international database for pesticide risk assessments and management." *Human and Ecological Risk Assessment: An International Journal* **22**(4): 1050-1064. DOI: <https://doi.org/10.1080/10807039.2015.1133242>.
- Liu, C. and Liu, J. (2016). "Aerobic biotransformation of polyfluoroalkyl phosphate esters (PAPs) in soil." *Environmental Pollution* **212**: 230–237. DOI: <https://doi.org/10.1016/j.envpol.2016.01.069>.
- Liu, M.; Dong, F.; Yi, S.; Zhu, Y.; Zhou, J.; Sun, B.; Shan, G.; Feng, J. and Zhu, L. (2020). "Probing Mechanisms for the Tissue-Specific Distribution and Biotransformation of Perfluoroalkyl Phosphinic Acids in Common Carp (*Cyprinus carpio*)." *Environmental Science & Technology* **54**(8): 4932–4941. DOI: <https://doi.org/10.1021/acs.est.0c00359>.
- Liu, S.; Lu, Y.; Xie, S.; Wang, T.; Jones, K. C. and Sweetman, A. J. (2015). "Exploring the fate, transport and risk of Perfluorooctane Sulfonate (PFOS) in a coastal region of China using a multimedia model." *Environment International* **85**: 15–26. DOI: <https://doi.org/10.1016/j.envint.2015.08.007>.
- Liu, Y.; D'Agostino, L.; Schymanski, E. and Martin, J. (2019b). "List of PFAS reported in Non-Target HRMS Studies (Liu et al 2019)." Retrieved 18.09.2024, from https://www.norman-network.com/sites/default/files/files/suspectListExchange/220319Update/Liu_etal_2019_HRMS_PFAS_1-s2.0-S0165993618306253-Table1.pdf. DOI: <https://doi.org/10.5281/zenodo.3653161>.
- Liu, Y.; D'Agostino, L. A.; Qu, G.; Jiang, G. and Martin, J. W. (2019a). "High-resolution mass spectrometry (HRMS) methods for nontarget discovery and characterization of poly- and per-fluoroalkyl substances (PFASs) in environmental and human samples." *TrAC Trends in Analytical Chemistry* **121**: 115420. DOI: <https://doi.org/10.1016/j.trac.2019.02.021>.
- Liu, Y.; Qian, M.; Ma, X.; Zhu, L. and Martin, J. W. (2018). "Nontarget Mass Spectrometry Reveals New Perfluoroalkyl Substances in Fish from the Yangtze River and Tangxun Lake, China." *Environmental Science & Technology* **52**(10): 5830-5840. DOI: <https://doi.org/10.1021/acs.est.8b00779>.
- Lohmann, R. and Letcher, R. J. (2023). "The universe of fluorinated polymers and polymeric substances and potential environmental impacts and concerns." *Current Opinion in Green and Sustainable Chemistry* **41**: 100795. DOI: <https://doi.org/10.1016/j.cogsc.2023.100795>.
- Lozano, J.; Moleón, M. and Virgós, E. (2006). "Biogeographical patterns in the diet of the wildcat, *Felis silvestris Schreber*, in Eurasia: factors affecting the trophic diversity." *Journal of Biogeography* **33**(6): 1076-1085. DOI: <https://doi.org/10.1111/j.1365-2699.2006.01474.x>.
- Ma, J.; Zhu, H. and Kannan, K. (2020). "Fecal Excretion of Perfluoroalkyl and Polyfluoroalkyl Substances in Pets from New York State, United States." *Environmental Science & Technology Letters* **7**(3): 135–142. DOI: <https://doi.org/10.1021/acs.estlett.9b00786>.
- Martin, D.; Munoz, G.; Mejia-Avenidaño, S.; Duy, S. V.; Yao, Y.; Volchek, K.; Brown, C. E.; Liu, J. and Sauvé, S. (2019). "Zwitterionic, cationic, and anionic perfluoroalkyl and polyfluoroalkyl substances integrated into total oxidizable

precursor assay of contaminated groundwater." *Talanta* **195**: 533–542. DOI: <https://doi.org/10.1016/j.talanta.2018.11.093>.

Massei, G.; Kindberg, J.; Licoppe, A.; Gačić, D.; Šprem, N.; Kamler, J.; Baubet, E.; Hohmann, U.; Monaco, A.; Ozoliņš, J.; Cellina, S.; Podgórski, T.; Fonseca, C.; Markov, N.; Pokorny, B.; Rosell, C. and Náhlik, A. (2015). "Wild boar populations up, numbers of hunters down? A review of trends and implications for Europe." *Pest Management Science* **71**(4): 492-500. DOI: <https://doi.org/10.1002/ps.3965>.

Minet, L.; Wang, Z.; Shalin, A.; Bruton, T. A.; Blum, A.; Peaslee, G. F.; Schwartz-Narbonne, H.; Venier, M.; Whitehead, H.; Wu, Y. and Diamond, M. L. (2022). "Use and release of per- and polyfluoroalkyl substances (PFASs) in consumer food packaging in U.S. and Canada." *Environmental Science: Processes & Impacts* **24**(11): 2032-2042. DOI: <https://doi.org/10.1039/d2em00166g>.

Morganti, M.; Polesello, S.; Pascariello, S.; Ferrario, C.; Rubolini, D.; Valsecchi, S. and Parolini, M. (2021). "Exposure assessment of PFAS-contaminated sites using avian eggs as a biomonitoring tool: A frame of reference and a case study in the Po River valley (Northern Italy)." *Integrated Environmental Assessment and Management* **17**(4): 733-745. DOI: <https://doi.org/10.1002/ieam.4417>.

Muir, D. and Miaz, L. T. (2021). "Spatial and Temporal Trends of Perfluoroalkyl Substances in Global Ocean and Coastal Waters." *Environmental Science & Technology* **55**(14): 9527–9537. DOI: <https://doi.org/10.1021/acs.est.0c08035>.

Müller, C. E.; Silva, A. O. d.; Small, J.; Williamson, M.; Wang, X.; Morris, A.; Katz, S.; Gamberg, M. and Muir, D. C. G. (2011). "Biomagnification of perfluorinated compounds in a remote terrestrial food chain: Lichen-Caribou-wolf." *Environmental Science & Technology* **45**(20): 8665–8673. DOI: <https://doi.org/10.1021/es201353v>.

Munoz, G.; Liu, J.; Vo Duy, S. and Sauvé, S. (2019). "Analysis of F-53B, Gen-X, ADONA, and emerging fluoroalkylether substances in environmental and biomonitoring samples: A review." *Trends in Environmental Analytical Chemistry* **23**: e00066. DOI: <https://doi.org/10.1016/j.teac.2019.e00066>.

Muschket, M.; Keltsch, N.; Paschke, H.; Reemtsma, T. and Berger, U. (2020). "Determination of transformation products of per- and polyfluoroalkyl substances at trace levels in agricultural plants." *Journal of Chromatography A* **1625**: 461271. DOI: <https://doi.org/10.1016/j.chroma.2020.461271>.

Nguyen, T. M. H.; Bräunig, J.; Thompson, K.; Thompson, J.; Kabiri, S.; Navarro, D. A.; Kookana, R. S.; Grimison, C.; Barnes, C. M.; Higgins, C. P.; McLaughlin, M. J. and Mueller, J. F. (2020). "Influences of Chemical Properties, Soil Properties, and Solution pH on Soil–Water Partitioning Coefficients of Per- and Polyfluoroalkyl Substances (PFASs)." *Environmental Science & Technology* **54**(24): 15883–15892. DOI: <https://doi.org/10.1021/acs.est.0c05705>.

Numata, J.; Kowalczyk, J.; Adolphs, J.; Ehlers, S.; Schafft, H.; Fuerst, P.; Müller-Graf, C.; Lahrssen-Wiederholt, M. and Greiner, M. (2014). "Toxicokinetics of Seven Perfluoroalkyl Sulfonic and Carboxylic Acids in Pigs Fed a Contaminated Diet." *Journal of Agricultural and Food Chemistry* **62**(28): 6861–6870. DOI: <https://doi.org/10.1021/jf405827u>.

OECD (2018). "Toward a New Comprehensive Global Database of Per- and Polyfluoroalkyl Substances (PFASs): Summary Report on Updating the OECD 2007 List of Per- and Polyfluoroalkyl Substances (PFASs)." *OECD Environment, Health and Safety Publications Series on Risk Management*, OECD Publishing. **39**: 1–24. [https://one.oecd.org/document/ENV/JM/MONO\(2018\)7/en/pdf](https://one.oecd.org/document/ENV/JM/MONO(2018)7/en/pdf).

OECD (2020). "PFASs and Alternatives in Food Packaging (Paper and Paperboard): Report on the Commercial Availability and Current Uses." *OECD Series on Risk Management of Chemicals* **58**: 1–65. DOI: <https://doi.org/10.1787/6db0c033-en>.

- OECD (2021). "Reconciling Terminology of the Universe of Per- and Polyfluoroalkyl Substances: Recommendations and Practical Guidance." *OECD Series on Risk Management of Chemicals* **61**: 1–45. DOI: <https://doi.org/10.1787/e458e796-en>
- Pan, Y.; Zhang, H.; Cui, Q.; Sheng, N.; Yeung, L. W. Y.; Sun, Y.; Guo, Y. and Dai, J. (2018). "Worldwide Distribution of Novel Perfluoroether Carboxylic and Sulfonic Acids in Surface Water." *Environmental Science & Technology* **52**(14): 7621-7629. DOI: <https://doi.org/10.1021/acs.est.8b00829>.
- Parolini, M.; De Felice, B.; Rusconi, M.; Morganti, M.; Polesello, S. and Valsecchi, S. (2022). "A review of the bioaccumulation and adverse effects of PFAS in free-living organisms from contaminated sites nearby fluorochemical production plants." *Water Emerging Contaminants & Nanoplastics* **1**(4): 18. DOI: <https://doi.org/10.20517/wecn.2022.15>.
- Paulus, M.; Klein, R.; Tarricone, K. and Teubner, D. (2018b). "Guideline for Sampling and Sample Processing Herring Gull (*Larus argentatus*)." *Standard Operating Procedure (SOP)*. Retrieved 25.06.2024, from <https://www.umweltprobenbank.de/en/documents/publications/26523>.
- Paulus, M.; Klein, R. and Teubner, D. (2018a). "Guideline for Sampling and Sample Processing Blue Mussel (*Mytilus edulis* complex)." *Standard Operating Procedure (SOP)*. Retrieved 25.06.2024, from <https://www.umweltprobenbank.de/en/documents/publications/26658>.
- Powley, C. R.; George, S. W.; Ryan, T. W. and Buck, R. C. (2005). "Matrix effect-free analytical methods for determination of perfluorinated carboxylic acids in environmental matrices." *Analytical Chemistry* **77**(19): 6353-6358. DOI: <https://doi.org/10.1021/ac0508090>.
- Prevedouros, K.; Cousins, I. T.; Buck, R. C. and Korzeniowski, S. H. (2006). "Sources, fate and transport of perfluorocarboxylates." *Environmental Science & Technology* **40**(1): 32–44. DOI: <https://doi.org/10.1021/es0512475>.
- PubChem. (2022). "PFAS and Fluorinated Compounds in PubChem." Retrieved 15.05.2024, from <https://pubchem.ncbi.nlm.nih.gov/classification/#hid=120>.
- Quack, M.; Bartel-Steinbach, M.; Klein, R.; Paulus, M.; Tarricone, K.; Teubner, D. and Wagner, G. (2010). "Richtlinie zur Probenahme und Probenbearbeitung Blasentang (*Fucus vesiculosus*)." *Standard Operating Procedure (SOP)*. Retrieved 25.06.2024, from <https://www.umweltprobenbank.de/en/documents/publications/20550>.
- Rand, A. A. and Mabury, S. A. (2014). "Protein Binding Associated with Exposure to Fluorotelomer Alcohols (FTOHs) and Polyfluoroalkyl Phosphate Esters (PAPs) in Rats." *Environmental Science & Technology* **48**: 140205115442006-140205115442006. DOI: <https://doi.org/10.1021/es404390x>.
- Rankin, K.; Mabury, S. A.; Jenkins, T. M. and Washington, J. W. (2016). "A North American and global survey of perfluoroalkyl substances in surface soils: Distribution patterns and mode of occurrence." *Chemosphere* **161**: 333–341. DOI: <https://doi.org/10.1016/j.chemosphere.2016.06.109>.
- Reemtsma, T.; Berger, U.; Arp, H. P. H.; Gallard, H.; Knepper, T. P.; Neumann, M.; Quintana, J. B. and Voegt, P. d. (2016). "Mind the Gap: Persistent and Mobile Organic Compounds—Water Contaminants That Slip Through." *Environmental Science & Technology* **50**(19): 10308-10315. DOI: <https://doi.org/10.1021/acs.est.6b03338>.
- Ricking, M.; Keller, M.; Heininger, P. and Körner, A. (2017). "Richtlinie zur Probenahme und Probenbearbeitung Schwebstoffe." *Standard Operating Procedure (SOP)*. Retrieved 25.06.2024, from <https://www.umweltprobenbank.de/en/documents/publications/25629>.
- Ricking, M.; Winkler, A. and Schneider, M. (2012). "Richtlinie zur Probenahme und Probenbearbeitung Schwebstoffe." *Standard Operating Procedure (SOP)*. Retrieved 25.06.2024, from <https://www.umweltprobenbank.de/en/documents/publications/21303>.

- Riebe, R. A.; Falk, S.; Georgii, S.; Brunn, H.; Failing, K. and Stahl, T. (2016). "Perfluoroalkyl Acid Concentrations in Livers of Fox (*Vulpes vulpes*) and Chamois (*Rupicapra rupicapra*) from Germany and Austria." Archives of Environmental Contamination and Toxicology **71**(1): 7–15. DOI: <https://doi.org/10.1007/s00244-015-0250-8>.
- Roos, A.; Berger, U.; Järnberg, U.; van Dijk, J. and Bignert, A. (2013). "Increasing Concentrations of Perfluoroalkyl Acids in Scandinavian Otters (*Lutra lutra*) between 1972 and 2011: A New Threat to the Otter Population?" Environmental Science & Technology **47**(20): 11757–11765. DOI: <https://doi.org/10.1021/es401485t>.
- Rupp, J.; Guckert, M.; Berger, U.; Drost, W.; Mader, A.; Nödler, K.; Nürenberg, G.; Schulze, J.; Söhlmann, R. and Reemtsma, T. (2023). "Comprehensive target analysis and TOP assay of per- and polyfluoroalkyl substances (PFAS) in wild boar livers indicate contamination hot-spots in the environment." Science of The Total Environment **871**(January): 162028-162028. DOI: <https://doi.org/10.1016/j.scitotenv.2023.162028>.
- Ruyle, B. J.; Thackray, C. P.; McCord, J. P.; Strynar, M. J.; Mauge-Lewis, K. A.; Fenton, S. E. and Sunderland, E. M. (2021). "Reconstructing the Composition of Per- and Polyfluoroalkyl Substances in Contemporary Aqueous Film-Forming Foams." Environmental Science & Technology **8**(1): 59-65. DOI: <https://doi.org/10.1021/acs.estlett.0c00798>.
- Saito, N.; Sasaki, K.; Nakatome, K.; Harada, K.; Yoshinaga, T. and Koizumi, A. (2003). "Perfluorooctane sulfonate concentrations in surface water in Japan." Archives of Environmental Contamination and Toxicology **45**(2): 149–158. DOI: <https://doi.org/10.1007/s00244-003-0163-9>.
- Scheringer, M.; Trier, X.; Cousins, I. T.; de Voogt, P.; Fletcher, T.; Wang, Z. and Webster, T. F. (2014). "Helsingør Statement on poly- and perfluorinated alkyl substances (PFASs)." Chemosphere **114**: 337-339. DOI: <https://doi.org/10.1016/j.chemosphere.2014.05.044>.
- Scheurer, M.; Nödler, K.; Freeling, F.; Janda, J.; Happel, O.; Riegel, M.; Müller, U.; Storck, F. R.; Fleig, M.; Lange, F. T.; Brunsch, A. and Brauch, H.-J. (2017). "Small, mobile, persistent: Trifluoroacetate in the water cycle - Overlooked sources, pathways, and consequences for drinking water supply." Water Research **126**: 460–471. DOI: <https://doi.org/10.1016/j.watres.2017.09.045>.
- Seiber, J. N. and Cahill, T. M. (2022). "Pesticides, organic contaminants, and pathogens in air: chemodynamics, health effects, sampling, and analysis." Taylor & Francis. ISBN/ISSN: 1032108940. DOI: <https://doi.org/10.1201/9781003217602>.
- Shukla, I.; Kilpatrick, A. M. and Beltran, R. S. (2021). "Variation in resting strategies across trophic levels and habitats in mammals." Ecology and Evolution **11**(21): 14405-14415. DOI: <https://doi.org/10.1002/ece3.8073>.
- Simonnet-Laprade, C.; Budzinski, H.; Maciejewski, K.; Le Menach, K.; Santos, R.; Alliot, F.; Goutte, A. and Labadie, P. (2019). "Biomagnification of perfluoroalkyl acids (PFAAs) in the food web of an urban river: assessment of the trophic transfer of targeted and unknown precursors and implications." Environmental Science: Processes & Impacts **21**(11): 1864–1874. DOI: <https://doi.org/10.1039/c9em00322c>.
- Söregård, M.; Kikuchi, J.; Wiberg, K. and Ahrens, L. (2022). "Spatial distribution and load of per- and polyfluoroalkyl substances (PFAS) in background soils in Sweden." Chemosphere **295**: 133944. DOI: <https://doi.org/10.1016/j.chemosphere.2022.133944>.
- Stahl, T.; Falk, S.; Failing, K.; Berger, J.; Georgii, S. and Brunn, H. (2012). "Perfluorooctanoic Acid and Perfluorooctane Sulfonate in Liver and Muscle Tissue from Wild Boar in Hesse, Germany." Archives of Environmental Contamination and Toxicology **62**(4): 696–703. DOI: <https://doi.org/10.1007/s00244-011-9726-3>.
- Stockholm Convention. "The new POPs under the Stockholm Convention." Retrieved August 30, 2022, from <https://chm.pops.int/TheConvention/ThePOPs/TheNewPOPs/tabid/2511/Default.aspx>.
- Sun, M.; Cui, J. n.; Guo, J.; Zhai, Z.; Zuo, P. and Zhang, J. (2020). "Fluorochemicals biodegradation as a potential source of trifluoroacetic acid (TFA) to the environment." Chemosphere **254**: 126894. DOI: <https://doi.org/10.1016/j.chemosphere.2020.126894>.

- Sznajder-Katarzyńska, K.; Surma, M. and Cieślík, I. (2019). "A Review of Perfluoroalkyl Acids (PFAAs) in terms of Sources, Applications, Human Exposure, Dietary Intake, Toxicity, Legal Regulation, and Methods of Determination." *Journal of Chemistry* **2019**: 1–20. DOI: <https://doi.org/10.1155/2019/2717528>.
- Tarricone, K.; Klein, R.; Paulus, M. and Teubner, D. (2018a). "Guideline for Sampling and Sample Processing Roe Deer (*Capreolus capreolus*)." *Standard Operating Procedure (SOP)*. Retrieved 25.06.2024, from <https://www.umweltprobenbank.de/en/documents/publications/26427>.
- Tarricone, K.; Klein, R.; Paulus, M. and Teubner, D. (2018b). "Guideline for Sampling and Sample Processing Red Beech (*Fagus sylvatica*)." *Standard Operating Procedure (SOP)*, from <https://www.umweltprobenbank.de/en/documents/publications/26604>.
- Tarricone, K.; Klein, R.; Paulus, M. and Teubner, D. (2018c). "Guideline for Sampling and Sample Processing Lombardy Poplar (*Populus nigra 'Italica'*)." *Standard Operating Procedure (SOP)*. Retrieved 25.06.2024, from <https://www.umweltprobenbank.de/de/documents/publications/26646>.
- Taupp, T. (2022). "Against all odds: Harbor porpoises intensively use an anthropogenically modified estuary." *Marine Mammal Science* **38**(1): 288-303. DOI: <https://doi.org/10.1111/mms.12858>.
- Teubner, D.; Klein, R.; Tarricone, K. and Paulus, M. (2018a). "Guideline for Sampling and Sample Processing Zebra Mussel (*Dreissena polymorpha*)." *Standard Operating Procedure (SOP)*. Retrieved 25.06.2024, from <https://www.umweltprobenbank.de/de/documents/publications/26988>.
- Teubner, D.; Paulus, M.; Tarricone, K. and Klein, R. (2018b). "Guideline for Sampling and Sample Processing Earthworm (*Lumbricus terrestris*, *Aporrectodea longa*)." *Standard Operating Procedure (SOP)*. Retrieved 25.06.2024, from <https://www.umweltprobenbank.de/en/documents/publications/27147>.
- Tobajas, J.; Oliva-Vidal, P.; Piqué, J.; Afonso-Jordana, I.; García-Ferré, D.; Moreno-Opo, R. and Margalida, A. (2021). "Scavenging patterns of generalist predators in forested areas: The potential implications of increase in carrion availability on a threatened capercaillie population." *Animal Conservation* **25**(2): 259-272. DOI: <https://doi.org/10.1111/acv.12735>.
- Uhlig, S.; Hettwer, K.; Baldauf, H.; Krügener, S. and Simon, K. (2014). "Umweltstatistische Auswertung der Umweltprobenbank des Bundes." *Quodata GmbH Qualitätsmanagement und Statistik*, from <https://www.umweltprobenbank.de/de/documents/publications/24783>.
- Ulenaers, J. (2020). "The impact of artificial intelligence on the right to a fair trial: towards a robot judge?" *Asian Journal of Law and Economics* **11**(2). DOI: <https://doi.org/10.1515/ajle-2020-0008>.
- UNEP. (2022). "POPRC Recommendations for listing Chemicals." *Stockholm Convention on Persistent Organic Pollutants (POPs)*. Retrieved 19.09.2024, from <http://chm.pops.int/Convention/POPsReviewCommittee/Chemicals/tabid/243>.
- EPA's Non-CBI Summary Tables for 2015 Company Progress Reports (Final Progress Reports): 1-4. https://www.epa.gov/sites/production/files/2017-02/documents/2016_pfoa_stewardship_summary_table_0.pdf.
- Letter Inviting Participation in the PFOA Stewardship Program, US EPA: 2-2. <https://www.epa.gov/sites/production/files/2015-10/documents/dupont.pdf>.
- van de Vijver, K. I.; Hoff, P. T.; Das, K.; van Dongen, W.; Esmans, E. L.; Jauniaux, T.; Bouqueneau, J. M.; Blust, R. and Coen, W. d. (2003). "Perfluorinated Chemicals Infiltrate Ocean Waters: Link between Exposure Levels and Stable Isotope Ratios in Marine Mammals." *Environmental Science & Technology* **37**(24): 5545–5550. DOI: <https://doi.org/10.1021/es0345975>.
- van de Vijver, K. I.; Holsbeek, L.; Das, K.; Blust, R.; Joiris, C. and Coen, W. d. (2007). "Occurrence of perfluorooctane sulfonate and other perfluorinated alkylated substances in harbor porpoises from the Black Sea." *Environmental Science & Technology* **41**(1): 315–320. DOI: <https://doi.org/10.1021/es060827e>.

- Verreault, J.; Berger, U. and Gabrielsen, G. W. (2007). "Trends of perfluorinated alkyl substances in herring gull eggs from two coastal colonies in northern Norway: 1983-2003." *Environmental Science & Technology* **41**(19): 6671-6677. DOI: <https://doi.org/10.1021/es070723j>.
- Wagner, A.; Raue, B.; Brauch, H.-J.; Worch, E. and Lange, F. T. (2013). "Determination of adsorbable organic fluorine from aqueous environmental samples by adsorption to polystyrene-divinylbenzene based activated carbon and combustion ion chromatography." *Journal of Chromatography A* **1295**: 82-89. DOI: <https://doi.org/10.1016/j.chroma.2013.04.051>.
- Wallington, T. J.; Schneider, W. F.; Worsnop, D. R.; Nielsen, O. J.; Sehested, J.; Debruyne, W. J. and Shorter, J. A. (1994). "The Environmental Impact of CFC Replacements HFCs and HCFCs." *Environmental Science & Technology* **28**(7): 320A-326A. DOI: <https://doi.org/10.1021/es00056a714>.
- Wang, Q.; Wang, X. and Ding, X. (2014). "Rainwater trifluoroacetic acid (TFA) in Guangzhou, South China: Levels, wet deposition fluxes and source implication." *Science of The Total Environment* **468-469**: 272-279. DOI: <https://doi.org/10.1016/j.scitotenv.2013.08.055>.
- Wang, S.; Huang, J.; Yang, Y.; Hui, Y.; Ge, Y.; Larssen, T.; Yu, G.; Deng, S.; Wang, B. and Harman, C. (2013). "First report of a Chinese PFOS alternative overlooked for 30 years: its toxicity, persistence, and presence in the environment." *Environmental Science & Technology* **47**(18): 10163–10170. DOI: <https://doi.org/10.1021/es401525n>.
- Wang, Z.; Cousins, I. T.; Scheringer, M. and Hungerbühler, K. (2013). "Fluorinated alternatives to long-chain perfluoroalkyl carboxylic acids (PFCAs), perfluoroalkane sulfonic acids (PFASs) and their potential precursors." *Environment International* **60**: 242-248. DOI: <https://doi.org/10.1016/j.envint.2013.08.021>.
- Wang, Z.; DeWitt, J. C.; Higgins, C. P. and Cousins, I. T. (2017). "A Never-Ending Story of Per- and Polyfluoroalkyl Substances (PFASs)?" *Environmental Science & Technology* **51**(5): 2508–2518. DOI: <https://doi.org/10.1021/acs.est.6b04806>.
- Washington, J. W.; Rankin, K.; Libelo, E. L.; Lynch, D. G. and Cyterski, M. (2019). "Determining global background soil PFAS loads and the fluorotelomer-based polymer degradation rates that can account for these loads." *Science of the Total Environment* **651**(Pt 2): 2444–2449. DOI: <https://doi.org/10.1016/j.scitotenv.2018.10.071>.
- Wegge, P. and Kastdalen, L. (2008). "Habitat and diet of young grouse broods: resource partitioning between Capercaillie (*Tetrao urogallus*) and Black Grouse (*Tetrao tetrix*) in boreal forests." *Journal of Ornithology* **149**(2): 237-244. DOI: <https://doi.org/10.1007/s10336-007-0265-7>.
- Weinfurter, K. and Kördel, W. (2012). "Guideline for Sampling and Sample Treatment Soil." *Standard Operating Procedure (SOP)*. Retrieved 25.06.2024, from <https://www.umweltprobenbank.de/en/documents/publications/15883>.
- Weppner, W. (2000, 07.03.2006). "Letter, with Attachments, from William Weppner, 3M, to Charles Auer, EPA OPPT, regarding the Phase-out Plan for PFOS-Based Products." Retrieved 27.02.2023, from <https://www.regulations.gov/document?D=EPA-HQ-OPPT-2002-0051-0006>.
- Wilhelm, M.; Kraft, M.; Rauchfuss, K. and Hölzer, J. (2008). "Assessment and Management of the First German Case of a Contamination with Perfluorinated Compounds (PFC) in the Region Sauerland, North Rhine-Westphalia." *Journal of Toxicology and Environmental Health. Part A* **71**(11-12): 725–733. DOI: <https://doi.org/10.1080/15287390801985216>.
- Wirth, O.; Bliklen, R.; Rödig, L.; Wichmann, P.; Zimmermann, T.; Posner, S. and Hildenbrand, J. (2019). "Potential SVHC in environment and articles – information collection with the aim to prepare restriction proposals for PFAS." *Umweltbundesamt* **144/2019**.

- Wolf, C. J.; Takacs, M. L.; Schmid, J. E.; Lau, C. and Abbott, B. D. (2008). "Activation of mouse and human peroxisome proliferator-activated receptor alpha by perfluoroalkyl acids of different functional groups and chain lengths." *Toxicological Sciences* **106**(1): 162-171. DOI: <https://doi.org/10.1093/toxsci/kfn166>.
- Yamashita, N.; Kannan, K.; Taniyasu, S.; Horii, Y.; Petrick, G. and Gamo, T. (2005). "A global survey of perfluorinated acids in oceans." *Marine Pollution Bulletin* **51**(8-12): 658–668. DOI: <https://doi.org/10.1016/j.marpolbul.2005.04.026>.
- Yeung, L. W. Y.; Robinson, S. J.; Koschorreck, J. and Mabury, S. A. (2013). "Part II. A temporal study of PFOS and its precursors in human plasma from two german cities in 1982-2009." *Environmental Science & Technology* **47**(8): 3875-3882. DOI: <https://doi.org/10.1021/es4004153>.
- Yi, S.; Yang, D.; Zhu, L. and Mabury, S. A. (2022). "Significant Reductive Transformation of 6:2 Chlorinated Polyfluorooctane Ether Sulfonate to Form Hydrogen-Substituted Polyfluorooctane Ether Sulfonate and Their Toxicokinetics in Male Sprague–Dawley Rats." *Environmental Science & Technology* **56**(10): 6123–6132. DOI: <https://doi.org/10.1021/acs.est.1c00616>.
- Yoo, H.; Washington, J. W.; Jenkins, T. M. and Ellington, J. J. (2011). "Quantitative determination of perfluorochemicals and fluorotelomer alcohols in plants from biosolid-amended fields using LC/MS/MS and GC/MS." *Environmental Science & Technology* **45**(19): 7985-7990. DOI: <https://doi.org/10.1021/es102972m>.
- Zabaleta, I.; Bizkarguenaga, E.; Izagirre, U.; Negreira, N.; Covaci, A.; Benskin, J. P.; Prieto, A. and Zuloaga, O. (2017). "Biotransformation of 8:2 polyfluoroalkyl phosphate diester in gilthead bream (*Sparus aurata*)." *Science of the Total Environment* **609**: 1085-1092. DOI: <https://doi.org/10.1016/j.scitotenv.2017.07.241>.
- Zhang, C.; Hopkins, Z. R.; McCord, J.; Strynar, M. J. and Knappe, D. R. U. (2019). "Fate of Per- and Polyfluoroalkyl Ether Acids in the Total Oxidizable Precursor Assay and Implications for the Analysis of Impacted Water." *Environmental Science & Technology Letters* **6**(11): 662-668. DOI: <https://doi.org/10.1021/acs.estlett.9b00525>.
- Zhao, S. and Zhu, L. (2017). "Uptake and metabolism of 10:2 fluorotelomer alcohol in soil-earthworm (*Eisenia fetida*) and soil-wheat (*Triticum aestivum* L.) systems." *Environmental Pollution* **220**: 124-131. DOI: <https://doi.org/10.1016/j.envpol.2016.09.030>.
- Zhao, S.; Zhu, L.; Liu, L.; Liu, Z. and Zhang, Y. (2013). "Bioaccumulation of perfluoroalkyl carboxylates (PFCAs) and perfluoroalkane sulfonates (PFASs) by earthworms (*Eisenia fetida*) in soil." *Environmental Pollution* **179**: 45-52. DOI: <https://doi.org/10.1016/j.envpol.2013.04.002>.
- Zhao, Z.; Xie, Z.; Tang, J.; Sturm, R.; Chen, Y.; Zhang, G. and Ebinghaus, R. (2015). "Seasonal variations and spatial distributions of perfluoroalkyl substances in the rivers Elbe and lower Weser and the North Sea." *Chemosphere* **129**: 118-125. DOI: <https://doi.org/10.1016/j.chemosphere.2014.03.050>.
- Zhou, J.; Shu, R.; Yu, C.; Xiong, Z.; Xiao, Q.; Li, Z.; Xie, X. and Fu, Z. (2020). "Exposure to low concentration of trifluoromethanesulfonic acid induces the disorders of liver lipid metabolism and gut microbiota in mice." *Chemosphere* **258**(6). DOI: <https://doi.org/10.1016/j.chemosphere.2020.127255>.
- Zweigle, J.; Bugsel, B.; Fabregat-Palau, J. and Zwiener, C. (2024). "PFA Screen—an open-source tool for automated PFAS feature prioritization in non-target HRMS data." *Analytical and Bioanalytical Chemistry* **416**(2): 349-362. DOI: <https://doi.org/10.1007/s00216-023-05070-2>.

A Additional Information on Chemicals and Samples

A.1 PFAS reference standards and reagent purity

For method A, acetonitrile (Chromasolv™ LC-MS, ≥99.9%) and methanol (Rotisolv®, ≥99.95 %, LC-MS Grade) were purchased from Honeywell (Seelze, Germany), potassium peroxydisulfate (p. a., ≥99.0%) and sodium hydroxide (p. a., ≥98.0 %) from Merck (Darmstadt, Germany) and ammonium bicarbonate (≥99.5 %), formic acid (LC-MS grade, ≥98.0 %) and ammonium acetate (UHPLC-MS Optigrade) from Sigma-Aldrich (Bellefonte, USA). Ultrapure water was produced in an arium® 611 UV water purification system from Sartorius (Göttingen, Germany).

For method B, LC/MS grade methanol, acetonitrile, glacial acetic acid and ammonium acetate were obtained from Biosolve (Valkenswaard, the Netherlands) and ultrapure water from a Milli-Q system (Merck KGaA, Darmstadt, Germany).

Table A 1: List of target compounds and internal standards with acronym, corresponding PFAS family and group and information from the manufacturer

Compound	Acronym	Family	Group	Manufactured reference substance	CAS	Manufacturer	Concentration
Perfluorobutanesulfonic acid	PFBS	PFSA	A	KPFBS	375-73-5	Wellington	50 µg mL ⁻¹
Perfluorohexanesulfonic acid	PFHxS	PFSA	A	PFHxS	355-46-4	Wellington	50 µg mL ⁻¹
Perfluorooctanesulfonic acid	PFOS	PFSA	A	PFOS	1763-23-1	Wellington	50 µg mL ⁻¹
Perfluorodecanesulfonic acid	PFDS	PFSA	A	PFDS	335-77-3	Wellington	50 µg mL ⁻¹
Trifluoroacetate	TFA	PFCA	A	NaTFA	406-93-9	ABCR	neat
Perfluoropropanoic acid	PFPrA	PFCA	A	NaPFPrA	422-64-0	ABCR	neat
Perfluorobutanoic acid	PFBA	PFCA	A	PFBA	375-22-4	Wellington	50 µg mL ⁻¹
Perfluoropentanoic acid	PFPeA	PFCA	A	PFPeA	2706-90-3	Wellington	50 µg mL ⁻¹
Perfluorohexanoic acid	PFHxA	PFCA	A	PFHxA	307-24-4	Wellington	50 µg mL ⁻¹
Perfluoroheptanoic acid	PFHpA	PFCA	A	PFHpA	375-85-9	Wellington	50 µg mL ⁻¹
Perfluorooctanoic acid	PFOA	PFCA	A	PFOA	335-67-1	Wellington	50 µg mL ⁻¹
Perfluorononanoic acid	PFNA	PFCA	A	PFNA	375-95-1	Wellington	50 µg mL ⁻¹
Perfluorodecanoic acid	PFDA	PFCA	A	PFDA	335-76-2	Wellington	50 µg mL ⁻¹
Perfluoroundecanoic acid	PFUnDA	PFCA	A	PFUnDA	2058-94-8	Wellington	50 µg mL ⁻¹
Perfluorododecanoic acid	PFDoDA	PFCA	A	PFDoDA	307-55-1	Wellington	50 µg mL ⁻¹
Perfluorotridecanoic acid	PFTTrDA	PFCA	A	PFTTrDA	72629-94-8	Wellington	50 µg mL ⁻¹
Perfluorotetradecanoic acid	PFTeDA	PFCA	A	PFTeDA	376-06-7	Wellington	50 µg mL ⁻¹

Compound	Acronym	Family	Group	Manufactured reference substance	CAS	Manufacturer	Concentration
4:2 Fluorotelomer phosphate monoester	4:2 monoPAP	monoPAP	A	NA	150065-76-2	NA	NA
6:2 Fluorotelomer phosphate monoester	6:2 monoPAP	monoPAP	A	6:2 monoPAP	57678-01-0	Wellington	50 µg mL ⁻¹
8:2 Fluorotelomer phosphate monoester	8:2 monoPAP	monoPAP	A	8:2 monoPAP	57678-03-2	Wellington	50 µg mL ⁻¹
10:2 Fluorotelomer phosphate monoester	10:2 monoPAP	monoPAP	A	10:2 monoPAP	57678-05-4	Chiron	neat
4:2 Fluorotelomer phosphate diester	4:2 diPAP	diPAP	A	NA	135098-69-0	NA	NA
6:2 Fluorotelomer phosphate diester	6:2 diPAP	diPAP	A	6:2 diPAP	57677-95-9	Wellington	50 µg mL ⁻¹
6:2/8:2 Fluorotelomer phosphate diester	6:2/8:2 diPAP	diPAP	A	6:2/8:2 diPAP	943913-15-3	Wellington	50 µg mL ⁻¹
6:2/10:2 Fluorotelomer phosphate diester	6:2/10:2 diPAP	diPAP	A	NA	NA	NA	NA
6:2/12:2 Fluorotelomer phosphate diester	6:2/12:2 diPAP	diPAP	A	NA	NA	NA	NA
8:2 Fluorotelomer phosphate diester	8:2 diPAP	diPAP	A	8:2 diPAP	678-41-1	Wellington	50 µg mL ⁻¹
8:2/10:2 Fluorotelomer phosphate diester	8:2/10:2 diPAP	diPAP	A	NA	NA	NA	NA
8:2/12:2 Fluorotelomer phosphate diester	8:2/12:2 diPAP	diPAP	A	NA	NA	NA	NA
10:2 Fluorotelomer phosphate diester	10:2 diPAP	diPAP	A	10:2 diPAP	1895-26-7	Chiron	neat
Perfluorooctane sulfonamido phosphate diester	diSAmPAP	diSAmPAP	A	Na(diSAmPAP)	NA	Wellington	50 µg mL ⁻¹
4:2 Fluorotelomer sulfonic acid	4:2 FTSA	FTSA	A	4:2 FTSA	757124-72-4	Wellington	50 µg mL ⁻¹
6:2 Fluorotelomer sulfonic acid	6:2 FTSA	FTSA	A	6:2 FTSA	27619-97-2	Wellington	50 µg mL ⁻¹
8:2 Fluorotelomer sulfonic acid	8:2 FTSA	FTSA	A	8:2 FTSA	39108-34-4	Wellington	50 µg mL ⁻¹
Perfluorobutane sulfonamide	FBSA	FASA	A	FBSA	30334-69-1	ABCR	neat
Perfluorohexane sulfonamide	FHxSA	FASA	A	FHxSA	41997-13-1	ABCR	neat

Compound	Acronym	Family	Group	Manufactured reference substance	CAS	Manufacturer	Concentration
Perfluorooctane sulfonamide	FOSA	FASA	A	FOSA	754-91-6	Wellington	50 µg mL ⁻¹
<i>N</i> -Methyl perfluorooctane sulfonamide	MeFOSA	FASA	B	MeFOSA	31506-32-8	Wellington	50 µg mL ⁻¹
<i>N</i> -Ethyl perfluorooctane sulfonamide	EtFOSA	FASA	B	EtFOSA	4151-50-2	Wellington	50 µg mL ⁻¹
Perfluorobutane sulfonamidoethanol	FBSE	FASE	B	NA	34454-99-4	NA	NA
Perfluorohexane sulfonamidoethanol	FHxSE	FASE	B	NA	106443-63-4	NA	NA
Perfluorooctane sulfonamidoethanol	FOSE	FASE	B	NA	10116-92-4	NA	NA
<i>N</i> -Methyl perfluorooctane sulfonamidoethanol	MeFOSE	FASE	B	MeFOSE	24448-09-7	Wellington	50 µg mL ⁻¹
<i>N</i> -Ethyl perfluorooctane sulfonamidoethanol	EtFOSE	FASE	B	EtFOSE	1691-99-2	Wellington	50 µg mL ⁻¹
Perfluorobutane sulfonamidoacetic acid	FBSAA	FASAA	B	NA	347872-22-4	NA	NA
Perfluorohexane sulfonamidoacetic acid	FHxSAA	FASAA	B	NA	1003193-99-4	NA	NA
Perfluorooctane sulfonamidoacetic acid	FOSAA	FASAA	B	FOSAA	2806-24-8	Wellington	50 µg mL ⁻¹
<i>N</i> -Methylperfluorooctane sulfonamidoacetic acid	MeFOSAA	FASAA	B	MeFOSAA	2355-31-9	Wellington	50 µg mL ⁻¹
<i>N</i> -Ethylperfluorooctane sulfonamidoacetic acid	EtFOSAA	FASAA	B	EtFOSAA	2991-50-6	Wellington	50 µg mL ⁻¹
9-chlorohexadecafluoro-3-oxanonane-1-sulfonate	6:2 Cl-PFESA	Cl-PFESA	B	K(9Cl-PF3ONS)	73606-19-6	Wellington	50 µg mL ⁻¹
11-chloroeicosafluoro-3-oxaundecane-1-sulfonate	8:2 Cl-PFESA	Cl-PFESA	B	K(11Cl-PF3OUdS)	83329-89-9	Wellington	50 µg mL ⁻¹
4,8-dioxa-3 <i>H</i> -perfluorononanoic acid	DONA	PFECA	B	NaDONA	NOCAS_892452	Wellington	50 µg mL ⁻¹

Compound	Acronym	Family	Group	Manufactured reference substance	CAS	Manufacturer	Concentration
Perfluoro-2-methyl-3-oxahexanoic acid	HFPO-DA	PFECA	B	HFPO-DA	13252-13-6	Wellington	50 µg mL ⁻¹
6:2 fluorotelomer sulfonamide amine oxide (Capstone A)	6:2 FTNO	FTNO	A	DPOSA	80475-32-7	HPC Standards	neat
6:2 fluorotelomer sulfonamidopropyl betaine (Capstone B)	6:2 FTSA-PrB	FTSA-PrB	A	CDPOS	34455-29-3	HPC Standards	neat
Internal standards							
Sodium perfluoro-1-[2,3,4- ¹³ C ₃]butanesulfonate	PFBS-13C3	PFSA	A	MPFBS	NA	Wellington	50 µg mL ⁻¹
Sodium perfluoro-1-hexane[¹⁸ O ₂]sulfonate	PFHxS-18O2	PFSA	A	MPFHxS	NA	Wellington	50 µg mL ⁻¹
Sodium perfluoro-1-[1,2,3,4- ¹³ C ₈]octanesulfonate	PFOS-13C8	PFSA	A	MPFOS	NA	Wellington	50 µg mL ⁻¹
Perfluoro-n-[1,2,3,4- ¹³ C ₄]butanoic acid	PFBA-13C4	PFCA	A	MPFBA	NA	Wellington	50 µg mL ⁻¹
Perfluoro-n-[1,2,3,4,5- ¹³ C ₅]pentanoic acid	PFPeA-13C5	PFCA	A	MPFPeA	NA	Wellington	50 µg mL ⁻¹
Perfluoro-n-[1,2- ¹³ C ₂]hexanoic acid	PFHxA-13C2	PFCA	A	MPFHxA	NA	Wellington	50 µg mL ⁻¹
Perfluoro-n-[1,2,3,4- ¹³ C ₄]heptanoic acid	PFHpA-13C4	PFCA	A	MPFHpA	NA	Wellington	50 µg mL ⁻¹
Perfluoro-n-[1,2,3,4- ¹³ C ₄]octanoic acid	PFOA-13C4	PFCA	A	MPFOA	NA	Wellington	50 µg mL ⁻¹
Perfluoro-n-[1,2,3,4,5- ¹³ C ₅]nonanoic acid	PFNA-13C5	PFCA	A	MPFNA	NA	Wellington	50 µg mL ⁻¹
Perfluoro-n-[1,2- ¹³ C ₂]decanoic acid	PFDA-13C2	PFCA	A	MPFDA	NA	Wellington	50 µg mL ⁻¹
Perfluoro-n-[1,2- ¹³ C ₂]undecanoic acid	PFUndA-13C2	PFCA	A	MPFUndA	NA	Wellington	50 µg mL ⁻¹
Perfluoro-n-[1,2- ¹³ C ₂]dodecanoic acid	PFDoA-13C2	PFCA	A	MPFDoA	NA	Wellington	50 µg mL ⁻¹

Compound	Acronym	Family	Group	Manufactured reference substance	CAS	Manufacturer	Concentration
Perfluoro-n-[1,2- ¹³ C ₂]tetradecanoic acid	PFTeDA- ¹³ C ₂	PFCA	A	MPFTeDA	NA	Wellington	50 µg mL ⁻¹
Sodium 1 <i>H</i> ,1 <i>H</i> ,2 <i>H</i> ,2 <i>H</i> -[1,2- ¹³ C ₂]perfluorooctylphosphate	6:2 monoPAP- ¹³ C ₂	monoPAP	A	M6:2 monoPAP	NA	Wellington	50 µg mL ⁻¹
Sodium 1 <i>H</i> ,1 <i>H</i> ,2 <i>H</i> ,2 <i>H</i> -[1,2- ¹³ C ₂]perfluorodecylphosphate	8:2 monoPAP- ¹³ C ₂	monoPAP	A	M8:2 monoPAP	NA	Wellington	50 µg mL ⁻¹
Sodium bis(1 <i>H</i> ,1 <i>H</i> ,2 <i>H</i> ,2 <i>H</i> -[1,2- ¹³ C ₂]perfluorooctyl)phosphate	6:2 diPAP- ¹³ C ₂	diPAP	A	M6:2 diPAP	NA	Wellington	50 µg mL ⁻¹
Sodium bis(1 <i>H</i> ,1 <i>H</i> ,2 <i>H</i> ,2 <i>H</i> -[1,2- ¹³ C ₂]perfluorodecyl)phosphate	8:2 diPAP- ¹³ C ₂	diPAP	A	M8:2 diPAP	NA	Wellington	50 µg mL ⁻¹
Sodium bis(1 <i>H</i> ,1 <i>H</i> ,2 <i>H</i> ,2 <i>H</i> -[d ⁴]-perfluorodecyl)phosphate	10:2 diPAP- ² H ₄	diPAP	A	M10:2 diPAP	NA	Chiron	neat
Perfluoro-1-[¹³ C ₈]octanesulfonamide	FOSA- ¹³ C ₈	FASA	A	MFOSA	NA	Wellington	50 µg mL ⁻¹
<i>N</i> -methyl-d ³ -perfluoro-1-octanesulfonamide	MeFOSA- ² H ₃	FASA	B	d-N-MeFOSA	NA	Wellington	50 µg mL ⁻¹
<i>N</i> -ethyl-d ⁵ -perfluoro-1-octanesulfonamide	EtFOSA- ² H ₅	FASA	B	d-N-EtFOSA	NA	Wellington	50 µg mL ⁻¹
2-(<i>N</i> -deuteriomethylperfluoro-1-octanesulfonamido)- 1,1,2,2-tetradeuterioethanol	MeFOSE- ² H ₇	FASE	B	d ⁷ -N-MeFOSE	NA	Wellington	50 µg mL ⁻¹
2-(<i>N</i> -deuterioethylperfluoro-1-octanesulfonamido)- 1,1,2,2-tetradeuterioethanol	EtFOSE- ² H ₉	FASE	B	d ⁹ -N-EtFOSE	NA	Wellington	50 µg mL ⁻¹
<i>N</i> -deuteriomethylperfluoro-1-octanesulfonamidoacetic acid	MeFOSAA- ² H ₃	FASAA	B	d ³ -N-MeFOSAA	NA	Wellington	50 µg mL ⁻¹

Compound	Acronym	Family	Group	Manufactured reference substance	CAS	Manufacturer	Concentration
<i>N</i> -deuterioethylperfluoro-1-octanesulfonamidoacetic acid	EtFOSAA- ² H ₅	FASAA	B	d5-N-EtFOSAA	NA	Wellington	50 µg mL ⁻¹
2,3,3,3-Tetrafluoro-2-(1,1,2,2,3,3,3-heptafluoropropoxy)- ¹³ C ₃ -propanoic acid	HFPO-DA- ¹³ C ₃	PFECA	B	MHFPO-DA	NA	Wellington	50 µg mL ⁻¹
Sodium 1 <i>H</i> ,1 <i>H</i> ,2 <i>H</i> ,2 <i>H</i> -perfluoro-1-[1,2- ¹³ C ₂]-hexane sulfonate(4:2)	4:2 FTSA- ¹³ C ₂	FTSA	A	M4:2 FTSA	NA	Wellington	50 µg mL ⁻¹
Sodium 1 <i>H</i> ,1 <i>H</i> ,2 <i>H</i> ,2 <i>H</i> -perfluoro-1-[1,2- ¹³ C ₂]-octane sulfonate(6:2)	6:2 FTSA- ¹³ C ₂	FTSA	A	M6:2 FTSA	NA	Wellington	50 µg mL ⁻¹
Sodium 1 <i>H</i> ,1 <i>H</i> ,2 <i>H</i> ,2 <i>H</i> -perfluoro-1-[1,2- ¹³ C ₂]-decane sulfonate(8:2)	8:2 FTSA- ¹³ C ₂	FTSA	A	M8:2 FTSA	NA	Wellington	50 µg mL ⁻¹

A.2 Sample overview

Table A 2: Sample overview

English name	Latin name	Code	Sample type	Class	Ecosystem
Herring gull	<i>Larus argentatus</i>	LAE	Egg	bird	marine/freshwater carnivore
Great crested grebe	<i>Podiceps cristatus</i>	PCE	Egg	bird	freshwater carnivore
Great cormorant	<i>Phalacrocorax carbo</i>	PCU	Lung	bird	freshwater carnivore
Great cormorant	<i>Phalacrocorax carbo</i>	PCL	Liver	bird	freshwater carnivore
Common eider duck	<i>Somateria mollissima</i>	SML	Liver	bird	freshwater carnivore
Black grouse	<i>Tetrao tetris</i>	TTE	Egg	bird	terrestrial herbivore
Emerald rockcod	<i>Trematomus bernachii</i>	TBF	Musculature	fish/cod icefish	marine
Viviparous eelpout	<i>Zoarces viviparus</i>	ZVL	Liver	fish/Perciformes	marine benthic carnivore
Viviparous eelpout	<i>Zoarces viviparus</i>	ZVF	Musculature	fish/Perciformes	marine benthic carnivore
Common bream	<i>Abramis brama</i>	ABL	Liver	fish/leucesidae	freshwater
Common bream	<i>Abramis brama</i>	ABF	Musculature	fish/leucesidae	freshwater
Common barbel	<i>Barbus barbus</i>	BBL	Liver	fish/crypnidae	freshwater omnivore
Common barbel	<i>Barbus barbus</i>	BBF	Musculature	fish/crypnidae	freshwater omnivore
Roach	<i>Rutilus rutilus</i>	RRF	Musculature	fish/leucesidae	freshwater
European chub	<i>Squalius cephalus</i>	SCF	Musculature	fish/leucesidae	freshwater
Pike-perch	<i>Sander lucioperca</i>	SLF	Musculature	fish/Perciformes	freshwater carnivore
Blue mussel	<i>Mytilus edulis complex</i>	MEM	Mussel	mussel/Mytilidae	marine detritivore
Quagga mussel	<i>Dreissena rostriformis</i>	DRM	Mussel	mussel/Dreissenidae	freshwater

English name	Latin name	Code	Sample type	Class	Ecosystem
Zebra mussel	<i>Dreissena polymorpha</i>	DPM	Mussel	mussel/Dreissenidae	freshwater
Harbour porpoise	<i>Phocoena phocoena</i>	PPL	Liver	porpoise	marine/freshwater carnivore
Harbour porpoise	<i>Phocoena phocoena</i>	PPF	Musculature	porpoise	marine/freshwater carnivore
Grey seal	<i>Halichoerus grypus</i>	HGL	Liver	caniformia/pinniped	marine/freshwater carnivore
Grey seal	<i>Halichoerus grypus</i>	HGF	Musculature	caniformia/pinniped	marine/freshwater carnivore
Harbour seal	<i>Phoca vitulina</i>	PVL	Liver	caniformia/pinniped	marine/freshwater carnivore
Harbour seal	<i>Phoca vitulina</i>	PVF	Musculature	caniformia/pinniped	marine/freshwater carnivore
Common otter	<i>Lutra lutra</i>	LLL	Liver	caniformia/mustelidae	freshwater carnivore
Common otter	<i>Lutra lutra</i>	LLF	Musculature	caniformia/mustelidae	freshwater carnivore
Earthworm	<i>Lumbricus terrestris</i> + <i>Aporrectodea longa</i>	LTF	Musculature	lumbricidae	terrestrial
Chamois	<i>Rupicapra rupicapra</i>	RRL	Liver	ruminantia/caprinae	terrestrial herbivore
Red deer	<i>Cervus elaphus</i>	CEL	Liver	CEL/Cervidae	terrestrial herbivore
Roe deer	<i>Capreolus capreolus</i>	CCL	Liver	ruminantia/Cervidae	terrestrial herbivore
Common hare	<i>Lepus europaeus</i>	LEL	Liver	glires/lagomorphs(leoporidae)	terrestrial herbivore
Eurasian beaver	<i>Castor fiber</i>	CFL	Liver	glires/rodent	freshwater herbivore
Coypu	<i>Myocastor coypus</i>	MCL	Liver	glires/rodent	freshwater omnivore
Wild boar	<i>Sus scrofa</i>	SSL	Liver	pig	terrestrial omnivore
Wildcat	<i>Felis silvestris</i>	FSL	Liver	cat	terrestrial carnivore
Bladder wrack	<i>Fucus vesiculosus</i>	FVP	Plant material	plant/brown algae	marine
European beech	<i>Fagus sylvatica</i>	FSP	Plant material	plant/fagales	broadleave tree

English name	Latin name	Code	Sample type	Class	Ecosystem
Norway spruce	<i>Picea abies</i>	PAP	Plant material	plant/pinales/Pinaceae	coniferous tree
Scots pine	<i>Pinus sylvestris</i>	PSP	Plant material	plant/pinales/Pinaceae	coniferous tree
Lombardy poplar	<i>Populus nigra 'Italica'</i>	PNP	Plant material	plant/willow	broadleave tree
Suspended matter	NA	SPS	Solid material	Suspended matter	freshwater
Soil A horizon / Top soil	NA	TSS	Solid material	soil	terrestrial

Table A 3: Samples from the German ESB for initial screening

Sample number	Matrix	Sampling site	Sampling year
A001	LAE	Trischen (North Sea)	2017
A002	LAE	Mellum (North Sea)	2001
A003	LAE	Mellum (North Sea)	2014
A004	LAE	Mellum (North Sea)	2018
A005	ZVF	Darß (Baltic Sea)	2001
A006	ZVF	Darß (Baltic Sea)	2015
A007	ZVF	Darß (Baltic Sea)	2018
A008	ZVF	Varel-Mellum	2017
A009	ABL	Lake Belau	2017
A010	ABL	Rehlingen (Saar)	2018
A011	ABL	Wettin (Saale)	2017
A012	ABL	Jochenstein (Danube)	2018
A013	ABL	Dessau (Mulde)	2018
A014	ABL	Cumlosen (Elbe)	2018
A015	ABL	Blankenese (Elbe)	2018
A016	ABL	Koblenz (Rhine)	2017
A017	ABL	Bimmen (Rhine)	2001
A018	ABL	Bimmen (Rhine)	2018
A019	BBL	Weil (Rhine)	2018
A020	ABF	Lake Belau	2017
A021	ABF	Rehlingen (Saar)	2018
A022	ABF	Wettin (Saale)	2017
A023	ABF	Jochenstein (Danube)	2018
A024	ABF	Dessau (Mulde)	2018
A025	ABF	Cumlosen (Elbe)	2015
A026	ABF	Cumlosen (Elbe)	2018
A027	ABF	Blankenese (Elbe)	2018
A028	ABF	Koblenz	2017
A029	ABF	Bimmen (Rhine)	2001
A030	ABF	Bimmen (Rhine)	2018
A031	BBF	Weil (Rhine)	2018

Sample number	Matrix	Sampling site	Sampling year
A032	MEM	Königshafen (North Sea)	2000
A033	MEM	Königshafen (North Sea)	2017
A034	MEM	Eckwarderhörne (North Sea)	2017
A035	MEM	Darß (Baltic Sea)	2017
A036	DPM	Lake Belau	2017
A037	DPM	Rehlingen (Saar)	1998
A038	DPM	Rehlingen (Saar)	2018
A039	DPM	Jochenstein (Danube)	2018
A040	DPM	Wettin (Saale)	2018
A041	DPM	Prossen (Elbe)	2018
A042	DPM	Cumlosen (Rhine)	2018
A043	DPM	Blankenese (Elbe)	2018
A044	DPM	Koblenz (Rhine)	2018
A045	LTF	Leipzig	2017
A046	LTF	Leipzig	2019
A047	LTF	Saartal	2018
A048	LTF	Scheyern	2017
A049	LTF	Saartal	2018
A050	CCL	Duebener Heide	2015
A051	CCL	Duebener Heide	2018
A052	CCL	Harz	2018
A053	CCL	Berchtesgaden	2018
A054	CCL	War<LODt	2018
A055	CCL	Bavarian Forest	2018
A056	CCL	Bornhoeveder lake district	2017
A057	CCL	Solling	2017
A058	CCL	Palatinate Forest	2017
A059	CCL	Scheyern	2017
A060	FVP	Königshafen (North Sea)	2012
A061	FVP	Eckwarderhörne (North Sea)	2012
A062	FVP	Cap Arkona (Baltic Sea)	2012
A063	PAP	Hochharz	2018

Sample number	Matrix	Sampling site	Sampling year
A064	PAP	Berchtesgaden	2018
A065	PAP	Warndt	2018
A066	PAP	Bavarian Forest	2018
A067	PAP	Bornhoeved	2017
A068	PAP	Solling	2017
A069	PAP	Palatinate Forest	2017
A070	PAP	Scheyern	2017
A071	PSP	Duebener Heide	2015
A072	PSP	Duebener Heide	2018
A073	FSP	Hochharz	2018
A074	FSP	Berchtesgaden	2018
A075	FSP	Bavarian Forest	2018
A076	FSP	Bornhoeved	2017
A077	FSP	Solling	2017
A078	FSP	Palatinate Forest	2017
A079	FSP	Scheyern	2017
A080	PNP	Leipzig	1991
A081	PNP	Leipzig	2016
A082	PNP	Leipzig	2018
A083	SPS	Jochenstein (Danube)	2019
A084	SPS	Cumlosen (Rhine)	2019
A085	SPS	Wettin (Saale)	2019
A086	SPS	Weil (Rhine)	2019
A087	SPS	Koblenz (Rhine)	2018
A088	SPS	Koblenz (Rhine)	2019
A089	SPS	Bimmen (Rhine)	2019
A090	TSS	Leipzig	2018
A091	TSS	Staaden	2018
A092	TSS	Duebener Heide	2018
A093	TSS	Berchtesgaden	2018
A094	TSS	Warndt	2018
A095	TSS	Bavarian Forest	2018

Sample number	Matrix	Sampling site	Sampling year
A096	TSS	Bornhoeveder lake district	2019
A097	TSS	Solling	2014
A098	TSS	Solling	2019
A099	TSS	Palatinate Forest	2019
A100	TSS	Scheyern	2019

Table A 4: Samples from the German ESB for spatiotemporal trend analyses

Sample number	Matrix	Sampling site	Sampling year
C023	ZVL	Darß (Baltic Sea)	2001
C024	ZVL	Darß (Baltic Sea)	2018
C025	ABL	Prossen (Elbe)	2001
C026	ABL	Prossen (Elbe)	2018
C027	ABL	Dessau (Mulde)	2001
A013	ABL	Dessau (Mulde)	2018
C028	ABL	Blankenese (Elbe)	2001
C029	ABL	Blankenese (Elbe)	2018
C034	ABL	Koblenz (Rhine)	2001
A016	ABL	Koblenz (Rhine)	2017
A017	ABL	Bimmen (Rhine)	2001
A018	ABL	Bimmen (Rhine)	2018
C051	DPM	Prossen (Elbe)	2001
A041	DPM	Prossen (Elbe)	2018
C056	DPM	Blankenese (Elbe)	2001
C071	DPM	Blankenese (Elbe)	2018
C072	DPM	Koblenz (Rhine)	2001
A044	DPM	Koblenz (Rhine)	2018
C073	DPM	Bimmen (Rhine)	2001
C050	DRM02	Bimmen (Rhine)	2018

Table A 5: Details on samples and sampling procedures of the German ESB

Sample	Specimen	Method	Sampling frequency	Sampling time	SOP reference
Soil	Organic layer, A-horizon	Cutting frame, split tube sampler. Particle size: ≤5 mm (organic layer); 2 mm (soil), amount: ≥ 5 kg (ww) organic layer and ≥12 kg (ww) soil per site. Immediate freezing at -130 °C	Every 4 years	Late summer/autumn before leaves fall	(Weinfurtnner and Kördel 2012)
Red Beech (<i>Fagus sylvatica</i>) Lombardy Poplar (<i>Populus nigra 'Italica'</i>)	Leaves	Beech: 25 leaves per tree without stalks from branches from upper outside crown. Poplar: leaves without stalks from branches from a height of 5 – 7 m. ≥15 trees per site, 75 g (ww) leaves per tree. Immediate freezing at -130 °C	annually	Late summer (before leaf discoloration)	(Tarricone et al. 2018b, Tarricone et al. 2018c)
Norway Spruce (<i>Picea abies</i>) Scots Pine (<i>Pinus sylvestris</i>)	Shoots	One-year-old shoots from upper crown region; ≥15 trees per site, 150 g (ww) shoots per tree. Immediate freezing at -130°C	annually	March – May (end of the dormancy)	(Klein et al. 2018c)
Earthworm (<i>Lumbricus terrestris</i> , <i>Aporrectodea longa</i>)	Defecated body	captured individuals remain at 8 – 12 °C for 5 days for intestinal evacuation, then for 1 – 2 days at -20 °C followed by -130°C	annually	October – mid-December	(Teubner et al. 2018b)
Roe Deer (<i>Capreolus capreolus</i>)	Liver	Livers of yearlings of both sexes; ≥ 10 individuals per site and period; killed by professional shooting. Immediately frozen at ≤ -15 °C for ≤ 4 weeks, then -130 °C	annually	Early May – mid-July (before rutting season)	(Tarricone et al. 2018a)
Suspended matter	Particles < 2 mm	Sampling with sedimentation boxes. 12 monthly samples per site, pooled to one annual sampled of ≥6 kg (ww). Immediate freezing at -130 °C; freeze-drying at cooled conditions	annually	January - December	(Ricking et al. 2012)
Zebra Mussel (<i>Dreissena polymorpha</i>)	Soft body	Adult mussels of ≥12 mm shell length; 1000 g soft body (about 2000 – 5000 mussels) per site;	annually	May – end of August (after spawning)	(Teubner et al. 2018a)

Sample	Specimen	Method	Sampling frequency	Sampling time	SOP reference
		samples from plate racks or wild samples. Immediate freezing at -130 °C			
Blue Mussel (<i>Mytilus edulis complex</i>)	Soft body	Has to be checked and added later			(Paulus et al. 2018a)
Barbel (<i>Barbus barbus</i>)	Filet	n. a.	n. a.	n. a.	n. a.
Barbel (<i>Barbus barbus</i>)	Liver	n. a.	n. a.	n. a.	n. a.
Bream (<i>Abramis brama</i>)	Filet	Adult individuals (8 – 12 years old) of both sexes; ≥20 bream per site; net fishing of electrofishing. Immediate freezing after dissection at -130 °C	annually	Mid-July – end of October (after spawning)	(Klein et al. 2018a)
Bream (<i>Abramis brama</i>)	Liver	See bream filet	annually	Mid-July – end of October (after spawning)	(Klein et al. 2018a)
Bladder wrack (<i>Fucus vesiculosus</i>)	Thallus	≥20 forked thalli per site and sampling; cut by scissors. Immediate freezing at – 130 °C. All samples taken at one site in one year are combined to annual pool samples	annually	North Sea: every second month, Baltic Sea: June + November	(Quack et al. 2010)
Eelpout (<i>Zoarces viviparous</i>)	Filet	Adult individuals (≥15 cm length) of both sexes; ≥200 fish per site; net fishing. Immediate freezing after dissection at -130 °C	annually	Early May – end of June (before mating)	(Klein et al. 2018b)
Herring gull (<i>Larus argentatus</i>)	Egg	2nd egg in clutch; ≥25 eggs per site. Stored at 5± 2 °C for ≤2 weeks, then egg content stored at -130 °C	annually	April – March (during nesting season)	(Paulus et al. 2018b)

Table A 6: Samples from other collections and sampling campaigns

Sample number	English name	Latin name	Organ	Origin	Sampling date	Pooled (p) /individual (I)	Number in pool	Female (f)/male (m)	Age class
B043	Nutria	<i>Myocastor coypus</i>	liver	Bremen	2019	I	-	m	adult
B044	Nutria	<i>Myocastor coypus</i>	Liver	Bremen	2019	I	-	m	adult
B045	Nutria	<i>Myocastor coypus</i>	Liver	Bremen	2019	I	-	m	juvenile
B046	Nutria	<i>Myocastor coypus</i>	Liver	Bremen	2019	I	-	f	adult
B038	Hare	<i>Lepus europaeus</i>	Liver	Schleswig-Holstein	2016/2017	P	5	m	adult
B020	Harbour porpoise	<i>Phocoena phocoena</i>	Liver	Schleswig-Holstein	2015-2018	P	5	m	adult
B022	Harbour porpoise	<i>Phocoena phocoena</i>	Musculature	Schleswig-Holstein	2015-2018	P	5	m	adult
B021	Harbour porpoise	<i>Phocoena phocoena</i>	Liver	Schleswig-Holstein	2016-2019	P	5	m	adult
B023	Harbour porpoise	<i>Phocoena phocoena</i>	Musculature	Schleswig-Holstein	2016-2019	P	5	m	adult
B024	Grey seal	<i>Halichoerus grypus</i>	Liver	Schleswig-Holstein	2015-2020	P	5	m	adult

Sample number	English name	Latin name	Organ	Origin	Sampling date	Pooled (p) /individual (I)	Number in pool	Female (f)/male (m)	Age class
B025	Grey seal	<i>Halichoerus grypus</i>	Musculature	Schleswig-Holstein	2015-2020	P	5	m	adult
B026	harbour seal	<i>Phoca vitulina</i>	Liver	Schleswig-Holstein	2015-2020	P	5	f	adult
B027	harbour seal	<i>Phoca vitulina</i>	Musculature	Schleswig-Holstein	2015-2020	P	5	f	adult
B013	Common eider duck	<i>Somateria mollissima</i>	Liver	Denmark	2017/2018	P	5	m	adult
B028	Otter	<i>Lutra lutra</i>	Liver	Schleswig-Holstein	2016-2020	P	5	m	adult
B030	Otter	<i>Lutra lutra</i>	Musculature	Schleswig-Holstein	2016-2020	P	5	m	adult
B029	Otter	<i>Lutra lutra</i>	Liver	Lower Saxony	2016-2019	P	5	m	adult
B031	Otter	<i>Lutra lutra</i>	Musculature	Lower Saxony	2016-2019	P	5	m	adult
B015	Emerald rockcod	<i>Trematomus bernachii</i>	Musculature	Anarktica	2015/2016	P	8	f/m	-
B047	Wild boar	<i>Sus scrofa</i>	Liver	Area BC	19.10.2019	P	5	m	squeaker
B048	Wild boar	<i>Sus scrofa</i>	Liver	Area BC	19.10.2019	P	5	f	squeaker
B049	Wild boar	<i>Sus scrofa</i>	Liver	Area BC	11.11.2019	P	5	m	juvenile
B050	Wild boar	<i>Sus scrofa</i>	Liver	Area BC	19.10.2019	P	5	f	juvenile
B051	Wild boar	<i>Sus scrofa</i>	Liver	Area BC	19.10.2019	P	3	m	adult

Sample number	English name	Latin name	Organ	Origin	Sampling date	Pooled (p) /individual (I)	Number in pool	Female (f)/male (m)	Age class
B052	Wild boar	<i>Sus scrofa</i>	Liver	Area BC	19.10.2019	P	4	f	adult
B053	Wild boar	<i>Sus scrofa</i>	Liver	Area BC	25.10.2019	P	5	m	squeaker
B054	Wild boar	<i>Sus scrofa</i>	Liver	Area BC	26.10.2019	P	5	f	squeaker
B055	Wild boar	<i>Sus scrofa</i>	Liver	Area BC	25.10.2019	P	5	m	juvenile
B056	Wild boar	<i>Sus scrofa</i>	Liver	Area BC	25.10.2019	P	5	f	juvenile
B057	Wild boar	<i>Sus scrofa</i>	Liver	Area BC	25.10.2019	P	3	m	adult
B083	Soil		-	Bavaria	09.04.2019	P	>10	-	-
B084	Soil		-	Bavaria	26.07.2018	P	>10	-	-
B085	Soil		-	IE	04.04.2019	P	>10	-	-
B017	European chub	<i>Squalius cephalus</i>	Musculature	Bavaria	30.06.2016	P	10	f/m	adult
B016	Roach	<i>Rutilus rutilus</i>	Musculature	Bavaria	14.11.2018	P	8	f/m	adult
B018	European chub	<i>Squalius cephalus</i>	Musculature	Bavaria	19.07.2016	P	6	f/m	adult
B019	European chub	<i>Squalius cephalus</i>	Musculature	Bavaria	25.06.2018	P	10	f/m	adult
B014	Black grouse	<i>Tetrao tetris</i>	egg	Bavaria	01.08.2020	P	2	-	-

Sample number	English name	Latin name	Organ	Origin	Sampling date	Pooled (p) /individual (I)	Number in pool	Female (f)/male (m)	Age class
B032	Chamois	<i>Rupicapra rupicapra</i>	Liver	Bavaria	06.09.2020	I	-	F	juvenile
B033	Chamois	<i>Rupicapra rupicapra</i>	Liver	Bavaria	17.09.2020	I	-	F	juvenile
B034	Chamois	<i>Rupicapra rupicapra</i>	Liver	Bavaria	17.09.2020	I	-	m	adult
B035	Red deer	<i>Cervus elaphus</i>	Liver	Bavaria	16.09.2020	I	-	F	juvenile
B036	Red deer	<i>Cervus elaphus</i>	Liver	Bavaria	16.09.2020	I	-	F	adult
B037	Red deer	<i>Cervus elaphus</i>	Liver	Bavaria	16.09.2020	I	-	F	juvenile
B001	Great crested grebe	<i>Podiceps cristatus</i>	egg	Bavaria	01.08.2020	I	-	-	-
B002	Great crested grebe	<i>Podiceps cristatus</i>	egg	Bavaria	01.08.2020	I	-	-	-
B077	Riverine suspended matter		-	Bavaria	22.11.2019	I	-	-	-
B078	Riverine suspended matter		-	Bavaria	14.01.2019	I	-	-	-
B079	Riverine suspended matter		-	Bavaria	08.04.2019	I	-	-	-
B080	Riverine suspended matter		-	Bavaria	07.07.2019	I	-	-	-

Sample number	English name	Latin name	Organ	Origin	Sampling date	Pooled (p) /individual (I)	Number in pool	Female (f)/male (m)	Age class
B081	Riverine suspended matter		-	Bavaria	28.07.2016	I	-	-	-
B082	Riverine suspended matter		-	Bavaria	17.10.2016	I	-	-	-
B058	Wild boar	<i>Sus scrofa</i>	Liver	Bavaria	12.05.2020	I	-	F	juvenil
B069	Wildcat	<i>Felis silvestris</i>	Liver	Saxony-Anhalt	14.11.2019	I	-	F	immature
B070	Wildcat	<i>Felis silvestris</i>	Liver	Saxony-Anhalt	26.12.2019	I	-	F	immature
B071	Wildcat	<i>Felis silvestris</i>	Liver	Saxony-Anhalt	18.03.2020	I	-	m	adult
B076	Wildcat	<i>Felis silvestris</i>	Liver	Saxony-Anhalt	14.03.2019	I	-	F	adult
B068	Wildcat	<i>Felis silvestris</i>	Liver	Saxony-Anhalt	26.10.2019	I	-	m	immature
B072	Wildcat	<i>Felis silvestris</i>	Liver	Saxony-Anhalt	25.09.2019	I	-	m	adult
B073	Wildcat	<i>Felis silvestris</i>	Liver	Saxony-Anhalt	04.05.2018	I	-	m	adult
B074	Wildcat	<i>Felis silvestris</i>	Liver	Saxony-Anhalt	19.12.2019	I	-	m	adult
B075	Wildcat	<i>Felis silvestris</i>	Liver	Saxony-Anhalt	19.12.2019	I	-	m	adult
B039	Eurasian beaver	<i>Castor fiber</i>	Liver	Berlin	2015-2020	P	4	f/m	juvenil
B040	Eurasian beaver	<i>Castor fiber</i>	Liver	Berlin	2016-2019	P	3	F	subadult

Sample number	English name	Latin name	Organ	Origin	Sampling date	Pooled (p) /individual (I)	Number in pool	Female (f)/male (m)	Age class
B042	Eurasian beaver	<i>Castor fiber</i>	Liver	Berlin	2015-2020	P	6	F	adult
B041	Eurasian beaver	<i>Castor fiber</i>	Liver	Berlin	2016-2019	P	6	m	adult
B059	Wild boar	<i>Sus scrofa</i>	Liver	Baden-Württemberg	02.11.2020	I	-	f	squeaker
B060	Wild boar	<i>Sus scrofa</i>	Liver	Baden-Württemberg	05.11.2020	I	-	F	squeaker
B061	Wild boar	<i>Sus scrofa</i>	Liver	Baden-Württemberg	25.10.2020	I	-	F	squeaker
B062	Wild boar	<i>Sus scrofa</i>	Liver	Baden-Württemberg	10.11.2020	I	-	m	juvenile
B063	Wild boar	<i>Sus scrofa</i>	Liver	Baden-Württemberg	05.11.2020	I	-	m	juvenile
B067	Wild boar	<i>Sus scrofa</i>	Liver	Baden-Württemberg	11.11.2020	I	-	F	adult
B064	Wild boar	<i>Sus scrofa</i>	Liver	Baden-Württemberg	11.11.2020	I	-	m	adult
B065	Wild boar	<i>Sus scrofa</i>	Liver	Baden-Württemberg	03.11.2020	I	-	m	adult
B066	Wild boar	<i>Sus scrofa</i>	Liver	Baden-Württemberg	09.11.2020	I	-	m	adult
B003	Great cormorant	<i>Phalacrocorax carbo</i>	Lunge	Bavaria	Nov./Dez. 2020	I	-	F	Juvenil

Sample number	English name	Latin name	Organ	Origin	Sampling date	Pooled (p) /individual (I)	Number in pool	Female (f)/male (m)	Age class
B004	Great cormorant	<i>Phalacrocorax carbo</i>	Lunge	Bavaria	Nov./Dez. 2020	P	3	m	Juvenil
B006	Great cormorant	<i>Phalacrocorax carbo</i>	Liver	Bavaria	Nov./Dez. 2020	I	-	F	Juvenil
B005	Great cormorant	<i>Phalacrocorax carbo</i>	Liver	Bavaria	Nov./Dez. 2020	P	3	m	Juvenil
B007	Great cormorant	<i>Phalacrocorax carbo</i>	Liver	Bavaria	30.09.2020	I	-	m	Juvenil
B008	Great cormorant	<i>Phalacrocorax carbo</i>	Liver	Bavaria	27.11.2020	I	-	m	Adult
B009	Great cormorant	<i>Phalacrocorax carbo</i>	Liver	Bavaria	12.10.2020	I	-	F	Juvenil
B012	Great cormorant	<i>Phalacrocorax carbo</i>	Liver	Bavaria	25.11.2020	I	-	F	Adult
B010	Great cormorant	<i>Phalacrocorax carbo</i>	Liver	Bavaria	25.11.2020	I	-	m	Adult
B011	Great cormorant	<i>Phalacrocorax carbo</i>	Liver	Bavaria	25.11.2020	P	3	m	Adult

B Overview of Analytical Methods Applied

B.1 Method A

Extraction

For group A PFAS, 0.5 g of sample (or 0.1 g for monoPAP analysis in soil and suspended matter) was weighed into a 15 mL centrifuge tube and internal standard (IS) solution(s) (50 μL for PAP analysis (10 $\mu\text{g L}^{-1}$ diPAP/50 $\mu\text{g L}^{-1}$ monoPAP) and 25 μL for the other analyses (20 $\mu\text{g L}^{-1}$) were added. No IS was added to the TOP assay samples. For biota samples, 5 mL acetonitrile/water (9/1, v/v), for all other sample matrices 5 mL methanol (or methanol/water 7/3, v/v, for monoPAP analysis) were added. After initial vortex-mixing, the samples were incubated in an ultrasonic bath for 15 min at 25 °C, followed by shaking for 15 min in a vortex mixer at 2000 rpm. After centrifuging the samples for 5 min at $2968 \times g$, the supernatant was transferred into an additional 15 mL centrifuge tube and the extraction process was repeated with fresh solvents. The extracts were combined and subject to further sample treatment (clean-up or TOP assay).

Clean-Up

Extracts from biota samples were stored at -18 °C overnight to achieve a phase separation into an organic and aqueous layer and then centrifuged for 5 min. The organic layer was transferred into an additional 15 mL tube. Extracts from other matrices were not subject to freezing and processed straight. The solvent was evaporated to dryness using a slight stream of N_2 at 40 °C and 1.3 mL acetonitrile was added to the residues. After vortex-mixing, the extracts were treated in an ultrasonic bath for 15 min and subsequently agitated for 30 min at 2000 rpm on a horizontal shaker. The shaking step is crucial for breaking the salt structure after TOP assay and for process unity, this step was also adopted in the normal clean up. The supernatant was transferred into a 2 mL microcentrifuge tube. This fraction was centrifuged for 10 min at $12,000 \times g$ before transferring the liquid phase to another microcentrifuge tube. The clean-up process was repeated with 0.8 mL acetonitrile and 30 s shaking time before combining the supernatants. The acetonitrile was evaporated using a gentle stream of N_2 at 40 °C, and the residues dissolved in 0.2 mL methanol/water 8/2, v/v (or 0.2 mL methanol/water (8/2, v/v) with 0.1% ammonia for PAP analysis). The extracts were once again centrifuged at $12,000 \times g$ for 10 min and the supernatant was transferred to a 200 μL PP vial for instrumental analysis.

TOP Assay

The extracts were concentrated to 5 mL using a gentle stream of N_2 at 40 °C. Extracts of biota samples were stored at -18 °C overnight to achieve a phase separation into an organic and an aqueous layer and were then centrifuged for 5 min. The organic layer was transferred into a new 15 mL tube. Subsequently, the extract was divided into two 2 mL aliquots (in 15 mL tubes), one for the oxidation process and the other one for reference (without oxidation) to determine the formation potential of PFCAs from precursors. A volume of 10 μL IS (20 $\mu\text{g L}^{-1}$) was added to the reference aliquot before evaporating the solvent using N_2 . The pre-TOP assay extract was subject to the described clean-up process. After division of the raw extract, the aliquot for oxidation was also evaporated to dryness but then 8 mL $\text{K}_2\text{S}_2\text{O}_8$ solution (20 g L^{-1}) and 0.15 mL 10 N NaOH solution were added and the mixture was vortex-mixed. For oxidative digestion, the samples were incubated for 20 h at 85 °C. To ensure that the oxidation was complete, QA samples for each matrix (wild boar liver, soil, suspended matter, bream musculature) were spiked with 10 μL EtFOSAA solution (250 $\mu\text{g L}^{-1}$) prior oxidation. After cooling the samples using an ice bath, 10 μL IS (20 $\mu\text{g L}^{-1}$) were

added before evaporating the liquid phase at 10 mbar and 60 °C for 5 h using a rotational vacuum concentrator. Afterwards, the dried extracts were subject to the prior described clean-up, which was slightly modified by adding 6 glass beads before shaking it for 30 min to break the salt structure.

Calculations of Organofluorine (OF) concentrations

For calculation of the OF concentrations, all concentrations were normalized to the molecular fluorine content and expressed in $\mu\text{g L}^{-1}$ OF. The PFCA formation potential from precursor PFAS was calculated as the difference between the sum concentrations in the oxidized extract and the reference extract from the TOP assay (ΔTOP). However, concentrations are more accurate when using IS for quantification as done in target analysis e. g. for the PFCAs. However, in the TOP assay, IS cannot be used. So, in this study, the sum of the IS-corrected ΣPFCA concentration from target analysis and of the ΔTOP from TOP assay are considered the closest estimate of the PFAS total concentration. Hereafter, this concentration is called “After TOP assay”.

After TOP assay = $\Delta\text{TOP} + \Sigma\text{PFCA}(\text{target analysis})$ [$\mu\text{g L}^{-1}$ OF].

Instrumental Analysis

Instrumental analysis for the 50 PFAS of group A, including 19 analytes for qualitative analysis, was performed by applying three separate methods based on ion chromatography quadrupole time-of-flight mass spectrometry (IC-QTOF-MS) (TFA, PFPrA, PFBA, PFPeA), reversed-phase liquid chromatography tandem mass spectrometry (RP-LC-MS/MS) method 1 (PAP analysis) and RP-LC-MS/MS method 2 (all other group A PFAS).

IC-QTOF analysis was performed by injection of 10 μL extract on an Infinity 1290 HPLC system (Agilent Technologies, Waldbronn, Germany) coupled to a hybrid quadrupole time-of-flight mass spectrometer mass analyser (QTOF) (Sciex TripleTOF 6600, Darmstadt, Germany), using the negative ion mode for the electrospray ionization (ESI). The high-resolution mass spectrometer was used to avoid false positive results due to analytical difficulties for short chain PFCAs (i.e., PFPrA and PFBA) as described by Abraham et al. (2021) (i.e., only one mass transition).

Chromatographic separation was achieved on a Dionex IonPAC AS17 C column (2 \times 250 mm, Thermo Fisher, Darmstadt, Germany) equipped with a pre-column (Dionex IonPAC AG17-C, 2 \times 50 mm). Eluent A was 100 mM ammonium bicarbonate in water/methanol (8/2, v/v), eluent B was methanol. The binary gradient started with 20% A and increased to 40 % A within 4.5 min, holding for 3 min before increasing to 80 % A within 10 s. The gradient was held for 3 min before decreasing to 20 % A within 10 s and held for another 5.5 min. The applied flow rate was 0.18 mL min^{-1} , and the column was thermostated at 40 °C. The mass spectrometer was recalibrated automatically after five measurements using an automated calibrant delivery system (CDS). The quantification by QTOF based on parallel measurement of product ion experiments (m/z 60–410 Da) for the four analytes and the related three internal standards. A full scan experiment (m/z 100–800 Da) was measured in parallel as proof of identity since a second fragment is missing for the small analytes.

Both RP-LC-MS/MS methods were performed on an Infinity 1260 HPLC system (Agilent Technologies) coupled to a triple quadrupole mass spectrometer (Sciex Triple Quad 6500+) using ESI-negative mode with a Turbo V ESI source. The schedule multiple-reaction monitoring (SMRM) was used with two mass transitions for a compound if available. The chromatographic separation of the PAPs (RP-LC-MS/MS 1) was achieved on an Acquity UPLC® BEH column (2.1 \times 100 mm, 1.7 μm , Waters, Eschborn, Germany) with a guard column (KrudKatcher ULTRA HPLC In Line Filter 2 μm , Phenomenex, Aschaffenburg, Germany). Eluent A was water, eluent B was methanol, both containing 0.1 % ammonium hydroxide. The binary gradient started with 25 % B, increased to

98 % B within 8 min, holding for 6 min before decreasing to 25 % again within 10 s and holding for another 6 min. Sample volumes of 10 μL were injected, the applied flow rate was 0.18 mL min^{-1} , and the column was thermostated at 40 $^{\circ}\text{C}$.

For the RP-LC-MS/MS 2 method, a Luna® Omega 1.6 μm polar C18 column (100 mm \times 2.1 mm, 1.6 μm , Phenomenex) with a pre-column (KrudKatcher ULTRA HPLC In-Line Filter 2 μm , Phenomenex) was used. To handle potential contamination from fittings, an isolator column (2.1 \times 50 mm, Waters, Eschborn, Germany) was installed between the solvent mixing unit and the autosampler. Due to the high organic solvent content in the final extracts, an injector program was implemented for the RP-LC-MS/MS 2 method (Janda et al., 2019). To adjust the ratio of water and organic solvent to avoid unfavourable chromatographic effects, 20 μL formic acid (1 %) were drawn into the sample loop before drawing 10 μL sample and another 20 μL formic acid until the mixture was injected. The needle was rinsed with methanol/water (1/1, v/v) after each drawing step. Eluent A was 10 mM ammonium acetate in water/methanol (9/1, v/v) and eluent was methanol. The binary gradient started with 20% B, increased to 70 % B within 7 min and to 98 % B until minute 7.5. After holding 98 % B for 7 min, it decreased to 20 % B within 0.5 and was held for another 8 min. The flow rate was 0.18 mL min^{-1} and the column was thermostated at 40 $^{\circ}\text{C}$.

B.2 Method B

Extraction

The extraction protocol for PFAS of group B (Table A 1) is adapted from Verreault et al. (2007) and includes a purification step first applied by Powley et al. (2005). A sample aliquot of 1 g was weighed into a 15-mL falcon tube. Depending on the sample appearance 0–3 mL acetonitrile (methanol for soil and suspended matter) were added for sample wetting before the addition of 50 μL IS solution (20 $\mu\text{g L}^{-1}$ in methanol, for individual PFAS up to 100 $\mu\text{g L}^{-1}$). The sample was left overnight or, for specific matrices requiring intensive wetting, longer (up to 4 days for abiotic material) to let the solvent evaporate. Subsequently, they were extracted with 5 mL acetonitrile, vortex-mixed vigorously, treated in an ultrasonic bath for 15 min and centrifuged (5 min at 2,000 rpm). Soil and suspended matter were extracted with methanol instead of acetonitrile. The extraction was repeated and the supernatants combined in a 15-mL Falcon tube.

Clean-Up

The raw extract was concentrated to approximately 1 mL under a gentle stream of N_2 . A 2-mL centrifuge tube containing 20 mg graphitized carbon (ENVI-Carb, Supelclean, 120/400 mesh, Supelco, Sigma-Aldrich, Bellefonte, USA) and 50 μL glacial acetic acid was prepared for sample clean-up. After addition of the concentrated extract, the tube was vortex-mixed thoroughly and centrifuged (10 min at 10,000 rpm). A volume of 500 μL supernatant was mixed with 500 μL 4 mM aqueous ammonium acetate solution in a 1.5-mL centrifuge tube. Biotic samples were purified further by density separation after freeze-out. For this purpose, the extracts were stored at -18°C overnight and centrifuged at -4°C (15 min at 11,000 rpm). Before analysis, all extracts were filtered through a 0.2 μm RC4 filter (Minisart, PP-housing, Sartorius, Stonehouse, UK) into PP autosampler vials. The extracts of abiotic samples were filtered after adaptation to the mobile phase without prior freeze-out.

Instrumental Analysis

Analysis for 16 PFAS of group B, including 5 analytes for qualitative analysis, was performed on an ultra-high-performance liquid chromatograph (Acquity I Class system) coupled to a tandem mass spectrometer (Xevo TQ-S, both Waters, Eschborn, Germany). MassLynx v4.2 was used for

instrument control and data processing. The chromatographic program was adapted from Muschket et al. (2020). An exact volume of 5 μL extract was injected and separated on an Acquity UPLC BEH Shield RP18 column (50 \times 2.1, 1.7 μm , Waters) at a flow rate of 0.35 mL min^{-1} at 40 $^{\circ}\text{C}$. A 'PFC IsolatorTM' column (50 \times 2.1 mm, Waters) was installed downstream the solvent mixing unit to prevent interfering PFAS signals from background contaminations in the mobile phase. The gradient program started with 90 % solvent A (2 mM ammonium acetate in water/methanol, 95/5, v/v) and 10 % B (2 mM ammonium acetate in water/methanol/acetonitrile, 5/75/20, v/v/v). After 1.5 min, the proportion of solvent B was ramped to 65 % within the next 3.0 min and to 80 % within the following 3.75 min. Then the column was flushed by 99.9 % B for 2.75 min before changing back to the initial conditions. The total run time was 15 min. The MS/MS was operated in ESI-negative mode employing N_2 as desolvation and cone gas (600 and 150 L hr^{-1} , respectively). The capillary voltage was set to 1.0 kV and the desolvation and source temperature to 350 and 150 $^{\circ}\text{C}$, respectively.

B.3 Method C

Sample Preparation

PFAS of group C were analysed using solid-phase microextraction (SPME) followed by GC-MS analysis. The SPME-method developed by Bach et al. (2016) for quantification of neutral PFAS in sediment was optimized for poplar leaves and applied also to other plant and abiotic materials and earthworm exemplary for animal tissue.

A weight of 1.5 g biotic sample material was weighed into a 10-mL headspace vial (Gerstel, Mühlheim a/R, Germany) containing a glass-coated PTFE stirring bar (Carl Roth GmbH, Karlsruhe, Germany). Afterwards, 5 mL ultrapure water were added to facilitate headspace (HS) sampling. The sample and water amount were optimized for poplar leaves and adapted to sample density when applied to abiotic material to keep HS volume constant throughout all extractions. This affected the ratio of sample to water which was adjusted accordingly. Taking all factors into account, a slurry of 1.7 g soil (ww) and 5.666 mL water and for suspended matter a slurry of 1.7 g sample (dw) and 5.2 mL water was prepared for analysis. Before HS-sampling, 1.5 or 2.0 μL IS solution and the same amount of recovery standard 7:1 FTOH (both 1000 $\mu\text{g L}^{-1}$) were added. The vial was capped immediately and put in the autosampler. Stability tests showed a decreasing response after approximately 90 min sample preparation. As a consequence, no more than two samples were prepared at the same time for immediate analysis.

Automated Solid-Phase Microextraction

The neutral PFAS were extracted by a DVB/PDMS fiber (65 μm , Supelco, Bellefonte, USA) employing the autosampler MPS robotic XL installed to the GC-MS system and controlled by Maestro Control software V1.4 (Gerstel, Mühlheim a/d Ruhr, Germany). The fiber was conditioned according to the manufacturer's recommendations. The sample was incubated at 30 $^{\circ}\text{C}$ for 30 min and the analytes were extracted from the headspace at the same temperature during the following 30 min. Stirring was set to pulsed mode (20 s at 250 rpm after 2 s rest).

Instrumental Analysis

The instrumental analysis was carried out on an Agilent 8890 GC coupled to a 5977B GC/MS (Agilent, Waldbronn, Germany). MassHunter Workstation V10.0 was used for control of the instrument and data processing. The extracted analytes were desorbed thermally from the fiber for 3 min at 230 $^{\circ}\text{C}$ using splitless injection mode. The injector was equipped with a merlin low-pressure microseal and a 0.75 mm I.D. liner (Agilent). For chromatographic separation a CP-WAX

57 CB column (25 m x 0.25 mm x 2 μ m, Agilent) and He as carrier gas was used at a constant flow of 1.1 mL min⁻¹. The detection method was adapted from Jahnke et al. (2007). The GC oven program was as follows: 50 °C (3.2 min); 3 °C min⁻¹ 80 °C; 20 °C min⁻¹ 160 °C (4 min) and 30 °C min⁻¹ 200 °C (2 min) with a total run time of 24.5 min. The MS was operated in single ion monitoring (SIM) and positive chemical ionisation (PCI) mode with methane (20 %) as reaction gas. The interface to the MS and the source were heated at 250 °C and the quadrupole at 150 °C.

Figure B 1: Sample volume of beech leaves and soil in 10-mL headspace vials

The influence of density on the filling volume for constant mass.



Source: own illustration, UFZ.

B.4 Instrumental parameters for MS/MS detection of target compounds

Table B 1: Target compounds and selected instrumental parameters for LC-MS/MS detection

Compound (quantitative)	MS mode	Q _n (Q _i) m/z	Collision energy / eV	Internal standard
PFBS	ESI-/MRM	299 > 99 (80)	-45 (-50)	MPFBS
PFHxS	ESI-/MRM	399 > 99 (80)	-52 (-75)	MPFHxS
PFOS	ESI-/MRM	499 > 99 (80)	-60 (-90)	MPFOS
PFDS	ESI-/MRM	599 > 99 (80)	-75 (-110)	MPFOS
TFA	ESI-/MRM (HRMS)	112.9856 > 68.9948	-16±2	MTFA
PFPrA	ESI-/MRM (HRMS)	162.9824 > 118.992	-16±2	MTFA
PFBA	ESI-/MRM (HRMS)	212.9792 > 168.9858	-16±2	MPFBA
PFPeA	ESI-/MRM (HRMS)	262.9760 > 218.9858	-16±2	MPFPeA
PFHxA	ESI-/MRM	313 > 269 (119)	-13 (-30)	MPFHxA
PFHpA	ESI-/MRM	363 > 319 (169)	-14 (-24)	MPFHpA
PFOA	ESI-/MRM	413 > 369 (169)	-13 (-25)	MPFOA
PFNA	ESI-/MRM	463 > 419 (219)	-15 (-24)	MPFNA
PFDA	ESI-/MRM	513 > 469 (219)	-16 (-25)	MPFDA
PFUnDA	ESI-/MRM	563 > 519 (269)	-18 (-26)	MPFUnDA
PFDoDA	ESI-/MRM	613 > 569 (169)	-19 (-38)	MPFDoDA
PFTrDA	ESI-/MRM	663 > 619 (169)	-19 (-40)	MPFTrDA
PFTeDA	ESI-/MRM	713 > 669 (169)	-40 (-50)	MPFTeDA
6:2 monoPAP	ESI-/MRM	443 > 423 (97)	-16 (-20)	M6:2 monoPAP

Compound (quantitative)	MS mode	Q _n (Q _i) m/z	Collision energy / eV	Internal standard
8:2 monoPAP	ESI-/MRM	543 > 523 (97)	-20 (-22)	M8:2 monoPAP
10:2 monoPAP	ESI-/MRM	643 > 623 (97)	-24 (-54)	M6:2 monoPAP
6:2 diPAP	ESI-/MRM	789 > 443 (423)	-30 (-36)	M6:2 diPAP
6:2/8:2 diPAP	ESI-/MRM	889 > 443 (543)	-32 (-32)	M8:2 diPAP
8:2 diPAP	ESI-/MRM	989 > 543 (523)	-36 (-42)	M8:2 diPAP
10:2 diPAP	ESI-/MRM	1189 > 643 (623)	-38 (-48)	M10:2 diPAP
diSAmPAP	ESI-/MRM	1203 > 526 (650)	-62 (-54)	M10:2 diPAP
FOSA	ESI-/MRM	498 > 78 (48)	-40 (-125)	MFOSA
MeFOSA	ESI-/MRM	512 > 169 (219)	28 (24)	d-N-MeFOSA
EtFOSA	ESI-/MRM	526 > 169 (219)	28 (24)	d-N-EtFOSA
MeFOSE (acetate adduct)	ESI-/MRM	616 > 59	12	d7-N-MeFOSE (acetate adduct)
EtFOSE (acetate adduct)	ESI-/MRM	630 > 59	16	d9-N-EtFOSE (acetate adduct)
FOSAA	ESI-/MRM	556 > 498 (419)	30	d3-N-MeFOSAA
MeFOSAA	ESI-/MRM	570 > 419 (483)	20 (14)	d3-N-MeFOSAA
EtFOSAA	ESI-/MRM	584 > 419 (526)	22 (22)	d5-N-EtFOSAA
6:2 Cl-PFESA	ESI-/MRM	531 > 351 (83)	26 (26)	MPFOS
8:2 Cl-PFESA	ESI-/MRM	631 > 451 (83)	26 (26)	MPFOS
DONA	ESI-/MRM	377 > 251 (85)	14 (24)	MPFOA
HFPO-DA	ESI-/MRM	285 > 169 (185)	10 (20)	MHFPO-DA
6:2 FTNO (Capstone A)	ESI-/MRM	527 > 507 (120)	-16 (-44)	MPFDA
6:2 FTSA-PrB (Capstone B)	ESI-/MRM	569 > 223 (120)	-22 (-42)	MPFUnDA
4:2 FTSA	ESI-/MRM	327 > 307 (81)	-28 (-70)	M4:2 FTSA
6:2 FTSA	ESI-/MRM	427 > 407 (81)	-34 (-68)	M6:2 FTSA
8:2 FTSA	ESI-/MRM	527 > 507 (81)	-40 (-40)	M8:2 FTSA

B.5 Further Information on LC-HRMS screening

Table B 2: Mix of standards used for quality control in LC-HRMS screening

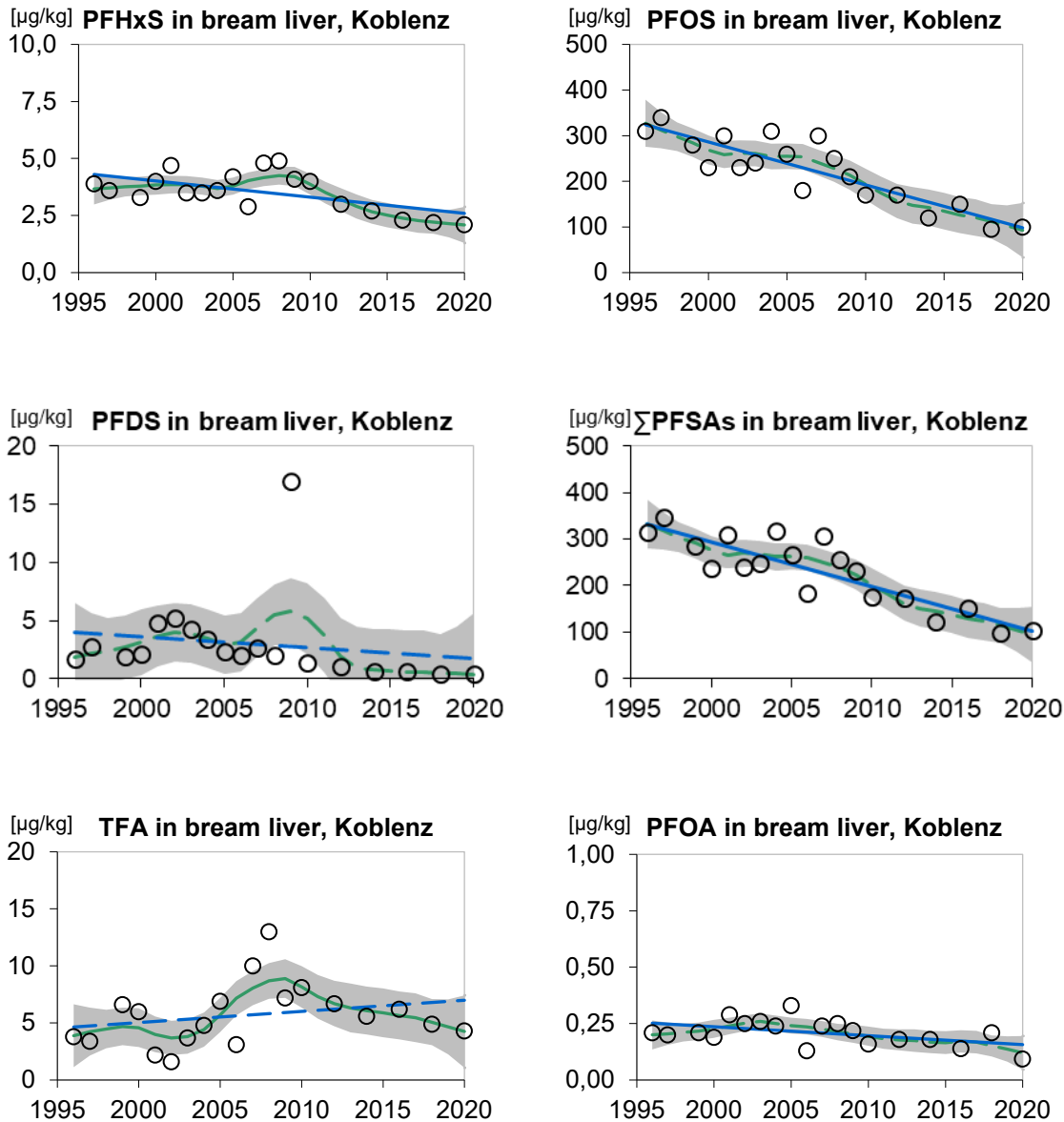
Analyte	Concentration in the measurement solution (ng/mL)
F53B-9Cl	2
F53B-11Cl	2

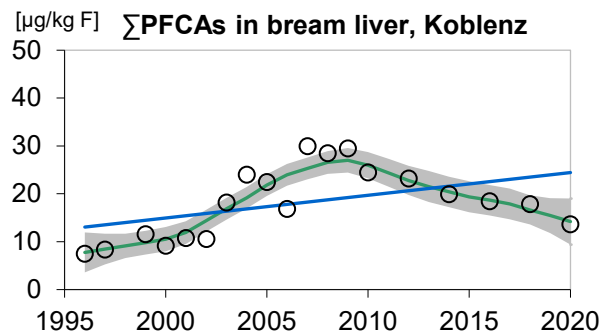
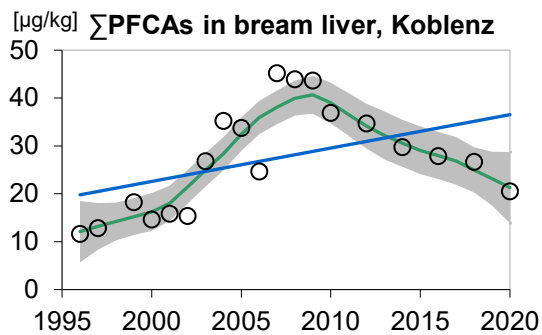
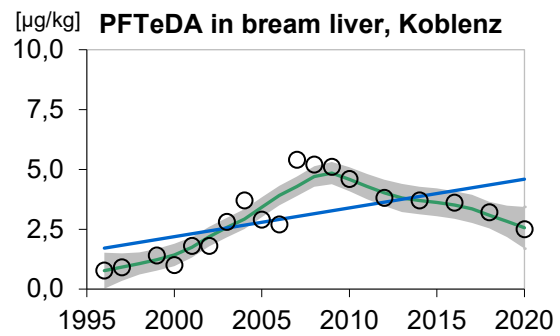
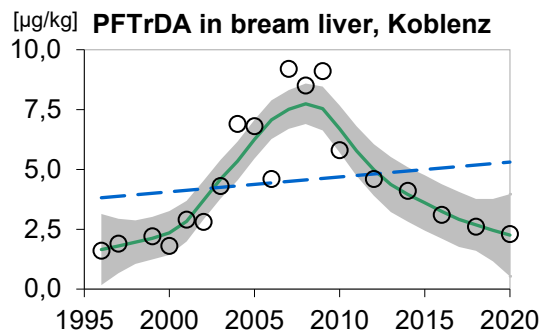
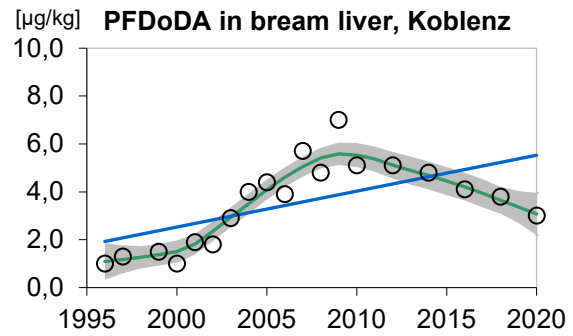
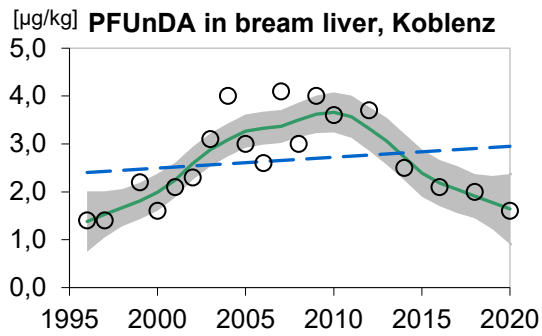
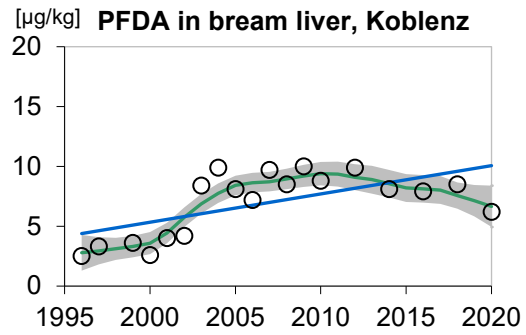
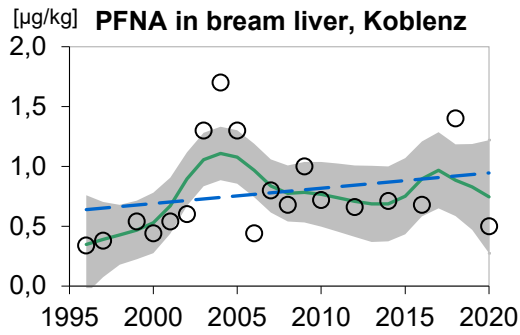
Analyte	Concentration in the measurement solution (ng/mL)
FOSAA	2
MeFOSAA	2
EtFOSAA	2
NaDONA	2
HFPO-DA	4
PFOS	2
PFHxS	2
PFDA	2
PFOA	2
MeFOSE	4
EtFOSE	4
FOSA	4
MeFOSA	4
EtFOSA	4
D3-MeFOSAA	2
D5-EtFOSAA	2
M3HFPO-DA	2
M8-PFOS	2
M-PFHxS	2
M-PFDA	2
M8-PFOA	2
d7-MeFOSE	10
d9-EtFOSE	10
M8FOSA	2
dMeFOSA	2
dEtFOSA	2

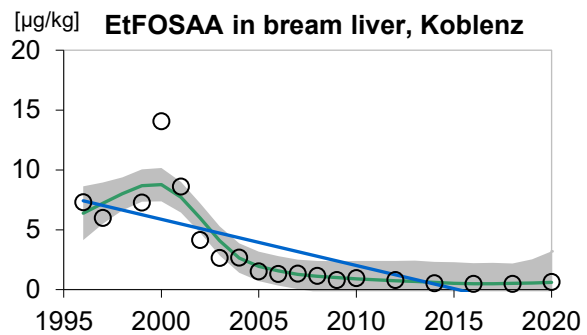
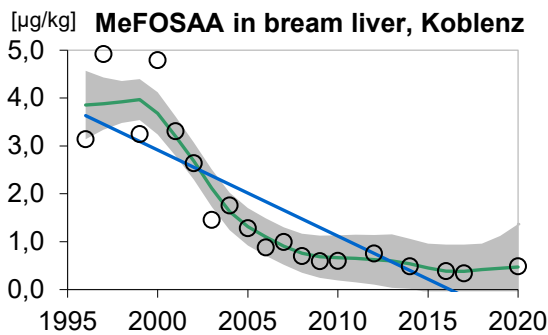
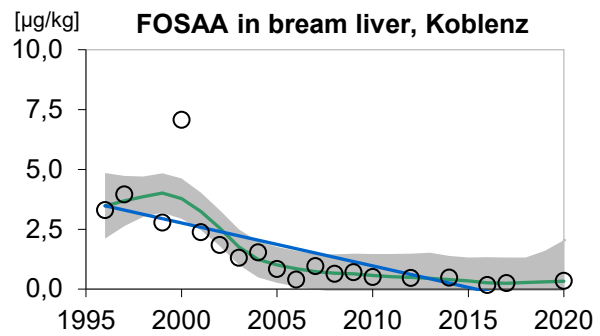
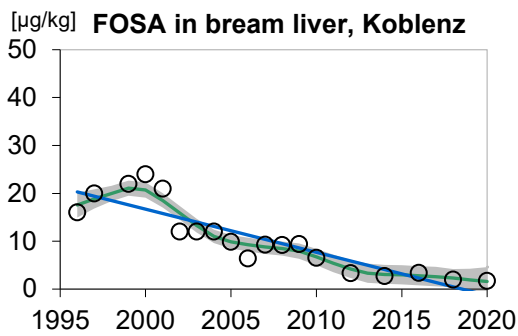
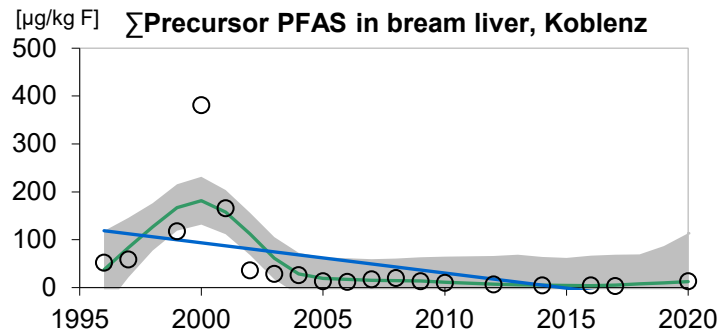
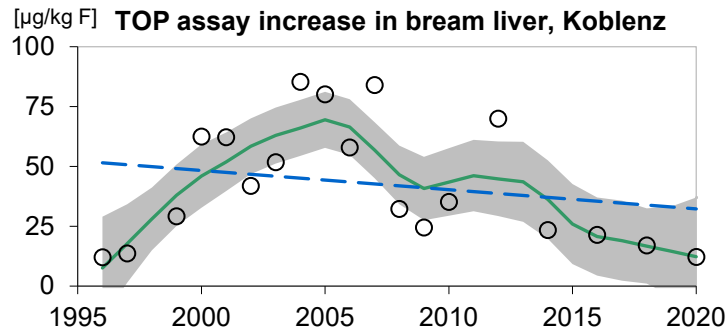
C Screening Results

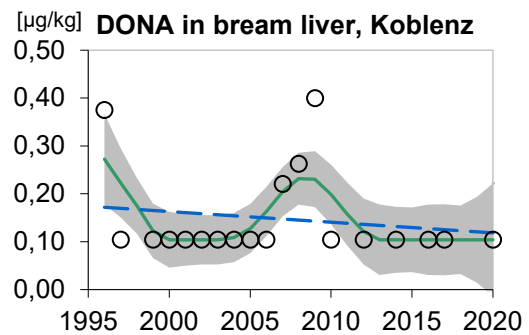
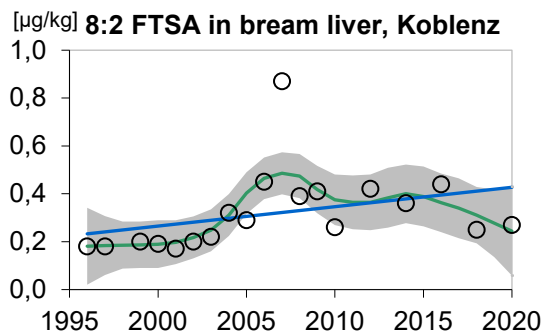
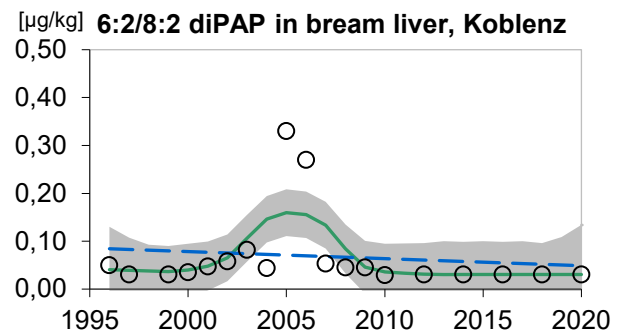
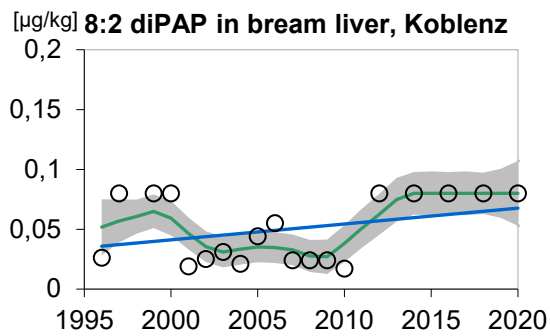
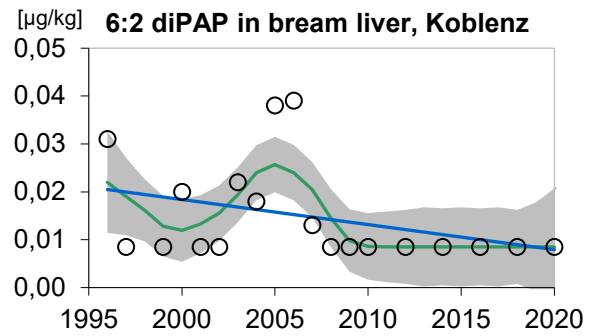
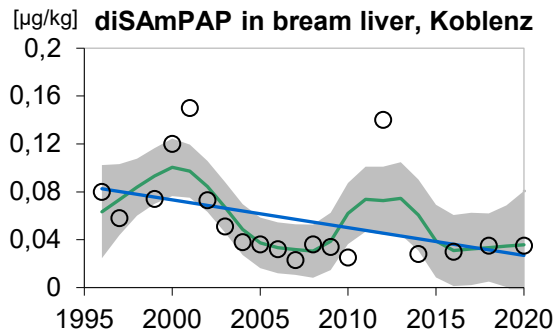
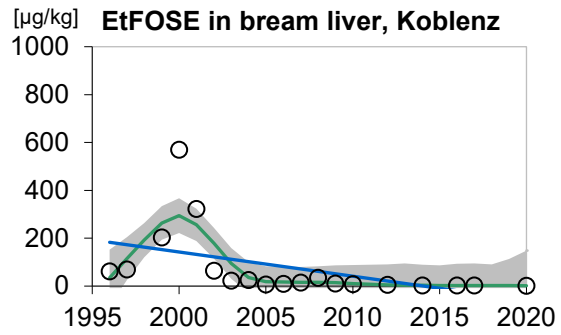
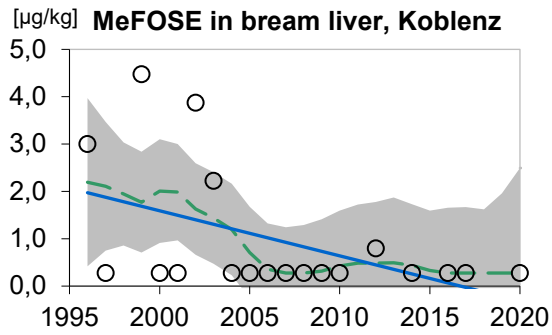
C.1 Time Series Analyses by LOESS Trend

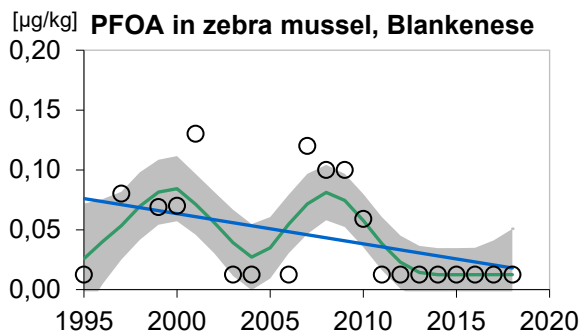
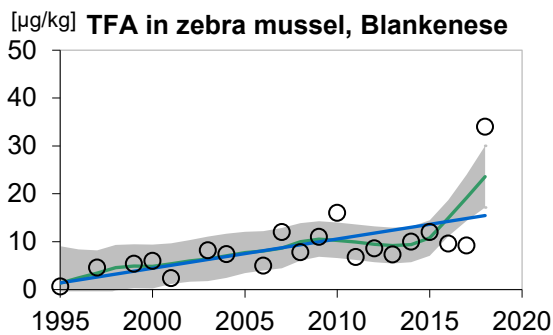
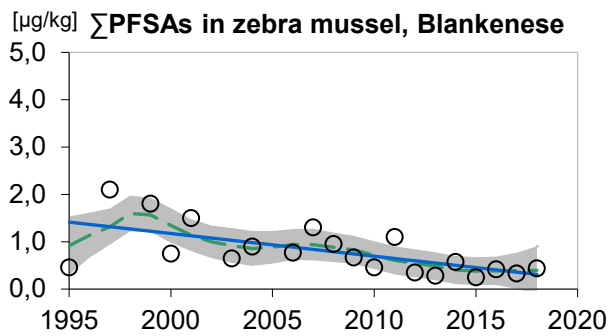
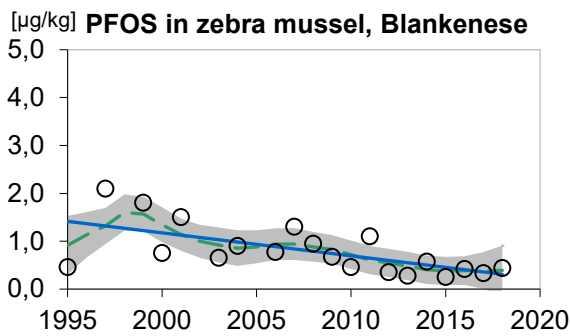
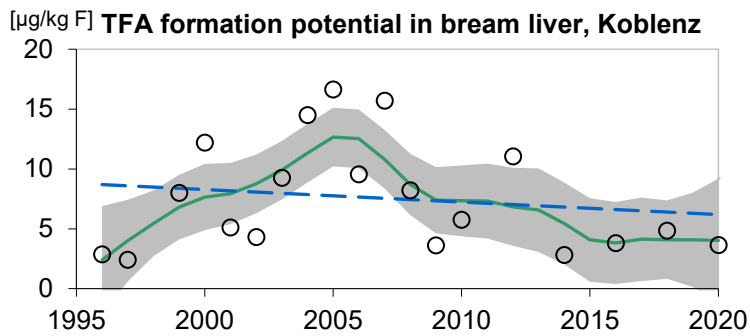
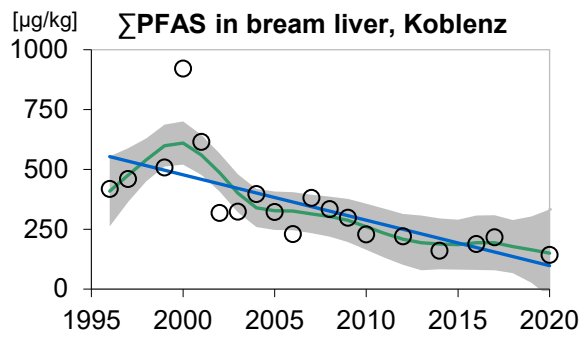
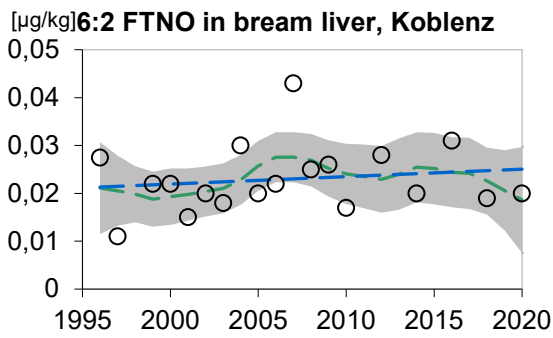
Figure C 1: Time Series Analyses by LOESS Trend

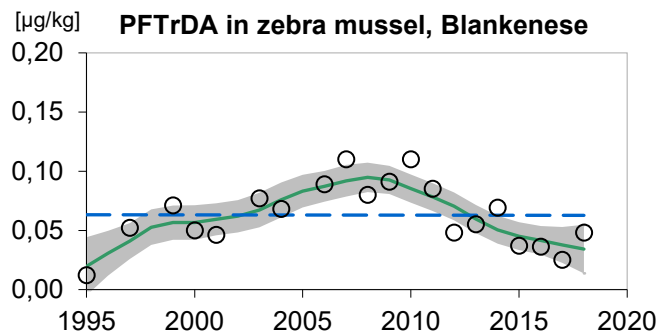
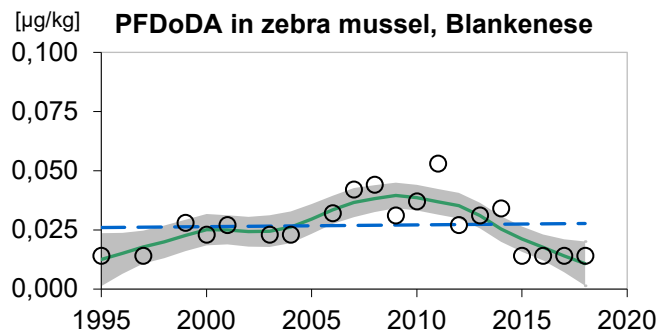
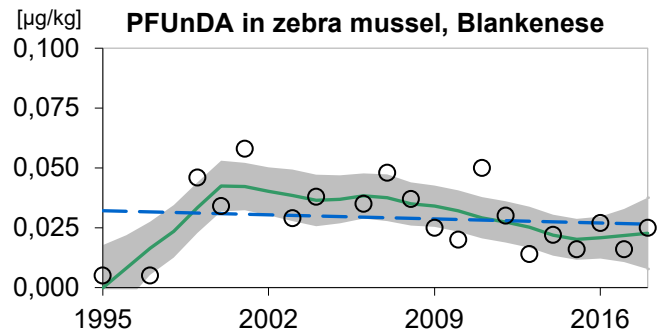
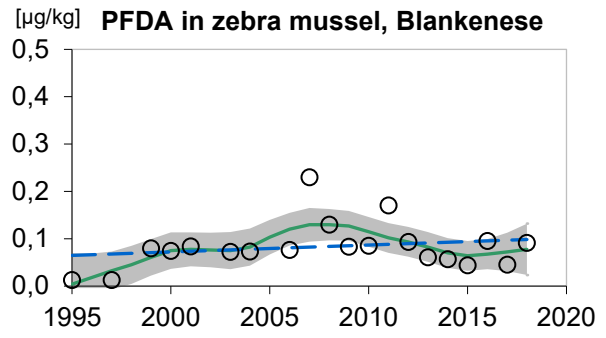
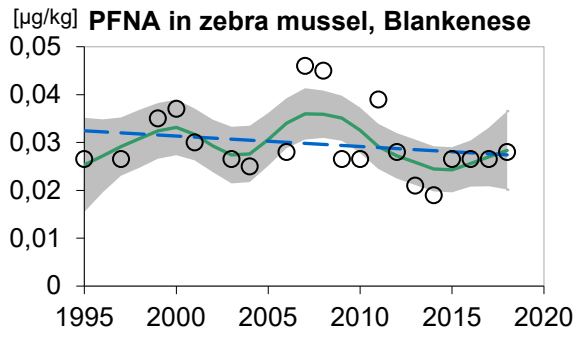


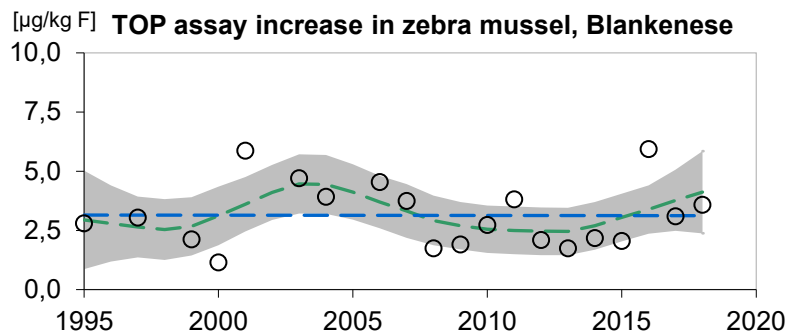
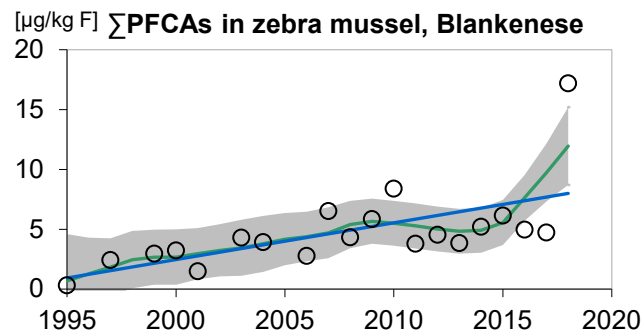
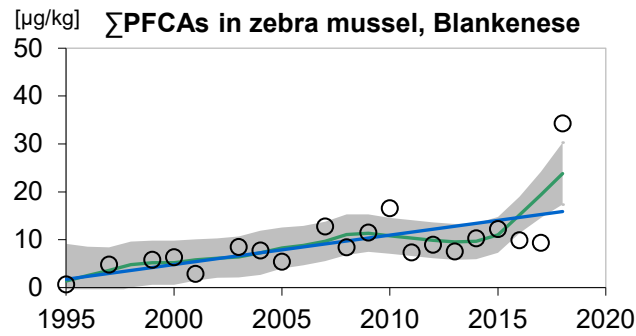
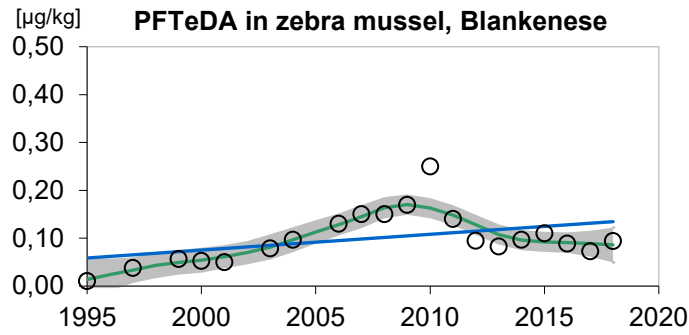


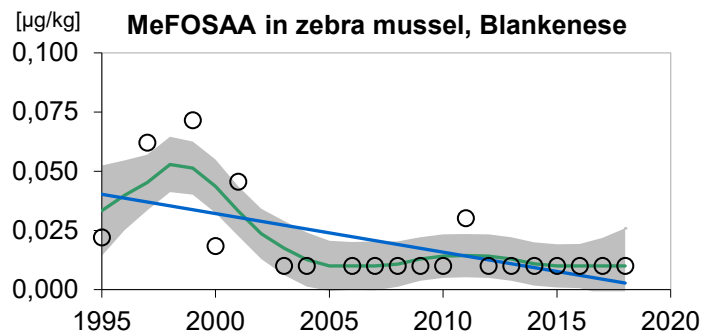
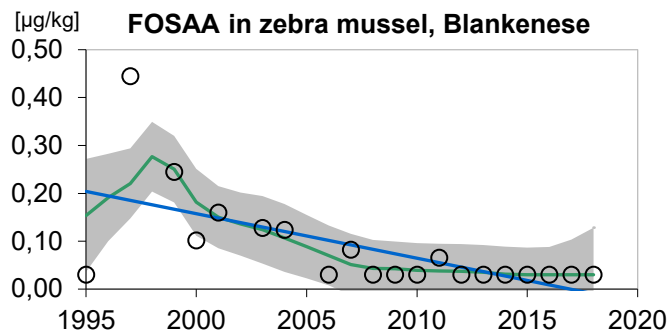
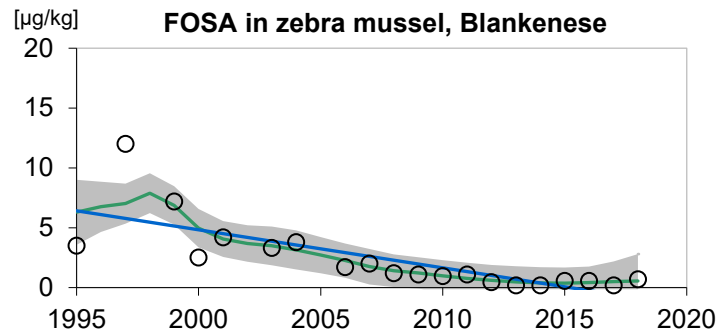
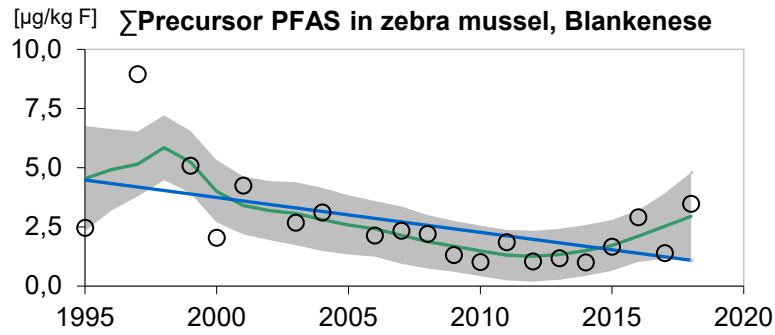


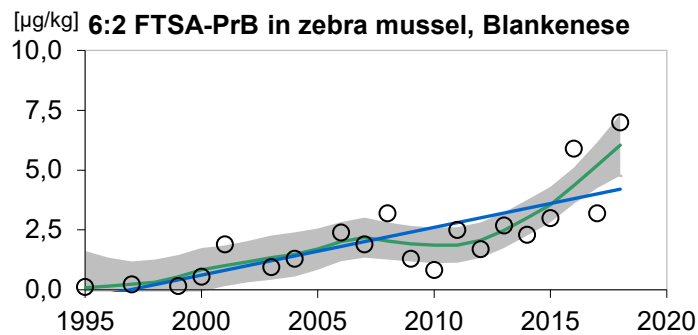
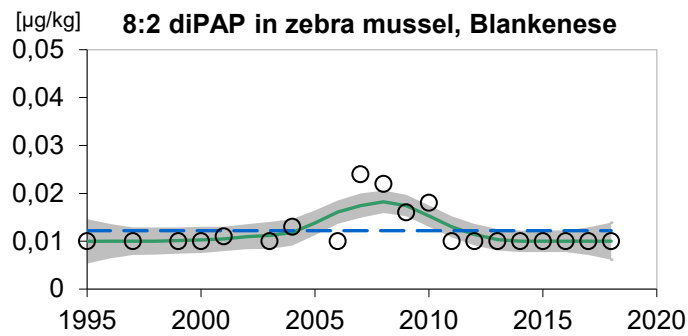
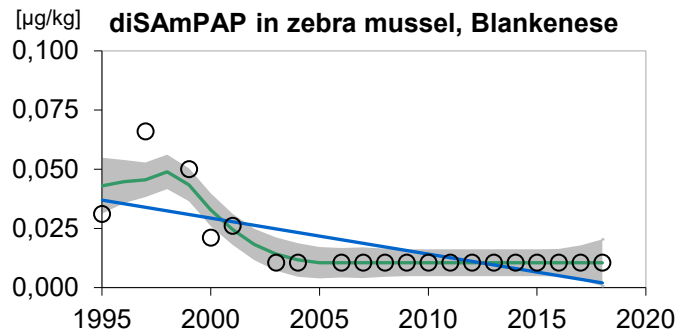
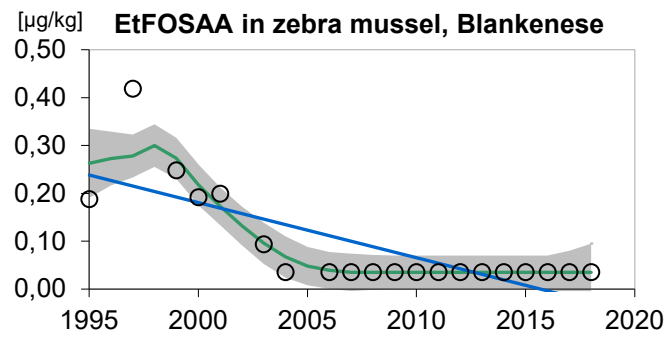


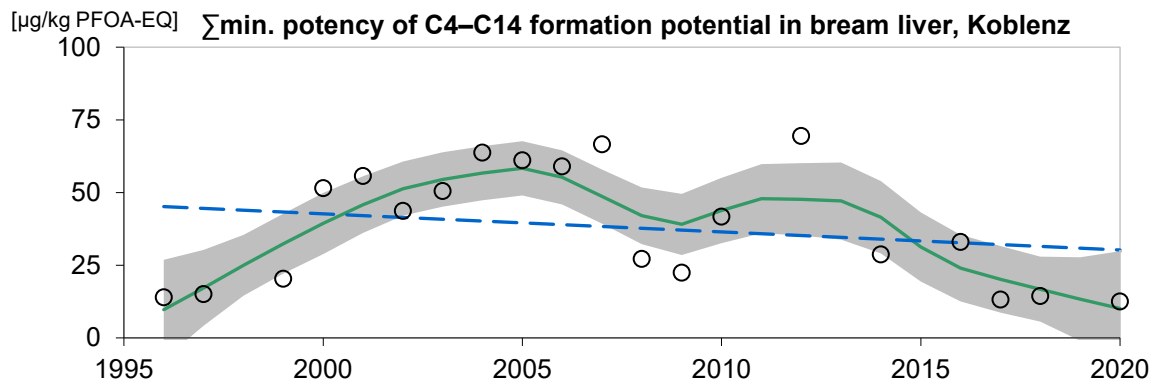
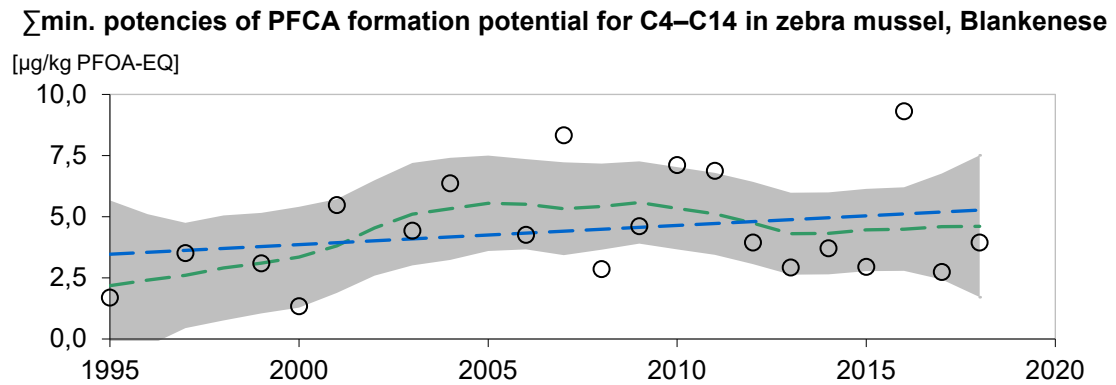
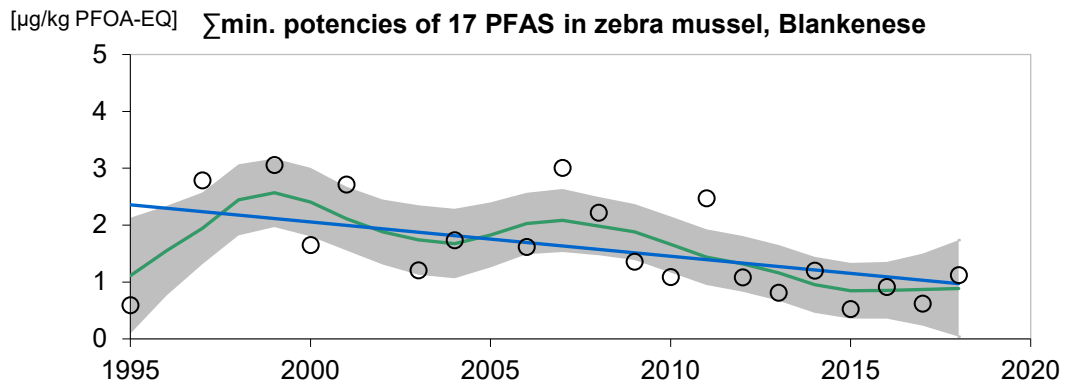
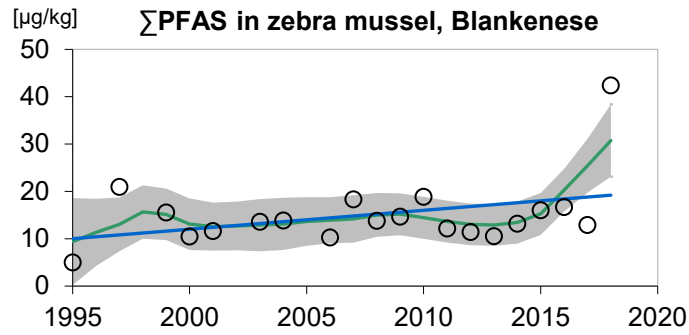












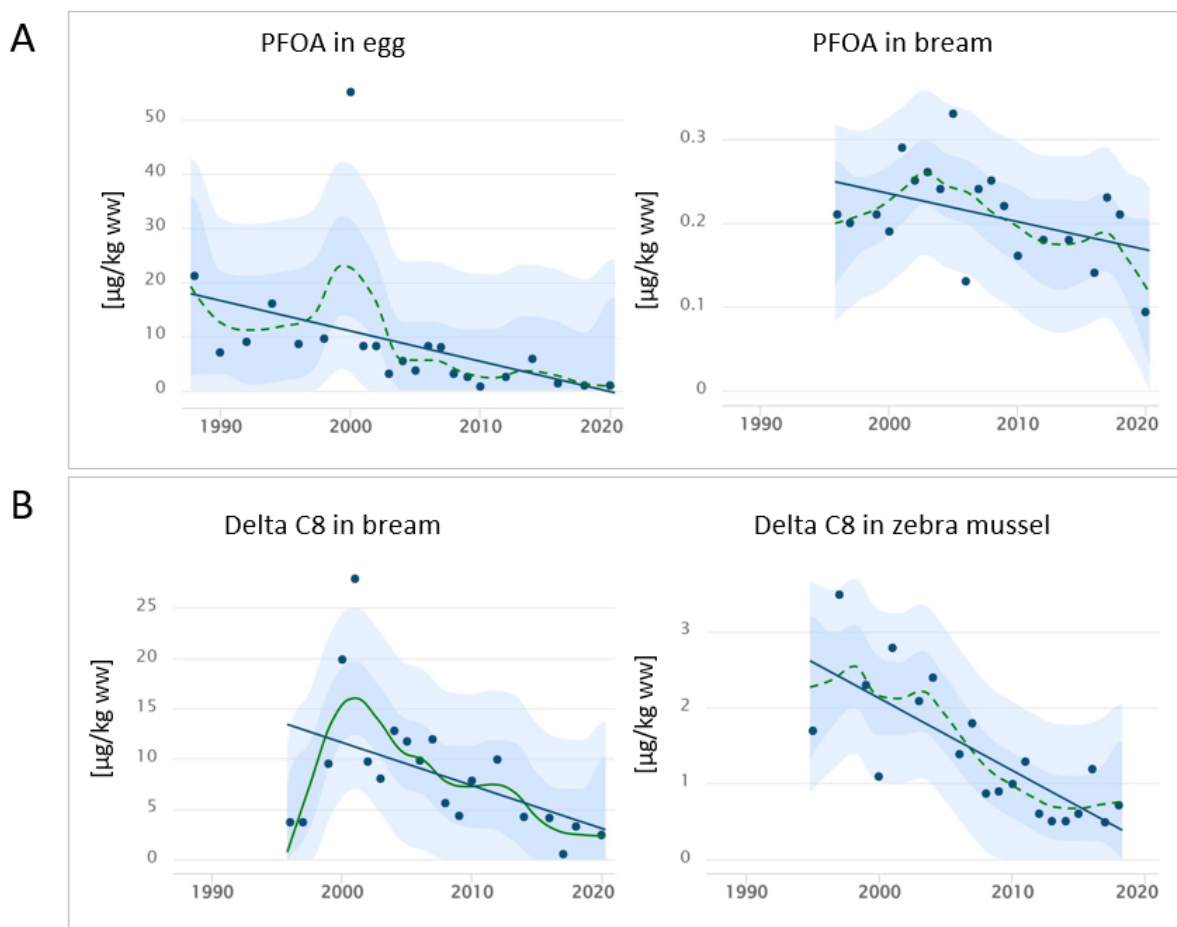
Source: Own illustration, UFZ.

D Additional Information on Work Packages

D.1 Additional information on work package 4

Figure D 1: Temporal trends of (A) PFOA (target analysis) and (B) Delta C8 (TOP assay) in samples from the German Environmental Specimen Bank

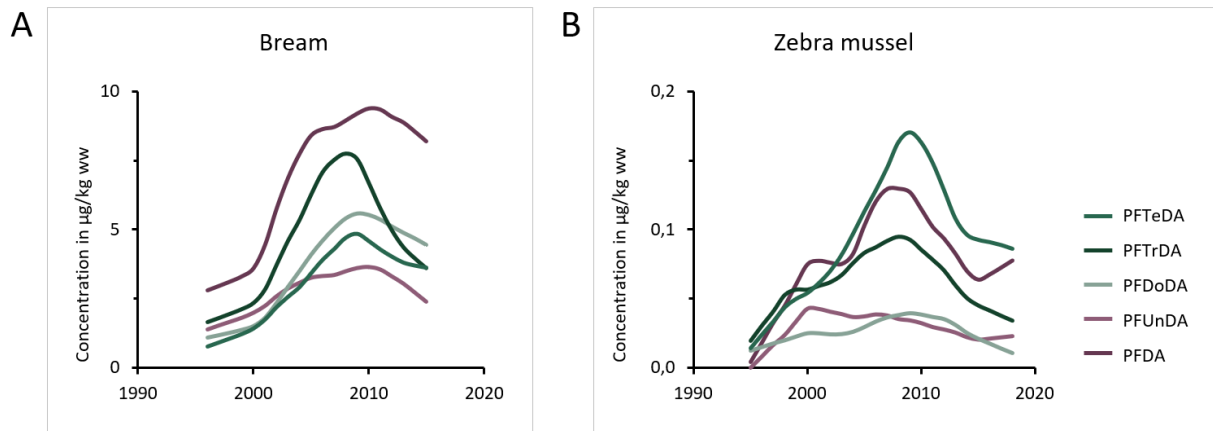
Eggs (n=22; pool size \geq 25 eggs) were from herring gulls in Mellum (North Sea), bream livers (n=19; pool size \geq 20 fish) from Koblenz (Rhine) and zebra mussels (n=19; pool size: 2000–5000 mussels) from Blankenese (Elbe). Solid line: significant linear or non-linear fit; dashed line: not significant; blue line: linear fit; green line: non-linear; shadowed areas: 95 % confidence (dark blue) and 95 % prediction interval (light blue). Note the different scaling of the y-axis.



Source: Own illustration, UFZ.

Figure D 2: Non-linear time trends of C10–C14 perfluoroalkyl carboxylic acids in (A) bream liver from Koblenz and (B) zebra mussel from Blankenese.

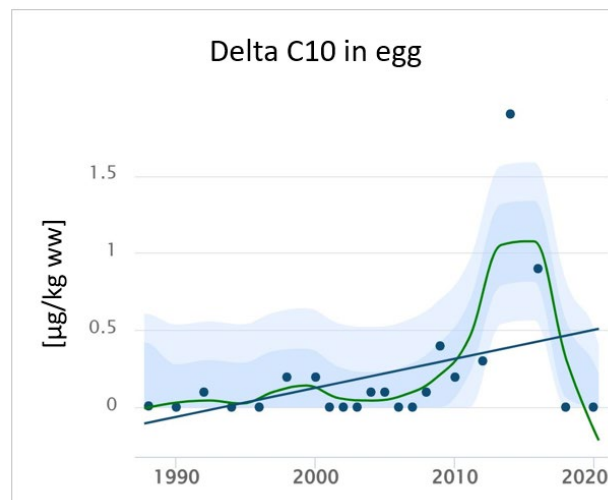
All trends are significant. Note the different scaling of the y-axis.



Source: Own illustration, UFZ.

Figure D 3: Temporal trend of Delta C10 in herring gull egg (n=22; pool size ≥ 25 eggs) from Mellum (North Sea).

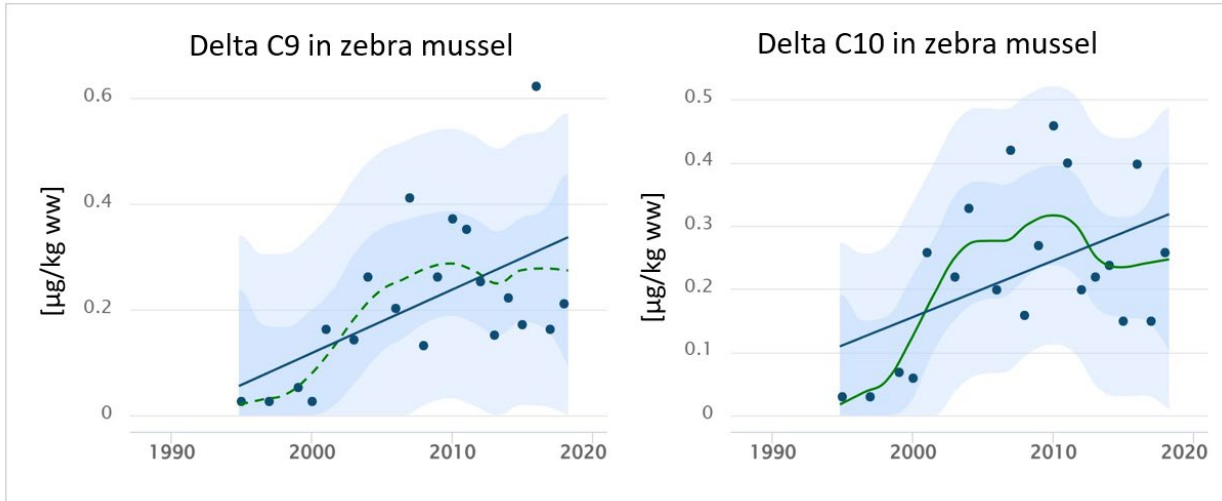
The concentrations indicate the formation potential of PFDA in the TOP assay. Blue line: significant linear fit; green line: significant; shadowed areas: 95 % confidence (dark blue) and 95% prediction interval (light blue). Values < LOQ were set to LOQ/2 ($0.005 \mu\text{g kg}^{-1}$).



Source: Own illustration, UFZ.

Figure D 4: Temporal trends of Delta C9 and C10 in zebra mussels (n=19; pool size: 2000–5000 mussels) from Blankenese (Elbe).

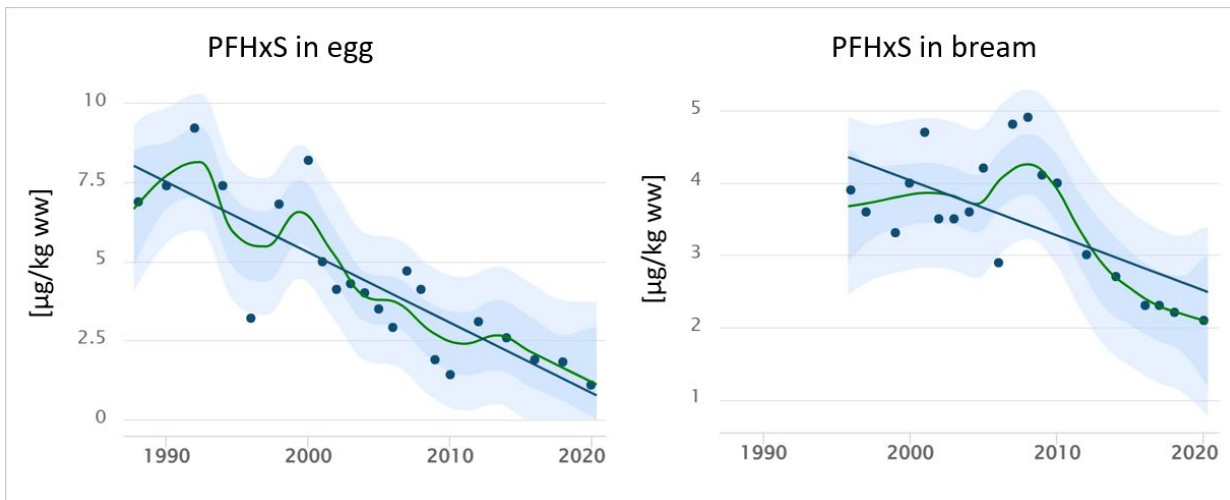
The concentrations indicate the formation potential of PFNA and PFDA in the TOP assay. Blue line: linear fit; green line: non-linear fit; solid line: significant; dashed line: not significant; shadowed areas: 95% confidence (dark blue) and 95 % prediction interval (light blue).



Source: Own illustration, UFZ.

Figure D 5: Temporal trends of PFHxS in herring gull egg from Mellum (North Sea; n=22; pool size ≥25 eggs) and bream liver from Koblenz (Rhine; n=19; pool size ≥20 fish).

Blue line: linear fit; green line: non-linear fit; shadowed areas: 95 % confidence (dark blue) and 95 % prediction interval (light blue). All fits are significant. Note the different scaling of the y-axis.

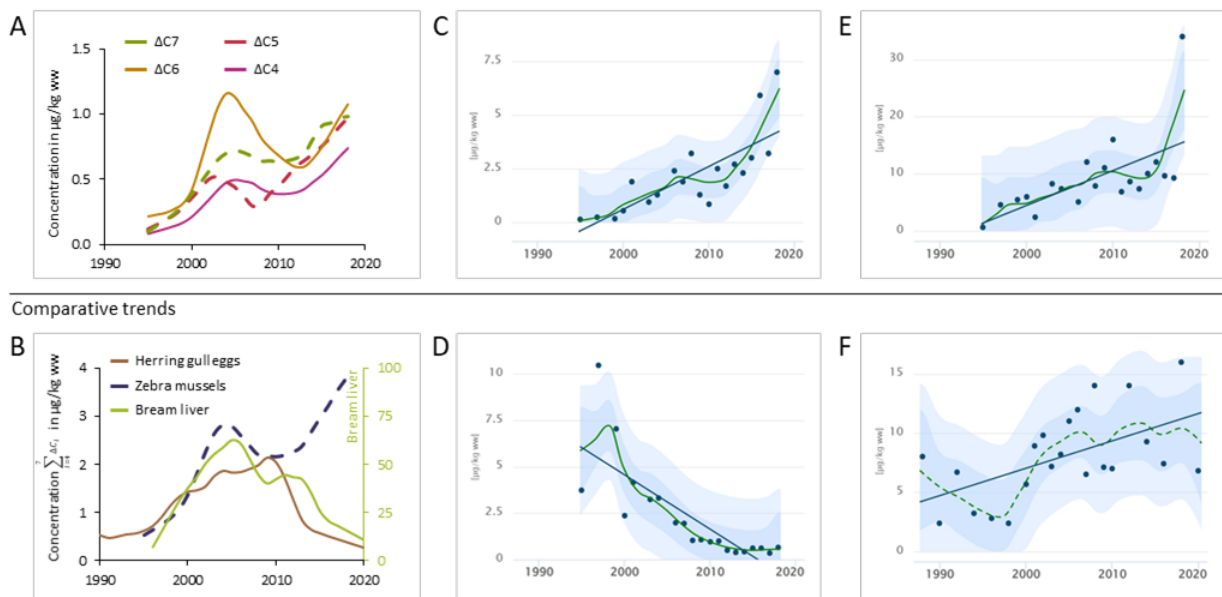


Source: Own illustration, UFZ.

Figure D 6: Temporal trends of (top) (ultra)short-chain PFAS in zebra mussels (n=19; pool size: 50–100 mussels) from Blankenese (Elbe) in comparison to (bottom) related trends in zebra mussels and other biota

(A) the formation potential of short-chain perfluorocarboxylic acids from precursors in the TOP assay ($\Delta C4$ – $\Delta C7$) in zebra mussels as opposed to (B) their sum concentration in zebra mussels, herring gull eggs and bream liver; (C) the precursor 6:2 FTSA–PrB as opposed to (D) FOSA in zebra mussels and, (E) trifluoroacetic acid (TFA) in zebra mussels as opposed to (F) TFA in herring gull eggs. Blue lines: linear curve fit; other colours: non-linear fit; solid line: significant fit; dashed line: not significant; shadowed areas: 95 % confidence (dark blue) and 95% prediction interval (light blue). Note the different scaling of the y-axes.

(Ultra)short-chain PFAS in zebra mussels



Source: Own illustration, UFZ.

D.2 Additional information on chapter 6.3

Table D 1: Mean sum concentrations in $\mu\text{g kg}^{-1}$ in liver samples from different species analysed within this study.

Concentrations refer to wet weight. Values < LOQ were considered as zero for arithmetic mean and standard deviation (SD) calculation. Used abbreviations: chamois liver (RR); red deer liver (CE); roe deer liver (CC); hare liver (LE); beaver liver (CF); nutria liver (MC); common eider duck liver (SM); wild boar liver (SS); wildcat liver (FS); otter liver (LL); cormorant liver (PC); harbour porpoise (PP); grey seal (HG); harbour seal (PV). ¹⁾ target analysis + PFCAs formed in the TOP assay.

		RR	CE	CC	LE	CF	MC	SM	SS [#]	FS	LL	PC	PP	HG	PV
	Number of samles	n=3	n=3	n=10	n=1	n=4	n=4	n=1	n=9	n=9	n=2	n=8	n=2	n=1	n=1
	Individual (I) / Pooled (P)	I	I	P	P	P	I	P	P	I	P	P	P	P	P
Σ PFAS	Detection frequency	3/3	3/3	10/10	1/1	4/4	4/4	1/1	11/11	9/9	2/2	8/8	2/2	1/1	1/1
Σ PFAS	Max	30.1	39.2	53.7	38.3	25.2	26.9	19.3	533.7	55.0	1329.8	647.9	326.0	82.4	214.9
Σ PFAS	Min	19.9	23.5	12.9	38.3	12.9	14.6	19.3	71.3	23.5	1217.8	41.0	245	82.4	214.9
Σ PFAS	Median	20.7	31.8	23.1	38.3	15.0	21.1	19.3	122.3	30.9	1273.8	198.1	286	82.4	214.9
Σ PFAS	Mean	23.6	31.5	21.7*	38.3	17.0	20.9	19.3	121.6*	36.9	1273.8	232.8	285.8	82.4	214.9
Σ PFAS	SD	5.7	7.9	6.3*	-	5.6	5.9	-	28.3*	11.2	79.2	219.8	57	-	-
Σ PFSA	Detection frequency	3/3	3/3	0/10	1/1	4/4	4/4	1/1	11/11	9/9	2/2	8/8	2/2	1/1	1/1
Σ PFSA	Max	1.0	1.2	-	1.9	7.7	9.8	7.3	453.3	12.0	1012.0	640.6	271	55.5	173.7
Σ PFSA	Min	0.6	0.8	-	1.9	4.5	4.0	7.3	46.2	6.2	820.2	29.0	201	55.5	173.7
Σ PFSA	Median	0.9	1.1	-	1.9	5.7	6.3	7.3	89.0	9.4	916.1	185.0	236	55.5	173.7
Σ PFSA	Mean	0.9	1.0	-	1.9	5.9	6.6	7.3	82.3*	9.4	916.1	219.3	235.7	55.5	173.7
Σ PFSA	SD	0.2	0.2	-	-	1.4	2.5	-	29.3*	1.5	135.6	220.5	49	-	-

TEXTE How rapidly do per- and polyfluoroalkyl substances (PFAS) accumulate in different environmental compartments? – Monitoring of Samples from the German Environmental Specimen Bank

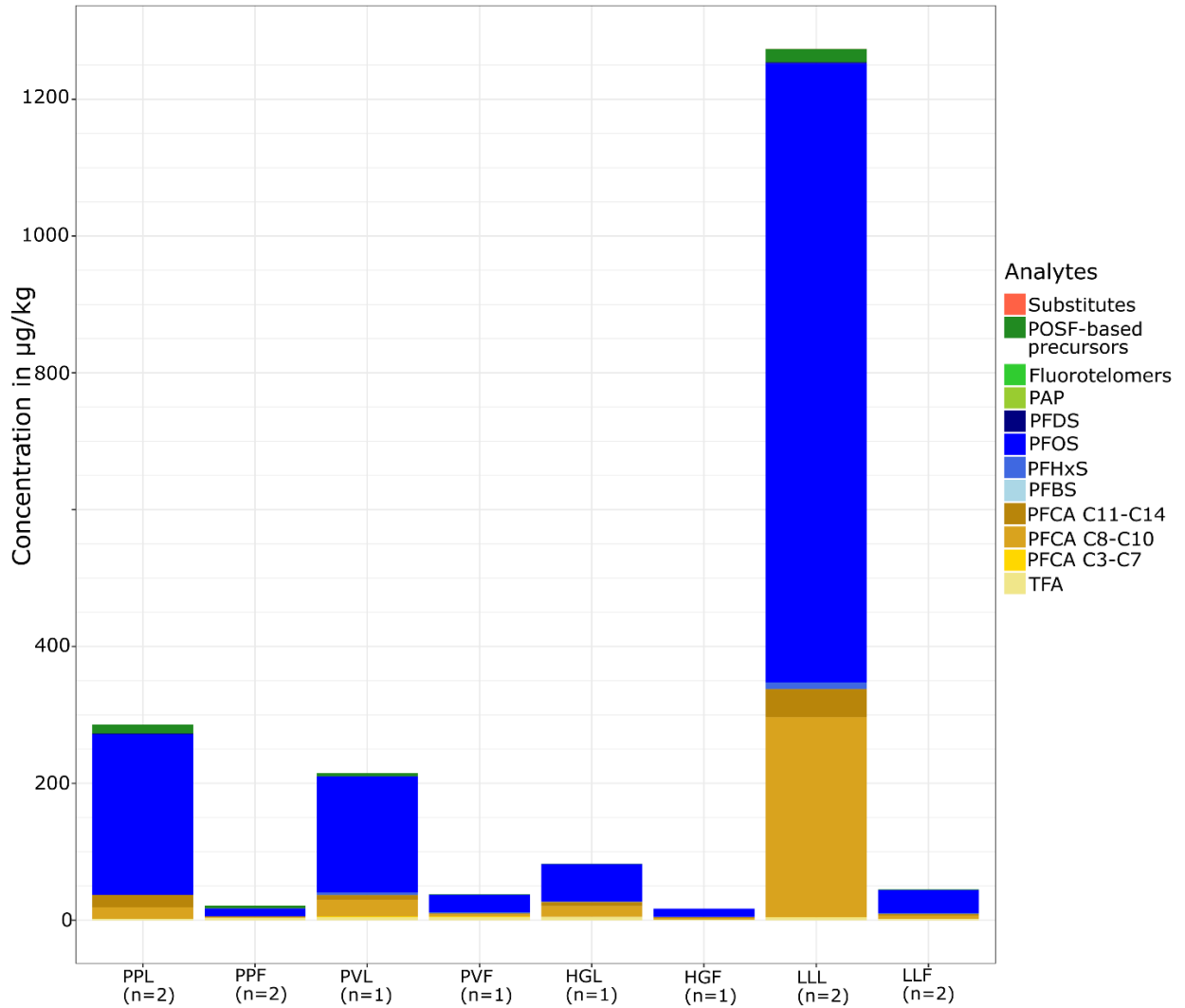
		RR	CE	CC	LE	CF	MC	SM	SS [#]	FS	LL	PC	PP	HG	PV
ΣPolyfluorinated compounds	Detection frequency	2/3	1/3	0/10	1/1	4/4	4/4	0/1	11/11	7/9	2/2	8/8	2/2	1/1	1/1
ΣPolyfluorinated compounds	Max	-	-	-	-	0.8	1.1	0.3	6.2	0.1	24.5	2.0	14	0.3	4.6
ΣPolyfluorinated compounds	Min	-	-	-	-	0.4	0.1	0.3	0.3	-	15.2	0.4	12	0.3	4.6
ΣPolyfluorinated compounds	Median	-	-	-	-	0.5	0.3	0.3	1.3	-	19.8	1.1	13	0.3	4.6
ΣPolyfluorinated compounds	Mean	-	-	-	-	0.6	0.4	0.3	1.3*	-	19.8	1.1	13.1	0.3	4.6
ΣPolyfluorinated compounds	SD	-	-	-	-	0.1	0.4	-	1.0*	-	6.5	0.6	2	-	-
ΣSubstitute compounds	Detection frequency	0/3	0/3	0/10	0/1	0/4	0/4	0/1	6/11	0/9	2/2	1/8	0/2	0/1	0/1
ΣSubstitute compounds	Max	-	-	-	-	-	-	-	0.035	-	0.120	0.020	-	-	-
ΣSubstitute compounds	Min	-	-	-	-	-	-	-	-	-	0.110	-	-	-	-
ΣSubstitute compounds	Median	-	-	-	-	-	-	-	0.016	-	0.115	-	-	-	-
ΣSubstitute compounds	Mean	-	-	-	-	-	-	-	0.012	-	0.115	0.003	-	-	-
ΣSubstitute compounds	SD	-	-	-	-	-	-	-	0.035	-	0.120	0.020	-	-	-
ΣPFCA	Detection frequency	3/3	3/3	10/10	1/1	4/4	4/4	1/1	11/11	9/9	2/2	8/8	2/2	1/1	1/1

TEXTE How rapidly do per- and polyfluoroalkyl substances (PFAS) accumulate in different environmental compartments? – Monitoring of Samples from the German Environmental Specimen Bank

		RR	CE	CC	LE	CF	MC	SM	SS [#]	FS	LL	PC	PP	HG	PV
ΣPFCA	Max	29.5	38.5	53.7	36.4	20.2	21.1	11.7	77.8	45.9	373.0	24.1	44	26.7	36.6
ΣPFCA	Min	18.9	22.3	12.9	36.4	5.7	10.0	11.7	23.7	13.4	302.5	6.3	30	26.7	36.6
ΣPFCA	Median	19.7	30.7	23.1	36.4	8.3	12.2	11.7	37.2	21.7	337.8	11.8	37	26.7	36.6
ΣPFCA	Mean	22.7	30.5	21.7*	36.4	10.6	13.9	11.7	40.1	27.4	337.8	12.3	37.0	26.7	36.6
ΣPFCA	SD	5.9	8.1	6.3*	-	6.7	5.1	-	15.5	11.3	49.8	5.4	9	-	-
ΣPFCA after TOP assay ¹⁾	Detection frequency	3/3	3/3	10/10	1/1	4/4	4/4	1/1	11/11	9/9	2/2	8/8	2/2	1/1	1/1
ΣPFCA after TOP assay ¹⁾	Max	38.4	49.6	53.7	36.4	52.3	21.1	11.7	120.5	46.0	386.4	73.6	55.7	47.6	38.2
ΣPFCA after TOP assay ¹⁾	Min	18.9	22.3	12.9	36.4	6.1	11.4	11.7	38.1	13.6	308.1	11.7	36.4	47.6	38.2
ΣPFCA after TOP assay ¹⁾	Median	28.6	42.5	23.1	36.4	9.9	14.0	11.7	48.1	21.7	347.3	15.8	46.0	47.6	38.2
ΣPFCA after TOP assay ¹⁾	Mean	28.7	38.1	21.7**	36.4	11.5**	15.1	11.7	48.8**	27.7	347.3	17.3**	46.0	47.6	38.20
ΣPFCA after TOP assay ¹⁾	SD	9.7	14.2	6.3*	-	6.1*	4.2	-	10.9*	11.3	55.4	9.5**	13.6	-	-

Figure D 7: Total PFAS concentrations in liver (L) and musculature (F) tissue in grey seal (HG), harbour seal (PV), harbour porpoise (PP), cormorant (PC) and otter (LL)

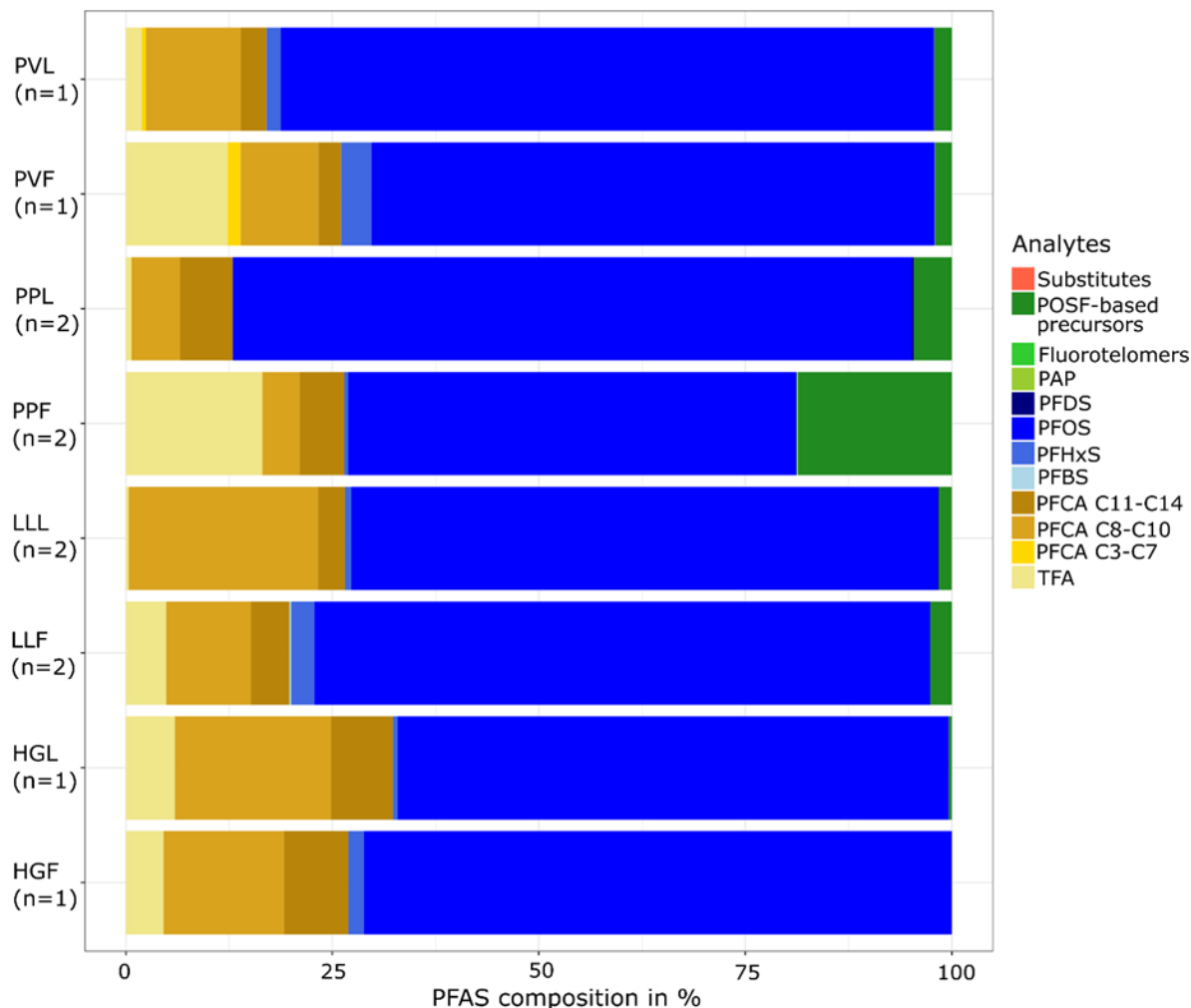
n represents the number of samples analysed. The samples are pooled and consist of 5 individuals. Only data from target analysis is represented. Abbreviations to be read as species plus organ.



Source: Own illustration, TZW.

Figure D 8: Differences in the PFAS composition between liver (L) and musculature (F) tissue in grey seal (HG), harbour seal (PV), harbour porpoise (PP), cormorant (PC) and otter (LL).

n represents the number of samples analysed. The samples are pooled and consist of 5 individuals. Only data from target analysis is represented. Abbreviations to be read as species plus organ.



Source: own illustration, TZW.

Table D 2: Mean sum concentrations in $\mu\text{g kg}^{-1}$ in pooled samples of musculature tissue from selected species analysed within this study.

Concentrations refer to wet weight. Values < LOQ were considered as zero for arithmetic mean calculation.

¹⁾ target analysis + PFCAs formed in the TOP assay.

PFAS group	parameter	Otter	Harbour porpoise	Harbour seal	Grey seal
	Number of samples	n=2	n=2	n=1	n=1
Σ PFAS	Detection frequency	2/2	2/2	2/2	2/2
Σ PFAS	Max	54.8	21.9	38.1	16.7
Σ PFAS	Min	35.0	20.5	38.1	16.7

PFAS group	parameter	Otter	Harbour porpoise	Harbour seal	Grey seal
∑PFAS	Mean	44.9	21.2	38.1	16.7
∑PFSA	Detection frequency	2/2	2/2	2/2	2/2
∑PFSA	Max	41.4	12.0	27.4	12.3
∑PFSA	Min	28.3	11.2	27.4	12.3
∑PFSA	Mean	34.8	11.6	27.4	12.3
∑Polyfluorinated compounds	Detection frequency	2/2	2/2	2/2	0/0
∑Polyfluorinated compounds	Max	1.5	5.0	0.8	-
∑Polyfluorinated compounds	Min	0.8	4.0	0.8	-
∑Polyfluorinated compounds	Mean	1.2	4	0.8	-
∑Substitute compounds	Detection frequency	0/0	0/0	0/0	0/0
∑Substitute compounds	Max	-	-	-	-
∑Substitute compounds	Min	-	-	-	-
∑Substitute compounds	Mean	-	-	-	-
∑PFCA target analysis	Detection frequency	2/2	2/2	2/2	2/2
∑PFCA target analysis	Max	12.0	5.7	9.9	4.6
∑PFCA target analysis	Min	5.6	5.5	9.9	4.6
∑PFCA target analysis	Mean	8.9	5.6	9.9	4.6
∑PFCA after TOP assay ¹⁾	Detection frequency	2/2	2/2	2/2	2/2
∑PFCA after TOP assay ¹⁾	Max	19.6	21.0	11.8	6.4
∑PFCA after TOP assay ¹⁾	Min	7.2	16.9	11.8	6.4
∑PFCA after TOP assay ¹⁾	Mean	13.4	18.9	11.8	6.4

D.3 Additional information on chapter 6.4

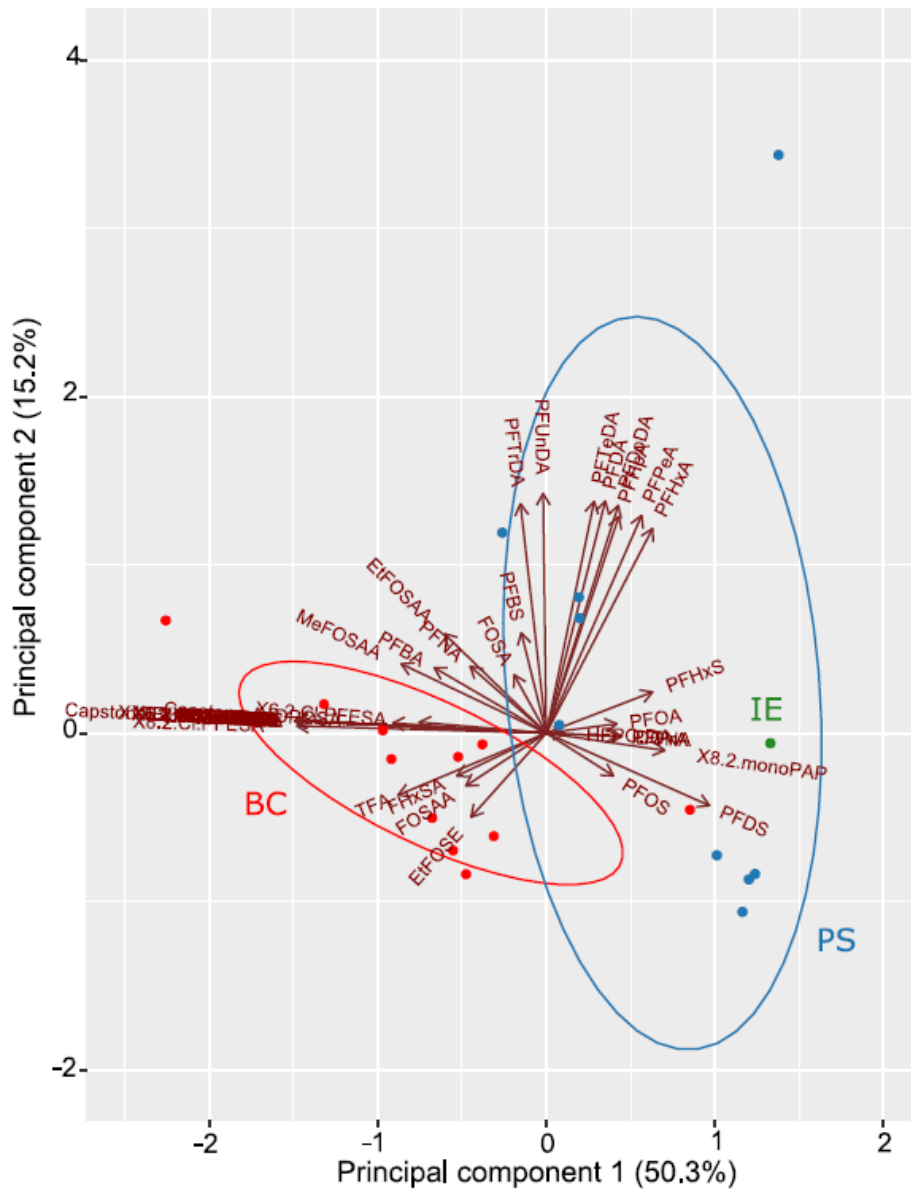
Table D 3: p-values after testing for significant differences between the wild boar livers from areas “background contamination” (BC, n=11) and “paper sludges” (PS, n=9).

Tests for significant differences of individual analytes were only conducted when all concentrations were >LOQ. p-values <0.05 indicate significant differences between the two groups investigated. They are indicated in bold. The samples were collected in Germany in 2019 and 2020.

Single Analyte	<i>p-value</i>
PFBS	0.0029
PFHxS	0.0076
PFOS	0.0052
TFA	0.0059
PFHpA	0.0015
PFOA	0.3612
PFNA	0.2431
PFDA	1.69E-07
PFUnDA	4.11E-07
PFDoDA	0.0001
PFTTrDA	2.50E-06
PFTeDA	6.79E-06
6:2 FTSA	0.0038
8:2 FTSA	1.49E-05
Grouped Analytes	
ΣPFAS	0.0027
ΣPFASs	0.0052
ΣPFCA _s	0.1071
ΣPFCA C2–C7	0.0383
ΣPFCA C8–C14	3.34E-05
ΣPolyfluorinated compounds	0.7493
ΣIncrease organic fluorine by TOP assay	0.3364
ΣPFASs in %	0.0033
ΣPFCA _s in %	0.39

Figure D 9: Scores along principle components (PC) 1 and 2 from the principle component analysis (PCA) of PFAS in wild boar liver from the paper sludge (PS, n=9), industrial emission (IE, n=1) and background contamination (BC, n=11) sites in Germany (collected in 2019 and 2020).

To display the PFAS pattern, the raw data was transformed to molar masses and later normalized. The loadings show individual analytes, dots indicate individual scores. PC 1 and 2 combined explain 65.5% of the total variance inherent in the data. A different pattern between wild boars from sites with background contamination towards sites with contamination due to agricultural practice or industrial emissions can be observed. Wild boars from contaminated sites are determined by long-chained PFCA and PFOS, whereas wild boars with background contamination are characterized by short chained PFCA and certain precursors such as EtFOSE.



Source: Own Illustration, TZW.

Table D 4: Organofluorine concentrations of PFCAs C2–C14 upon target analysis and TOP assay and the significance of their difference for wild boar liver from areas “background contamination” (BC, n=11) and “paper sludges” (PS, n=9), respectively.

Mean and standard deviation (sd) of the results from one method (“target analysis”) and both methods in combination (“after TOP assay”) are given as well as the p-value from significance testing. Tests for significant differences of individual analytes were only conducted when all concentrations were >LOQ. p values <0.05 indicate significant differences between the PFCA concentrations from target analysis and after TOP assay analysis. They are indicated in bold. The samples were collected in Germany in 2019 and 2020.

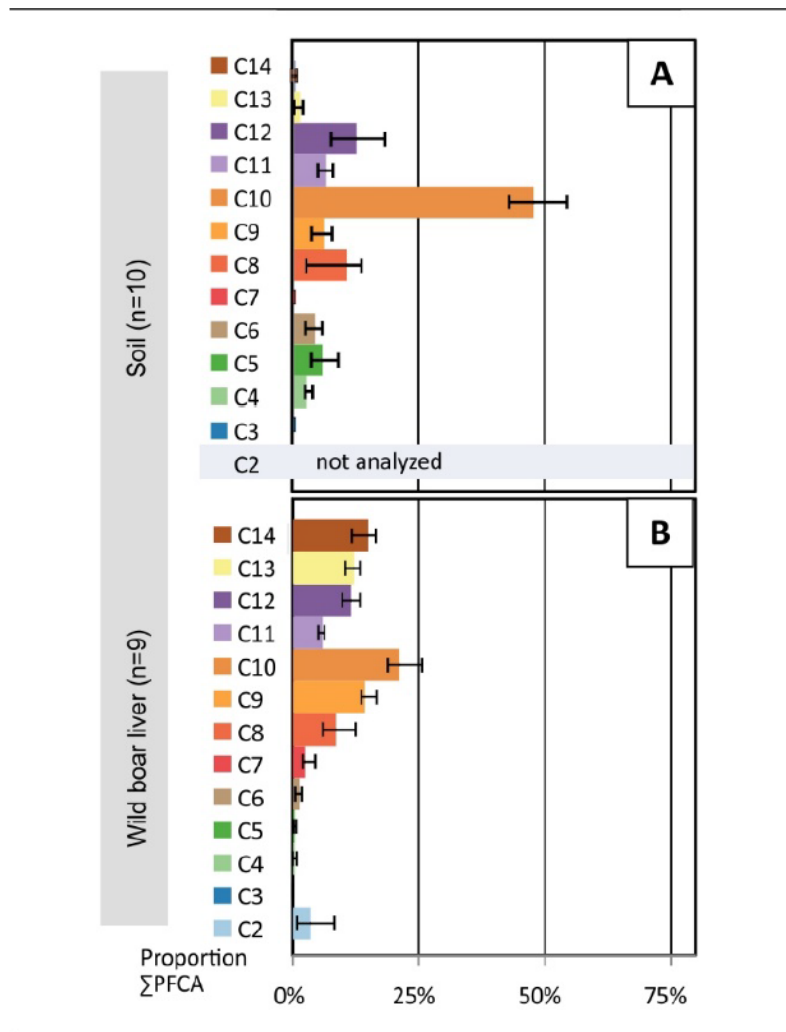
PFCA	BC (n=11)					PS (n=9)				
	OF detected as PFCAs in target analysis		OF detected as PFCAs after TOP assay (target analysis + TOP assay)		p value between target analysis and after TOP assay	OF detected as PFCAs in target analysis		OF detected as PFCAs after TOP assay (target analysis + TOP assay)		p value between target analysis and after TOP assay
	mean	sd	mean	sd	p	mean	sd	mean	sd	p
TFA	5.64	4.18	11.44	4.34	0.0014	1.17	1.02	6.85	2.01	0.0051
PFPrA	-	-	-	-	-	-	-	-	-	-
PFBA	0.11	0.09	0.11	0.09	1.0000	0.15	0.13	0.13	0.13	0.9808
PFPeA	-	-	-	-	-	0.12	0.07	0.31	0.20	0.0035
PFHxA	-	-	-	-	-	0.35	0.28	0.89	0.43	0.0004
PFHpA	0.28	0.15	0.28	0.15	0.9999	0.91	0.50	1.57	0.60	0.0083
PFOA	2.56	1.91	2.56	1.91	1.0000	3.46	2.28	3.88	2.26	0.9769
PFNA	7.35	4.85	7.35	4.85	1.0000	5.22	1.17	5.57	1.23	0.9978
PFDA	2.70	0.65	2.73	0.65	0.9999	7.66	1.65	7.66	1.65	1.0000
PFUnDA	0.84	0.21	0.87	0.23	0.9987	2.11	0.43	2.32	0.70	0.7450
PFDoDA	0.94	0.34	1.01	0.33	0.9987	4.06	1.24	5.11	1.85	0.2201
PFTTrDA	2.09	0.70	2.37	0.78	0.8654	4.50	0.73	5.31	1.00	0.2008
PFTeDA	1.42	0.59	1.45	0.61	0.9999	5.46	1.85	5.50	1.85	0.9999

TEXTE How rapidly do per- and polyfluoroalkyl substances (PFAS) accumulate in different environmental compartments? – Monitoring of Samples from the German Environmental Specimen Bank

PFCA	BC (n=11)					PS (n=9)				
	OF detected as PFCAs in target analysis		OF detected as PFCAs after TOP assay (target analysis + TOP assay)		<i>p</i> value between target analysis and after TOP assay	OF detected as PFCAs in target analysis		OF detected as PFCAs after TOP assay (target analysis + TOP assay)		<i>p</i> value between target analysis and after TOP assay
	mean	sd	mean	sd	<i>p</i>	mean	sd	mean	sd	<i>p</i>
ΣPFCA	23.91	5.80	30.17	3.84	0.3375	35.16	6.73	45.10	8.90	0.0225

Figure D 10: Median PFCA pattern in soil (A, n=10) and wild boar liver (B, n=9) from area paper sludges (PS) in Germany.

Soil data is obtained from (Kotthoff et al. 2020).



Source: Own Illustration, TZW.

Table D 5: Sample overview for the areas PS, IE and BC.

Samples are allocated to their source of contamination and reference sample pool and hypothesis.

Sample type	Source of contamination	Sample pooled?	n (after pooling)	N (before pooling)
Wild boar liver	Paper sludges (PS)	No	9	9
Wild boar liver	Industrial emissions (IE)	No	1	1
Wild boar liver	Background contamination (BC)	Yes	11	40
Wild boar liver	Reference	No	1	1
Soil	Industrial emissions (IE)	Yes	1	24
Soil	Reference	Yes	10	160
Suspended matter	Industrial emissions (IE)	No	1	For 130 days collected in sedimentation trap
Suspended matter	Reference	No	6	12 monthly samples each, collected in sedimentation traps
European chub filet	Industrial emissions (IE)	Yes	1	10
European chub filet	Reference	Yes	2	16

Table D 6: Detailed information on individual sample materials and allocated source of contamination.

	Sample (Spec.)	Source of contamination	Sampling area (Federal state)	Sampling time	Individual/Pool sample (I/P)	Number of subsamples	Sex (m/f)	Age class	Weight [kg]	Origin
001	European chub filet (<i>Squalius cephalus</i>)	IE	Area IE	2016	P	10	f/m	adult	0.95	NA
002	European chub filet (<i>Squalius cephalus</i>)	Reference	German river A	2016	P	6	f/m	adult	0.82	NA
003	European chub filet (<i>Squalius cephalus</i>)	Reference	German river B	2018	P	10	f/m	adult	0.79	NA
004	Wild boar liver (<i>Sus scrofa</i>)	IE	Area IE	2020	I	NA	f/m	juvenile	27*	NA
005	Wild boar liver (<i>Sus scrofa</i>)	BC/Ref.	Area BC	2019	P	5	m	young	NA	BfR
006	Wild boar liver (<i>Sus scrofa</i>)	BC/Ref.	Area BC	2019	P	5	f	young	NA	BfR
007	Wild boar liver (<i>Sus scrofa</i>)	BC/Ref.	Area BC	2019	P	5	m	juvenile	NA	BfR
008	Wild boar liver (<i>Sus scrofa</i>)	BC/Ref.	Area BC	2019	P	5	f	juvenile	NA	BfR
009	Wild boar liver (<i>Sus scrofa</i>)	BC/Ref.	Area BC	2019	P	3	m	adult	NA	BfR
010	Wild boar liver (<i>Sus scrofa</i>)	BC/Ref.	Area BC	2019	P	4	f	adult	NA	BfR
011	Wild boar liver (<i>Sus scrofa</i>)	BC/Ref.	Area BC	2019	P	5	m	young	NA	BfR
012	Wild boar liver (<i>Sus scrofa</i>)	BC/Ref.	Area BC	2019	P	5	f	young	NA	BfR

	Sample (Spec.)	Source of contamination	Sampling area (Federal state)	Sampling time	Individual/Pool sample (I/P)	Number of subsamples	Sex (m/f)	Age class	Weight [kg]	Origin
013	Wild boar liver (<i>Sus scrofa</i>)	BC/Ref.	Area BC	2019	P	5	m	juvenile	NA	BfR
014	Wild boar liver (<i>Sus scrofa</i>)	BC/Ref.	Area BC	2019	P	5	f	juvenile	NA	BfR
015	Wild boar liver (<i>Sus scrofa</i>)	BC/Ref.	Area BC	2019	P	3	m	adult	NA	BfR
016	Wild boar liver (<i>Sus scrofa</i>)	PS	Hügelsheim (Nord), BW	2020	I	NA	f	young	19*	District office Rastatt
017	Wild boar liver (<i>Sus scrofa</i>)	PS	Hügelsheim (Nord), BW	2020	I	NA	f	young	17*	District office Rastatt
018	Wild boar liver (<i>Sus scrofa</i>)	PS	Hügelsheim (Nord), BW	2020	I	NA	f	young	22*	District office Rastatt
019	Wild boar liver (<i>Sus scrofa</i>)	PS	Hügelsheim (Nord), BW	2020	I	NA	m	juvenile	44*	District office Rastatt
020	Wild boar liver (<i>Sus scrofa</i>)	PS	Hügelsheim (Nord), BW	2020	I	NA	m	juvenile	41	District office Rastatt
021	Wild boar liver (<i>Sus scrofa</i>)	PS	Hügelsheim (Nord), BW	2020	I	NA	f	adult	48*	District office Rastatt
022	Wild boar liver (<i>Sus scrofa</i>)	PS	Hügelsheim (Nord), BW	2020	I	NA	m	adult	58*	District office Rastatt
023	Wild boar liver (<i>Sus scrofa</i>)	PS	Hügelsheim (Nord), BW	2020	I	NA	m	adult	46*	District office Rastatt
024	Wild boar liver (<i>Sus scrofa</i>)	PS	Hügelsheim (Nord), BW	2020	I	NA	m	adult	49*	District office Rastatt
025	Soil (18.3% water)	IE	Area IE	2019	P	>10	NA	NA	NA	NA

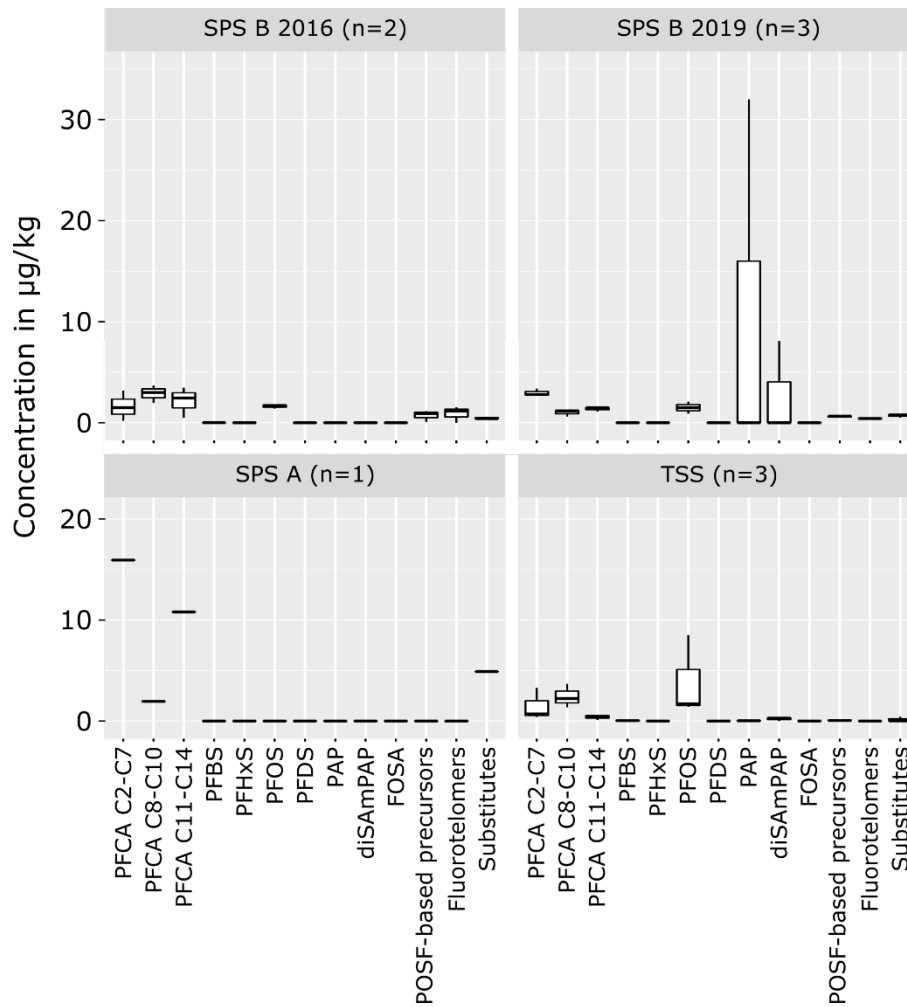
	Sample (Spec.)	Source of contamination	Sampling area (Federal state)	Sampling time	Individual/Pool sample (I/P)	Number of subsamples	Sex (m/f)	Age class	Weight [kg]	Origin
026	Soil	Reference	Warndt, SL	2018	P	16	NA	NA	NA	German ESB
027	Soil	Reference	Leipzig, Rosental, SA	2018	P	16	NA	NA	NA	German ESB
028	Soil	Reference	Bavarian Forest, VY	2018	P	16	NA	NA	NA	German ESB
029	Soil	Reference	National park Berchtesgaden, BY	2018	P	16	NA	NA	NA	German ESB
030	Soil	Reference	Bornhoeveder lake district, SH	2019	P	16	NA	NA	NA	German ESB
031	Soil	Reference	Duebener Heide, SAA	2018	P	16	NA	NA	NA	German ESB
032	Soil	Reference	Staadten, SL	2018	P	16	NA	NA	NA	German ESB
033	Soil	Reference	Solling, LS	2019	P	16	NA	NA	NA	German ESB
034	Soil	Reference	Palatinate Forest, RP	2019	P	16	NA	NA	NA	German ESB
035	Soil	Reference	Großpalmberg/Scheyern, BY	2019	P	16	NA	NA	NA	German ESB
036	Suspended matter	IE	Area IE	2019	I	NA	NA	NA	NA	NA
037	Suspended matter	Reference	River Danube (Jochenstein), BY	2019	P	12	NA	NA	NA	German ESB
038	Suspended matter	Reference	River Elbe (Cumlosen), BB	2019	P	12	NA	NA	NA	German ESB
039	Suspended matter	Reference	River Saale (Wettin), SAA	2019	P	12	NA	NA	NA	German ESB
040	Suspended matter	Reference	River Rhine (Weil), BW	2019	P	12	NA	NA	NA	German ESB
041	Suspended matter	Reference	River Rhine (Koblenz), RP	2019	P	12	NA	NA	NA	German ESB

	Sample (Spec.)	Source of contamination	Sampling area (Federal state)	Sampling time	Individual/Pool sample (I/P)	Number of subsamples	Sex (m/f)	Age class	Weight [kg]	Origin
042	Suspended matter	Reference	River Rhine (Bimmen), NW	2018	P	12	NA	NA	NA	German ESB

D.4 Additional information on chapter 6

Figure D 11: PFAS profiles of abiotic materials

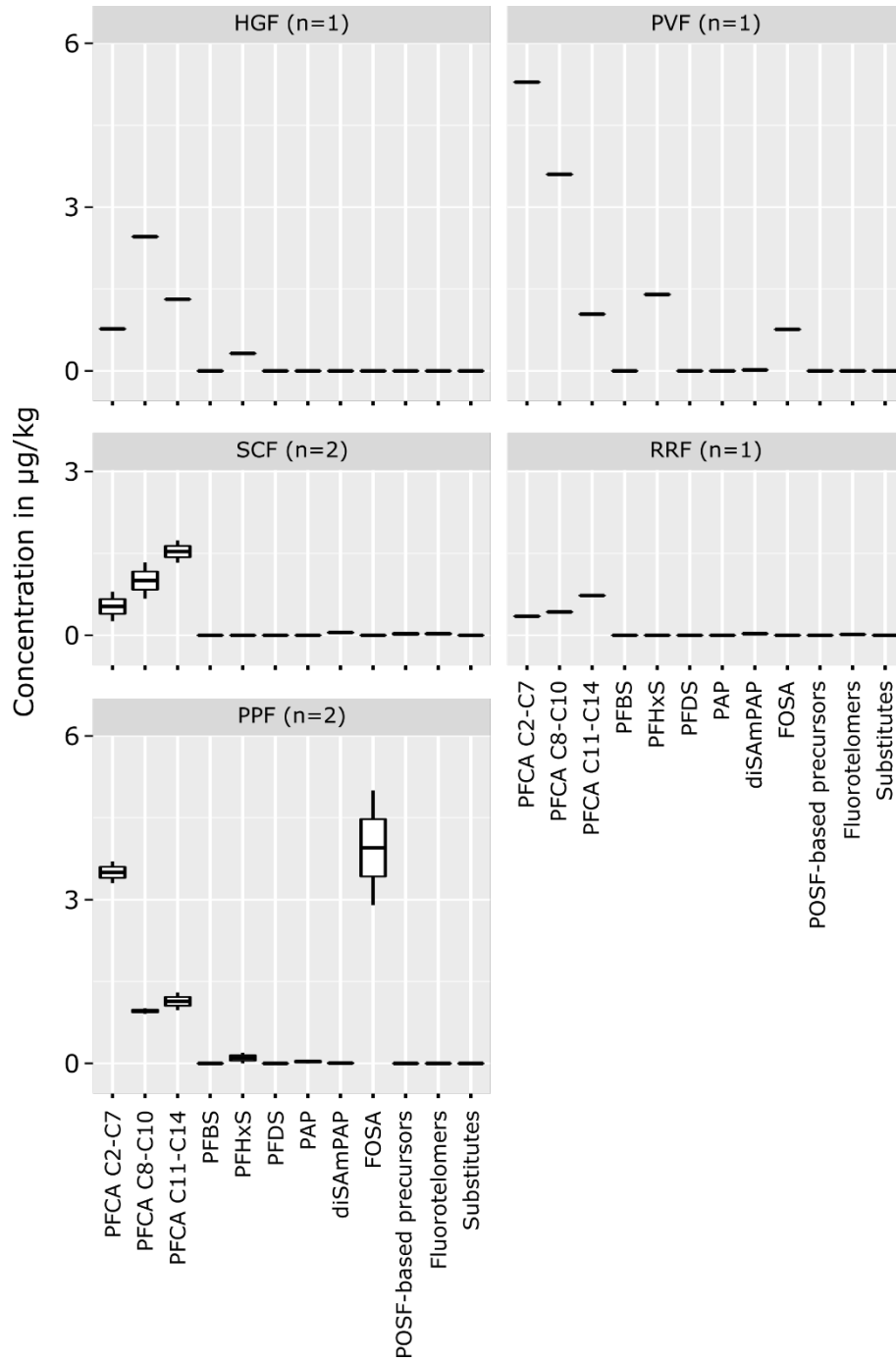
Riverine suspended matter (SPS) and top soil (TSS). Boxplots show median, first and third quartile; whiskers show range. Concentration levels of single samples are shown as a line.



Source: Own illustration, UFZ.

Figure D 12: PFAS profiles of aquatic samples – Filets

Used abbreviations: emerald rockcod filet (TBF); European chub filet (SCF); roach filet (RRF); harbour porpoise filet (PPF); grey seal filet (HGF); harbour seal filet (PVF). Boxplots show median, first and third quartile; whiskers show range. Concentration levels of single samples are shown as a horizontal line.



Source: Own illustration, UFZ.

D.5 Samples of the study “Wild Boars Livers as Bioindicators for the Terrestrial Environment”

In area IE, top soil (0–15 cm, n = 1 after pooling from 24 individual samples) and aquatic specimens were sampled as proxies for the terrestrial and riverine contamination in addition to the wild boar. The aquatic specimens are musculatures of European chubs (n = 10) and suspended matter (n = 1) originating from 3 and 13 km downstream the industrial wastewater treatment plant, respectively. The soil sample was from an acre 3 km downwind the industrial facility. For each sample type, a set of reference samples without known contamination history was gathered across Germany. For wild boar, the pool samples of the BC area are defined as reference. Reference samples of soil and suspended matter were archived composite samples of different origin from the German environmental specimen bank (n = 10 and 6 after pooling from 16 and 12 individual samples, respectively). They were sampled according to standard operating procedures described by Weinfurtner and Kördel (2012) and Ricking et al. (2017). For the fish musculature, the six and ten reference fish originated from two rivers without known contamination, respectively.

Wild boar livers from areas PS (n = 9) and IE (n = 1) were studied individually and wild boar livers from area BC as pool samples because here at least three boars of the same age class and sex were available. For these 40 samples from area BC, pooling resulted in eleven liver pool samples. Fish musculatures from area IE and the two reference rivers were pooled from six to ten individuals. Soil samples were pooled from at least 16 individual samples. All pool samples were obtained by mixing equal weight proportions of individual samples. An overview of the samples, their related source of contamination and the pooling is provided in Table D 5 as well as further information on individual samples in Table D 6.

E Attended Scientific Events as Part of the Project

Table E 1: Attended events as part of the project

Date	Title of the presentation and the event	Meeting place	Type of presentation
03.– 05.06.19	FLUORBANK – Targeting an Organofluorine Mass Balance in Samples of the German Environmental Specimen Bank International Conference on Environmental Specimen Banks	Stockholm, Sweden	Poster
10.– 12.05.21	A generic method for the quantification of legacy, precursor and substitute PFAS in various sample matrices	online	Poster
07.09.21	Ergebnisse aus dem FLUORBANK-Projekt: PFAS im Wildschwein 16. Sitzung AG „Wald, Wild & One Health“	Berlin & online	oral
07.– 08.09.21	Eine generische Methode zur Quantifizierung von Legacy PFAS, ihren Vorläufern und Substituten in Proben verschiedener Umweltkompartimente Umwelt 2021	online	oral
02.– 03.11.21	Projekt FLUORBANK: Ergebnisse & Diskussion Von der Nordsee bis in die Alpen – PFAS-Belastungen in Deutschland FLUORBANK Workshop: PFAS-Analytik für die Umweltüberwachung	Leipzig, Germany	oral
05.– 07.09.22	Retrospektive Trendanalysen von PFAS in Biotaprobenn der Umweltprobenbank Umwelt 2022	Emden, Germany	oral